UNIVERSITÀ DEGLI STUDI DELLA TUSCIA DI VITERBO

DIPARTIMENTO DI SCIENZE DELL'AMBIENTE FORESTALE E DELLE SUE RISORSE
(Di.S.A.F.Ri)

CORSO DI DOTTORATO DI RICERCA

in ECOLOGIA FORESTALE - XVIII CICLO.

ANALYSIS OF THE CARBON CYCLE OF STEPPE AND OLD FIELD ECOSYSTEMS OF CENTRAL ASIA

ANALISI DEL CICLO DEL CARBONIO DI STEPPE ED AREE AGRICOLE ABBANDONATE DELL'ASIA CENTRALE

settore scientifico-disciplinare AGR05

Coordinatore: Prof. Paolo De Angelis

Tutor: Prof. Riccardo Valentini

Dottorando: Dott. Luca Belelli Marchesini

The scientist, by the very nature of his commitment, creates more and more questions, never fewer. Indeed the measure of our intellectual maturity, one philosopher suggests, is our capacity to feel less and less satisfied with our answers to better problems.

(G.W. Allport; Becoming)

Never fall in love with your hypothesis.

(Peter Medawar)

Whenever I have found out that I have blundered, or that my work has been imperfect, and when I have been contemptuously criticized, and even when I have been overpraised, so that I have felt mortified, it has been my greatest comfort to say hundreds of time to myself that "I have worked as hard and as well as I could, and no man can do more than this".

(Charles Darwin; Autobiography)

Some scientists work so hard there is no time left for serious thinking.

(Francis Crick; What mad persuit)

Abstract

Eurasian steppes cover a vast area of about $8 \cdot 10^6$ km^2, of which a fraction between 60% and 70% was converted to agricultural use in the past, and have been poorly investigated in respect with the exchanges of CO_2 with the atmosphere while they could play a relevant role in the carbon uptake located over the northern hemisphere lands at temperate latitudes. In particular, old agricultural fields abandoned after 1990 in former Soviet Union could contribute actively to the sequestration of atmospheric carbon, since after land use change they tend to restore the original stock of carbon of steppe ecosystems, that went partly lost with the agricultural use of the land. This study provides a quantitative characterization of the carbon pools, of the patterns of carbon allocation within the ecosystems, of the CO_2 exchanges between the biosphere and the atmosphere, as well as of the response of CO_2 fluxes to environmental drivers of true bunchgrass steppes and neighbouring old agricultural fields hosting different temporal stages of recovering grassland located in the Republic of Hakasia and in the Republic of Tuva (Russian Federation).

Within about 40 years, cultivations caused a loss of organic carbon not lower than 46%-52% in respect with the level of steppes (average carbon sotck: 140.9 $tCha^{-1}$ in Hakasia and 45.5 $tCha^{-1}$ in Tuva) and affected both the soil organic carbon pool, 80-92% of the lost carbon, and the belowground biomass pool for the remaining part.

The biomass carbon stock of steppes of Hakasia and Tuva was found to be stored mainly in the belowground pool, with a proportion ranging 88-94%, due to the highly developed root system of perennial species. In old agricultural fields, belowground biomass was still predominant but the share of biomass found in the aboveground pool, from 12% to 42%, was larger than in steppes.

The assessment of net primary productivity (NPP) at sites of Hakasia by different biometric methods ranged between 6.0 ad 13.1 t d.m. ha^{-1}, and organicated carbon was allocated primarily to the root system, with a fraction varying between 70% and 90% for both steppe and old field ecosystems.

CO_2 fluxes at ecosystem scale were monitored by eddy covariance technique over three stages of an old field succession in Hakasia represented by an early stage (5 years since land use change), an intermediate stage (10 years) and a mature stage (steppe). Yearly CO_2 exchange estimates disclosed all the sites to act as carbon sinks, with a strenght declining from the early stage (2.1 tC ha^{-1}) to the steppe ecosystem (1.1 tC ha^{-1}). Also the amounts of carbon assimilated by photosynthesis (GPP) and released to the atmosphere through ecosystem respiration (R_{eco}) decreased over the stages of the succession, yielding the observed trend in the net ecosystem productivity (NEP).

The steppe ecosystem, even if characterized by lower carbon assimilation than old field ecosystems, displayed a less pronounced reduction of the photosynthetic process in response to extreme high air temperature and air dryness conditions, maintaining its efficiency in carbon uptake.

The steppe ecosystem was also found resilient to disturbances since after a fire burst before the onset of the growing season, it showed an enhanced carbon sequestration that could completely offset the amount of carbon lost from the burnt biomass.

The carbon budget of the true steppe, estimated additionally using the ecological inventory methodology based on the difference between net primary productivity and heterotrophic respiration (NEP=NPP-Rh), agreed with the result obtained with the micrometeorological technique.

The spatialization of the carbon balance observed at sites in the steppe region of the Republic of Hakasia, to assess the magnitude of the sink of steppes and old fields ecosystems in the Russian Federation, suggests a carbon sequestration of 0.17 PgC yr^{-1}.

Keywords: carbon cycle, steppe, old agricultural fields, net primary productivity, eddy covariance, CO_2 flux partitioning.

Sommario

Le steppe eurasiatiche, che si estendono su di un'area di circa $8 \cdot 10^6$ km^2 di cui tra il 60% e il 70% convertito in passato all'uso agricolo, sono state scarsamente oggetto di ricerche sugli scambi di CO_2 con l'atmosfera, nonostante possano rivestire un ruolo rilevante nell'assorbimento di carbonio attualmente in atto da parte degli ambienti terrestri nelle zone temperate dell'emisfero boreale. In particolare i campi agricoli abbandonati a partire dal 1990 nell'ex-URSS possono contribuire attivamente al sequestro di carbonio dato che tendono a ripristinare lo stock originario di carbonio tipico delle steppe che si è parzialmente depauperato con l'uso agricolo del suolo.

Il presente studio ha come obiettivo la caratterizzazione quantitativa del ciclo del carbonio di steppe e campi agricoli abbandonati ospitanti diversi stadi temporali di una successione ecologica secondaria, di cui la vegetazione steppica rappresenta lo stadio finale, nella Repubblica dell'Hakasia e nella Repubblica di Tuva (Federazione Russa). Si analizzano gli stock di carbonio la loro distribuzione nei comparti (pools) degli ecosistemi, la produttività primaria netta e la sua allocazione, gli scambi di CO_2 tra ecosistema e atmosfera ed il controllo esercitato dai fattori ambientali su flussi di carbonio.

In seguito a circa 40 anni di coltivazione, lo stock di carbonio negli agroecosistemi ha subito una diminuzione non inferiore al 46%-52% rispetto ai livelli degli ecosistemi di steppa (pari in media a 140.9 $tCha^{-1}$ in Hakasia e a 45.5 $tCha^{-1}$ a Tuva) a carico principalmente del carbonio organico del suolo (in ragione del 80%-92%) e della biomassa radicale per la restante parte.

Il carbonio nella biomassa delle steppe in Hakasia e a Tuva è risultato stoccato per l'88%-94% nella biomassa ipogea, costituita dall'apparato radicale particolarmente sviluppato delle specie perenni. Nei campi abbandonati, la biomassa ipogea rimane prevalente sebbene la biomassa epigea rappresenti una frazione, tra il 12% e il 42%, maggiore rispetto a quanto osservato per le steppe.

La produttività primaria netta (NPP) stimata con diversi metodi biometrici per i siti dell'Hakasia è risultata compresa tra 6.0 e 13.1 t ha^{-1} di sostanza secca ed allocata prevalentemente nell'apparato radicale sia negli ecosistemi di steppa che negli ex-coltivi in proporzione variabile tra il 70% e il 90%.

La tecnica della correlazione turbolenta (eddy covariance) è stata impiegata in Hakasia per monitorare i flussi di CO_2 a scala ecosistemica su tre stadi serali della successione innescata dalla ricolonizzazione dei campi agricoli da parte della vegetazione spontanea (pioniero-5 anni; intermedio-10 anni; finale-steppa). Il bilancio del carbonio su base annuale che ne è risultato ha evidenziato la capacità di sequestro del carbonio di tutti gli stadi analizzati che è massima nello stadio pioniero (2.1 tC ha^{-1}) e decrescente nel tempo fino allo stadio di steppa (1.1 tC ha^{-1}). Lo stesso andamento temporale caratterizza il carbonio assimilato per fotosintesi (GPP) e rilasciato in atmosfera per mezzo della respirazione ecosistemica (R_{eco}), sebbene con tassi di variazione distinti che determinano le differenze osservate nella produzione netta ecosistemica (NEP).

L'ecosistema di steppa, nonostante sia caratterizzato da una minore capacità assimilativa rispetto agli stadi successionali precedenti, ha invece mostrato una maggiore capacità di mantenere l'efficienza nell'assorbimento netto di carbonio in condizioni ambientali di alta temperatura dell'aria e deficit di pressione di vapore. L'ecosistema di steppa è risultato anche dotato di buon livello di resilienza dato che ad un evento di incendio è seguita un'aumentata capacità assimilativa che nel corso di una singola stagione vegetativa ha portato a recuperare la quantità di carbonio perduto.

L'impiego di un approccio inventariale basato sulla differenza tra produzione primaria netta e respirazione eterotrofa (NEP=NPP-Rh) per la stima del bilancio del carbonio del sito di steppa è risultato convergente con quanto prodotto dal metodo dell'eddy covariance.

La spazializzazione delle stime di bilancio del carbonio ottenuto per i siti dell'Hakasia, finalizzata alla valutazione del potenziale del sequestro del carbonio atmosferico di steppe e campi agricoli abbandonati della Federazione Russa, indica un sink di 0.17 PgC yr^{-1}.

Keywords: ciclo del carbonio, steppe, ex-coltivi, produttività primaria netta, eddy covariance, partizione dei flussi di CO_2.

CONTENTS

Introduction

Background of scientific research on the carbon cycle

The atmosphere in the last century has experienced rapid changes in its chemistry due to human activities, at unprecedented rates at least during the last 20000 years: global atmospheric concentrations of carbon dioxide (CO_2), methane (CH_4) and nitrous oxide (N_2O), the main greenhouse gases (GHGs), have indeed increased remarkably, starting already since 1750, and presently far exceed pre-industrial values.

This increase of carbon dioxide was determined in the first place by the burning of fossil fuels and, with a smaller but significant contribution, by the deterioration of the original carbon stocks of terrestrial ecosystems induced by deforestation, agricultural practices and generally associated with land use changes. Emissions of methane and nitrous oxide are primarily due to agricultural activities and are proportional to the intensity of the agricultural management.

Although the tendency of the scientific research at present is to investigate on all the GHGs, tracking the exchanges of these gases between the biosphere and the atmosphere, in the last decade the largest part of the efforts was focused on the quantitative study of the carbon cycle, the ensemble of the exchanges of carbon, in the form of CO_2, among the atmosphere, the terrestrial ecosystems and the oceans by means of the processes of photosynthesis, respiration and dissolution.

Carbon dioxide is the most important greenhouse gas, and its global atmospheric concentration has increased from a pre-industrial value of about 280 ppm to 379 ppm in 2005. The analysis of the this trend reveals that, despite of the year to year variability in the growth rates, the annual carbon dioxide concentration growth-rate was larger during the last 10 years (1995 – 2005 average: 1.9 ppm per year), than it has been since the beginning of continuous direct atmospheric measurements (1960–2005 average: 1.4 ppm per year). The picture becomes concerning when we consider that the atmospheric concentration of carbon dioxide in 2005 exceeds by far the natural range over the last 650000 years (180 to 300 ppm) as determined from ice cores, and that at the same time annual anthropogenic carbon dioxide emissions are increasing worldwide. Fossil carbon dioxide emissions passed from an average of 6.4 [6.0 to 6.8] GtC per year in the 1990s, to 7.2 [6.9 to 7.5] GtC per year in 2000–2005, while carbon dioxide emissions associated with land-use change are estimated to be 1.6 [0.5 to 2.7] GtC per year over the 1990s, although these estimates have a large uncertainty.

The influence of anthropogenic GHG emissions on the global climate has been an extremely vivid matter of debate among the scientific community, interesting also the public opinion in recent years as long as the awareness of the drastic impacts of climate warming over human life spread wider.

The climatic records show that eleven of the last twelve years (1995 -2006) rank among the 12 warmest years in the instrumental record of global surface temperature (since 1850) and that the linear warming trend over the last 50 years (0.13 [0.10 to 0.16]°C per decade) is nearly twice that for the last 100 years. The global atmospheric temperature increase from 1850 – 1899 to 2001 – 2005 is 0.76 [0.57 to 0.95]°C.

If on the one hand the warming of the climate system is considered unequivocal, as it is more and more evident from observations of increases in global average air and ocean temperatures, widespread melting of snow and ice, and rising global mean sea level, on the other hand the effect of anthropogenic GHG emissions over climate has been at first only cautiously related to the climate warming as a hypothesis to explain global warming. That hypothesis started to be corroborated by an increasing bulk of experimental data, as long as new research projects were launched to address the new challenging issue.

In 2001, the Intergovernmental Panel on Climate Change (IPCC) concluded in the Third Assessment Report that "most of the observed warming over the last 50 years was likely to have been due to the increase in greenhouse gas concentrations". Since then a considerable breakthrough in the understanding of anthropogenic warming influence was achieved: in the latest Fourth Assessment Report of the IPCC, partly released in February 2007, the human activities since 1750 are claimed to be have been responsible, at a high level of confidence, for the climate warming with a radiative forcing of +1.6 [+0.6 to +2.4] Wm^{-2} and discernible human influences are extended to other aspects of climate, including ocean warming, continental-average temperatures, temperature extremes and wind patterns.

The future scenarios projected by IPCC for the next two decades imply a warming of about 0.2°C per decade and even if the concentrations of all greenhouse gases and aerosols had been kept constant at year 2000 levels, a further warming of about 0.1°C per decade would be expected.

Nevertheless the rate of emission of CO_2 due to human activities exceeds the actual rate of increase of CO_2 concentration measured in the atmosphere. This imbalance was noted in the early 1990's and could not be explained only by the amount of CO_2 dissolving in the oceans, leading to postulate the existence of a net uptake of atmospheric CO_2 by terrestrial ecosystems. The amount of this term of the global carbon cycle, generally indicated as "missing sink", is estimated to be about 2.9±1.1 GtG (Houghton, 2003).

Therefore, since the 1990's there was a major research effort to resolve uncertainties in the location and magnitude of sinks. The issue was tackled either by the establishment of global networks of research sites worldwide for surface flux measurements such as in the Euroflux, Ameriflux and LBA projects, and by intensifying the monitoring of CO_2 and other carbon cycle relevant tracers in the lower troposphere.

Current knowledge, relevance at global scale, and steps forward in the understanding of the carbon cycle of Siberia: the TCOS-Siberia project

The research activities upon which the present doctoral thesis is based, were carried out in the framework of a EU project, the Terrestrial Carbon Observing System–Siberia (TCOS-Siberia, EVK2-CT 2001-00131), aimed at enhancing the understanding the carbon cycle of this particular region of the Northern Hemisphere.

The selection of Siberia as a target for investigation relies behind the fact that from atmospheric measurements of the CO_2 concentration it has been inferred that a substantial net carbon uptake takes place in temperate latitudes of the northern hemisphere (Keeling et al., 1989, Tans et al. 1990), with a significant fraction over the continents.

It is reasonable to state that Siberia contributes in an important way to the northern hemisphere sink as it constitutes one of the most important terrestrial components of the global carbon cycle with an area of $13 \cdot 10^6$ km^2, an amount of 74 PgC stocked in vegetation and 249 PgC in soils (Dixon et al., 1994), and an estimated Net Primary Productivity of 1-3 PgC yr^{-1} (Schulze et al., 1999).

At present there is still a modest understanding of the role of this region in the global carbon cycle, due to the scatter in the results produced by the few researches on the topic, although substantially they confirmed the hypothesis of Siberia being a hotspot in the global biogeochemical cycles.

From the side of a top-down approach, based on inversion models, Bousquet et al. (1999) located the area with the largest sink in the North Asian continent, with a strength of the Asian boreal area of 1.5±0.7 Pg C yr^{-1}, whereas they found a source in the global arctic area, North of 65 °N, of 0.2 ± 0.3 Pg C yr^{-1}. Gurney et al. (2002) found a sink of 0.5 Pg C yr^{-1} in Boreal Asia and Rödenbeck et al. (2003) found a sink of 0.4 Pg C yr^{-1} in the Northern Hemisphere lands, largely located in North America, but a roughly balanced budget for Eurasia.

The TCOS-Siberia project implemented a continental scale observing system for an evaluation of the net Siberian carbon balance and its inter-annual variability. This objective was pursued by an integration of a “top-down” and “bottom-up” approaches where the first implies that atmospheric measurements of the concentration of the greenhouse gases are assimilated in inversion models to estimate magnitude and uncertainty of surface sources and sinks that are consistent with the observations, while the latter is based “bottom-up” point-wise flux measurements for various ecosystems, which are then aggregated to the regional scale.

Under the TCOS-Siberia project a network of long-term surface CO_2 flux-measuring stations was developed. These were located in a west-east transect (Bialystok, Fedorovskoje, Zotino, Yakutsk) cutting the boreal forest (taiga) of Russian Federation along 60°N , and were complemented by stations in the steppes of Hakasia in the south (54°N) and in tundra ecosystems (Cherskii, Chokurdakh) in the north (70°N).

The creation of such a network comprising the major ecosystem types (taiga, tundra, steppe) has a fundamental importance because the contribution of the different biomes to the aggregated continental flux is still a largely open question.

In particular, the role of forest biome has been approached by several studies based on biomass inventory that converged in reckoning the Russian taiga as a sink of atmospheric carbon: Kolchugina and Vinson (1993) suggested a sink of 0.485 Pg C yr^{-1}; Nilsson et al. (2000) and Shvidenko & Nilsson (2003) found sinks of 0.42±0.07 Pg C yr^{-1} between 1961–1998 including land-use change and peat-land dynamics, while Liski et al. (2003) suggest a sink of 0.43 Pg C yr^{-1}.
On the contrary there is a poor knowledge of the steppe biome in respect with its role as a carbon source/sink, since former studies focused mainly on the assessment of net primary productivity of these ecosystems (IGBP Programme) and its relation to the degree of grazing pressure. In the global distribution of the monitoring stations of CO_2 fluxes, gathered in the FLUXNET network, Eurasian steppes are very weakly represented, and apart from the stations established during the TCOS-Siberia activities, in the knowledge of the writer there exists only one long term site, located in Mongolia, that produced published results on the net ecosystem exchange of a steppe ecosystem (Li et al., 2005).

Focus on steppe ecosystems: motivations and objectives of the study

Eurasian steppes cover an extremely vast area of about $8 \cdot 10^6$ km^2, and are a relevant tile in the reconstruction of the continental carbon cycle of Siberia. Yet an analysis of the ecology of the steppes in respect with the carbon balance cannot avoid to take into consideration their land use history and actual management. A fraction between 65-70% of the steppes area was converted to agricultural use in the past, particularly during Soviet times, in order to create the so called “wheat field of Russia”. Since the breakdown of the USSR, a noticeable fraction of agricultural land (lowest estimate: $22 \cdot 10^6$ ha between 1992-2003) was abandoned and is currently in the stage of recovering steppe. The recover of the natural communities typical of steppe, after a disturbance that is widely associated to an impoverishment of the carbon stock, may represent a pre-eminent factor leading to carbon sequestration since these ecosystems tend to restore their carbon stocks to the original levels.
The aim of this study was to characterize the carbon cycle of natural and recovering steppe ecosystems of Central Asia. The location selected for the study were the steppes of the Shira region, in the Republic of Hakasia (Russian Federation), where the largest part of research efforts were concentrated, and the steppes of Ubs-Nur Hollow Reserve, in the Republic of Tuva (Russian Federation), differing in a higher climatic continentality and lower productivity.
In the Shira region, activities were carried out over a natural bunchgrass steppe and two successional stages of recovering steppe (old fields) aged 5 and 10 years since abandonment of agriculture were monitored during a 3 year campaign (2002-2004).
The overarching aim was approached by the use of different methods pursuant to the following specific objectives of the research:

1. Quantification of the carbon stock and analysis of pattern of distribution of carbon within aboveground biomass, belowground biomass and soil organic matter over the old field ecological succession. (Chapter 5)

2. Assessment of Net Primary Productivity, comparing different computational methods and field techniques for the assessment of aboveground and belowground NPP. (Chapter 6)

3. Assessment of the Net Ecosystem Productivity, by micrometeorological (eddy covariance) technique; partitioning of fluxes into Gross Primary Productivity and Total Ecosystem Respiration; analysis of the response of CO_2 fluxes to the main environmental forcings. (Chapter 7)

4. Chamber based measurements of soil CO_2 effluxes in the context of experiments aimed at: (i) partitioning soil respiration into autotrophic and heterotrophic component by root exclusion technique; (ii) testing the control of photosynthesis over soil CO_2 effluxes. (Chapter 8)

5. Constraint of Net Ecosystem Productivity by multiple methodological approaches: eddy covariance versus ecological inventory. (Chapter 9)

In the case of the steppes of Tuva, the investigated sites included a natural dry bunchgrass steppe and an abandoned agricultural field since 12 years. Results are limited to objective 1, for both sites, and objective 3, for the natural dry steppe only, of which results from a short-term record of CO_2 fluxes measured by eddy covariance technique are presented.

1 Steppes of Eurasia

The steppes of Eurasian continent form a well defined region occupying a vast area between 48 °N and 57 °N latitude and 27 °E to 128 °E longitude. Given the great expanse of steppe region, stretching for 800-1000 km from north to south and about 8000 km from west to east, a remarkable diversity of steppe communities is found.

1.1 Main features of vegetation and classification of steppes

Perennial microtherm xerophilous, and often sclerophyllous, bunch grasses predominate in steppe communities. These grasses are usually species of the genera *Agropyron sp.*, *Cleistogenes sp.*, *Festuca sp.*, *Helictotrichon sp.*, *Koeleria sp.* and *Stipa sp.*. Dominants also include bunch species of sedges (*Carex sp.*), and, in central Asia, of species of bunch forbs (*Allium sp.* and *Filifolium sp.*).

Dominant bunch grasses form the basis of plant community and provide most of the phytomass: these are usually composed of a combination of relatively tall bunch grasses, mostly species of *Stipa*, of shorter bunch grasses of the genera *Cleistogenes sp.* and *Festuca sp.*, and sometimes of dwarf bunch species of *Carex spp.*or dwarf species of *Stipa spp.*.

Forbs (herbaceous dycotiledons and non gramineous monocotyledons, usually of the families *Iridaceae* and *Liliaceae*) are often associated to bunch grasses. The number of species of forbs and their proportional contribution to biomass decreases from north to south within the steppe region, because of increased aridity of climate. In the most arid semi-desert and desert steppes communities of dwarf half shrubs also occur, consisting mostly of species of the genus *Artemisia sp.*.

The rhizomatous grasses and sedges do not form a clearly defined structural group in zonal steppe communities, but they are abundant in more northerly grasslands. The relative vigour of the various species and of the one structural group compared to another, change with fluctuation in precipitation, therefore the vegetative cover exhibits considerable inter-annual variation.

Plants in the dominating structural part of the plant community grow during the whole vegetative period , but during droughty months in summer (July and early August) their rate of development is retarded overmuch of the steppe region. This period of semi-dormancy occurs throughout the steppes of the European part of the former Soviet Union, as well as in the northern part of Kazakhstan and south western Siberia. In these regions growth is most rapid during June, the month of greatest precipitation. To the east, in the Daurian steppes, maximum precipitation occurs in July and August and the maximum development of vegetation takes place later than in western regions.

1.1.1 Zonal types of steppes

In the steppe region different zonal types of steppe which successively replace one another from north to south are met, following conditions of decreasing precipitation, increasing aridity and temperature summations and lengthening of growing season.

The classification of steppe according to Lavrenko (1970) distinguishes four types of steppe:

1. meadow steppe (forest steppe), in semi humid climate.
2. true or typical steppe divided into: (a) bunch-grass steppes with many forbs in semi-arid climate; (b) bunch-grass steppes with few forbs, in arid climate.
3. desertified bunch grass and dwarf half shrub-bunch grass (semi-desert steppe), in very arid climate.
4. desert dwarf half shrub bunch grass steppe in hyperarid climate.

The northern meadow steppes are characterized by the dominance of mesoxerophilous bunch grasses and sedges and by the abundance of xeromesophilous.

The typical or true steppes are distinguished by greater aridity of habitat, domination of xerophilous species of bunch grasses, and by a lower abundance of forbs (which are of a more xerophilous character than those in the meadow steppe).

The southern semi-desert and desert steppes are more arid than the preceding types, the most xerophilous bunch grasses and dwarf half shrubs being dominant.

Many other structural features change with increasing aridity. Species diversity is reduced from 40-50 species per square meter in meadow steppe to 12-15 species in semi desert and desert steppes. The height of the grass canopy decreases from 80-100 cm in the north to 15-20 cm in the south and foliage cover decreases from 70-90% to 10-20% and even less.

The vegetative cover of the forest steppe zone was, in the past, a mosaic of meadow, grassland and forest. In the European part of the former Soviet Union the principal tree was *Quercus robur* L:. These forest stands occurred on well drained catchments along the slopes of rather large rivers. At present they have been preserved only as small tracts. In the zone of true steppes, patches of trees grow only along the slopes of ravines. In the western Siberian forest steppe, as well as in the low mountain ranges of Central Kazakhstan, small tract of *Betula pendula* Roth., *B.pubescens* and *Populus tremula* L. are typical around shallow depressions. More or less steppified forests of *Pinus sylvestris* L. also grow along the flood plains and terraces of rivers throughout the Eurasian forest steppe and in low mountain ranges in Central and Northern Kazakhstan. *Larix gmelinii* Rupr. and *L.sibirica* Ledeb. occur in the mountainous forest steppe of Transbaikal and Mongolia.

1.1.2 Distribution of vegetation according to edaphic characteristics

Most types of steppes typically grow on Chernozem and chestnut (Kastanozem) soils (FAO soil classification). However, much of the variation in vegetation within each of the zonal types of

steppe is related to edaphic characteristics. The vegetation growing over flat, well drained plains with loamy soils, defined as *plakor*, most fully reflects zonal climate. Variations from this which affect the nature of vegetation are found in sands and loamy sands (psammophytic and hemi-psammophytic conditions), in stony and gravely soils (petrophytic conditions) and in soils with high salt content (halophytic conditions).

In hemi-psammophytic and psammophytic subtypes of steppes, the principal dominants are specific groupings of bunch grass species of *Agropyron spp.*, *Festuca spp.*, *Koeleria spp.* and *Stipa spp.*.

Areas of gravely soils, in low hills and intermountain plains, are characterized by communities of dwarf half-shrubs of several families, especially *Asteraceae, Cariophyllaceae, Lamiaceae* and *Scrophulariaceae*. Communities of dwarf half-shrubs with or without scattering of bunch grasses and sedges are often formed on rock outcrops almost devoid of soil. In some places within the steppe zone, shrubs are dominant in diluvial loamy, sandy and gravely deposits.

These shrub steppes are widely distributed over the steppe region of Eurasia, especially in Eastern Kazahstan and in Mongolia. And are characterized by abundance of the species *Caragana* and *Spirea spp.*.

Thickets of steppe shrubs occur on the slopes of ravines, in gullies formed by water erosion and in the margins of forest steppes. These are composed by the representatives of many genera, including *Amygdalus sp.*, *Calophaca sp.*, *Caragana sp.*, *Cerasus sp.* and *Cotoneaster sp.*.

1.2 Structure and ecological strategies of steppe communities

1.2.1 Community structure

Considerable variability exists in the structure of the above-ground and below-ground parts of communities in different subzones of the steppe, driven by differences in aridity. The proportion of soil covered by the vegetative canopy decreases from approximately 90% in the meadow steppe of the Black Sea region to about 10% in the desert steppe of Mongolia. Species diversity decreases along this same gradient from 22-36 species per square meter to only 7-10 species. Similarly also the height of grasses decreases from 80 cm or more in meadow steppes to only 5-8 cm (10 cm in moist years) in desert steppes.

Although the layer of grasses and dwarf-half shrubs constitutes the basic canopy of steppe vegetation, other strata are usually present. In meadow steppes a layer of mosses is often present (most commonly of *Thiudium abietinum*). In dry and semi-desert steppes of Kazakhstan, especially on sandy and stony soils, lichens (mainly *Parmelia vagans* Nyl..) form a rather thick cover on the soil surface.

The whole Eurasian steppe region is characterized by a well formed, but rarefied shrub layer (particularly of species of *Caragana* and *Spirea*) which is usually taller than grasses, reaching a height of 30 to 100 cm.

In the grass canopy of the forb-bunch-grass steppes, three sublayers are clearly distinguished: one of tall grasses (species *Helictotrichon* and *Stipa*) and of dicotyledonous forbs; a second of low bunch grasses and dicotyledonous forbs; and a third stratum of ephermerals, often reaching several centimetres in height. Similar sublayering occurs in semi-desert and desert steppes.

1.2.2 Phenology

Phenological development of steppe species is highly diverse, both in the duration of the vegetative period and in the timing of the phenological phases (aspects), their number and their prominence, in response to variations in temperature and moisture supply.

In the steppified meadows of the central chernozem region (forest steppe) of the European part of former Soviet Union, where the vegetative period is from April to September, some species are flowering at all times and as many as eleven flowering phases can be identified.

In more xerophitic steppes of the same region, where growth begins in the second half of April and continues until early October, no pronounced period of semi-dormancy occurs, as in southern steppe.

In the bunch grass dry steppe of the Black Sea region and Kazakhstan where the vegetative period is still longer (from March to early November), a well pronounced period of semi-dormancy occurs during summer (late June and early July).

In the semi-desert steppe of Kazakhstan, where the vegetative period is from 7 to 8 months long, as well as in the dry steppe, the period of semi-dormancy lasts for one to one and a half months.

In the extremely adverse environment in the desert steppe of Mongolia, growth begins between early April and early June depending on the occurrence of rainfall; nevertheless there is a general tendency towards an increasing number of species growing from spring to summer, the time of maximum precipitation.

1.2.3 Morphological adaptations

The dominating species in steppe communities are bunch grasses with pronounced xeromorphy of aboveground organs. The main feature of their xeromorphism is the presence of narrow, almost threadlike, more or less folded leaves. The stomata are located on the inner surface of the folded leaves, where they are protected during dry and hot weather. They are able to open at the moment of unfolding of the leaf during moist periods. These characteristics of leaves are very important adaptive features of steppe grasses.

The bunch life-form which predominates among species of the steppe, evidently has an advantage over the other life forms in adjusting to a tenuous supply of moisture. This is achieved by burial of vegetative buds, so that the basis of the tillers are positioned deeper in the soil. This protects them better than species of other life forms from grazing and trampling by wild and domesticated

ungulates. The bunches assist in the accumulation of snow and dust, which add to the supply of moisture and nutrients.

The underground parts of steppe plants also have characteristics that facilitate survival under adverse conditions such as a fibrous root system, typical of most plants of the steppe, providing a great number of small roots and root hairs which penetrate densely throughout the soil. The surface area of the root system is very great in relation to mass, a characteristic that is very important under conditions of low soil moisture.

The major amount of under-ground biomass was found to be in uppermost 50 cm, in the humus layer of the soil, whereas in the shallower soil of the southern steppes (Black sea steppes) the roots are concentrated in the uppermost 30 cm (Shalyt, 1950, 1952). In semi-desert steppes, the major portion of the root biomass is located in the top 20 cm of soil. In meadows the root system is also concentrated in the upper 50 cm, but the roots do not penetratre as deeply as in the steppe, where the moisture supply is more limited (Lavrenko, 1941).

1.2.4 Functional adaptations

An adaptive feature to survive in environments with low temperatures throughout the vegetative period, as in southern Mongolia, is the plasticity in respect with photosynthesis. For example, *Stipa gobica* Roschev. has a rather high photosynthetic performance at temperatures much lower than its optimal for this activity. At 0° and 10°C it is able to absorb, respectively, 22% and 56% of the amount of carbon dioxide which it fixes at optimum temperature (which varies from 20° to 25°C). This plasticity is a feature of the adaptation of many species to survive in southern Mongolia, where low temperatures are throughout the vegetative period. Such plasticity is not inherent in desert species.

Other adaptive features operate at the population level. For example, the steppe community is able to compensate for an adverse environment by rare and irregular peaks in rates of germination of seeds and survival of seedlings. This is especially important in the dry conditions of dry steppes. Even in the meadow of the Black Sea region indeed, where the annual precipitation reaches 600 mm, great fluctuations are observed in the time of appearance and abundance of seedlings as well as the numbers of juvenile individuals (Kamenetskaya, 1949).

Most steppe species are both anemphilous and anemochoric. The regimes of flower opening and pollination are generally controlled by humidity of the air and the wind, which is almost constant over steppes, is the controlling factor of distribution of fruits and seeds.

1.2.5 Steppe ecosystems sustainability

Steppe ecosystem sustainability is defined as capability of a steppe vegetation community to maintain its structure and functions for an infinite period of time under moderate grazing activity and recover back to the initial state once a moderate or a high grazing stress is removed.

The main steppe sustainability contributors are rapidly changing species composition, the effective use of various plant survival strategies, high dominant species productivity, accumulation of live plant parts mostly below ground, as well as spatial and temporal variability of soil nutrient availability.

Like other grass ecosystems, steppes are permanently under succession, as their biota species composition depends on management regime and particularly on grazing activity whose level varies place to place.

Dominant plant species structure is known to change drastically during post-grazing steppe recovery and during steppe degradation due to heavy grazing. In central Asian steppes it was found that the greater the grazing stress the bigger the proportions of *Artemisia frigida* (Willd.) and *Potentilla acaulis* L. and the less the stress, the greater the graminoids proportion in green biomass.

In degrading dry Tuva steppes, for example, the graminoids proportion in aboveground biomass decreases compared to stable steppes and increases in recovering steppes of the same type.

It is rapid replacement (succession) of pre-disturbance species by others, which are more adapted to a given grazing level, that provides green biomass load recovery and makes a certain vegetation structure sustainable and maintains also the productivity potential of steppe ecosystems.

Grazing has been a direct influence historically inherent in steppe ecosystem evolution. As a result, steppe plants developed certain strategies of adaptation to grazing. One of them is redistribution of assimilates between green and below-ground plant parts when a stress gets severer.

Studies on steppes of Tuva (Tilianova, 1999) evidenced how species appeared to transport more than 70% of dry matter to their below-ground parts. The plants were found to have different strategies of carbon allocation between their above- and below-ground parts in response to increasing grazing stress. Sedges and *Stipa krylovii* Roschev. showed a sudden increase in the rate of transporting organic substances to roots with severe grazing. *Helictotrichon desertorum* Less. seemed incapable of redistributing organic substances rapidly among its parts to result in decreasing the species abundance under moderate grazing and almost complete elimination of the species from the grass cover under overgrazing. *Festuca valesiaca* (Schleicher ex Gaud.) and *Cleistogenes squarrosa* (Trin.) Keng are known to be very resistant to biting tops off and trampling, although the rate of organic substance transport to the roots decreases for these species under heavy grazing. Their capability to recover, once their green biomass is consumed, is due to shooting from auxiliary buds and the ability of their terminal buds to produce two leaf generations. Such strategies can promote species survival and growth under increasing aridity and grazing. Coexistence of species having different stress adaptation strategies maintains biodiversity and functional heterogenity of a steppe ecosystem and, hence, its sustainability.

Below-ground accumulation of the plant parts playing the key role in regeneration reflects the steppe strategy developed in the course of evolution as a survival tool for vegetation suffering from long, cold and often dry winters and periodical severe summer droughts. In early spring and following drought spells, below-ground plant parts may support the development of above ground organs and the viability of photosynthetic tissues.

The below-ground layer can be defined as the steppe biodiversity storehouse. There seeds, the genetic fund of a community, are stored. This is where species manage to survive not only short-term frost or droughts, but also long-term (tens and hundreds of years) grazing influence. Moreover, rapid replacement of the dominant species above ground would be impossible if their rhizomes and regeneration nodes could not survive in the soil.

1.3 Longitudinal division of Eurasian steppes

The structure and floristic composition of vegetation of Eurasian steppes change from west to east accordingly to the degree of continentality of the climate which is expressed particularly in sharp fluctuations in the amount of precipitation and heat in different seasons of the year, as well as between years. The following sections can be recognized:

1. the temperate continental southern European part of the former Soviet Union and Romania
2. the continental southern part of Western Siberia and Northern Kazakhstan
3. the hyper-continental southern part of Eastern Siberia and Central Asia (including steppes of Trans-Baikal and Mongolia)
4. the temperate continental plains of north eastern China and adjacent meadow steppe.

The boundary layer between the continental and hyper continental zones is used as a basis for dividing the Eurasian steppe into two sub regions: Black Sea-Kazakhstan and Central Asian (Dauro-Mongolian).

1.3.1 The Black Sea-Kazakhstan subregion

This includes the extensive plains of eastern Europe, the plain in the southern part of the Western Siberian lowland, the plain of western Kazakhstan to the east and south of the Ural mountains, the low hills and low mountains of central and eastern Kazakhstan respectively. Mountains are situated only in the extreme south–east , including the southern Altai, the Kalbinsk mountain ridge and the Targabatai and Saur ridges, which all exhibit a well pronounced altitudinal zonality of vegetation. The Ural mountains and the Ural river constitute an inner boundary that separates the western part of the subregion, where climate is temperate continental, from the continental block of zones on the east.

In this subregion spring (April-May) is relatively warm, with considerable precipitation and June is the month of highest precipitation. The soils over the most of this subregion are typical deep

southern chernozems, while chestnut soils occur only in the south. Salinized, solonetz and solonchak soils are common in the chestnut soil area and also in the chernozem soils of south-western Siberia.

The dominants include the following species of *Stipa*: *S.dasyphylla* Lindem., *S.pennata* L., *S.pulcherrima* Koch, *S.tirsa* Steven, *S.ucrainica* P.Smirn, *S.zalesskii* Wilensky (section Stipa); *S.capillata* L., *S.sareptana* A.Beck (section Leiostipa); *S. korshinskyi* Roschev., *S.orientalis* Trin., *S.lessingiana* Trin. et Rupr. (section Barbatae).

Festuca valesiaca Schleich. ex Gaudin is another important short bunch grass together with *Koeleria cristata* L., and species of *Agropyron* and *Poa spp.*.

1.3.2 The Central Asian subregion

Central Asian steppes cover about $223 \cdot 10^6$ hectares (56°-41°N; 90°-120°E) and more than half of this area is in Mongolia (Table 1.1). Unlike more westward Eurasian steppes, Central Asian steppes are discontinuous, as they are dissected by mountains in many places and often have an island distribution pattern. Tytlianova (2003) argues that would be probably more correct to name these steppes "east Siberian-central Asian" steppes, although steppe areas that occur far beyond Central Asia are often defined as "central Asian steppes" in literature.

Prominent features of this subregion are small hills and high mountain ranges (Mongolian and Gobi Altai, the Hangayn Nuruu, Bulnai, Targabatai) with well defined altitudinal differentiation of vegetation. To the east, highly elevated (500-1000 m or more), well drained plains are situated between the eastern foothills of the Hangayn Nuruu and the western edge of the greater Khingan Mountains. In part, steppes occur in basins, river valleys, and on lake terraces. Bedrock type, a high break-stone content of soil, and slope aspect are the major controls of vegetation type.

Geographic location	Coordinates range		Area	Share of total area
	N	E	Mha	%
Central Siberia (Krasnoyarsk, Hakasia, Tuva)	$56\text{-}50^0$	$90\text{-}97^0$	9.85	4.4
Eastern Siberia (Irkutsk, Buryatiya, Chita)	$52\text{-}48^0$	$97\text{-}120^0$	16.88	7.6
Mongolia	$50\text{-}42^0$	$90\text{-}116^0$	117.56	52.7
China, Inner Mongolia	$46\text{-}41^0$	$110\text{-}118^0$	78.8	35.3

Table 1.1. Geographic location and area of steppes of Central Asia.

Central Asian steppes are markedly different from Black Sea-Kazakhstan steppes in that they do not exhibit a single latitudinal climatic gradient within which increasing mean annual air temperature would be accompanied by decreasing precipitation. Here, the climatic gradient is disturbed due to, among other reasons, a strong impact of Siberian anticyclone that is developed in autumn and winter over vast plains of central Asia as a result of intensive cooling of the area and long prevalence of dense and heavy air.

The climate is distinctly continental with frequent droughts during the growing season. July and August are the months of maximum precipitation. Spring (April – May) is cold, windy and dry. Air temperatures are very low in winter. The mean coldest winter month air temperature is, for example, -33.7 °C in the geometric center of Asia, which is in Kyzyl, Tuva, -29.2 °C in Ulan-Bator, Mongolia, and –28.0 °C in Borz, Dahuria. The warmest month mean temperatures are 19.6, 18.3, and 20.0 °C, respectively. Tuva, the center of Asia, is the coldest region with the greatest aridity and continentality. Continentality decreases north and eastward and monsoon climate has a mitigating effect in the east of central Asian steppes (Isachenko and Shlapnikov 1989).

Of all meadow, true, and dry steppes along the Yenisei meridian, the warmest are those in Minusinsk basin, where maximum air temperatures do not correspond to the minimum, but to the mean precipitation in this meridian section.

Widely varying combinations of heat and moisture amounts, mountain topography, big influences of the bedrock and a high break-stone content of soils in basins, foothills, and landscapes of the cuesta-ridge complex: all these factors contribute to central Asian steppes' being different from big plain steppes.

The soils of the Mongolian steppe are mostly dark chestnut to light chestnut. They are usually free of salt, predominantly loamy sand or sandy loam in texture, and more or less gravely. In southern Mongolia, steppe vegetation also occurs in the brown desert-steppe soils, which is not in the case of Black Sea- Kazakhstan subregion. Chernozems only occur in the northern part of the forest steppe in Transbaykal and in the northern part of Mongolia.

A specific feature of central Asian steppes is that their type distribution is independent of soil type differences, except that meadow and native semi-desert steppe types are closely linked to soil: the former are limited to chernozem soils and the latter to chestnut desert soils. True and dry steppes, as well as those regressed to desert by secondary factors can be found on dark-chestnut and chestnut soils of any kind.

Wide occurrence of transitional desert steppe areas in Central Asia is, to a big extent, the result of continental climate and increasing grazing: these two factors account for secondary deserting of true short bunchgrass steppes (Kuminova 1982). The dominant species are as follows: *Agropyron cristatum* L., *Cleistogenes songorica* Roschev., *Cleistogenes squarrosa* Trin., *Festuca kryloviana* Reverd., *Festuca lenensis* Dobrov., *Koeleria macrantha* Ledeb., *Poa attenuate*, *Poa botryoides* Trin. ex Griseb., *Stipa baicalensis* Roschev., *Stipa glareosa* P.Smirn., *Stipa gobica* Roschev., *Stipa*

grandis P.Smirn., *Stipa klemenzii* Roschev., *Stipa krylovii* Roschev. Species of *Caragana spp.* are also very important contributors in the vegetative cover.

Dwarf half-shrubs of semi-desert and desert steppes include: *Ajana fruticolosa*, *Anabis brevifolia*, *Artemisia frigida* Willd., *Artemisia xerophytica* Krasch., *Reaumuria songorica* (Pall.) Mill..

Artemisa frigida occurs also in more northerly steppes. Ephemerals are absent or rare, those genera typical of the Black Sea-Kazakhstan subregion being absent from Central Asia or limited to its western edge. Summer-autumn annuals and biennials are abundant in steppes, especially during moist years.

1.4 Steppes of Hakasia

Steppe areas account for about one third of Hakasia ($2 \cdot 10^6$ ha of the total $6{,}15 \cdot 10^6$ ha) and occur mainly in the south of Minusinsk basin. Ploughland is $7{,}4 \cdot 10^6$ ha and hayfields and pastures total $6{,}25 \cdot 10^6$ ha in the steppe area. Minusinsk basin is lined by Kuznetsk Altai, West Sayan, and East Sayan mountain systems in the west, south, and east, respectively. The natural conditions of the basin are determined by its being situated in the central part of Asia and by mountain-basin topography.

Minusinsk basin steppes, as classified by E.M. Lavrenko (1956), fall within the category of Yenisei true *Stipa capillata*-dominated steppes and are found on slopes of hummocks (400-450m above sea level) and on flat surfaces elevated 250-300m and higher.

Helictotrichon desertorum Less./feather-grass steppes occupy mostly the southern part of the basin (Koibal, Bey and Sabin steppes). The canopy is made up by big bunchgrasses, such as *Helictotrichon desertorum* Less. and *Stipa krylovii* Roschev., whereas the second and third layers were represented by *Festuca valesiaca* Schleicher ex Gaudin*, Koeleria cristata* (L.) Pers.*, Galium verum* L.*, Cleistogenes squarrosa* Trin.*,* and *Carex pediformis.* C.A.Mey. Closer to the northern slopes of mountains and ridges, big bunchgrass/feather-grass steppes are replaced by tall wormwood/feather-grass steppes where *Stipa krylovii* Roschev.*, Artemisia glauca* Pallas ex Willd.*, Festuca valesiaca* Schleicher ex Gaudin*, Koeleria cristata* (L.) Pers.*,* and *Cleistogenes quarrosa* Trin. dominated. Small bunchgrass steppes with four co-dominating grass species (so called 4-grass steppes) are common in the driest, mostly central, parts of the basin. The grass layer consisted mainly of grasses, such as *Stipa krylovii* Roschev.*, Festuca valesiaca* Schleicher ex Gaudin*, Koeleria cristata* (L.) Pers*,* and *Cleistogenes squarrosa* Trin., with remarkable shares of *Caragana pygmaea* (L.)DC. and xerophitic herb species (Volkova et al. 1979).

However, Minusinsk basin vegetation cover has changed significantly due to long-term influence of intensive grazing (Volkova et al. 1979). Kuminova (1976) found 530 plant species in the flora of Hakasian steppes which characterizes its richness.

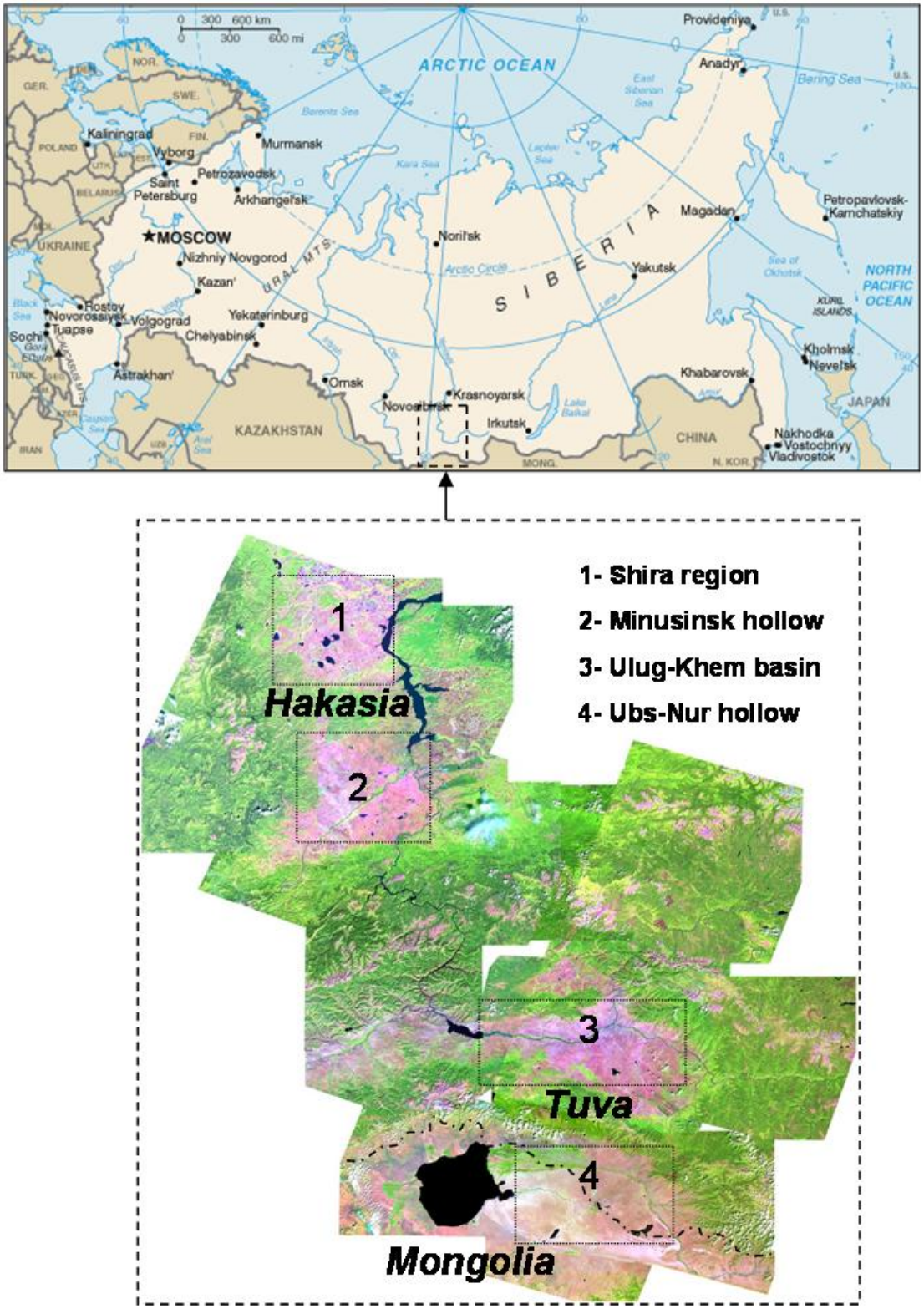

Figure 1.1. Corography of steppe areas of Hakasia and Tuva

compared to other steppe islands in southern Siberia. In the flora, 3 families are most numerous: Fabaceae, Asteraceae, and Poaceae. According to the biological analysis, herbaceous perennials, short shrubs, semishrubs and shrubs dominate the flora. According to ecological analysis, xerophytes dominate, followed by xeropetrophytes. Mesophytes are not numerous, only 14% of the composition. Psychrophytes and cryophytes are glacial relics. Halophytes and psammophytes caused by edaphic conditions are locally found. Kuminova (1976) found 369 species in meadow steppes, 310 species in tall bunchgrass steppes, 279 species in short bunchgrass steppes, and 103 species in desertificated steppes.

1.5 Steppes of Tuva

Steppes of Tuva occupy intermountain basins (550-1200m a.s.l.), the lower parts of mountain slopes, and high river terraces. Steppe areas are concentrated in two basins: the Ulug-Khem and the Ubs-Nur.

1.5.1 Ulug-Khem basin

Ulug-Khem basin (550-700m a.s.l.) is located in Central Tuva depression and stretches for about 100km. The basin is limited by Bur and Tanu-Ol mountain range slopes in the north and south, respectively.

Ulug-Khem basin's being situated in the center of Asia accounts for its severe environmental conditions – little precipitation and extremely continental climate. The total precipitation ranges 180-230 mm in the north (Kyzyl town) and 250 to 350 mm in the south of the basin (Sosnovka village). Spring and early summer are very dry and rains fall, usually as heavy showers, in July and August. Mean annual air temperature is very low (-5.7 °C), with absolute maximum (36-39 °C) in July, and it can drop as low as –55-60 °C in some days in winter. The frost-free period lasts for 100-120 days. Snow cover is not thick and does not exceed 24 cm around Kyzyl town. Soil freezes gradually down to 140 cm from the second half of November through early March and than it gradually thaws from late April to mid July (Gorshkova 1990).

Since meadow steppes typically occur in the forest-steppe belt, often on southern slopes, they are not characteristic of this basin. Here, petrophytic steppe vegetation, represented by true small and big bunchgrass communities, is widespread, as it is capable to develop on poorly developed soils with high stone content on steep southern slopes.

Tall bunchgrass steppes are represented by *Helictotrichon desertorum* Less., feather grass, sedge, and secondary forb communities (*Helictotrichon desertorum* Less*., Stipa capillata* L*., Carex pediformis* C.A.Mey*., Aster alpinus* L*., Bupleurum scorzonerifolium* Willd*., Artemisia glauca* Pallas ex Willd*., Poa botryoides* Trin. ex Griseb*)* (Kuminova 1982).

Short bunchgrass steppes occur on chestnut soil-dominated flat parts of well-developed river valleys, lake basins, and intermountain depressions. Grasses enjoy permanent predominance in sites that are only slightly damages by grazing. Heavy grazing results in bunchgrass decay, disturbs the general grass cover structure, and changes species composition. Secondary communities begin to establish where more grazing resistant plants prevail, such as *Carex duriuscula* C.A.Mey and *Artemisia frigida* Willd.. As reproductive buds of *Carex duriuscula* are located deeper in soil compared to grasses, this species spreads rapidly with increasing grazing activity. Grasses are broadcast, in small bunches, across the area. As grazing activity gets even heavier, *Artemisia frigida* steppe is formed on eroded light-textured soils (Yershova 1982).

The following species are common in small bunchgrass steppes: *Festuca valesiaca* Schleicher ex Gaudin*, Koeleria cristata* (L.) Pers.*, Stipa krylovii* Roschev.*, Poa botryoides* Trin. ex Griseb*, Agropyron cristatum* (L.) Gaertn.*, Carex duriuscula* C.A.Mey*, Veronica pinnata* L.*,* and *V.incana* L.. Transitional desert steppes are covered by *Artemisia frigida* Willd.*, Agropyron cristatum* (L.)Gaertn.*/Cleistogenes squarrosa* Trin.*,* and *Cleistogenes squarrosa* Trin.*/*small forb communities with characteristic steppe species, such as *Cleistogenes squarrosa* Trin.*, Artemisia frigida* Willd.*, Potentilla acaulis* L.*, Krascheninnikovia ceratoides* (L.) Guldenst*,* and desert steppe species, such as *Kochia prostrata* (L.) Schrad. *, Gypsophila desertorum* (Bunge) Fenzl*,* and *Convolvulus ammanii* Desr..

While transitional desertification associated with erosion, heavy grazing, and road building occurs fragmentarily in Hakasia, transitional desert steppes are extremely vast in Tuva and their characteristic vegetation cover type dominates in a number of large regions.

There are typical secondary semi-deserted steppes also in Ulug-Khem basin, primarily on alluvial fans of rivers running down from the southern slope of West Sayan Mountains. These steppes are limited to poorly developed light-chestnut soils and their communities are characterized by *Stipa glareosa* P.Smirn.*, S. orientalis* Trin.*, Psathyrostachys juncea* (Fisch.) Nevski*, Gypsophila desertorum* (Bunge) Fenzl*,* and *Convolvulus ammanii* Desr. (Kuminova 1982).

1.5.2 Ubs-Nur basin

Tuva includes the northern part of the basin of Ubs-Nur lake, whose water edge is at 760 m a.s.l. The lake basin is situated in Ubs-Nur basin, a depression in Altai-Sayan-Mongolian mountain belt.

Ubs-Nur basin, like entire Tuva, is subjected to strong anticyclone that results in extremely cold winters. Mean minimum December and March air temperature is lower than –35 °C and it can drop to –48 °C and lower in January and February. This basin is located where sharp contrasts in the climate, the greatest on global record, occur. Large divergence of mean daily air temperature between the seasons,, with long and non-thaw winter with severe frost and hot summer, along with little precipitation (a pronounced maximum in summer) are the main features of the climate,. The frost-free period lasts for 140-160 days. Growing season, i.e. a period of mean daily air temperature

above 10°C, starts during the first ten days of May and goes on up to the third ten-day period of September. A multiyear record shows that average annual precipitation is about 230 mm. According to data from Erzin weather station, annual precipitation has varied 180-290 mm over the 90's. Precipitation peaks in July-August. May and June are often very dry and steppes come to life as late as August, after late summer rains.

Ubs-Nur basin is remarkable for a complex and mosaic vegetation cover. Here, mountain steppes meet plain steppes. Steppe vegetation of the basin bottom can be divided, as stated by some authors, into two zones: true and transitional desert steppes (Kuminova 1985; Alekhno et al. 1995). True steppes include vegetation communities where xerophilous small bunch grasses account for the major proportion. They are mostly found in the north of the basin, and plant communities range widely. *Cleistogenes squarrosa* Trin./feather grass, small bunchgrass/feather grass, and feather grass/small bunchgrass are the most common steppe communities, whose dominants are *Stipa krylovii* Roschev., *Cleistogenes squarrosa* Trin., *Koeleria cristata* (L.) Pers., *Agropyron cristatum* (L.) Gaertn., *Festuca valesiaca* Schleicher ex Gaudin, and *Carex duriuscula* C.A.Mey.. Grass prevalence can drastically decrease as a result of grazing-induced digression and new dominants, such as *Carex duriuscula* C.A.Mey, *Artemisia frigida* Willd., and *Potentilla acaulis* L., can confer to steppe a quite aspect. As dominants are replaced rapidly, it is impossible to tell true steppe from dry areas based only on the dominating species criterion. We have no choice but to consider the communities of interest as dry steppe communities, since the steppes of the Tuva part of Ubs-Nur basin are confound to chestnut soils of usually light granulometric composition. In Mongolian part of the basin, true steppes are associated with dark-chestnut soils that are predominant mainly in broad valleys in the south-east of the basin (Deyeva et al. 1995). As was mentioned above, true steppes are widespread on dark-chestnut soil and sparse chernozem sites in Ulug-Khem basin, Tuva.

Transitional desert steppes account much of Ubs-Nur basin and are covered mostly by *Stipa glareosa* P.Smirn. communities where *Stipa krylovii* Roschev., *Clestogenes squarrosa* Trin., and *Artemisia frigida* Willd. prevail, while *Caragana pygmaea* (L.)DC. largely contributes to developing shrub steppes.

2 Carbon cycle and carbon sequestration capacity of temperate grassland ecosystems

Global estimates of the relative amounts of carbon in different vegetation types attribute to temperate and tropical grasslands, more than 10% of the total carbon store of the biosphere (Eswaran et al., 1993; Nosberger et al., 2000).

Of the temperate grasslands of the world, some have grasslands as their natural vegetation and some are anthropogenic in origin. In areas where grasslands are the natural climax vegetation (e.g. the steppes of central Asia and the prairies of North America) the rainfall is low enough to prevent the growth of forests. Where grasslands are non-natural (e.g. north-western and central Europe, New Zealand, parts of North and South America and Australia) rainfall is normally higher and the climax vegetation is forest. These climate differences mean that the productivity of natural grasslands is generally low while that of the non-natural grasslands is significantly higher, with the result that they tend to be used more for intensive agricultural production (Whitehead, 1995)

2.1 Carbon cycle of grassland ecosystems with emphasis on the role of soil

The paradigmatic carbon cycle of grassland ecosystems implies exchanges of carbon in form of organic matter among three compartments (soil, vegetation, herbivores) and under inorganic form as CO_2 between each of these and the atmosphere (fig.2.1). The vegetation exchanges actively CO_2 with the atmosphere through the biological processes of photosynthesis and respiration and contributes to inputs of organic matter into the soil by dead tissues that are partly decomposed and the carbon contained in released to the atmosphere as CO_2. The herbivores consume grass matter, return part of the ingested carbon through excrements, that naturally serve as fertilizing substrate for grass, and emit CO_2 to the atmosphere as a result of respiration. In managed grasslands the excreted carbon may be incorporated directly into soil as manure by farming practices. For natural steppe ecosystems, in absence of livestock, the fraction of primary productivity consumed by herbivores, typically rodents, is very small and generally does not exceed 1-2% of NPP. Moreover, grasslands contribute to the biosphere-atmosphere exchange of non-CO_2 greenhouse gases, with fluxes tightly depending on management practices: nitrous oxide (N_2O) is emitted by soils and methane (CH_4) is emitted by livestock at grazing and can be exchanged with the soil. Moreover, horizontal transfers of organic carbon to or from grassland plots may occur as a result of harvesting grass as silage or hay, on the one hand, and of farm manure applications on the other. Up to 98% of the total carbon store in temperate

grassland ecosystems can be found sequestered in the below ground pool (Hungate et al., 1997) which generally has much slower turnover rates than aboveground C (Schlesinger, 1977).

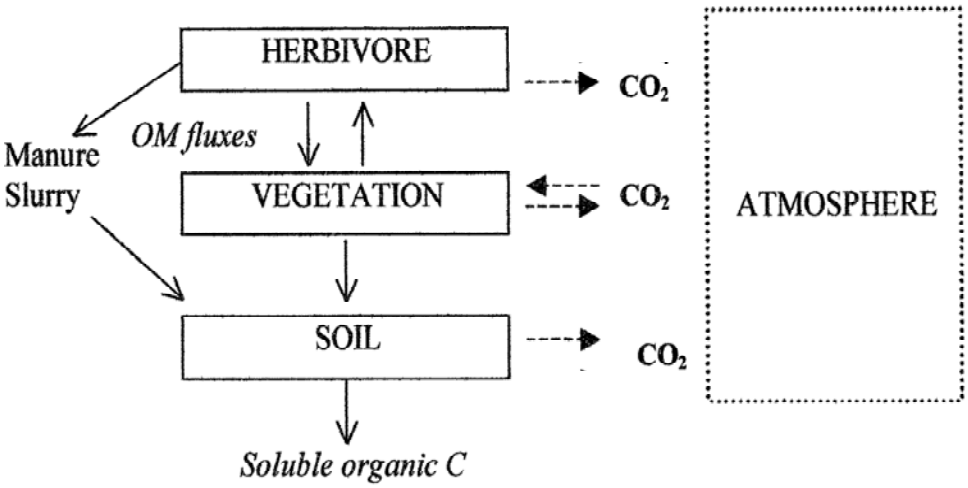

Figure 2.1. Schematic diagram of the greenhouse gas fluxes and main organic matter (OM) fluxes in a grazed grassland. (modified after Sousanna, 2004)

A significant proportion of soil organic matter (SOM) is physically protected from decomposition through occlusion by clay minerals and encapsulation within soil aggregates. A large amount of this SOM comprises a pool having an intermediate (10–15 yr) residence time, but this decomposes more quickly on disturbance. More active organic matter, consisting of microbial biomass and labile organic matter, such as plant detritus, cycles more rapidly but makes up only 3–5% of total organic matter (Darrah, 1996; Joffre & Ågren, 2001). At the other extreme is very old material that is physically or biochemically protected in a passive recalcitrant form with a turnover time of hundreds to thousands of years (Jenkinson, 1990; Post & Kwon, 2000).

Usually soil carbon stocks are quantified considering a soil depth ranging 30-100 cm (Jobbágy & Jackson, 2000; Gifford & Roderick, 2003), and information on vertical distribution of soil organic carbon (SOC) are not abundant. However, Jobbágy & Jackson (2000), in a survey of temperate grasslands, found that while only 64% of SOC occurred in the top 40 cm, this depth contained as much as 87% of the roots. Possible explanations for the presence of a large part of SOC in the deeper soil layers can be:

(i) decreasing SOC turnover with depth resulting in higher SOC accumulations, as carbon placed in depth is often protected physically and/or chemically from microbial attack (Ajwa et al., 1998);

(ii) increasing root turnover with depth causing higher C inputs per unit of standing biomass; this argument is supported by the observation that the lower nutrient content in deeper roots leads to reduced turnover rates (Gordon & Jackson, 2000);

(iii) SOC leaching from upper to lower levels;

(iv) vertical mixing by soil organisms (Jobbágy & Jackson, 2000).

2.1.1 The process of carbon sequestration in soils

Carbon from plants enters the SOC pool in the form of either above-ground litter or root material. Also, in grasslands a significant but variable proportion of plant material is consumed by herbivores and then enters the SOC pool from animal excretion (Bol et al., 2004). Within the soil, plant fragments become reduced in size to either the light fraction or the particulate organic matter fraction (Post & Kwon, 2000). In addition, plant residue leachate and microbial and plant-root exudates contribute to a more active carbon pool which consists of microbial biomass and microbial metabolites. The leachates and exudates from roots and microbes, together with fungal hyphae, earthworm casts and other biological binding mechanisms, effectively increase the light fraction of the plant material with clay and other mineral particles.

Post & Kwon (2000) indicated that there are many factors and processes that determine the direction and the rate of change in soil organic content when vegetation and soil management practices are changed. Ones that may be important for increasing soil carbon storage include:

i) increasing the input rates of soil organic matter;

ii) changing the decomposability of organic matter inputs that increase the light fraction of organic carbon;

(iii) placing organic matter deeper in the soil either directly by increasing belowground inputs or indirectly by enhancing surface mixing by soil organisms;

(iv) enhancing physical protection of the soil through either intra-aggregate or organomineral complexes. Conditions favouring these processes occur generally when soils are converted from cultivated use to permanent perennial vegetation, such as from crop to pasture.

High root production by grasses may explain why pastures accumulate so much soil organic carbon. On the other hand, episodic grazing or cutting of pastures may have a soil carbon " pumping action" owing to the rapid death of roots following each defoliation event followed by root re-growth as the pasture sward re-establishes. Under certain conditions grazing can lead to increased annual net primary production over ungrazed areas (Conant et al. 2001).

Most pasture plants (≈80%) are perennial and have well developed root systems that are used as a carbon storage of new growth in spring or after grazing (mowing). Hence, the relative belowground translocation of assimilated carbon by pasture plants can reach up to 80% (including C autotrophically respired by roots) but up to only 60% by trees (Kuziakov & Domanski, 2000). At he same time

grasslands have high inherent soil organic matter content that supplies plant nutrients, increases cation exchange and water logging capacity (Miller & Donahue, 1990).

A large proportion of the carbon that enters the soil is returned to the atmosphere through respiration carried out by roots and soil organisms. The distinction between autotrophic and heterotrophic respiration in soils is difficult to make (Trumbore, 2000), and estimates are extremely uncertain, but the fraction of CO_2 evolution attributable to root respiration can vary between 16% and 95% (Darrah, 1996). Other significant losses of carbon in grasslands are through soil erosion and soil water drainage containing dissolved organic carbon (Kalbitz et al., 2000).

2.1.2 Turnover of SOM and capacity for long term carbon sequestration

Soil organic carbon includes plant, animal and microbial residues in all stages of decomposition. Many organic compounds in the soil are intimately associated with inorganic soil particles. The turnover rate of the different soil organic carbon compounds varies due to the complex interactions between biological, chemical and physical processes in soil. Although there may be a continuum of soil organic carbon compounds in terms of their decomposability and turnover time, physical fractionation techniques are often used to define and delineate various relatively discrete soil organic carbon pools. Physically defined fractions, while containing a diverse array of organic compounds, integrate physical and structural properties of soil organic carbon. According to Christensen (1996), the organic carbon in the soil can be found in the form of light fraction, organomineral fraction or being part of microbial biomass.

The light fraction of organic carbon (LF-OC) is free (not complexed with mineral matter), particulate plant and animal residues undergoing decomposition (Spycher et al., 1983). Occasionally some of this material may be biologically resistant, such as charcoal (Skjemstad, 1990).

Part of the LF-OC can be physically stabilized in macroaggregates as intra-aggregate particulate carbon (Cambardella and Elliot, 1992, 1993). This fraction is highly decomposable and can show seasonal fluctuations and spatial variation with changes in litter inputs (Boone, 1994). The turnover of LF-OC in such ecosystems is linked to macroaggregate formation and its amount is greatly impacted by cropping and tillage (Bremer at al. 1994). Short term shifts in SOC storage and turnover are in large part due to the dynamic nature of this pool which has a bulk turnover time measured in months to a few years.

SOC is transformed by bacterial action and stabilized in clay or silt sized organomineral complexes where the majority of SOC is found. The highest concentrations of SOC are associated with < 5 μm mineral particles. Following the addition of simple substrates, new SOC is found to be associated with a range of mineral particles sizes. However, clay sized organomineral complexes often show greater

accumulations and subsequently more rapid loss rates than in silt sized particles, indicating a higher stability of silt-SOC (Christensen, 1996). Turnover times of HF-OC are in the order of decades.

Microbial biomass, while a small part of SOC, mediates the transfer of SOC among inputs, LF-OC and organomineral HF-OC. As a result, rates of transfer and transformation are influenced by biologically important factors including soil moisture and soil temperature. It is thought that passive SOC is comprised of nearly inert LF-OC component, as charcoal and some very chemically recalcitrant material in organomineral HF-OC complexes.

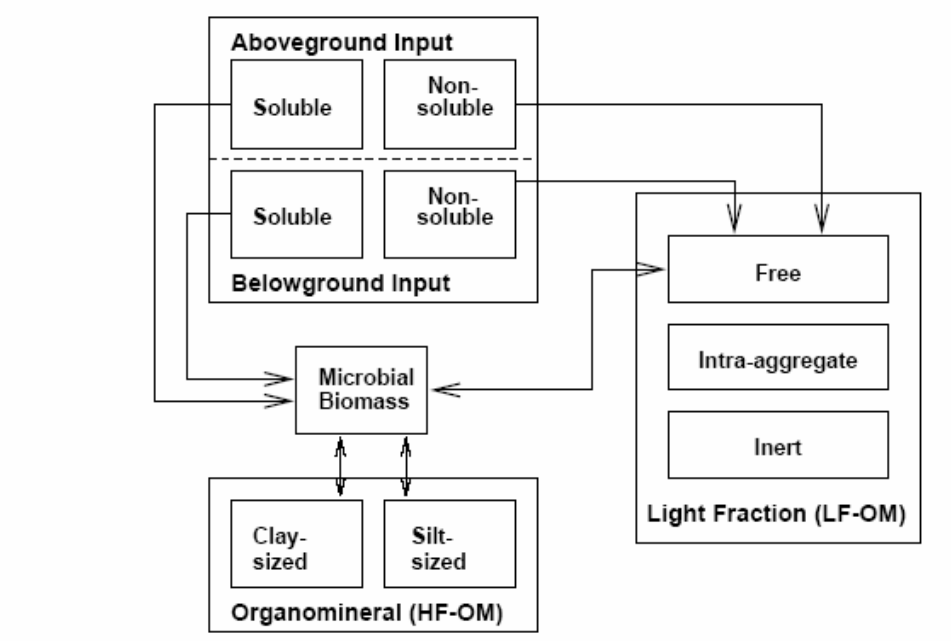

Figure 2.2 Scheme of mineralization and transfer of organic matter in soil according to Christensen (1996).

2.2 Carbon sequestrastion magnitude of temperate grassland ecosystems

The role of carbon sink or source of an ecosystem can be assessed by measuring the small changes in carbon stocks in the soil or by determining the carbon balance based on a the accounting of carbon gains and losses.

The measurement of carbon stocks has to account for the heterogeneous nature of the distribution of carbon in the soil and, if significant changes are to be detected, then measurements may need to be made over timescales of, at least, decades (Hungate et al., 1996; Conant et al., 2001). Nevertheless the carbon accounting depends on the reliable measurement of large fluxes into and out of the system.

A number of studies based on both these approaches have shown that most temperate grasslands worldwide are characterized by carbon sequestration capacity (Conant et al ., 2001) under a range of climatic and management conditions.

Location	Ecosystem type/management	Net Ecosystem Exchange (t C ha^{-1} yr^{-1})	Reference
Canada	Temperate grassland (ungrazed)	-1.09 to -0.18	Flanagan et al. (2002)
USA	Serpentine grassland	-1.33	Valentini et al. (1995)
North America	C_4 dominant	-0.5 to -0.8	Dugas et al. (1999)
USA (Oklahoma)	C_4 tall-grass prairie	-0.46 to -2.74	Sukyer et al. (2003)
USA (Nevada)	Grazed mixed prairie	-0.36	Franck (2002)
USA (Nevada)	Ungrazed mixed prairie	-0.45	Franck & Dugas (2001)
USA (Oklahoma)	Tall-grass prairie	0	Sukyer & Verma (2001)
USA (Oklahoma)	Grazed grassland	0.41	Meyers (2001)
Mongolia	Grazed steppe	-0.41	Li et al. (2005)
France	Grassland- high N input Grassland – low N input	-0.40 -1.40	Sousanna et al. (2004)
Hungary	Grassland	-1.20	Sousanna et al. (2004)
Italy	Alpine grassland	-4.31	Sousanna et al. (2004)
Switzerland	Grassland- high N input Grassland- low N input	-4.02 -2.81	Sousanna et al. (2004)
UK	Grassland – ploughed Grassland – cut	4.49 0.29	Sousanna et al. (2004)
US (North Carolina)	Grassland- cut annually	0.97	Novick et al. (2004)
US (Arizona)	Grassland	0.58 to 2.12	Emmerich (2004)

Table 2.1. Review of published results of annual net ecosystem exchange of temperate grasslands obtained by CO_2 eddy covariance flux measurements(negative NEE values denote an uptake of atmospheric carbon).

In the USA and Canada, Bruce et al. (1999) estimated that North American soils sequester, on average, 0.2 tC $ha^{-1}yr^{-1}$, while Conant et al. (2001) produced an estimate of 0.58 tC $ha^{-1}yr^{-1}$ for the same region. For Australia, Conant et al. (2001) give a value of 0.28 tC $ha^{-1}yr^{-1}$, while Gifford et al. (1992) estimated that the same soils can sequester between 0.5 and 0.6 tC $ha^{-1}yr^{-1}$. In a model prediction for Europe, under a business-as-usual scenario in 2008–12, Vleeshouwers & Verhagen (2002) propose that the majority of European grasslands will be sinks for C and the average sequestration could be 0.52 tC $ha^{-1}yr^{-1}$.

Annual Net Ecosystem Exchange estimates produced by monitoring of CO_2 fluxes by eddy covariance technique over temperate grasslands worldwide (table 2.1), range between a source of 4.49 tC $ha^{-1}yr^{-1}$ (for a ploughed grassland in the UK) and a sink of 4.31 tC $ha^{-1}yr^{-1}$ (for an alpine grassland in Italy), indicating on average a carbon sink capacity of 0.61±0.44 tC $ha^{-1}yr^{-1}$. Out of 19 studies, 10 have been conducted in North America, 9 in Europe, while Asian steppe ecosystems are represented by 1 study in Mongolia. The largest net losses of carbon were observed for grasslands, run under impacting

management practices such as ploughing or grass cutting, with the exception of a grassland site in Arizona (Emmerich, 2004), which is developed over high carbonate soils.

2.2.1 Climate-change effects on carbon sequestration of grasslands

Climate influences both the above and below-ground processes which drive the carbon cycle and ultimately determine how much carbon is sequestered in grassland soils. The components of the climate that are most important for soil processes are temperature and rainfall: according to IPCC (2001), the global average surface temperature increased over the 20th century by ≈0.6 °C and is projected to increase between 1.4 and 5.8 °C over the period 1990–2100. Winter rainfall is also expected to increase in regions occupied by temperate grasslands (IPCC, 2001).

Using the CENTURY model, Ojima et al. (1993) and Parton et al. (1995) assessed grassland production and soil carbon worldwide in response to temperature increases of 2–5 °C and predicted a substantial loss (3–4 Pg C after 50 yr) of SOC for all grassland areas. The losses from soil carbon were caused by higher decomposition rates which were increased by as much as 25% in temperate grasslands.

However, in contrast Thornley & Cannell (1997) and Cao & Woodward (1998) predicted net increases in the carbon sink of temperate grasslands with increases in temperature.

In response to evidence based on experimental observations that soil carbon pools may be much less depleted at elevated temperatures than predicted by most ecosystem models, Giardina & Ryan (2000) and Thornley & Cannell (2001) hypothesize that increasing temperatures may have a larger effect on the rate of physicochemical processes relative to biological processes, thus transferring increased amounts of organic carbon to more stable soil carbon pools. They suggest that, in the short term, accelerated microbial respiration caused by warming results in an increase in soil carbon loss, but that in the long term more carbon is sequestered because of higher NPP combined with accelerated physicochemical ‘stabilization’ reactions. Thus in the long term rising temperature tends to induce a negative feedback, enabling greater amounts of carbon to be sequestered at higher temperatures.

Experimental treatments that have exposed grassland monoliths to elevated temperatures have tended to support the more recent model predictions of Thornley & Cannell (2001). For example, Loiseau & Soussana (1999) found no effect of a 3 °C increase in temperature (under elevated CO_2) on soil carbon accumulation in organic matter fractions above 50 μm. Fitter et al. (1999) also recorded no change in soil carbon storage in an upland grass ecosystem soil warmed by 3 °C, presumably because root production and death rates increased by equivalent amounts. Evidence from global patterns of carbon stocks along gradients of mean annual temperature is mixed. In a survey of more than 2700 soil profiles from around the globe, Jobbágy & Jackson (2000) concluded that SOC decreased with increasing temperature and increased with higher rainfall and clay content. Their analysis also showed

that the importance of these controls switches with soil depth so that climate dominates in shallow layers and clay content dominates in deeper layers. On the other hand, Kirschbaum (2000) found no clear trend when global patterns of soil carbon were plotted against mean annual temperature as long as very wet and very dry locations were excluded.

2.2.2 Management effects on carbon sequestration

The amount of SOM retained by grassland soils is strongly influenced by management (Barnwell et al., 1992; Conant et al., 2001; Zan et al., 2001; Schuman et al., 2002). Management practices which eliminate disturbance to soil carbon in established pastures, have the greatest impact on carbon sequestration.

Management methods that increase forage production, such as fertilization, irrigation, intersowing of grasses and legumes, intensification of grazing, and introducing earthworms, also have the potential to increase SOM (Conant et al., 2001). The introduction of productive forage grasses also increases sequestration. For example, sowing tall fescue (*Festuca arundinacea*) and smooth bromegrass (*Bromus inermis*) has been shown to increase the soil carbon pool by 17.2%, equivalent to a carbon sequestration of ≈3 Mg C ha^{-1} yr^{-1} over a 6 years period (Lal et al., 1998).

In general, grasslands with the greatest potential for soil carbon increase are those that have been depleted in the past by poor management. On intensively managed grasslands, improved practices such as rotational grazing and fertilizer application have the greatest potential, while on extensively managed grassland, grazing intensity and frequency are the main management practices to affect soil carbon levels. Reeder & Schuman (2002) have shown that soil carbon content was highest in US mixed-grass and short-grass rangelands at the highest stocking density, while excluding grazing caused immobilization of carbon in excessive above-ground plant litter or an increase in species having annual life forms which lack the dense fibrous rooting systems conducive to SOM formation and accumulation. They concluded that soil carbon was increased by grazing, caused by a higher annual shoot turnover and a redistribution of carbon within the plant–soil system as a result of changes in plant species composition. Both LeCain et al. (2002) and Reeder & Schuman (2002) recommended a light-to-moderate stocking density to maintain a diverse plant community with a dense rooting system, enabling a greater degree of carbon sequestration in the soil.

According to Schuman et al. (1999), livestock grazing, both heavy and light, resulted in an increase in soil carbon and nitrogen in the top 30 cm of a soil profile after 12 years as compared with an ungrazed control. They attributed these increases to a redistribution of C and N within the plant–soil system, an increase in C and N cycling rates between the system components, and reduced losses of C and N from the plant–soil system. However, in that study the total mass of carbon in the plant–soil system to 60 cm depth was unaffected, suggesting that this form of management simply leads to a redistribution of C in

the soil profile. Bruce et al. (1999) have proposed that, over the next two decades, intensively managed pastures in North America have the potential for further C gains of 0.2 Mg ha^{-1} yr^{-1} through the use of improved grazing regimes, fertilization practices and irrigation management as well as the introduction of more productive species. However, they also suggest that most extensively managed rangelands and long-term (> 50 yr) pasture are probably near equilibrium with respect to carbon and will not be significant sinks without some additional inputs such as fertilizer.

3 Effect of land use change on carbon stocks of temperate grasslands and land use history of Eurasian steppes

3.1 Carbon dynamics associated to land use change

Land use change can cause a change in land cover and an associated change in carbon stocks (Bolin & Sukumar, 2000). The change from one ecosystem to another could occur naturally or be the result of human activity, such as for food or timber production. Each soil has a carrying capacity, i.e an equilibrium carbon content depending on the nature of the vegetation, precipitation and temperature (Gupta and Rao, 1994). The equilibrium carbon stocks is the result of the balance between inflows and outflows to the pool (Fearnside and Barbosa, 1998). The equilibrium between carbon inflows and outflows in soil is disturbed by land use change until a new equilibrium is eventually reached in the new ecosystem. During this process soil may act either as a carbon source or as a carbon sink depending on the ratio between inflows and outflows.

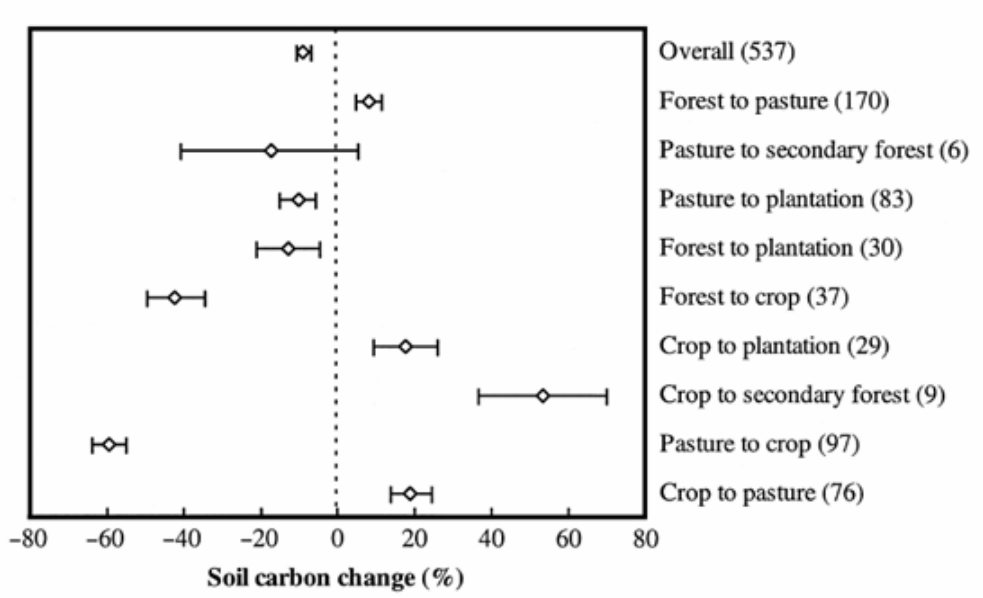

Figure 3.1. Change in soil carbon stock in response to various land use changes (horizontal bars show 95% confidence interval; number of studies are reported in parenthesis) (after Guo & Gifford, 2002)

Guo and Gifford (2002) included in a database 537 observations from 74 publication to analyze the change of soil organic carbon across all land use categories. Results showed that soil carbon stocks significantly increased after the conversion from forest to pasture (+8%), crop to plantation (+18%), crop to secondary forest (+53%), and crop to pasture (+19%) (fig.3.1). Soil carbon

declined after the conversion from pasture to plantation (-10%), forest to plantation (-13%) and particularly from forest and pasture to crop (-42% and -59%, respectively). The highest soil C loss occurred following land use change from pasture to crop. Wherever one of the land use changes decreased soil C (e.g. pasture to crop), the reverse process (e.g. crop to pasture) increased soil carbon, except the change from pasture to secondary forest, that leads either to a gain or loss of carbon.

3.1.1 Conversion from pasture to crop

The factors that show an effect on soil carbon stocks following conversion from pasture to crop are precipitation and age since land use change. The change was always associated to a reduction in soil C stocks by about 50% or more, but the highest carbon loss (-78%) was found in an area with 400-500 mm precipitation compared to lands with 300-400 mm (-54%) and greater than 500 mm (-50%). Also the magnitude of the C loss peaked 30-50 years after conversion at 85% recovering somewhat after.

Stable carbon may play some role in this age effect. The relatively stable part of soil carbon from previous land use (pasture) should be released gradually, but the part from current land use (crop) may be gradually accumulated at a slower rate. Therefore the equilibrium in the new land use could be reached only after 50 years.

3.1.2 Conversion from crop to pasture

The reverse process, the conversion from crop to pasture, significantly sequesters carbon from the atmosphere. Sousanna (2004) defines the kinetics of carbon accumulation following change in land use or in grassland management as:

(i) non linear, since they are more rapid during the first years after adopting a practice that enhances accumulation

(ii) asymmetric, since the accumulation arising from a conversion from arable to grassland use is on average half that of the release induced by conversion from grassland to arable use.

Carbon sequestration after the conversion from crop to pasture varied with soil sampling depth, as the top soil is more active at sequestering carbon for the atmosphere after land use change. However, pasture also caused substantial C accumulation below 100 cm depth: for instance a study of the grassland for a productive portion of U.S. Central Plains (Texas, Kansas, and Nebraska, Gebhart et al. 1994) indicates that SOC may accumulate at an average rate of 110.0 g C m^{-2} y^{-1} in the surface 300 cm after 12 years since agriculture. Carbon accumulation after conversion takes place irrespectively of the climate zone (table 3.1 and 3.3): results from subtropical moist forest zones demonstrate a potential for SOC gains when row crops are replaced with managed pasture

with a mean accumulation rate of 33.2 g C m^{-2} y^{-1} (Lugo et al. 1986); White et al. (1976) found lower values in South Dakota, an average of 21 g C m^{-2} y^{-1}, where the rates show considerable variation among plots with different species of plants established.

Site History	Years since Agriculture	Soil sample Depth (cm)	Average rate of C change (g m^{-2} yr^{-1})	Reference
Cool temperate grassland				
cultivated to perennial grass	12	300	110.0	Gebhart et al. 1994
cultivated to abandoned field	50	10	3.1	Burke et al. 1995
cultivated to seeded grass	6	5	0.0	Robles & Burke 1998
cultivated to improved pasture				White et al. 1976
Russian wildrye	8	7	6.86	
crested wheatgrass	8	7	18.87	
B-I-ALF(full)	8	7	14.01	
B-I-ALF(short)	8	7	34.15	
Subtropical moist forest				
cultivated to pasture				Lugo et al. 1986
Atlantic	37	18	-16.22	
Caonilas	37	18	-48.65	
Culebrinas	37	18	100.0	
Northwest	37	18	8.11	
West	37	18	37.84	
East	37	18	35.14	
Southeast	37	18	10.81	
Southwest	37	18	67.75	
South	37	18	113.51	
Turabo	37	18	24.32	

Table 3.1. Rates of carbon accumulation in soil after pasture establishment in cool temperate grassland and subtropical moist forest zones (modified after Post and Kwon, 2000)

In the shortgrass steppe of Colorado, Burke et al. (1995) found very low rates of SOC accumulation on unimproved abandoned crop fields They report an accumulation rate of 3.1 g C m^{-2} y^{-1} over a 50 year period. Robles and Burke (1998) did not find significant soil carbon gains in soils 6 years following cessation of cultivation in a semiarid grassland (Wyoming). Although there is now plenty of evidence to show that temperate grassland soils can sequester relatively large amounts of C, there is still uncertainty as to how long this can continue and whether there is an upper limit to C storage (Franck, 2002). Estimates of time to saturation range from 10 yr (Janzen et al., 1998) to 100 yr (Potter et al., 1999), but many models of SOC dynamics predict that soil C stocks can, in theory, be increased without limit (Six et al., 2002).

3.2 Land Use Change in arid and semi arid lands of East and Central Asia

Chuluun and Ojima (2002) analyzed the history and land use change of the whole area of arid and semi-arid lands of East and Central Asia, highlighting the ecological impact brought by drastic socio-economical changes.

The arid and semi-arid lands of Asia indeed have been used by nomads for the past several thousand years.

Rangeland ecosystems and pastoral systems co-adapted and co-evolved to increase the land use efficiency and sustainability strategy. Short term seasonal movements and long term migrations in search of better pastures were the main land use strategies enabling people to cope with climate variability in this region.

However, influence from settled societies of Russia and China began to impact the region since 16^{th}-17^{th} centuries. The most dramatic changes in land use and land cover occurred in the 20^{th} century due to political changes in the Soviet Union and China. Between 1700-1980 the total forest and grassland area in Asia decreased by 313 million hectares, the largest decrease in any region of the world (Grubler, 1994). Croplands increased with a maximum during the last 30 years, but UNEP has estimated that 60-70% of the grasslands in China, Mongolia and the Asian part of former USSR are affected by desertification due to overgrazing and overcropping (Graetz, 1994).

Land cover of arid East and Central Asia is dominated by rangelands including grasslands, steppe and desert systems. Changes in land use over the centuries have been defined by the physical climate and pastoral patterns of herding strategies. However recently, the increase in population pressures, political changes, and economic trends have modified the land use characteristics resulting in changes in carbon dynamics within the region.

More than 60% of the land in the five Central Asian countries (Kazakhstan, Uzbekistan, Turkmenistan, Kyrgyzstan and Tajikistan) is rangeland, accounting about 246 Mha (Kharin, 1996). Arable lands are 43 Mha. Out of 400 Mha of the grasslands in China only 224 Mha are usuable.

Currently, Inner Mongolia has about 8 Mha of croplands and 63 Mha of usable rangelands (Enkhee, 2000). Over 80% of land in Mongolia is rangelands and arable lands occupy only about 1% of total agricultural lands (Tserendash, 2000).

Major driving forces for land use change in the ASAL of East and Central Asia were population growth and policy. Total population of the central Asian countries increased from 23 million in 1959 to almost 54 million in 1996 (Kharin , 1999).

	Rangelands[Mha]	Croplands[Mha]	Collectivization	Privatization
Mongolia	123	1.35	late 1950s	early 1990s
China (usable)	224		in 1950s	early 1980s
Inner Mongolia	63	8	in 1950s	early 1980s
Central Asia	246	43	in 1930s	mid 1990s

Table 3.2. Major land use change events in arid and semi arid lands region of the East and Central Asia in the XX century (after Chuluun and Ojima, 2002).

Political changes of the past century have also impact on land use and its intensity in the region. The communist governments in China, Soviet Union and Mongolia forced conversion of some of the most productive grassland into cropland and collectivization programs (table 3.2).

These policies not only reduced the amount of rangeland available for livestock production, but also increased grazing intensity, often on less fertile grazing lands. For example, two million ha of grasslands were converted into cropland in Inner Mongolia during 1958-1976 (Enkhee, 2000) and the total number of grazing animals tripled from 100 million to nearly 340 million in the 1949-1989 period (Chuluun & Ojima, 2002). Land use practices with high mobility, diversity of coping mechanisms and traditional pastoral networks existed in Mongolia before collectivization. The countrywide collectivization of livestock occurred in Mongolia in the late 1950s.

The sedentarization of nomads was perceived as the main idea for rural development. Livestock mobility was reduced and dependence upon cultivated feed over the cold winters was increased with the collectivization of the pastoralists into state farms. Livestock populations increased steadily in the central Asian states during the collective period and, by the close of the Soviet period, they had over 63 million sheep or goats, 18 million cattle and 2 million horses as well as several hundred thousand camels and yaks (Kerven & Lunch, 1999). This increase in livestock numbers and the expansion of cultivation led to rangeland degradation and loss of soil fertility and carbon.Conversion of grasslands into croplands and improper management of these croplands caused large environmental damage, including carbon loss, in this part of the world.

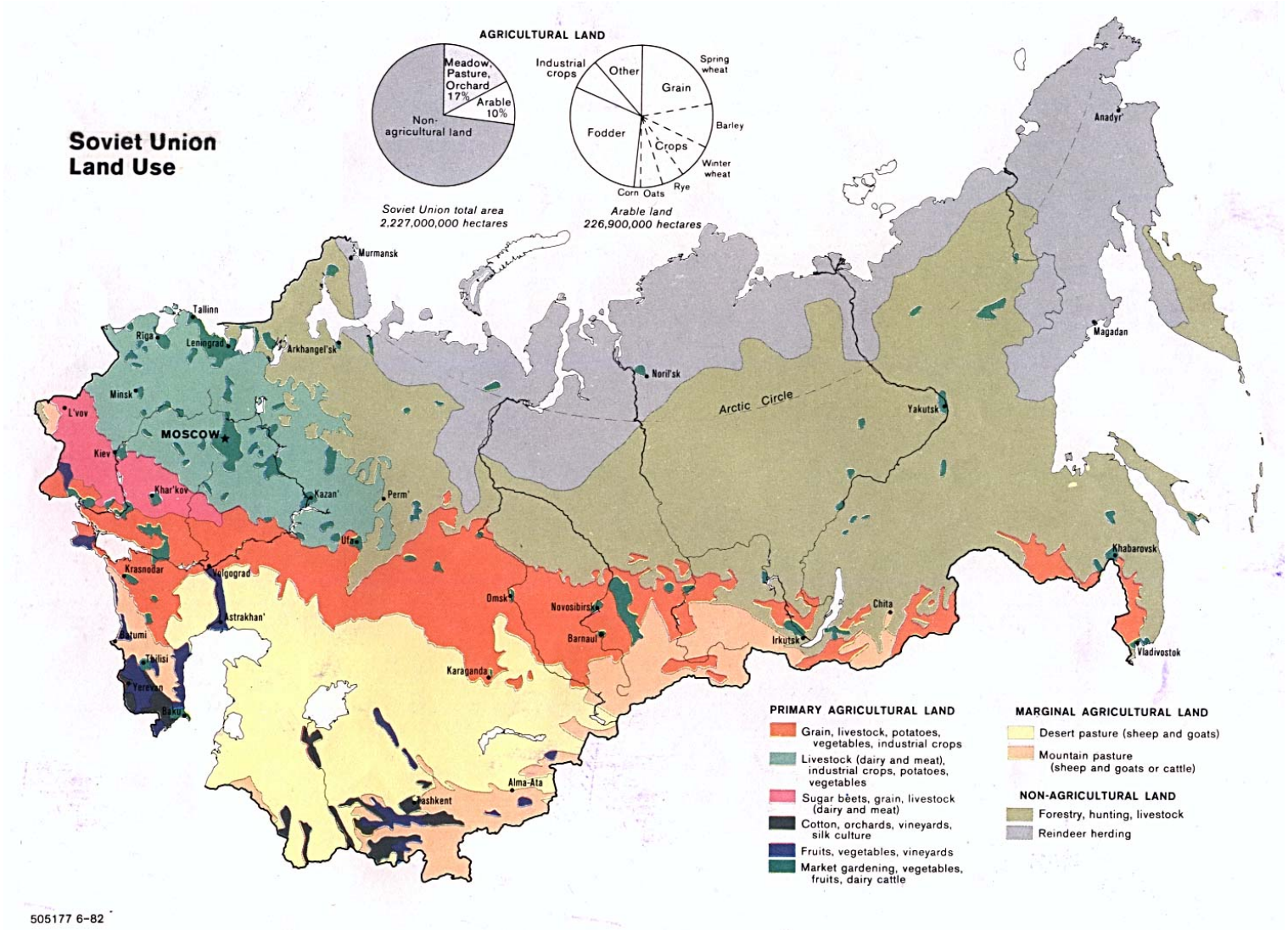

Figure 3.2. Map of Land Use of Soviet Union in 1982: most of steppe territory falls under primary agricultural use. (from Perry Castañeda Library Map Collection-http://www.lib.utexas.edu/maps/commonwealth.html)

The most dramatic environmental change in the Central Asia is the drying up of the Aral Sea caused by withdrawal of water from the Amudarya and the Syrdaria rivers for irrigation. Salinization of soils due to the drop of the Aral Sea level occurred in an area of 4.9 Mha (Kharin,1993). A 30-year study of the carbon balance of the chernozem soils in northern Kazakhstan showed 25%-30% reduction of humus reserves due to cultivation.

Overgrazing is also causing rangeland ecosystem degradation in this part of the world. For example, livestock population in Inner Mongolia was 9.2 million in 1947 (Orenchi, 2000) and reached 62 million by 1998 (Humprey, 1999). However, the total usable pasture decreased from 88 Mha in 1947 to 63 Mha at present (Chen, 1996; Enkhee, 2000). These 63 Mha of natural grassland can feed 44.2 million sheep units, and corn leaves and other fodder can support additional 10.5 million sheep units totaling 54.7 million sheep as maximum capacity. However, at present there are over 85 million sheep units. Grazing pressure has increased for the central and western regions of Mongolia during the recent decade, especially in Arhangai, Bayan-Olgii, Uvs and Hovd aimags by 50%-100% (Tserendash, 2000). Comparative study of culture and environment in Inner Asia show that pasture degradation was associated with loss of mobility in the pastoral systems (Humprey, 1999). Rangeland degradation was the most severe at the research sites from Buyatia and Chita Oblast' (Russia), where sedentarisation level was the highest, compared to other research sites from Mongolia, Tuva (Russia), Inner Mongolia and Xinjiang (China). A simulation study using Century (Chuluun & Ojima, 1999) showed that year-long or summer heavy grazing for 50 years result in the largest loss of total soil carbon relativein comparison to other seasonal grazing scenarios, as for instance, summer heavy grazing that resulted in a 15% soil carbon loss.

3.3 Land Use Change in steppe territory of former Soviet Union and potential of carbon accumulation

Analyzing in more detail the pattern of land use of temperate grassland ecosystems in the former Soviet Union it is possible to distinguish two distinct phases: the expansion of the agricultural land under rates varying according to historical periods of the 19^{th} and 20^{th} century, and the massive abandonment of cultivations since the last 10-15 years.

Conversions of native grasslands into croplands started in the 18^{th} century and progressively increased from 0.21 Mha yr^{-1} up to 1.11 Mha yr^{-1} during the 1930s when the Soviet government introduced collective farming systems (Houghton & Hackler, 2001). However, the most intensive land use change into croplands took place since the 50's (5.71 Mha yr^{-1}) until 1968. Since the second half of the 80's

the reverse process started, and since the beginning of the 90's large areas of croplands were abandoned, after the political breakdown of the Soviet system .

According to the FAO, the area of arable and permanent crops of the C.S.I (former Soviet Union) underwent a reduction of 22.7 Mha in the decade between 1992 and 2003. However there is a weak agreement on the exact area of abandoned land, as emerges from the comparison of different estimates found in literature. For instance, taking into account only the territory of the Russian Federation, Pankova and Navikova (2000) indicate that 34 Mha of arable soil area was abandoned during the period 1990-1995; Kluyev (2001) reports 29 Mha for the period 1990-1999 and on the lowest extreme Romanovskaya (2006) reports 21.6 Mha between 1990 and 2002.

Land-use change type	Years of grassing	Soil type	Soil depth, [cm]	Rate of C accumulation [gC $m^{-2}yr^{-1}$]	Reference
Sown grassland on arable land	18	Gray forest soil	60	161	Larionova et al. 2003
Grassland regrowth on abandoned arable land	47	Soddy-podzolic soil	60	43	Larionova et al. 2003
Sown grassland on eroded arable land	15	Gray forest soil	20	129	Kyrillova, 1999
Sown grassland on non-eroded arable land	15	Gray forest soil	20	47	Kyrillova, 1999
Pasture abandoned to uncut grassland	14	Chernozem	20	128	Afanasyev and Rotova, 1996
Grassland on coal mine spoil	25	Mine tailing	5	98	Titlyanova and Tesarova 1991
Grassland regrowth on coal mine spoil	30	Mine tailing	5	135	Yeterevskaya et al., 1985

Table 3.3. Rates of carbon accumulation in soils of taiga zone of Russia during grassland establishment.

(modified after Larionova et al., 2003).

In any case, given the great extension, the area of abandoned agricultural soils represents a significant potential carbon sink when converted to native vegetation. The magnitude of this potential was assessed by Larionova et al. (2003) using results of carbon accumulation rates in different soil types (chernozems, grey soils, sod-podzolic) reported in table 3.3. Among different soil types, gray forest soils and chernozems are characterised by high productivity in both European Russia and Siberia and their share in the total arable area of Russia comprises about 50%; up to 95% of chernozems and 80% of gray forest soils are used in agriculture and about 40% of area occupied by two soil types are degraded due to wind and water erosion (Dobrovolsky and Urusevskaya, 1984). The share of sandy soddy-podzolic soils in the total arable area of Russia does not exceed 1–2%. Taking into account the relative representativeness of the various soil types, the mean carbon accumulation in Russian soils due to agriculture abandonment was estimated in about 130 g C m^{-2} yr^{-1}. If applied to the area of abandoned land in Russia of 43 Mha, this rate yields a total accumulation of 44 Mt C yr^{-1}. This result is meant to likely represent an upper threshold for carbon sequestration potential in abandoned lands of Russia since it is based on the largest figure of abandoned land available from statistical sources. Moreover in the described approach, it was not taken into account the dependence on the time since land use change of the rate of carbon accumulation, which should be incorporated in the assessment procedure to yield more accurate predictions of the dynamics of C accumulation.

4 Research sites

The research activities of this study were carried out in the steppes of the Republic of Hakasia and in the Republic of Tuva, both part of the Russian Federation, and representative for two distinct areas of the Central Asiatic steppe region in terms of climate and environment.

4.1 Study area in the Republic of Hakasia

The investigated territory is situated in the Iyus-Shira steppe district of the Republic of Hakasia which forms a part of the Minusinsk hollow, covering an area of about 7000 km^2. The physical borders of this steppe area are the Kuznezk Altai and Batenevsk mountain-ridge on the west and south, the reservoir of the river Yenisey on the east and the the administrative border of Hakasia Republic on the north.

The hydrographical network is very poorly developed and represented by the lowest part of the rivers Bieloi Iyus and Chorny Iyus, and by a reach of Chulim river. Nevertheless the district hosts numerous relict lakes, (Shira, Bele, Itkul, Tus, Firkal, Shunet, etc.), some of which salted, formerly being included in a larger basin.

Zonal types of steppes in the Iyus-Shira region are true steppes, prevailing in flat areas or tall bunchgrass steppes, most often growing on steep south facing slopes, with *Stipa krylovii* Roschev. and *Helictotrichum desertorum* Less. as dominant species.

4.1.1 Research sites within the collective farm (sovkoz) of Solionoziornoe

4.1.1.1 Land use

The collective farm, indicated by the Russian word "*sovkoz*", of Solionoziornoe was established in the late 1958 with a total area of 8500 ha, in agreement with the program of land collectivization launched few years before by N. Kruscev, president of USSR at that time. Since then the agricultural activities started including cultivations of wheat (*Triticum aestivum* L.), barley (*Hordeum vulgare* L..), and forage grasses (*Melilotus, Megicago, Bromus*, the main), while animal breeding (cattle and sheep) brought to the use of natural grasslands as hayfields or pastures for grazing.

The economic crisis burst in 1991 due to the collapse of the socialist regime of former USSR, leading to a massive cessation of activities in the agricultural sector, invested the *sovkoz* of Solionoziornoe in 1992 and since then croplands were progressively set aside especially during the period 1992-1996.

The picture of situation at the year 2004 was made up of residual 4200 ha of croplands, divided into 2000 ha under cereals, 200 ha under forage and 2000 ha fallow, while the rest of the previously cultivated area, represented by 2000 ha (46% of sovhoz's area) had been already set-aside.

After the set-aside of croplands the encroachment by weeds starts and it constitutes the first stage of a secondary ecological succession that, through several stages of recovering grassland, ends with the restoration of the climax vegetation of steppes phytocenosis. This process should come to completion in a time span of 15 years, according to the study Cherepnin (1953), who described the ecological succession dynamics after the abandonment of croplands in the southern part of Krasnoyarsk province (fig.4.1), an area in ecological continuity with the republic of Hakasia. However, during a survey of the first cropfields that were set-aside (since 11 years), we observed only a modest presence of the species that are typical for steppe's vegetation, deducing that for our study area the climax stage will be reached in a longer time.

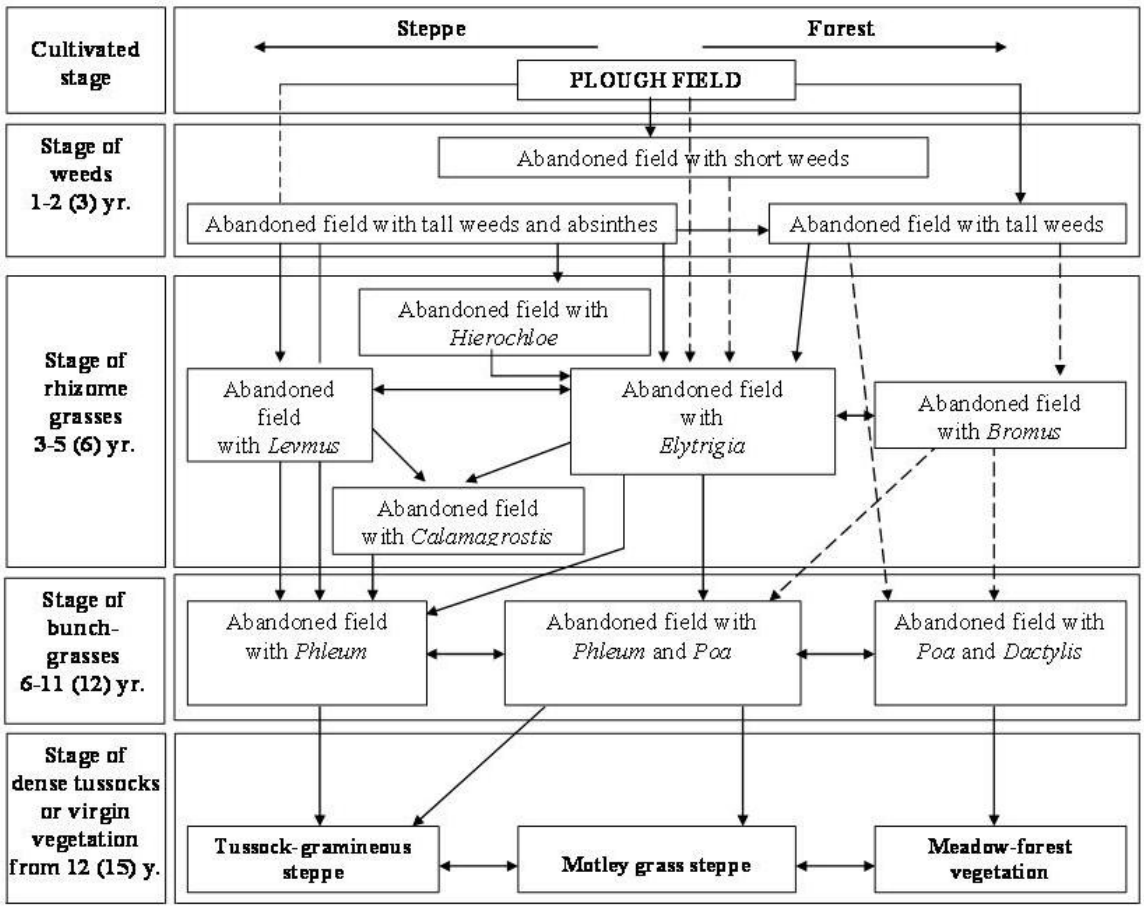

Figure 4.1. Scheme of ecological secondary succession on abandoned fields and restoration of climax in southern Krasnoyarsk region. (modified after Cherepnin, 1953).

4.1.1.2 Soil

The soil of the area is classified as a calcic chernozem (second level legend FAO-Unesco 1990) with fine surface texture and a proportion of clay ranging between 35% and 60% (Stolbovoi, 2000).

4.1.1.3 Climate

The climate at the research sites, according to the Koppen climate classification system (Thornthwaite, 1933), is semi-arid cool (BSk type). Climatic statistics determined on the base of archive data of Shira, a small town located approximately 30 km south of the research area, for the period 1942-1995, reveal a mean annual temperature of 0.4 °C, a seasonal temperature trend characterized by great continentality (mean temperature of January: -17 °C; mean temperature of July: +18 °C) and annual precipitation of 304 mm out of which 245 mm distributed during summer season from May to September (fig.4.2).

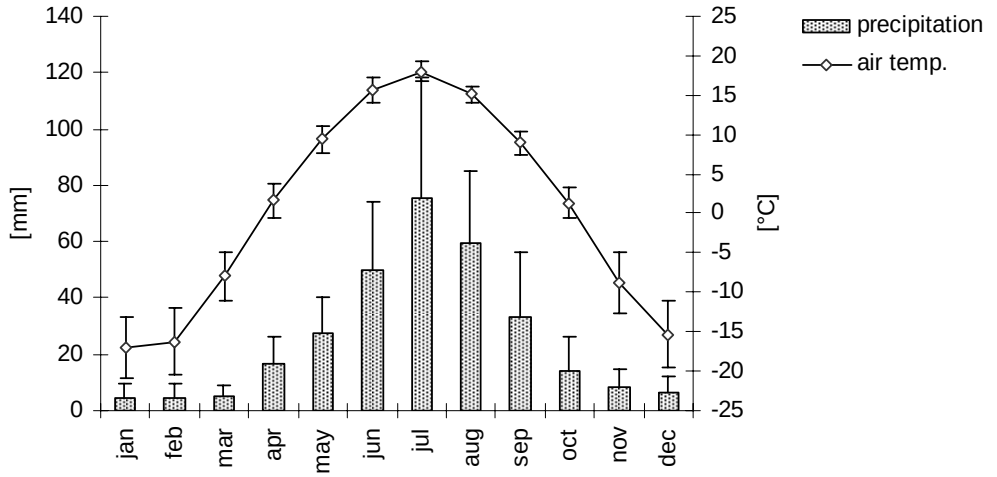

Figure 4.2. Monthly mean temperature and precipitation at Shira (Republic of Hakasia) determined on the base of archive meteorological data for the period 1942-1995.(error bars indicate standard deviation)

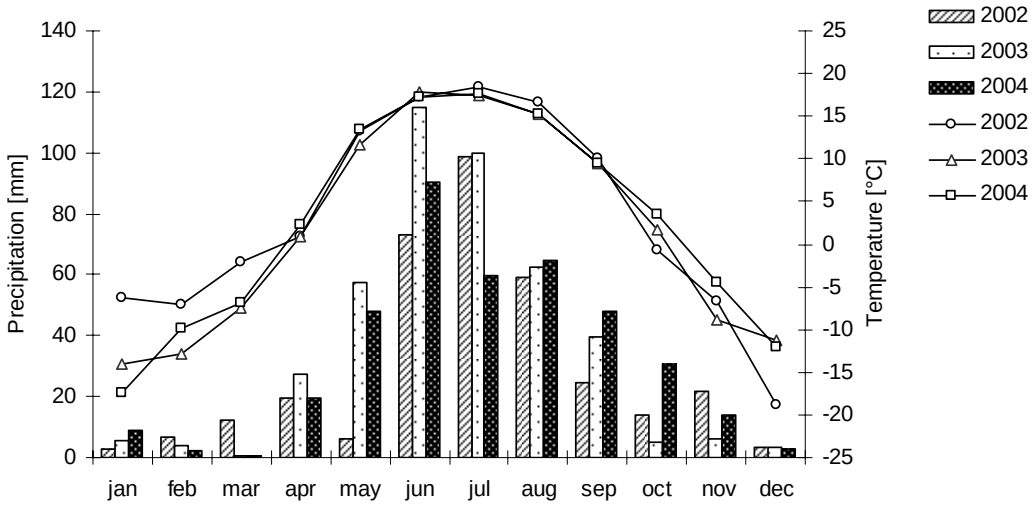

Figure 4.3. Mean monthly air temperature (lines) and precipitation (vertical bars) for the years 2002, 2003 and 2004 recorded at the site of Hak1. Missing data for winter months when the micrometeorological station was not operative, where filled with meteo data from the station of Shira.

In the years when the field campaigns were carried out (2002, 2003, 2004), the average annual temperature was 2.9, 1.6 and 2.3 °C respectively and annual precipitation was 341, 425, 388 mm respectively. In particular the year 2002 was characterized by temperatures from January to March above the average and by little precipitation in late spring-early summer (May-June), with a remarkably dry month of May (5.9 mm). The year 2003 showed, in contrast with the year 2002, a very rainy period at the beginning of the growing season (May: 57.3mm; June 115 mm) but a regular temperature records along the year. In the year 2004 it was recorded a dry month of July (60 mm) with only 2/3 of rain compared to previous years and a warmer temperature in September and October (fig.4.3).

4.1.1.4 Evidence of climate warming

The release in 2001 of the IPCC Third Assessment Report on Climate Change highlighted the increase of the global average surface temperature by 0.6±0.2 °C since the late 19th century, evidencing also the occurrence of the largest increases in temperature over the mid and high latitudes of the continents in the Northern Hemisphere (fig.4.4) during the most recent period of global warming (1976 to 1999).

The climatic records from 1942 to 1995 of Shira (Reference book on climate of the USSR. Gidrometeoizdat, Leningrad, issue 21, parts II, III, IV) are clearly representative for the climate warming in the Siberian region highlighted by IPCC (fig. 4.5), showing an increase in the average annual temperature of 0.3 °C per decade that led to warming effect over the considered period of +1.65 °C. The increase of temperatures was not evenly distributed over all the seasons but it was restricted to winter months from November to March, affecting particularly the temperature record of November, December and January, for which we observe a warming trend of 0.81, 0.81 and 0.85 °C/decade respectively (fig.4.6). On the contrary we do not observe any significant change in the precipitation regime during the examined set of years, either for the total annual precipitation and for the cumulated rain, falling during the vegetative season from May to September.

Future projections of globally averaged surface temperature, based on a full range of 35 scenarios from SRES (Special Report on Emission Scenarios) coupled with a number of climate models, reveal an increase of 1.4 to 5.8 °C over the period 1990 to 2100. It is very likely that nearly all land areas will warm more rapidly than the global average, particularly those at northern high latitudes in the cold season. Results from recent global circulation models (AOGCM) simulations forced with emissions scenarios accounting for different socio-economic paths of development, indicate that in winter the warming for all high-latitude northern regions exceeds the global mean warming in each model by more than 40% (1.3 to 6.3 °C for the range of models and scenarios considered).

Globally averaged water vapour, evaporation and precipitation are projected to increase. At the regional scale both increases and decreases in precipitation are seen. Results from recent AOGCM

simulations forced with SRES A2 and B2 emissions scenarios indicate that it is likely for precipitation to increase in both summer and winter over high-latitude regions.

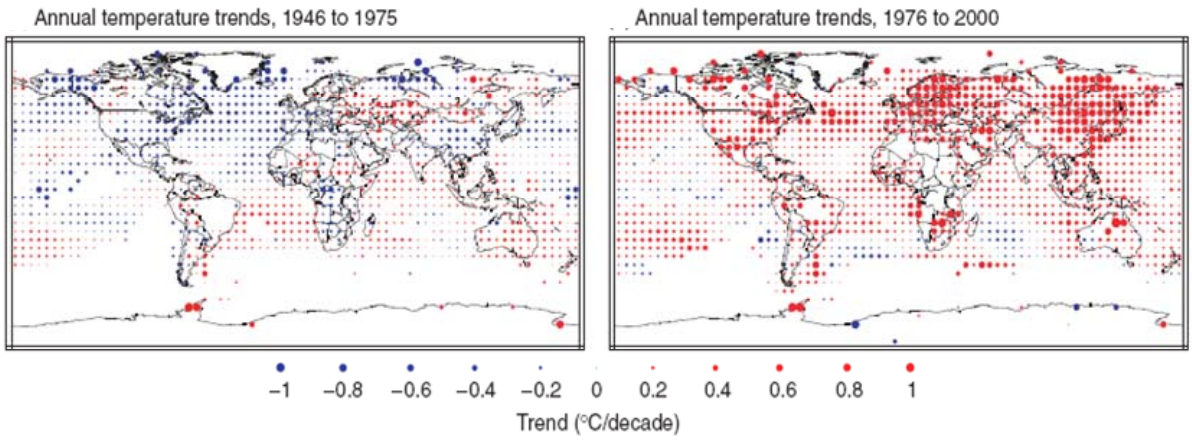

Figure 4.4. Annual temperature trends for the periods 1946 to 1975 and 1976 to 1999 respectively. Trends are represented by the area of the circle with red representing increases, blue representing decreases, and green little or no change. Trends were calculated from annually averaged gridded anomalies with the requirement that the calculation of annual anomalies include a minimum of 10 months of data. (IPCC, 2001).

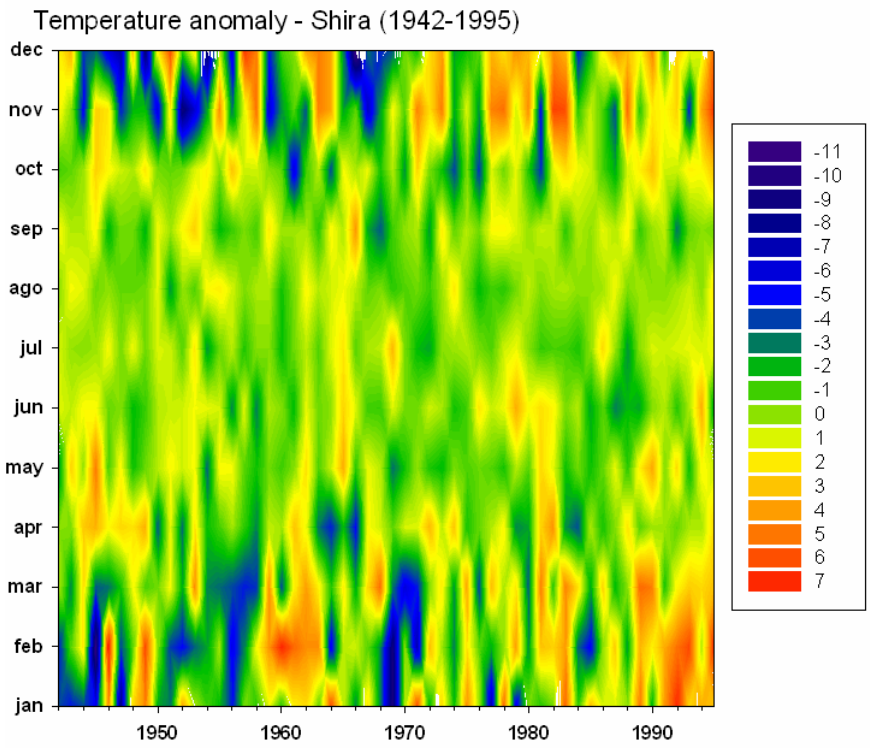

Figure 4.5. Monthly temperature anomalies [°C] in respect with the mean of the period 1942-1995 recorded at the meteorological station of Shira (Republic of Hakasia).

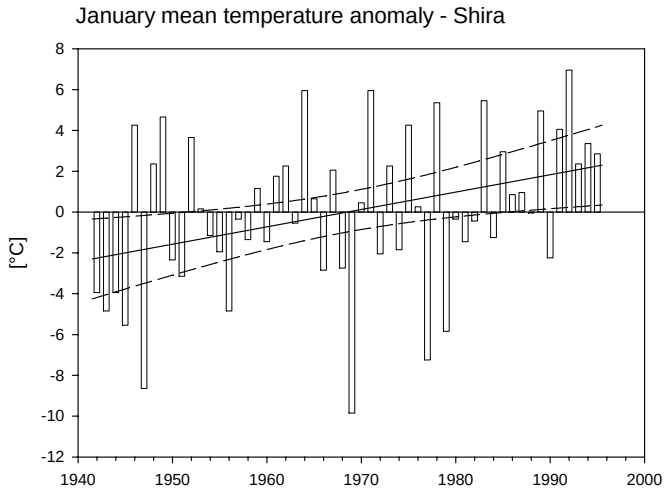

Figure 4.6.Anomalies in mean temperature of January in respect with the mean of the period 1942-1995 at Shira (Republic of Hakasia) from 1942 to 1995. Linear regression(solid line) with 95% confidence intervals (dashed lines:)ΔT[°C/yr]=0.0851±0.0316;P=0.009; R=0.35.

4.1.2 Sites equipped with micrometeorological (eddy covariance) systems

The selected sites for the establishment of eddy covariance towers and experimental areas were a natural true steppe (Hak1) and two former croplands abandoned respectively in 1999 (Hak2) and in 1994 (Hak3).

The classification of the vegetation at the sites of Hak2 and Hak3, described hereafter, was performed contemporarily to eddy covariance measurements, in 2002 and 2004 and it thus depicts the botanical features of the successional stages after 5 and 10 years since land use change. The botanical description at Hak 1 was carried out during summer 2004.

Hak1 (54°43.4'N; 89°59.5'E; 460 m a.s.l.)

True bunchgrass steppe.

This steppe site was grazed until 2001, after that the livestock , mostly flocks of sheep, was kept out of the area.

The vegetation cover reaches 60-70% on average and the grass stand is structured in multiple layers (dominant, middle lower), of which the dominant reaches an height of 0.4-0.8 m depending on seasonal productivity. The main species found in the dominant layer are *Festuca valesiaca* Schleicher ex Gaudin*, Koeleria cristata* (L.) Pers.*, Stipa krylovii* Roschev.*, Cleistogenes squarrosa* Trin.*, Poa botryoides* Trin. ex Griseb.. Plant composition counts 102 species (26 families). The most numerous families are in order of importance: *Asteraceae* (21 species), *Poaceae* (16 species), *Lamiaceae* (6 species), *Fabaceae* (6 species) and *Brassicaceae* (6 species).

The monitoring of vegetation in the year 2004 recorded a gradually increasing number of species along with the proceeding growing season, until it stabilized around 22 species/m^2 at the end of June.

The species with the highest frequency-abundance index were *Stipa krylovii* Roschev. (100%), *Poa botryoides* Trin. ex Griseb.(95%), *Thalictrum foetidum* (L.) (95%), *Thymus serpyllum* L. (90%), *Campanula sibirica* L. (85%), *Gentiana squarrosa* Ledeb.(85%).

Perennial grasses prevail and represent 76%, while other life forms are present in similar shares: annual grasses (8%), biennial grasses (7%) and semi dwarf-shrubs (9%).

The main ecological groups are represented by xerophytes (32%), mesoxerophytes (25%), xeropetrophytes (20%) and mesophyte (17%). The grass community is typical for natural steppes and its composition it is not influenced by previous grazing, due to the low density of livestock.

Hak2 (54.46.4'N, 89.57.4'E; 440 m a.s.l.)

Old agricultural field, uncultivated since 1999.

Vegetation was represented by an early successional stage with an equal presence of *Artemisia scoparia* Waldst. & Kit., *A. sieversiana* Ehrh. ex Willd., *A. jacutica* Drob., and the participation of a significant admixture of *Chamaerhodos erecta* (L.) Bunge., *Potentilla tanacetifolia* Willd. ex Schlecht., *Veronica incana* L., *Aster biennis* Greene, *Convolvulus fischerianum* V.Petrov., *Potentilla bifurca* L., *Stipa sibirica* (L.) Lam., *Leymus ramosus* (Trin.) Tzelev, to the floral composition. A number of weeds such as *Polygonum convolvulus* L., *Cirsium setosum* (Willd.) Bess. ex Bieb, *Cannabis ruderalis* Janisch., *Taraxacum sp., Salsola colina* Pall., *Urtica cannabina* L., *Lappula sp*. completes the composition.

Vegetation cover was homogeneous, on average reached about 40%, and the grass stand height did not overcome 0.6 m.

These steppe species were found in good state, not oppressed, normally following all phenological phases. Comparison to other neighboring fallow lands showed the same successional stage dominated by Artemisia spp. with significant but temporal participation of grasses (Agropyron repens L., Setaria viridis (L.) Beauv.) or typical weeds (Chenopodium album L., Cannabis ruderalis Janisch.).

Hak3 (54°42.2'N; 90°04.6'E; 401m a.s.l.)

Old agricultural field, abandoned in 1994.

Plant composition counts 97 species (29 families). The most numerous families are *Asteraceae* (22 species), *Fabaceae* (12 species) and *Poaceae* (12 species). The main species in the dominant layer are *Elytrigia repens* (L.) Desv., *Artemisia jacutica* Drob., *Artemisia scoparia* Walldst. & Kit.. The species found with the highest frequency are *Plantago media* L., *Taraxacum officinale* Weber, *Elytrigia repens* (L.) Desv., *Artemisia scoparia* Walldst. & Kit., *Convolvulus chinensis* Ker-Gawler Dahuria. Vegetation cover reached 60-70% and the maximum height of the canopy is 0.7 m at the end of summer. Perennial grasses prevail representing 73%, while other life forms are present in similar shares: annual grasses (16%), biennial grasses (7%) and semi dwarf-shrubs (4%).

The main ecological groups are represented by mesoxerophytes (35%), mesophytes (32%), xerophytes (22%) and xeropetrophytes (6%). Density of species is 11 /m^2, twice less than in natural steppe. The spatial distribution of the vegetation over this abandoned field, reflects the alternation of former fields sectors (100-120 meters wide) and border stripes between fields (5-7 meters wide): on the first *Elytrigia* prevails, while on the latter *Artemisia sp.* is mostly spread.

4.2 Study area in the Republic of Tuva

4.2.1 The Ubs-Nur Hollow and the Ubsunurskaya Kotlvina Biosphere Reserve

Ubsu-Nur is a mountain basin straddling the border between Mongolia and the Republic of Tuva in the Russian Federation. It stretches over 600 km from east to west, and 160 km from north to south; from 3000 meter high snow-capped peaks to the salty Ubs-Nur lake at about 1,000 meters above sea level, into which the entire depression drains. The more mountainous 20% lies within Tuva's territory, while the remaining 80%, composed primarily of steppe, desert-steppe and desert, lies within Mongolia.

The Ubsunorskaya Kotlavina is a cluster biosphere reserve consisting of five distinct units, covering a total of 284,300 hectares next to the Mongolian border. It has similar ecological characteristics to the Ubs-Nur Basin Biosphere Reserve in Mongolia but without the large lake: wetlands, large sand massifs, scattered dry steppe, rocky mountains, high altitude forests, tundra and alpine meadows.

Local communities (about 3,000 people in the biosphere reserve in 1997) are essentially nomadic and live from cattle breeding. The area has been inhabited by pastoral communities for the last two and a half millennia, as documented by burial mounds and rock paintings depicting the same animals as found today. The biosphere reserve contains one of the study sites of the International Geosphere Biosphere Programme for global change research.

Site of Yamaligh (Republic of Tuva) (50° 13.3' N; 94° 44.7' E; elevation: 1170 m a.s.l)

In July 2003 and August 2004, two research campaigns, were carried out at the site of Yamaligh, located about 30 km west from the village of Erzin, within a cluster of the Ubs-Nur Hollow Reserve.

The climate at the site of Yamaligh, according to the Koppen climate classification system (Thornthwaite, 1933), is semi-arid cool (BSk). Mean annual temperature is -5.7 °C, mean temperature of January and July is -31.5 °C and 17.7 °C respectively and annual precipitation ranges between 180 and 290 mm. The meteorological records of the year 2003 report a mean annual temperature of -2.92 °C and a precipitation of 226 mm (fig.4.7).

Climatic records in the last decades show a positive trend monthly mean air temperature anomalies increasing by 0.171 °C per year since 1985 (standard error: 0.04 °C) (fig.4.8); in comparison, the

global average land surface-air temperature increase since 1985 was around 0.03 $1Cyr^{-1}$ (Folland & Karl, 2001).

The site selected for the set-up of the eddy covariance station was a dry natural true steppe used as a pasture, however the vegetation community did not show signs of degradation due to overgrazing.

Vegetation cover was about 50%. The vegetation was mainly composed of *Stipa krylovii* Roschev., *Caragana pygmaea* L., which together formed 80% of the vegetation cover, *Kochia prostrata* L., *Artemisia frigida* Willd., and *Cleistogenes squarrosa* Trin.. (Kyrgys C., pers.com.). Soil type is kastanozem (Stebayev, 1993; Stolbovoii, 2000).

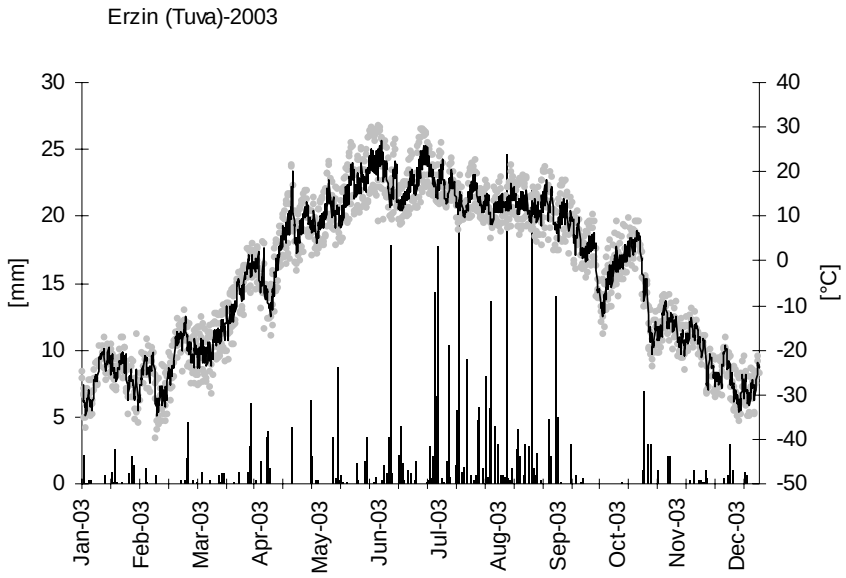

Figure 4.7. Air temperature (grey dots) measured at 6 hours time intervals (0:00, 6:00, 12:00, 18:00), trend of daily mean air temperature (black line) and daily precipitation (vertical bars) of Erzin meteo station (Republic of Tuva, 50°11.50' N, 95°10.90 E, 1114m a.s.l) in the year 2003.

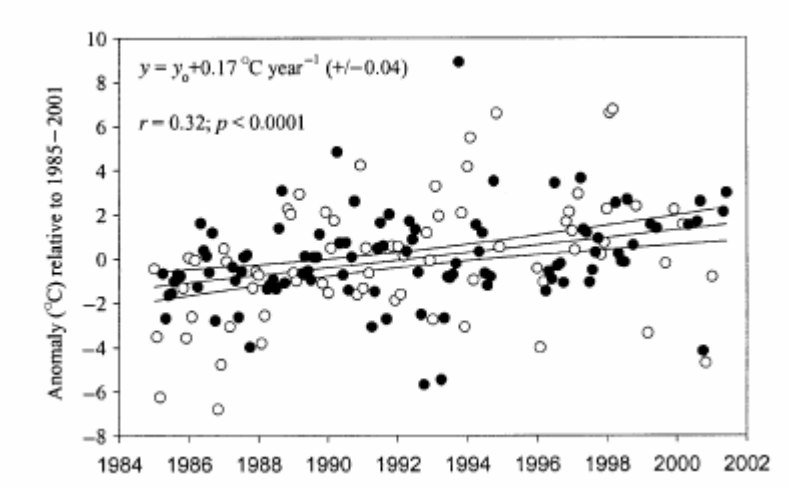

Figure 4.8. Monthly anomalies in mean air temperature at Erzin (50°11.50' N, 95°10.90 E, 1114m a.s.l.) relative to 1985–2001 averages. Black symbols represent summer month (April–October), white symbols represent winter months (November–March). The linear regression through all data, 95% confidence intervals and function are shown in the plot (after Conen at al., 2003).

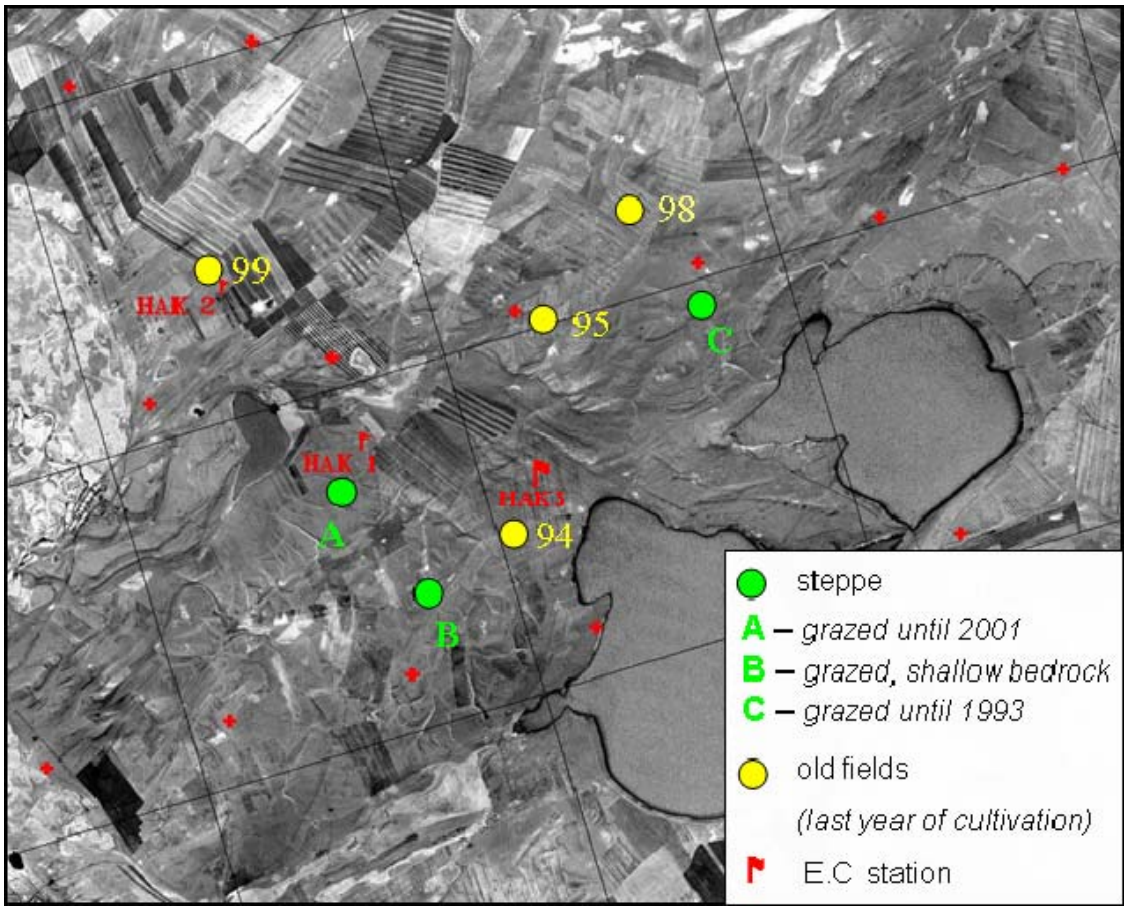

Figure 4.9. Satellite map of the study area in Hakasia centred on the sovkoz of Solionoziornoe. The steppe and old field sites surveyed for the determination of carbon stocks (see chapter 5) are marked with a circle. The position of the micrometeorological stations (eddy covariance) is marked with a red flag. Two of them (Hak1 and Hak2) coincide with the sites "steppe A" and "old field 99" respectively.

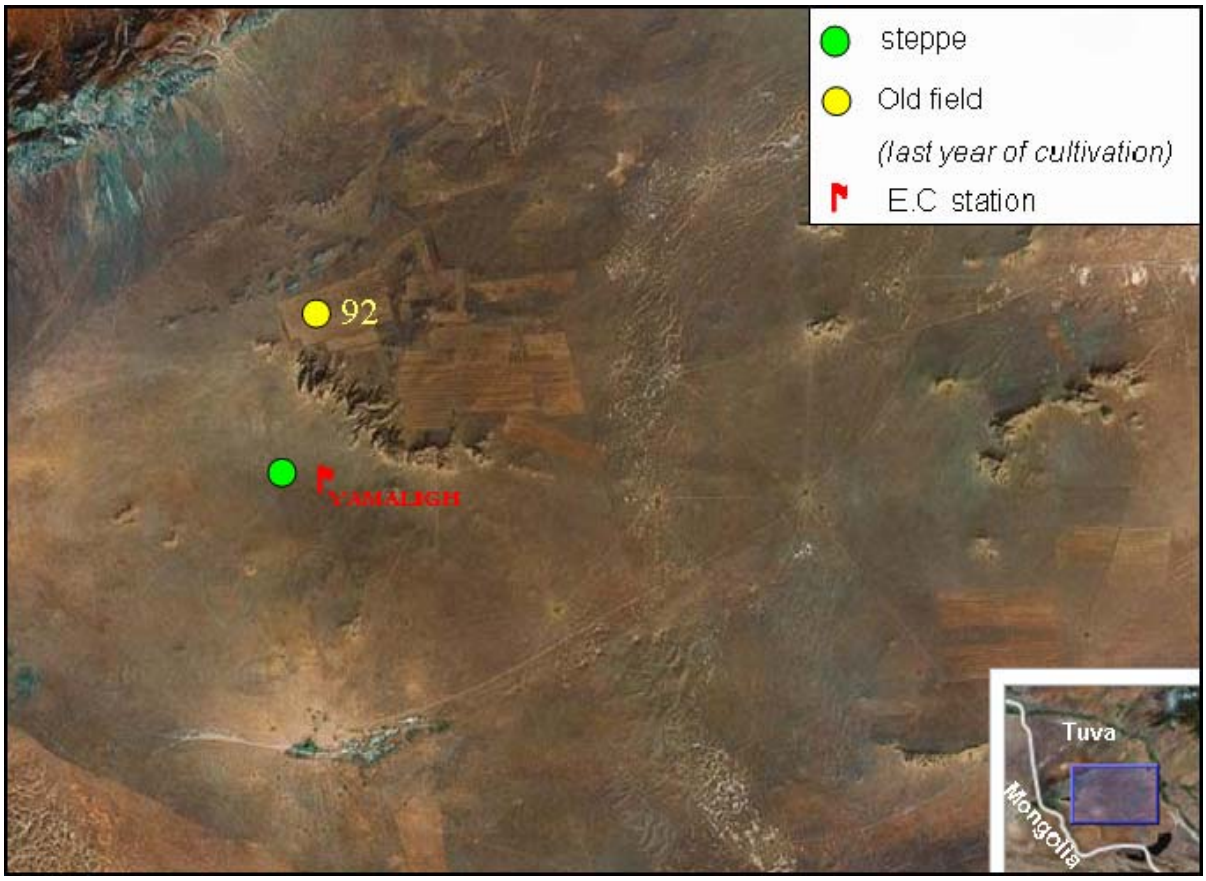

Figure 4.10. Satellite image of the study area of Tuva centred on the area of the Yamaligh cluster of the Ubs-Nur Biospshere Reserve. The steppe and old field sites surveyed for the determination of carbon stocks (see chapter 5) are marked with a circle. The position of the micrometeorological station (eddy covariance), operative during the second ten days of July 2003, is marked with a red flag.

5 Carbon stocks and distribution into pools

5.1 Introduction

In grassland ecosystems the carbon pools include the following: (i) the aboveground biomass, including live biomass and dead standing biomass, (ii) the litter represented by dead plant material lying on the ground, (iii) the belowground biomass, comprehensive of live and dead roots (belowground litter), and (iv) the soil organic matter, defined as carbon and associated nutrients entrained in the soil mineral horizons in forms no longer identifiable as plant residues.

The determination of the stock of carbon of an ecosystem is a key issue to understand its carbon storage capacity, to individuate the nature of sequestered carbon as long term or transient depending on the pool in which it is incorporated and, known the typical turnover rates of the pools, to determine the exchanges of carbon within the pools (i.e. carbon inputs into the soil due to root turnover) and the rates of carbon exchange between the ecosystem and the atmosphere.

In the particular case of steppes that were converted to croplands, the determination of the soil carbon stock may provide the quantitative effect of land use and management on the levels of carbon in respect with the soil carbon stock before the beginning of cultivations. This reference stock can be obtained by quantifying the carbon in soils of steppe ecosystems, located adjacently or at least in the same area of croplands, that on the contrary never experienced any disturbance linked to agricultural activities.

In early August 2004 a survey aimed at quantifying the carbon stocks and their distribution in the ecosystems compartments was carried out in several old agricultural fields and steppes located either in Hakasia and in Tuva. The choice of such time of the year was justified by the intention to sample the biomass once it reached its peak.

The selected sites in Hakasia were 3 natural steppes and 4 old agricultural fields situated within the boundary of the collective farm area of Solionoziornoe. The natural steppes (A,B,C) differed by land management history and physical features affecting their productivity. Site A, coinciding with the flux monitoring site of Hak 1, was grazed until 2001; site B located on a top of a hill was characterized by a shallow soil profile with the bedrock in some points not deeper than 30 cm, and it was ususally grazed; site C was no longer used as a pasture after 1993. All these sites were representative for the three main extensive areas of natural steppe study boundary.

The old fields differed by the year when land use change occurred, being 1994 for the oldest, (coinciding with the micrometeorological site of Hak 3), 1995 and 1998 for the other two. The site of Hak 2, an old field abandoned in 1999, was also included in the analysis, relying upon data collected in 2003, at the same time of the year.

The sites in Tuva were a true steppe located in Yamaligh, correspondening to the flux monitoring site chosen for the campaign of 2003, and an old agricultural field abandoned in 1992 situated contiguously to the steppe area.

The scope of the study was to characterize:

1. the carbon stocks of sites with different land use history.
2. the distribution of the carbon stocks into the pools of aboveground biomass, belowground biomass and soil organic matter.
3. the changes in the relative importance of carbon pools along the successional stages of recovering grassland.
4. The differences in the patterns of allocation carbon in respect with climatic/ecological conditions.

5.2 Materials and methods

5.2.1 Definition of pools

All the plant matter collected aboveground (live biomass, dead biomass, litter) was merged into a single group that is treated as a whole aboveground biomass pool. The belowground biomass pool is composed of roots biomass which was not sorted into live and dead.

5.2.2 Sampling design

Generally samples of biomass and soil were collected in each site over a number of 10 plots aligned along a randomly determined direction and spaced out systematically of 100 m. An exception was made for the sites of "steppe A" (Hak1), and "old field 94" (Hak3), and "old field 99" (Hak2) where the harvesting of biomass was performed according to a protocol of periodic samplings aimed at net primary productivity assessment, with a number of 20 samples collected over plots randomly located within the footprint of the flux tower. Specifically for these sites samples of biomass were collected within an area encompassing approximately a circle with a radius of 500 m, while soil samples for the determination of soil carbon stock were collected following the general protocol exposed above.

5.2.3 Aboveground biomass

All aboveground vegetation contained in square plots of 0.25 m^2 (0.5x0.5 m^2) was clipped at ground level and collected together with the litter. The matter of each sample was dried in oven at 70 °C in order to reach dry weight, determined subsequently by electronic scale. The amount of aboveground matter of the plots was converted into tonnes of dry matter per unit area [t d.m. ha^{-1}], applying the following:

$$AGb = \frac{AGb_{plot}}{A_{plot}} \cdot 10^{-2} \qquad \textit{(Equation 5.1)}$$

where AGb= aboveground biomass per unit of area [t d.m. /ha]; AGb_{plot}= aboveground biomass of the plot [g]; A_{plot}= area of the sampling plot [m^2];10^{-2}= scaling factor from [g d.m. /m^2] to [t d.m. /ha].

The carbon content of biomass was derived using a default conversion factor of 0.45 (IPCC, 2003).

5.2.4 Belowground biomass

In the middle of each harvested plot, a core of soil up to the depth of 30 cm was extracted. The depth of the core was set because of the largest proportion of roots, at least 80%, being indeed present in the soil layers above that value.

Roots and particulate organic matter were separated from the soil removing the larger roots by tweezers, the rest being washed in water to retrieve the floating fragments of roots and dead organic matter sieving them over multiple layers of 1 mm sieves.

All the collected matter was dried in a stove at 70 °C until completely dehydrated and weighed on an electronic scale; biomass was expressed as the weight of dry matter per unit area [t d.m. ha^{-1}] as:

$$BGb = \frac{BGb_{plot}}{\pi \cdot r^2} \cdot 10^{-2} \qquad \textit{(Equation 5.2)}$$

where BGb= belowground biomass per unit of area [tonne/ha]; r= radius of the core [m]; π= 3.14; 10^{-2}= scaling factor from [g d.m./m^2] to[t d.m./ha].

The carbon content of biomass was derived using a default conversion factor of 0.45 (IPCC, 2003).

5.2.5 Soil organic matter

In each plot a soil core was extracted and divided into two sub-samples: one for columns of soil between 0-5 cm of depth and another for the depth 5-30. All the sub-samples collected at each site were then mixed and homogenized to make one composite sample for each depth. To estimate the soil carbon stock, additional two samples were collected at each site for bulk density measurements at each depth.

Soil analyses were carried out at the University of South Boemia - Ceske Budejovice in Czech Republic by Dr. H. Santruckova applying the dry combustion method with a Carlo Erba elemental analyzer to quantify the carbon and nitrogen content. Because the dry combustion method includes

carbonates, samples were pre-treated with a solution of chloridric acid (HCl) at 20% to remove inorganic carbon.

The stock of soil organic carbon (SOC) per hectare [tC/ha] was calculated according to:

$$SOC = \sum_i [SOC]_i \cdot \rho_i \cdot h_i \cdot 10^{-1} \qquad \textit{(Equation 5.3)}$$

where $[SOC]_i$= concentration of soil organic carbon in a given soil mass of the layer i [%], ρ_i= soil bulk density of the layer i [kg m^{-3}]; h_i= thickness of soil layer *i*

The stock of soil total nitrogen was calculated accordingly, replacing in the formula the $[SOC]_i$ with $[N]_i$ the concentration of soil nitrogen per unit of soil mass of the layer *i*.

5.2.6 Statistical analysis

Differences in results of biomass stocks within and between the two groups of sites (steppes and old agricultural fields) were tested by one-way ANOVA and in case of significant differences found ($P<0.05$), the Tukey-Kramer multiple comparison test was performed. The assumptions that data are sampled from populations with the same standard deviation and that follow Gaussian distribution, both required for the applicability of ANOVA, were tested beforehand by the methods of Bartlett and Kolmogorov-Smirnov respectively. Results of biomass, soil organic carbon and total carbon stock from sites of Hakasia were analyzed by pooling them into two categories of steppes and old fields and testing the differences by unpaired t-test selecting a two tailed P value at 95% confidence level. In order to test differences in results of the sites of Tuva, an unpaired t-test with the same threshold as above was applied.

5.3 Results

5.3.1 Aboveground and belowground biomass

5.3.1.1 Hakasia

The stocks of total biomass in the steppe sites of Hakasia (table 5.1) ranged between a minimum of 17.08±2.34 t d.m/ha (mean±standard error) in steppe site B up to 33.19±2.34 t d.m/ha of site C, whereas the steppe site A (Hak 1) is collocated in the middle with 23.46±2.68 t d.m/ha. The total biomass stocks resulted significantly different among sites after ANOVA ($P<0.001$); such difference is explained by the amount of belowground biomass varying noticeably among sites ($P<0.001$), ranking the sites in the same order and being 31.47±2.57 t d.m/ha for steppe site B, 21.88±1.53 t d.m/ha for steppe site A (Hak1) and 15.14±2.40 t d.m/ha for steppe site B. On the contrary no significant differences arouse from the stock of aboveground biomass ($P<0.45$), that

was higher at steppe site B (1.85±0.23 t d.m/ha), intermediate at steppe site C (1.72±0.17 t d.m/ha) and lowest at steppe site A (Hak1) (1.60±0.97 t d.m/ha).

The results are in good agreement with the typical values of biomass stocks for steppes of Hakasia reported by Titlianova (2003), who found a total biomass of 32.15 t.d.m./ha for ungrazed steppes, a range of 18-26 t d.m./ha for steppes on transitional part of slopes (case of site A- Hak1) and a range of 11.6-21.5 t d.m./ha for steppes growing over flattened tops of the hills (case of site B).

	Steppe site			ANOVA
	A	B	C	
	[t d.m ha^{-1}]	[t d.m ha^{-1}]	[t d.m ha^{-1}]	
AG	1.60±0.08	1.99±0.24	1.72±0.18	n.s
BG	21.88±1.50 a	15.08±2.40 a	31.47±2.58 b	P<0.0001
Total	23.48±1.66 a	17.08±2.35 a	33.19±2.68 b	P<0.0001

Table 5.1. Aboveground (AG), belowground (BG) and total biomass stocks of natural steppe sites of Hakasia expressed in tonnes of dry matter per hectare (mean ± standard error; letters denote statistical difference at 95% confidence level). Site A - grazed until 2001, site B - grazed on hilltop, site C - ungrazed since 1993.

	Site				
	Old field 1999 –Hak2	Old field 1998	Old field 1995	Old field 1994-Hak3	ANOVA
	[t d.m ha^{-1}]	[t d.m ha^{-1}]	[t d.m ha^{-1}]	[t d.m ha^{-1}]	
AG	4.20±0.26 b	4.25±0.22 b	2.75±0.28 a	2.45±0.19 a	P<0.0001
BG	9.80±0.62 ab	5.88±0.99 a	8.81±0.97 a	13.74±0.64 b	P<0.0001
Total	14.00±0.99 b	10.12±1.09 a	11.56±1.03 a	16.20±1.15 b	P<0.0001
Years since Land Use Change	5	6	9	10	

Table 5.2. Aboveground (AG), belowground (BG) and total biomass stocks of former agricultural fields of Hakasia expressed in tonnes of dry matter per hectare (mean ± standard error; letters denote statistical difference at 95% confidence level). Site "old field 1999" coincides with the Hak2 micrometeorological station of and the site "old field 1994"with the Hak3 station.

The stocks of total biomass in the old fields of Hakasia (table 5.2) ranged between 10.12±1.09 to 16.29±1.51 t d.m/ha showing highly significant differences among sites (P<0.0001) although a pattern of change in respect with the time since the field abandonment is not evident. However, a more careful look at the result could individuate in the large quantity of biomass of the Hak2 site, abandoned in 1999, an anomaly in respect with the trend of increasing biomass versus time since land use change that characterizes the rest of the data. The large amount of biomass for that specific site, the only one referring to August 2003, can be explained by the more favourable conditions for productivity of that particular year compared to 2004, given especially by larger precipitation in July (>40 mm).

Both aboveground and belowground biomass showed significant differences among sites (P<0.0001); aboveground biomass ranged between 2.45±0.18 to 4.25±0.22 t d.m/ha, it was greater in the earlier stages of grassland recover (old field 99 and 98) and declined in the later stages (old field 95 and 94) (P<0.0001) while no particular tendency was found for belowground biomass, except in the case of assuming the value of the earliest stage (old field 99) overestimated for the above mentioned reasons. In such case we could figure out an increasing trend of root biomass over time.

Pooling the results obtained into two categories representative for the steppe and old field sites, the stock of total biomass resulted impoverished on average by -41.3% (P<0.0001) in the old fields. In particular belowground biomass was 51.2% (P<0.0001) less than in steppes, contrasted by a greater amount of aboveground biomass +88.5% (P<0.0001).

Steppe and old field ecosystems also differed in the pattern of distribution of the biomass into the above and belowground compartments: in the first indeed, 5.1% to 11.6% of the carbon is located aboveground and most of it, 88.3-94.2% is found belowground; in the latter a sensibly higher amount, ranging from 15.1% to 41.9% is aboveground and the share of belowground biomass is reduced to the range of 58.0-84.8%.

5.3.1.2 Tuva

The steppe and old field sites in Tuva (table 5.3) were characterized by similar stocks of aboveground biomass (P>0.05), being 2.30±0.17 and 2.07±0.42 t d.m./ha respectively. The difference in the stock of biomass located belowground, 16.59±0.01 t d.m /ha in the natural steppe site against 7.75±0.01 t d.m/ha in the old field, is responsible for the highly significant deviation (P<0.0001) in the amount of total biomass, reaching 22.39±1.14 and 11.45±0.71 t d.m/ha respectively. According to Titlianova (2003) the typical average stocks in aboveground, belowground pools in dry steppes of Tuva are 2.75 t d.m./ha and 20.77 t d.m./ha, confirming our estimates. In the case of Tuva the stage of recovering grassland at 12 years since the end of agricultural use hosts 51.1% (P<0.0001) of the biomass of the steppe's ecosystem. The proportion

of above and belowground biomass in respect with the total is 12.1% and 87.8% in the steppe ecosystem, 21.0% and 78.9% in the former cropfield.

	Site		
	steppe	old field 92	t-Test
	[t d.m ha^{-1}]	[t d.m ha^{-1}]	
AG	2.30±0.17	2.07±0.42	n.s
BG	16.59±0.26	7.75±0.15	P<0.0001
Total	22.39±1.14	11.45±0.71	P<0.0001

Table 5.3. Aboveground (AG), belowground (BG) and total biomass stocks of a former agricultural field abandoned in 1992 and a true dry bunchgrass steppe of Tuva expressed in tonnes of dry matter per hectare (mean ± standard error)..

5.3.2 Soil carbon and nitrogen stocks

5.3.2.1 Hakasia

Soil organic carbon stock in the soil layer (0-30cm) of the steppe sites of Hakasia ranged between 116.8 and 152.5 tC/ha, while in the old fields it resulted from 32.0 to 98.8 tC/ha. The average soil organic carbon stock of the former croplands was thus 51.7% less than what found in the steppe sites. The differences in the soil carbon content of the steppe sites is clearly correlated to the amount of belowground biomass, and likely dependent on the rates of carbon inputs by the root systems turnover. The large scatter in the soil organic carbon content observed in the formerly cultivated sites could be dependent, beyond factors attributable to spatial variability, on a diversification of agricultural management (crop types, rotations, soil preparation techniques, etc.) that affected the storage capacity of carbon in soil.

Soil nitrogen content, in the same layer (0-30cm) was found proportional to the soil organic carbon content at all examined sites, which were characterized by an average C/N ratio of 8.6. In the abandoned fields soil nitrogen ranged between 3.9 to 11.2 tN/ha while in steppes it varied from 14.0 to 17.9 tN/ha.

5.3.2.2 Tuva

Soil organic carbon stock in the steppe site of Tuva was 38.0 tC/ha, whereas in the abandoned field site it was smaller by 50.2% (18.9 tC/ha). Nitrogen content in soil was 5.8 and 2.4 tN/ha, revealing a C/N ratio of 15.3 and 12.6, for the steppe and the old field, respectively.

5.3.3 Total carbon stock and distribution into pools

The total carbon stock, given by the aggregation of biomass carbon stock (aboveground and belowground) and soil organic carbon for the steppe sites of Hakasia (table 5.4) resulted in an average of 140.9 tC/ha, distributed in the largest part in the soil organic matter (91.1-93.8%), by (5.5-8.4%) in the belowground biomass and only by (0.4-0.7%) in the aboveground pool.

	Carbon pool						
	Soil organic matter		AG biomass		BG biomass		TOTAL
	tC ha^{-1}	%	tC ha^{-1}	%	tC ha^{-1}	%	tC ha^{-1}
Steppe A (Hak1)	120.28	91.9	0.72	0.5	9.85	7.5	130.84
Steppe B	116.85	93.8	0.90	0.7	6.79	5.5	124.54
Steppe C	152.50	91.1	0.77	0.5	14.16	8.5	167.44
	129.88	**92.28**	**0.80**	**0.58**	**10.26**	**7.14**	**140.94**

Table 5.4. Stocks of carbon (tC ha^{-1}) and distribution (%) into aboveground (AG), belowground (BG), and soil organic matter (depth:0-30 cm) and total carbon of steppe sites of Hakasia.

	Carbon pool						
	Soil organic matter		AG biomass		BG biomass		TOTAL
	tC ha^{-1}	%	tC ha^{-1}	%	tC ha^{-1}	%	tC ha^{-1}
Old field 1999 (Hak 2)	32.04	83.6	1.89	4.9	4.41	11.5	38.33
Old field 1998	98.82	95.6	1.91	1.8	2.64	2.6	103.38
Old field 1995	67.18	92.8	1.24	1.7	3.96	5.5	72.38
Old field 1994 (Hak3)	53.21	88.0	1.10	1.8	6.18	10.2	60.50
	62.81	**89.98**	**1.54**	**2.58**	**4.30**	**7.44**	**68.65**

Table 5.5. Stocks of carbon (tC ha^{-1}) and distribution (%) into aboveground (AG), belowground (BG), and soil organic matter (depth:0-30 cm) and total carbon of former agricultural fields of Hakasia.

The abandoned fields (table 5.5) were characterized by total stock of carbon averaging 68.6tC/ha, allocated in the soil organic matter by (83.5-95.5%), in the belowground biomass by (2.5-11.5%) and in the aboveground pool by (1.7-4.9%).

At the sites of Tuva (table 5.6) the total carbon stock was 46.5 tC/ha for the steppe and 25.4 tC/ha for the old field, with a similar share of carbon in the various pools being 81.1% in the soil at both sites, 16.0% and 14.9% respectively in the belowground biomass, 2.2% and 3.6% in the aboveground biomass.

	Carbon pool						
	Soil organic matter		AG biomass		BG biomass		TOTAL
	tC ha^{-1}	%	tC ha^{-1}	%	tC ha^{-1}	%	tC ha^{-1}
Steppe	38.05 a	81.7	1.04	2.2	7.47	16.0	46.55
Old field 92	21.05 b	82.6	0.93	3.7	3.49	13.7	25.47

Table 5.6. Stocks of carbon (tC ha^{-1}) and distribution (%) into aboveground (AG), belowground (BG), and soil organic matter (depth:0-30 cm) and total carbon of a former agricultural field abandoned in 1992 and a true dry bunchgrass steppe of Tuva.

5.4 Discussion

The quantification of the reduction in soil organic carbon stock found in the old fields of Tuva and Hakasia as a consequence of the former agricultural use of the land is meant to indicate merely a minimum threshold, because after abandonment of agricultural practices the carbon stocks are supposed to build up again as shown in a number of similar studies (Post & Kwon, 2000; Knops & Tilman, 2000; Guo and Gifford, 2002). However, the accumulation of carbon in a given time arising from a conversion from arable to grassland use is on average half that of the release induced by conversion from grassland to arable use (Sousanna, 2004). In our study case the fields were firstly cultivated for about 40 years and then under grassland recover for 5-12 years; the results obtained may thus represent a fair approximation of the reduction of soil carbon induced by arable use of the land.

Interestingly, our results are in fair agreement with what generally observed for the conversion from grassland to cropland, that reduced soil carbon stock by about 50% or more (Guo and Gifford, 2002).

In particular, mechanical working of prairie soils lead over a period of 50 years to a loss of about 50% of the original C content (Matson at al., 1991) due to decomposition of easily mineralisable C compounds. It is unclear why decomposition of soil carbon stops at 50% despite further working. The fact that the black soils of steppes and prairies were formed, to a large extent, from charcoal and soot particles as a result of vegetation burning about 5000 years ago (Schmidt et al., 1999) and

that this black carbon is resistant to decomposition even with mechanical working, was hypothesised as a possible explanation.

Soil carbon stocks and the C/N ratio in steppes of Hakasia were found similar to other chernozem soils of natural steppes in Russia (Torn et al., 2002) storing about 100 tC ha^{-1} in the top 20 cm with a C/N level of 11. Lower carbon stocks are typical for chestnut soils (kastanozems) of southern steppes of Tuva, as confirmed by results of Conen et al. (2003), for the lower primary productivity and the highest fraction of sand.

The pattern of biomass distribution between the AG and BG compartments reflects the strategy of carbon allocation that differentiates annual plants, predominant in the early stages of recovering grassland, from perennial plants, characterizing the vegetation community of the climax stage in steppe ecosystems.

Annual plants are an example of investment type of plant, characterized by high photosynthetic capacity and a high proportion of photosynthetically active tissue in its total mass (at least 50%). During the growth phase the carbon income is mainly used for producing leaves, which then serves to increase the carbon gain of the plant. These plants have to make full use of a short period of time during which conditions are favourable for growth, flowering and setting of fruit; they must employ their photosynthetates in such a way that abundance of tissue is formed in the shortest possible time, and do this even when a fairly long time for growth is available. On the other hand, when local conditions are less favourable, particularly when water is short in supply, or when soil is poor in its nutrients, the plant is compelled to build up an extensive root system; this is done at the cost of the shoot and leads to a smaller photosynthetic yield and lower reproductive potential.

Perennial herbaceous plants follow a conservative pattern of utilization of photosynthetates, achieving a lower net carbon gain and thus grow more slowly than the investment type of plant. However, they have the advantage to survive under unfavourable conditions such as dry, cold or nutrient poor habitats. Any excess of assimilates will be allocated to shoot axes but primarily to belowground plant organs, which may eventually develop into massive storage organs (Eber, 1991; Sale, 1974; Larcher, 2003).

Steppe plants, which have to utilize the time between cold winters and dry summers to complete their life cycles, allocate any excess of assimilates primarily to belowground plant organs, which may eventually develop into massive storage organs, such as rhizomes, tubers, roots or bulbs. This allows a sufficient assimilation for vegetative growth as well as an early blooming even though leaf biomass has not reached the capacity yet to provide sufficient assimilates.

5.5 Conclusions

Soil organic matter represents by far the most important stock of carbon in steppes systems, reaching 91-93% in chernozem soils of Hakasia and 81% in kastanozem soils of Tuva.

The stock of carbon in old fields in Hakasia and Tuva resulted lower than that of steppes. The difference is to be related to the previous agricultural use of the old fields which lost on average, as a consequence of disturbance of soil, at least 50% of the soil organic matter stock.

The biomass carbon stock of steppes is stored mainly in the belowground pool, with a proportion ranging 88-94%. Levels of biomass in steppes of Hakasia resulted influenced by management history and geomorphology, being highest in a long term ungrazed steppe and higher in a steppe delevoped along a gentle slope of a hill than on its top.

Recovering steppes show a higher share of biomass in the aboveground pool (12-42%) than in climax steppes. Steppe vegetation indeed, composed by the largest part of perennial species, allocates preferably assimilated carbon to build up a dense fibrous root system, which constitutes an insurance against unfavourable environmental conditions. The earlier stages of recovering steppe is composed by an important fraction of annual species, which on the contrary tend to maximize growth and flowering, allocating carbon preferably to shoots.

View of the true bunchgrass steppe in the region of Shira (Republic of Hakasia) selected for the installation of a micrometeorological station (Hak1 site) - July 2002

View of the Hak2 site in the region of Shira (Republic of Hakasia), an old field 5 years after land use change .The eddy covariance station is visible in the middle of the picture – July 2002.

Horses grazing over a true bunchgrass steppe near Erzin (Republic of Tuva) - July 2003

View of the Hak3 site in the region of Shira (Republic of Hakasia), a former agricultural field abandoned 10 years before, at the beginning of the winter season – November 2003

6 Net primary productivity

6.1 Introduction

Net primary productivity (NPP) is defined as the total photosynthetic gain, less respiratory losses, of vegetation per unit of ground area. For natural vegetation, this is often expressed on an annual basis. For a given period of measurement, NPP is equal to the change in both aboveground and belowground plant mass plus any losses over this period due to death and subsequent decomposition, herbivory and exudation/volatilization (Long et al., 1989).

NPP is a key variable of terrestrial ecosystems and an important component of the global carbon cycle. The better understanding of NPP is essential to understand the terrestrial carbon cycle, biosphere-atmosphere interaction and response of ecosystem function to climate change and CO_2 fertilization (Melillo et al. 1993; Scurlock et al. 1999). However, a synthesis of NPP data based on field biomass measurements is lacking for all terrestrial worldwide ecosystems.

In order to compile global NPP data for model validation, a coordinated international programme, the Global Primary Productivity Data Initiative (GPPDI), has worked successfully since 1995. However, the lack of NPP data or their publication in languages other than English, still seriously inhibits the progress in estimating and modeling the global carbon cycle and in validating and evaluating the global NPP/carbon models (Scurlock et al., 1999; Ni, 2004).

This effort to quantify NPP is critical because of the central role of NPP in ecosystem functioning, determining plant biomass accumulation and herbivore production, as well as influencing nutrient cycling and ecosystem carbon exchange (McNaughton et al., 1989; Jackson et al., 2000; Sala & Austin, 2000).

Measuring NPP is also important to understand annual changes in organic matter in natural and managed systems and to understand the controls over carbon fluxes. Furthermore, understanding controls over NPP will be crucial in developing models of these processes at large spatial scales. While advances have been made in accurately determining aboveground NPP (Paruelo et al., 1997; Raich et al., 1997; Sala & Austin, 2000), the amount of NPP allocated below-ground remains among the most poorly understood attributes of ecosystems (Lauenroth, 2000).

However, many earlier estimates of grassland NPP ignored both turnover and belowground production and were based on aboveground peak of live and dead biomass only (Scurlock et al., 2002). Even the coordinated studies of the International Biological Programme (IBP) Grassland Biome in the late 1960's and early 1970's were based mainly on aboveground biomass changes, with relatively few estimates of belowground productivity (Singh and Joshi, 1979; Long et al., 1989).

Understanding below-ground NPP (BGNPP) is particularly important in grassland ecosystems. In most grasslands a large proportion of biomass is below-ground (Coupland, 1992), making estimates of total NPP in grasslands particularly sensitive to estimates of below-ground production.

Six algorithms are often used for estimating NPP from biomass measurements in grassland vegetation: peak live biomass, peak standing crop (live plus standing dead matter), maximum minus minimum live biomass, sum of positive increments in live biomass, sum of positive increments in live and dead plus litter, and sum of changes in live and dead biomass with adjustment from decomposition (Long et al., 1992; Scurlock et al., 2002). Certain methods may only apply within certain biomes (Scurlock et al., 2002). The peak live biomass and the maximum minus minimum live biomass methods for example, are only suitable for the temperate grasslands (Milner and Hughes, 1968; Long et al., 1989; Scurlock et al., 2002).

However, grassland NPP varies in the estimation of these six methods: Singh et al. (1975) and Surlock at al. (2002) showed that although many of the aboveground NPP estimates obtained using different computational methods were correlated with one another, they may yield to significantly different figures when applied to the same set of data. They raised concern about the statistical difference in measured biomass between successive harvests, but acknowledged that strict statistical constraints could prove logistically prohibitive. Although statistical procedures exist for determining the optimum number and size of plots for sampling within desired tolerances, it is generally not practicable to maximize the number of plots so as to obtain a statistically significant differences in biomass between consecutive samples (Long et al., 1992). The problem remains that the degree of underestimation using different methods may be strongly site-specific or may vary with the year of measurement (Scurlock, 2002).

In this study we assess the NPP of the steppe and recovering steppe (old field) sites of Hakasia, equipped with eddy covariance systems for CO_2 flux monitoring, where moving beyond the determination of the carbon balance, a more comprehensive analysis of the carbon cycle dynamics in respect with the carbon inputs was performed. The study was conducted thus parallel with the flux monitoring activities and regarded: the site of Hak2 (former crop field abandoned in 1999) from May 2002 to June 2003; the site of Hak3 (former crop field abandoned in 1994) from May to September 2004; the site of Hak 1 (steppe) from May 2002 to September 2004.

Given the divergence of NPP assessments based on biomass measurements, depending on the method used, we applied a multiple methodological approach in order to obtain a balanced set of results that include positively and negatively biased assessments.

In particular our attention was addressed to analyze the following issues:

1. Biomass growth dynamics patterns.
2. Performance of distinct methods for NPP assessment.

3. Differences in NPP among steppe ecosystem, recovering grasslands and between the two.
4. Allocation of primary productivity to shoots and roots.
5. Interannual variability of primary productivity and correlation of NPP with meteorological drivers (precipitation, air temperature).

6.2 Materials and methods

6.2.1 Biometric measurements

Biomass samplings were carried out during the whole length of the growing season from the beginning of May to the end of September of each year within the footprint area of the micrometeorological stations.

Aboveground phytomass was sampled at intervals of two weeks within 20 randomly located square plots of 0.25 m^2 each. The standing biomass was clipped at ground level and the litter was collected from the area of each plot; the matter was then sorted into live and dead biomass.

Belowground biomass was sampled once a month (every two weeks in 2002) from 0 to 30 cm using a corer in the same plots as for aboveground biomass estimation. The sampling depth was determined by trial sampling in order to retrieve at least 90% of belowground matter. Roots and particulate organic matter were separated from the soil removing the larger roots by tweezers, the rest being washed in water to retrieve the floating fragments of roots and dead organic matter sieving them over multiple layers of 1 mm sieves.

Samples of belowground biomass collected in 2002 were not washed in water, but after being sieved with 1 mm nylon grids, and having separated the main fraction of the roots, roots fragments and particulate organic matter were picked up by tweezers from the soil.

All the collected matter was dried in a stove at 70°C until completely dehydrated and weighed on an electronic scale; biomass was expressed as the weight of dry matter per unit area [t d.m. ha^{-1}].

The values of biomass were then converted to stock carbon per unit area, using 0.45 as conversion factor from biomass to carbon (IPCC, 2003).

6.2.2 NPP assessment

The methods for NPP assessment of grassland ecosystems can be applied only if specific assumptions (presence or absence of live or dead matter from previous years, negligibility of decomposition, simultaneity of biomass growth and death) are met. The algorithms used for the computation of NPP differ also in the number of inputs required to describe processes associated with biomass change over time (aboveground and belowground productivity, decomposition) and lead to different results in the assessment of NPP.

In this study net primary productivity was assessed using three methods, selected according to the criterion of using as input variables the temporal changes both in the aboveground and

belowground biomass levels. In doing so, the simplest approaches based on a single measure of peak biomass or derivation of belowground productivity from crude root/shoot ratios were rejected. Additionally belowground productivity at the natural steppe site was assessed by the use of the ingrowth cores technique.

The algorithms used for NPP assessment are the following:

1)

$$NPP(AG,BG) = MAX(AG,BG)Totmat - MIN(AG,BG)Totmat$$

Ni (2004) *(Equation 6.1)*

2)

$$NPP(AG,BG) = \Sigma(\Delta((AG,BG)bmass + (AG,BG)Totdead)) =$$
$$= \Sigma(\Delta(AGTotmat + BGTotmat)); \Delta > 0$$

Singh et al. (1975) *(Equation 6.2)*

3)

$$NPP(AG,BG) = \Sigma(\Delta(AG,BG)bmass + \Delta(AG,BG)Totdead + (r_{(ag,bg)} \cdot (AG,BG)Totdead))$$
$$= \Sigma(\Delta AGTotmat + \Delta BGTotmat + (r_{(ag,bg)} \cdot (AG,BG)Totdead))$$

Long et al. (1989); after Weigert & Evans (1964). *(Equation 6.3)*

where *AGbmass*= aboveground live matter; *AGTotdead*= aboveground total dead matter; *BGbmass*= belowground live biomass; *BGTotdea*d= belowground total dead matter; *AGr*= aboveground relative rate of decomposition; *BGr*= belowground relative rate of decomposition; *AGTotmat*= aboveground total matter; *BGTotmat*= belowground total matter.

Methods (1) and (2) assume that growth, death and decomposition do not occur simultaneously and it does not account for material lost by death during periods of biomass increase.

Method (3) assumes: a) that measured changes in parameters are statistically significant over each sample interval, although in practice this may be very hard to achieve as an impractically large number of samples would be required to detect real but modest changes over each sampling period (Scurlock et al., 2002), b) that decomposition rate is independent of the composition of dead matter, and c) that exports of biomass are negligible (i.e. grazing, root exudation, etc.); yet it is the only method which incorporates all components required for an accurate estimate of NPP, including adjustment for decomposition.

To retrieve the relative rates of decomposition, the decrease of decomposing dead matter over time (t) was assumed to follow a negative exponential trend (Olson, 1963; Koukura et al., 2003), described by the equation:

$$X = X_o e^{-kt} \qquad \textit{(Equation 6.4)}$$

where X = undecomposed matter quantity; Xo= initial quantity at time t [d]; k= rate constant [d^{-1}]
The fraction of dead matter which decomposes in time t as percentage of the initial quantity, corresponds to the relative rate of decomposition (r) and can be expressed as follows:

$$r = \frac{(X_o - X)}{X} = (1 - e^{-kt}) \qquad \textit{(Equation 6.5)}$$

inverting the equation the constant k may be retrieved

$$k = -\frac{\ln(1 - r)}{t} \qquad \textit{(Equation 6.6)}$$

Decomposition rates may be determined experimentally using litter bags containing dead aboveground matter placed at the ground surface, or dead belowground matter buried in the soil; at the end of the sample interval the bags are recovered and the loss of material is quantified. In this work we referred to results of observations of biomass decomposition (after 1 year) made in steppes of central Asia after Titlianova (1977), in order to retrieve specific constant rates (k): these were $1{,}18 \cdot 10^{-3}$ and $1{,}89 \cdot 10^{-3} d^{-1}$ for aboveground and belowground dead matter, respectively. The application of the adjustment for decomposition in method (2) requires the knowledge of the amount of dead matter which undergoes this process: as we did not separate belowground biomass into live and dead we assume the ratio between belowground live and total biomass to be 0.4, an average value for natural steppe ecosystems of Hakasia (Titlianova, 1977).
However the decomposition of dead matter depends strictly on the environmental conditions, being favoured by high temperature and moisture, and for this reason most of decomposition in steppe ecosystem takes place in summer months rather than in winter. A model of decomposition dynamic driven by time and parametrized by data of disappearance of dead matter in 1 year, can reproduce the process successfully on a yearly base, but tends to underestimate the quantity of decomposed dead matter in summer months, when the process is much more accelerated compared to winter months. In order to account for this bias, we used two variants of method 3: (3a) decomposed dead matter was estimated applying the above exposed model, for the time window between the start and the end of the biomass sampling (typically beginning of October); (3b) decomposed dead matter was estimated for a whole year assuming then that over a year period the greatest fraction of decomposition takes place during the growing season and that winter decomposition is negligible.

6.2.3 Ingrowth cores

This method consists of monitoring the regrowth of roots in a volume of soil where roots have been removed in advance (Jordan and Escalente, 1980; Persson, 1983; Cuevas and Medina, 1988; Neill, 1992; Fisk et al., 1998; Johnson and Matchett, 2001). In practice, a number of soil cores, up

to the depth of 30 cm, were collected and the roots contained in it were hand picked. The root free soil was then placed in mesh bags and returned to the holes in the ground. After a period of time the mesh bags were removed from the holes, the root biomass was separated from the soil and equalled the belowground productivity for that span of time. In this study mesh bags were prepared and placed in the ground at the beginning of the growing season (first week of May, except in 2002, when they were ready only at the beginning of July). A number of 8 replicates were sampled at time intervals of about 2 months until October.

This technique although is quite feasible and lets to avoid the necessary assumptions for the assessment of NPP by sequential biomass, on the other hand suffers from two major limitations: 1) it enhances root proliferation due to disturbance and altered nutrient availability in disturbed root-free soils and 2) it underestimates root growth because of disappearance of roots over the measurement period (Fahey and Hughes, 1994).

6.3 Results

6.3.1 Biomass dynamics

The growing season starts, as new green shoots appear, in the first half of May and lasts until the low air temperatures cause the senescence of the vegetation, typically in the month of September (fig. 6.1, 6.2, 6.3). The approximate duration of the growing season is 120 days (May –September), although a substantial extension of the growing season throughout the month of October is possible when temperature records keep high, as witnessed by the presence of live AG biomass on the occasion of mid October samplings in 2003 and 2004.

The peak of live aboveground (AG) biomass is found in the time window between mid July and mid August and its occurrence is adjusted by the climatic conditions of the season, particularly by precipitation. In the year 2002, characterized by a very dry spring particularly in the month of May, the vegetative season was delayed in its start of about 3 weeks, the growth rate was reduced despite the regular precipitation since the end of June and the peak of AG live biomass was reached not earlier than 5^{th}-10^{th} August both at Hak1 and Hak2. In 2003 and 2004, the growing season started promptly at the beginning of May but, if the peak of AG live biomass in the very rainy summer of 2003 was recorded around mid August, in 2004 it was anticipated to mid July because of low precipitation in that month.

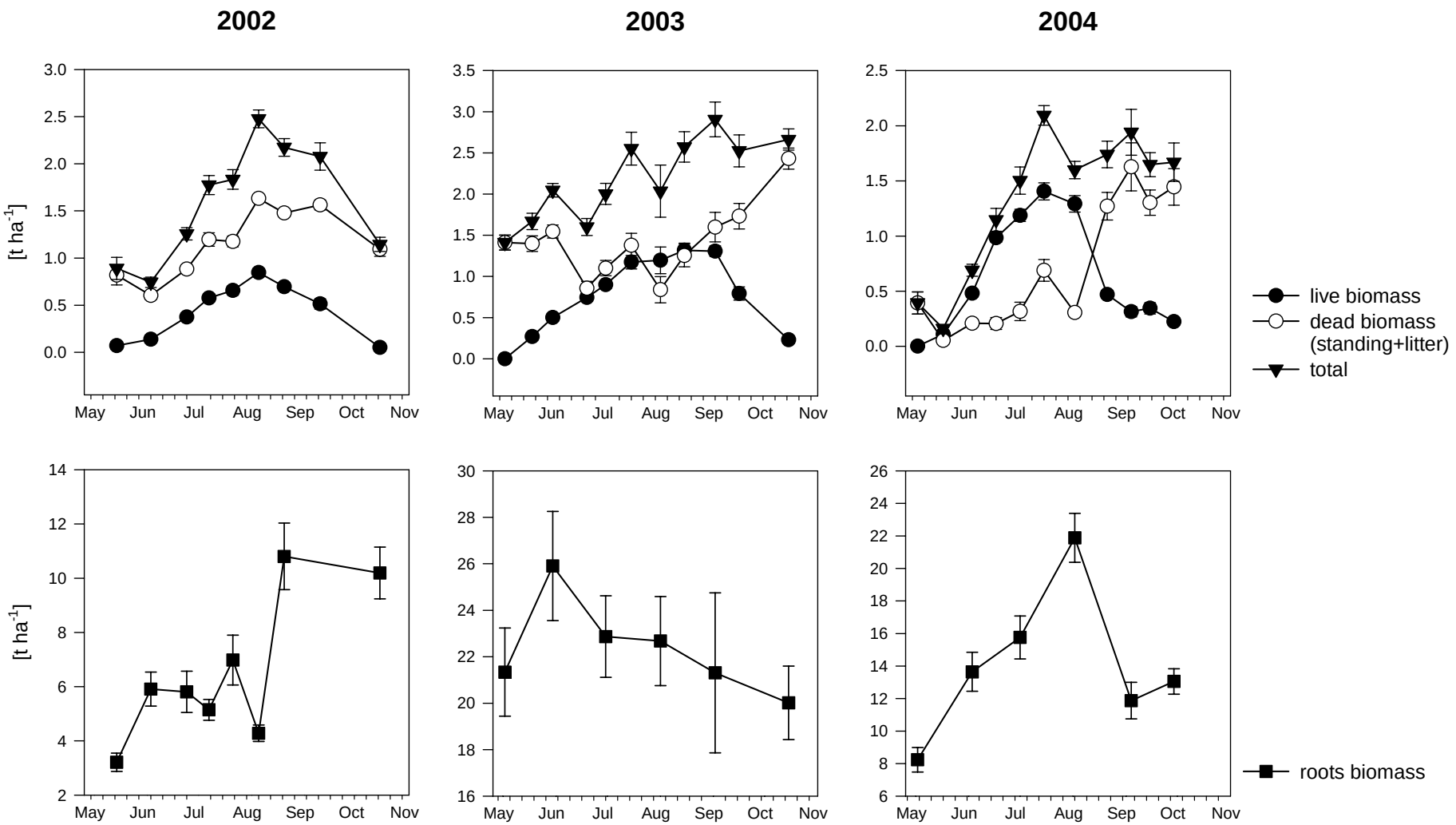

Figure 6.1. *Trend of aboveground (live,dead,total) and belowground biomass during the growing seasons of the years 2002,2003,2004 (mean ± standard error) at the site of Hak1.*

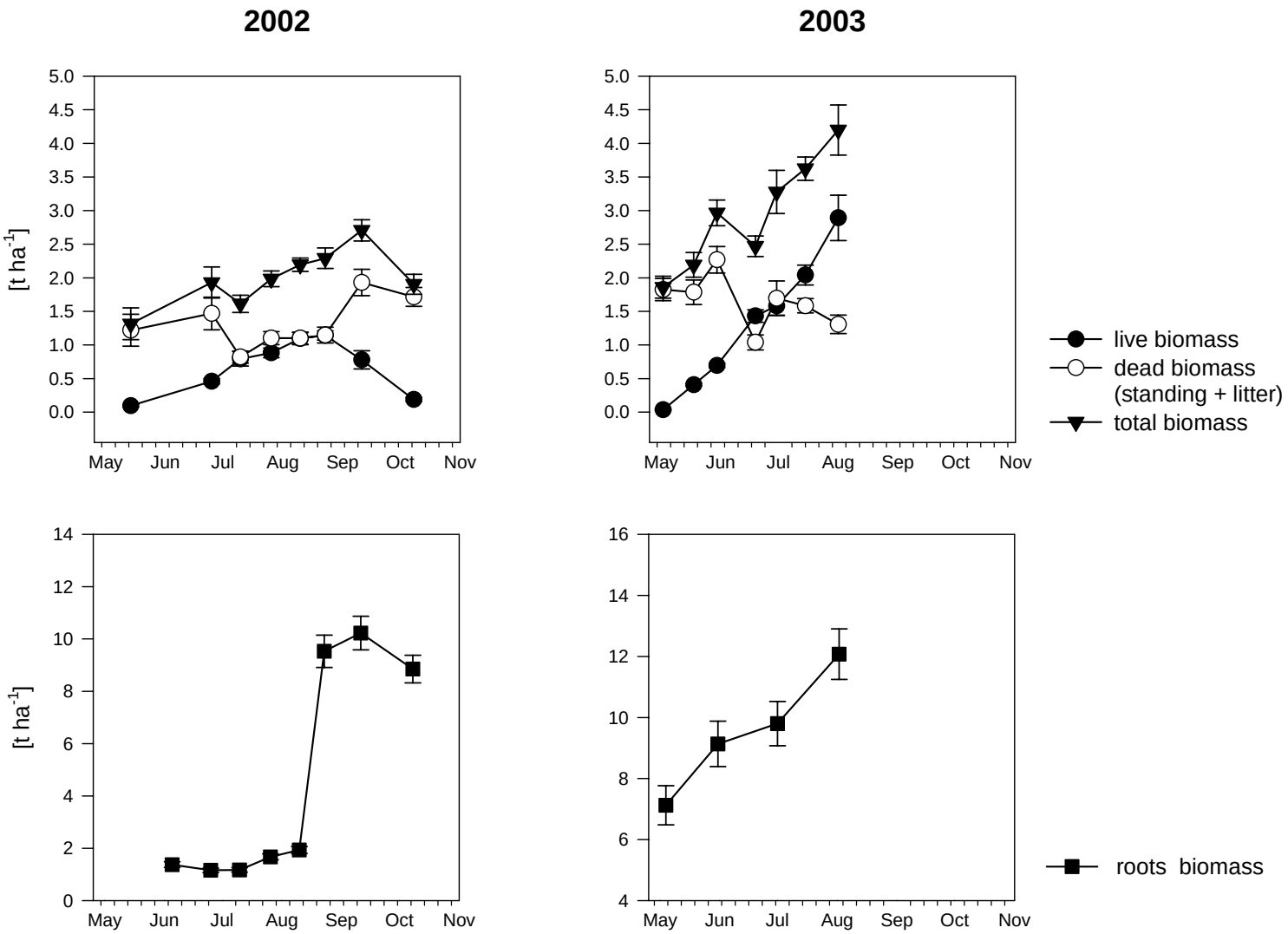

Figure *6.2. Trend of aboveground (live,dead,total) and belowground biomass during the growing season of the year 2002,and for the period May-August 2003 at the site of Hak2 (mean ± standard error).*

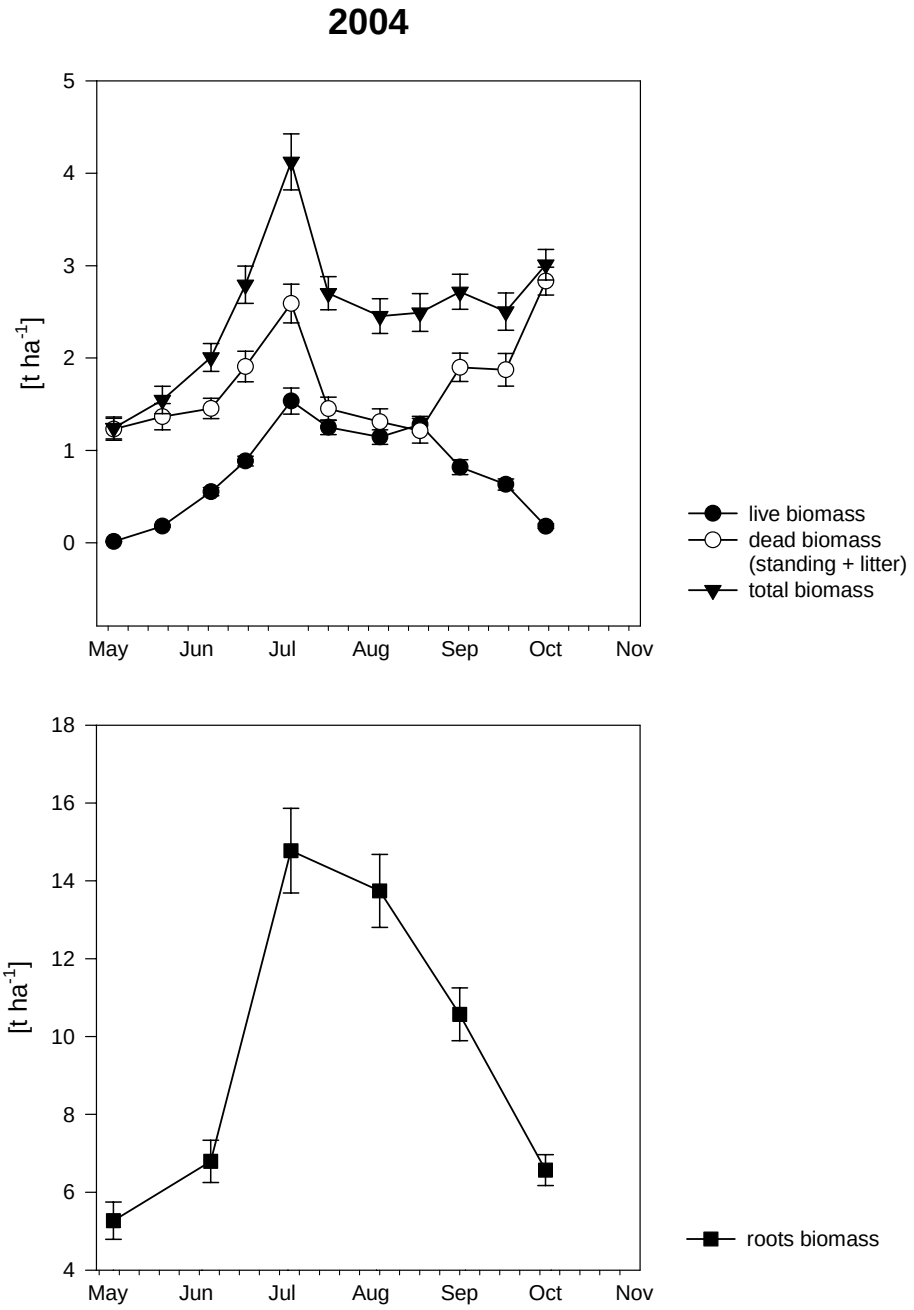

Figure *6.3. Trend of aboveground (live,dead,total) and belowground biomass during the growing season of the year 2004 at the site of Hak3 (mean ± standard error).*

The temporal pattern of roots growth follows approximately that of the shoots, however in the case of the dry year 2002, the development of BG biomass was uncoupled with AG biomass and it was shifted in the second half of the growing season, starting only after the aboveground biomass reached its maximum.

At the site of Hak1 it is evident the loss of AG biomass after a fire event in March 2004; however the low intensity fire burnt only most of the dead standing stems and part of the litter and no signs

of belowground biomass burning were found. In the following months there was a prompt recovery of AG live biomass which reached the maximum stock in the years of observation.

The smaller figures of BG biomass for the year 2002 compared to following years are imputable to the different quantity of detritus retrieved, due to the method used in separating the roots from the soil samples. Nevertheless, even if excluding part of the smallest biomass fragments, it is still possible to catch the amplitude of changes in BG biomass because roots formed within the season are accounted anyway.

6.3.2 NPP

Among the methods applied, method 2 (sum of positive changes in biomass) always yielded the highest figures of NPP, while method 3a (sum of changes with adjustment for decomposition) yielded the lowest. The estimates obtained by methods 1 (difference of max. minus min. biomass) and 3b (sum of changes with adjustment for decomposition of a year) tended to converge and were representative in general of a central value in the range of NPP estimates produced by all methods.

Hereafter estimates of NPP are expressed by the averaged results of all methods ± standard deviation.

The estimates of NPP for the natural steppe (Hak1) ranging from 6.55 to 13.17 t ha^{-1} are within the typical values of productivity for cold steppes reported in literature (Scurlock et al., 2002; Titlianova et al., 2002; Ni, 2004; Hiu & Jackson, 2005). In more detail, NPP was 10.71±1.69, 6.55±1.82 and 13.17±3.84 t $ha^{-1}yr^{-1}$ in the years 2002, 2003 and 2004 respectively, made up of an AG NPP of 1.13±0.62, 1.92±0.52, 1.79±0.38 t ha^{-1} yr^{-1} and a BG NPP of 9.58±1.28, 4.63±1.53, 11.38±3.50 t ha^{-1} yr^{-1} (table 6.1; fig. 6.5)

The assessment of BGNPP applying the ingrowth cores technique, resulted in systematically lower figures than using sequential sampling, being 7.06, 3.51, and 4.09 t ha^{-1} yr^{-1} over the period 2002-2004.

The NPP of the early stage of recovering grassland (Hak2) was 9.67±1.05 t ha^{-1} yr^{-1} in 2002 but, if referred to the 12 months period when eddy covariance measurements were carried on from July 2002 to June 2003, we obtain a NPP of 13.97±0.85 that was higher than that assessed for Hak 1 over the same period (11.58±2.69 t ha^{-1} yr^{-1}) (tab. 6.2; fig. 6.5).

The intermediate successional stage (Hak3), sampled in 2004, had a NPP of 9.26±4.09 t ha^{-1} yr^{-1} (tab. 6.3; fig. 6.5). Aware of the large uncertainty of this result, caused by particularly low NPP provided by methods 3a,3b, we focus only on the estimate yielded by method 1 to observe that this site shows lower NPP than Hak1 in 2004. However, productivity at Hak1 was noticeably higher in 2004 than in previous years, likely because of the “fertilizing” effect of fire.

Method	AG NPP [t ha^{-1}]				BG NPP [t ha^{-1}]				tot NPP [t ha^{-1}]			
	2002	**2003**	**2004**	**Jul02-Jun03**	**2002**	**2003**	**2004**	**Jul02-Jun03**	**2002**	**2003**	**2004**	**Jul02-Jun03**
1	1.59	1.49	1.78	1.86	8.87	4.57	13.65	9.56	10.46	6.06	15.43	11.42
2	1.73	2.59	2.30	2.26	11.06	4.57	14.82	12.92	12.79	7.16	17.12	15.18
3a	0.47	1.51	1.38	1.00	8.20	2.82	7.21	7.67	8.67	4.33	8.59	8.67
3b	0.71	2.08	1.70	1.23	10.20	6.58	9.82	9.80	10.91	8.66	11.52	11.03
mean	**1.13**	**1.92**	**1.79**	**1.59**	**9.58**	**4.63**	**11.38**	**9.99**	**10.71**	**6.55**	**13.17**	**11.58**
s.d.	**0.62**	**0.52**	**0.38**	**0.57**	**1.28**	**1.53**	**3.5**	**2.17**	**1.69**	**1.82**	**3.84**	**2.69**

Table 6.1. *NPP assessments at the Hak 1 site (steppe) for the years 2002, 2003, 2004 and for the 12 month window from July 2002 to June 2003. Figures in bold show mean ± standard deviation of the results yielded by methods (1,2,3a,3b).*

method	AG NPP [t ha^{-1}]		BG NPP [t ha^{-1}]		tot NPP [t ha^{-1}]	
	2002	**Jul02-Jun03**	**2002**	**Jul02-Jun03**	**2002**	**Jul02-Jun03**
1	1.39	2.20	8.44	11.75	9.83	13.95
2	1.71	3.01	9.07	11.75	10.78	14.76
3a	0.77	1.68	7.47	11.11	8.24	12.79
3b	1.16	2.07	8.67	12.31	9.83	14.38
mean	**1.26**	**2.24**	**8.41**	**11.73**	**9.67**	**13.97**
s.d.	**0.40**	**0.56**	**0.68**	**0.49**	**1.05**	**0.85**

Table 6.2. NPP assessments at the Hak 2 site (old field abandoned for 5 years) for the years 2002, and for the 12 month window from July 2002 to June 2003. Figures in bold show mean ± standard deviation of the results yielded by methods (1,2,3a,3b).

method	AG NPP [t ha^{-1}]	BG NPP [t ha^{-1}]	tot NPP [t ha^{-1}]
	2004	**2004**	**2004**
1	2.88	9.50	12.38
2	3.65	9.50	13.15
3a	2.11	2.99	3.46
3b	2.11	4.30	5.04
mean	**2.69**	**6.57**	**9.26**
s.d.	**0.73**	**3.42**	**4.09**

Table 6.3. NPP assessments of the Hak 3 site (old field abandoned for 10 years) for the year 2004. Figures in bold show mean ± standard deviation of the results yielded by methods (1,2,3a,3b).

	P(annual)	P (may-sep)	P (may)	T(annual)	T (may-sep)
AG NPP	0.95	**0.998***	**0.999***	**-0.908**	**-0.974**
BG NPP	-0.658	-0.421	-0.421	0.748	0.599
tot NPP	-0.566	-0.313	-0.313	0.665	0.502
fBGNPP	**-0.905**	-0.75	-0.75	**0.951**	0.87

Table 6.4. Pearson's correlation between net primary productivity of Hak1 site and climate. AGNPP: aboveground net primary productivity (t ha^{-1} yr^{-1}); BGNPP belowground net primary productivity (t ha^{-1} yr^{-1}); totNPP: total net primary productivity (t ha^{-1} yr^{-1}); fBGNPP: fraction of belowground net primary productivity (BGNPP/totNPP); P(annual): annual precipitation (mm); P(may-sep): cumulated precipitation from May to September (mm); P(may): precipitation of May (mm); T(annual): mean annual temperature (°C); T(may-sep): mean temperature of the months from May to Sep (°C)

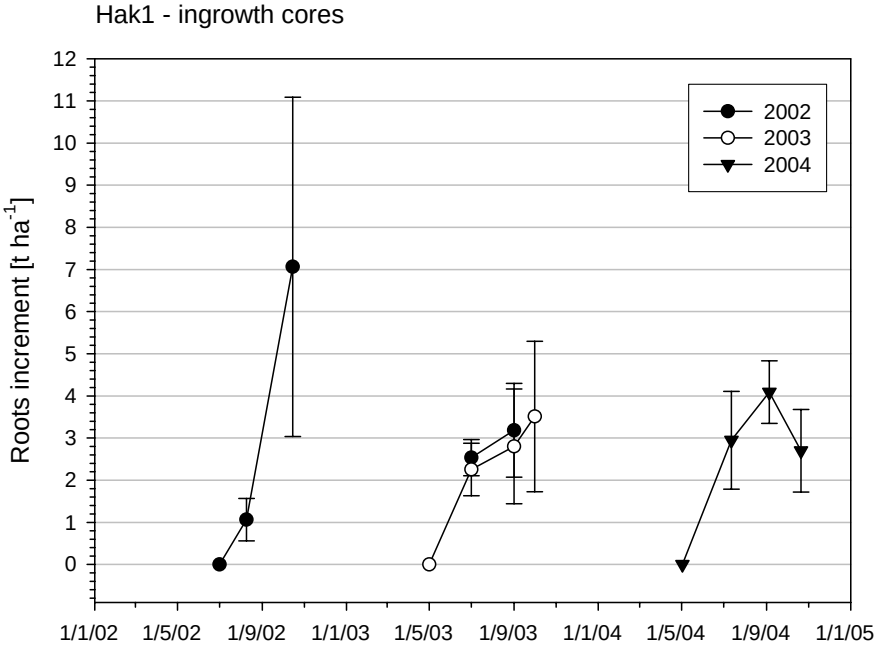

Figure 6.4. Belowground NPP assessed by the ingrowth cores technique at Hak1 site in the years 2002, 2003, 2004 (mean±standard deviation). Enclosures placed in the soil in 2002 and collected in the following year showed similar roots growth rates to those prepared in spring 2003.

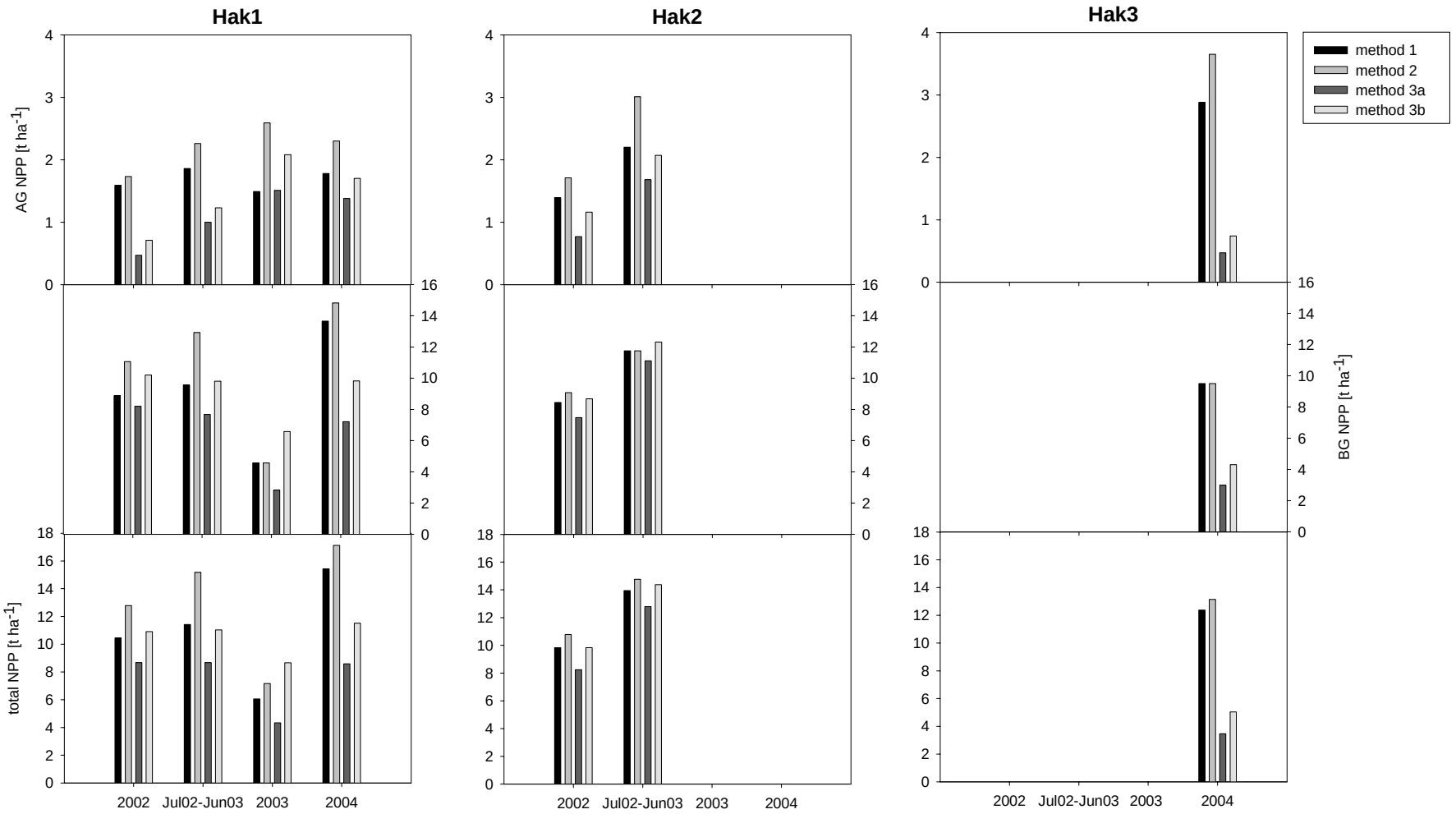

Figure 6.5. Aboveground (AG), belowground (BG) and total NPP estimates retrieved by the application of four distinct computational methods (1,2,3a,3b) for the sites of Hak1, Hak2, Hak3 during the years of the study (2002-2004)

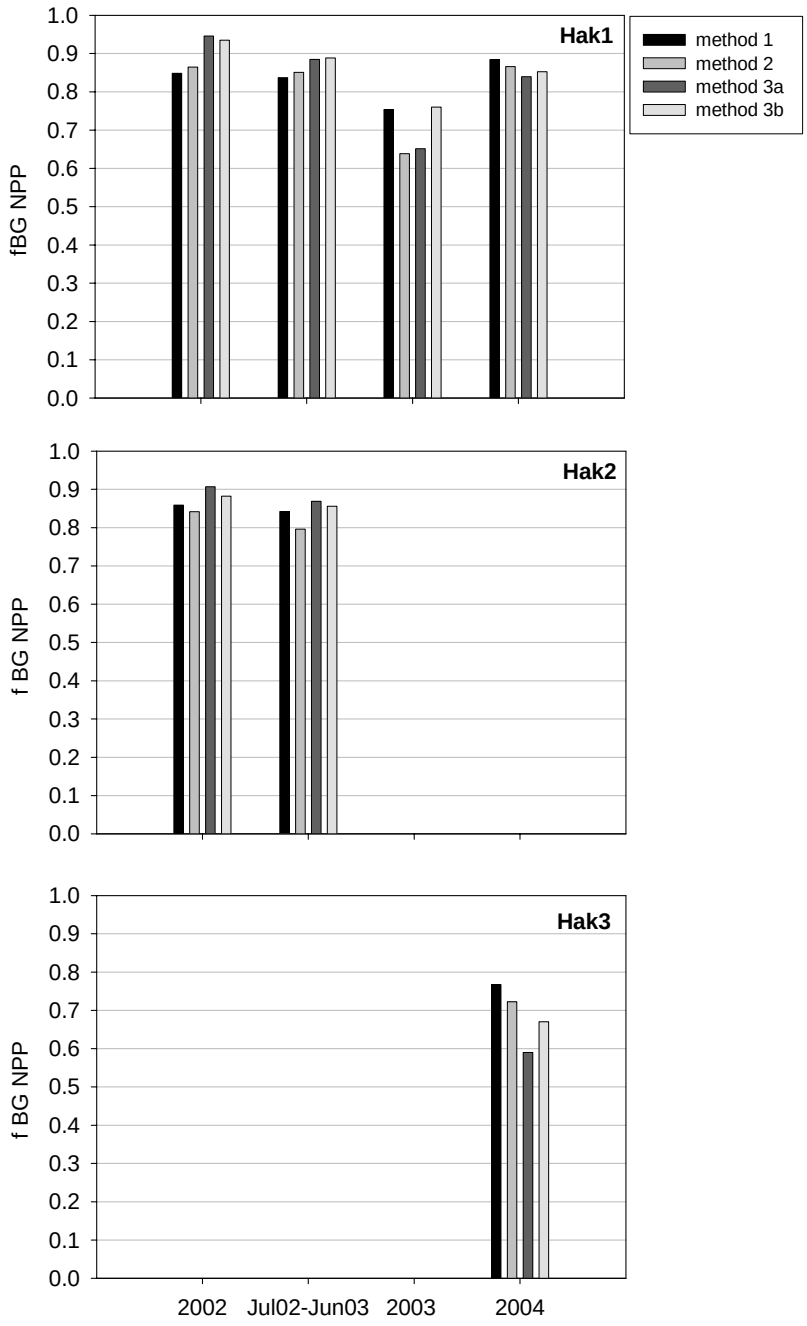

Figure 6.6. Fraction of net primary productivity allocated into the belowground biomass for the sites of Hak1 (top), Hak2(middle), Hak3 (bottom) according to different computational methods (1,2,3a,3b).

On average the largest fraction (60-90%) of net primary productivity was allocated to belowground biomass at all sites. The natural steppe was though characterized by a higher fraction of BG NPP (f_{BGNPP}) if compared to that of recovering grasslands over the same period. In 2002, f_{BGNPP} was 0.9 at Hak 1 against 0.87 at Hak 2; in 2003 it was 0.86 at Hak 1 and 0.69 at Hak3 (fig. 6.6).

AG NPP of the natural steppe, the only with an available dataset of 3 years, was found significantly ($P<0.05$) correlated (tab. 6.4) to annual precipitation (Pearson's r= 0.998) and precipitation of May (r=0.999), but negatively correlated to both mean annual temperature (r=-0.908) and mean

temperature of the growing season from May to September (r=-0.974). The fraction of net primary productivity allocated belowground ($f_{BGNPP)}$ increased with higher values of mean annual temperature (r=0.951), yet resulted anticorrelated to annual precipitation (r=-0.905).

6.4 Discussion

It is important to distinguish between methods that are conceptually more correct and methods that provide an answer that is closer to the true value. Methods that study the independent pattern of individual species or those that take into account numerous functional compartments are closer to the concept of primary productivity. However the results that they yield may be further from the real value than those resulting from simpler methods (Sala & Austin, 2000). Sources of underestimation of NPP come from not accounting for peaks of biomass and from the simultaneous nature of productivity and decomposition. Both this errors are reduced by increasing the sampling frequency, which on the other hand leads to a higher overall uncertainty in the NPP estimate because of the accumulation of the uncertainties in the differences of biomass stocks over time.

In the considered study case, method 1, based on the difference of (max-min) biomass, fairly converges with the more complex approach 3b, confirming what stated above. NPP estimates based on method 2 represent the upper threshold of the results of the methods comparison, as also found by Scurlock (2002) for steppe ecosystems. Monitoring belowground biomass dynamics was crucial in NPP assessment because: (i) BG NPP represented the largest fraction of NPP (60-90%); (ii) the root/shoot ratio was subdued to sensible interannual variations and any method based solely on measurements of aboveground biomass and derivation of belowground NPP would lead to large errors.

Although in 2002 mesh bags were prepared at the beginning of July, the BG productivity retrieved by this method can still be considered representative for the whole season because in that particular year the growth of roots, according to sequential biomass sampling, took place later on. Anyway, for all the examined years the estimates of BGNPP obtained by applying the ingrowth cores method (fig. 6.4) were lower than those obtained by sequential sampling (about -25% in 2002 and 2003); in 2004 the divergence was even remarkably larger (-60%), highlighting the limits of this technique, for the reasons already exposed in the methods section.

Aboveground net primary productivity was always higher in recovering grasslands compared to the steppe ecosystem; total NPP was higher (Δ=+2.39 t ha^{-1} yr^{-1}) in the early successional stage (Hak2) compared to the natural steppe (Hak1) in the period July 2002- June 2003 and the intermediate stage (Hak3) was more productive (Δ=+0.90 t ha^{-1} yr^{-1}) than Hak1 in 2004. It should be though noticed that in 2004 the productivity of the natural steppe ecosystem could have been enhanced by the availability of nutrients and improved irradiance thanks to the burning of grass in spring. However, considering the uncertainty in the assessments it is not possible to individuate a determined trend of NPP along the temporal stages of the ecological succession.

Net primary productivity and biomass partitioning are known to be strongly influenced by climate (Lieth, 1975; Melillo et al., 1993; Gill & Jackson, 2000; Gower et al., 2001) although most of experimental studies on the relation between NPP and climatic variables have been mostly related to aboveground NPP. In this study case, AG NPP resulted to increase linearly both with annual precipitation and precipitation of the month of May, similarly to what found by Miyazaki et al. (2004) for grassland vegetation in central Mongolia. The fraction of NPP allocated belowground responded negatively to precipitation, accordingly to the findings from several studies on grassland ecosystems, gathered in meta-analysis of grasslands NPP data by Ni (2004) and Hui & Jackson (2005).

6.5 Conclusions

Net primary productivity of a natural steppe of Hakasia assessed for the years from 2002 to 2004 on the basis of four distinct biometric methods ranged between 6.05 to 13.17 t ha^{-1} yr^{-1}, typical values for steppe ecosystems.

Aboveground NPP of recovering grasslands (old agricultural fields) was found systematically higher than in the steppe, however it was not possible to establish a clear ranking of total NPP among the sites because of the uncertainties in the results.

A variable fraction of NPP, included between 70% and 90% (average 83%), was allocated to belowground biomass either in steppe and recovering steppe ecosystems.

Monitoring belowground biomass dynamics assumes thus a fundamental importance for an accurate assessment of NPP, considering that methods based on the extrapolation of BGNPP on the base of root/shoot ratios may turn into very crude estimates. The fraction of NPP allocated belowground showed indeed an interannual variability with values increasing linearly with mean annual temperature and decreasing with annual precipitation.

The use of ingrowth cores may turn of great utility in the task of quantifying BG NPP, because it substantially reduces the amount of time and labour that is behind a campaign of sequential biomass sampling and the uncertainty of the assessment of roots growth. BG NPP, when applying the ingrowth cores technique, is directly measured and not assessed by differences of biomass stocks. Nevertheless in the presented case study the estimates of BGNPP obtained by such technique were systematically lower by not less than 25% than those using other methods, confirming that the ingrowth cores method fails to account for the real biomass increments of roots.

7 CO_2 fluxes at ecosystem scale by eddy covariance technique

7.1 Use of the eddy covariance technique as a tool to characterize the carbon cycle

The eddy covariance method is a micrometeorological technique that provides a direct measure of net carbon (CO_2), water vapour and sensible heat fluxes between vegetated canopies and the atmosphere (Baldocchi, 2003; Aubinet et al., 2000). With the use of the eddy covariance method it is possible to measure continuously mass and energy fluxes over variable timescales, from a minimum of an hour or less (typically 30 minutes) to days, seasons, and years. The merits of the method include the minimal disturbance to the underlying vegetation and its ability to sample an area of land large enough to be representative for the targeted ecosystem. The requirements for the applicability of the eddy covariance method are steady atmospheric conditions and locations with relatively flat terrain and vegetation cover extending horizontally about 100 times the sampling height.

In a systematic approach to the study of the carbon cycle, the net CO_2 flux between an ecosystem and the atmosphere is termed Net Ecosystem Exchange (NEE) and is the result of different physiological components. Each component is responsible for a separate flux to or from the atmosphere of which NEE represents the sum (Ruimy et al., 1995); for a grassland ecosystem this concept can be expressed as:

$$NEE = -A + R_l + R_r + R_h \qquad \textbf{(}\textit{Equation 7.1)}$$

Where A is the carbon assimilated from the atmosphere by the photosynthetic process, while R_l, R_r and R_h stand for the carbon released to the atmosphere by leaf (and other aboveground tissues of plants), root and heterothrophic respiration respectively. According to the meteorological conventions positive signs denote an upward flux (release of carbon to the atmosphere).

The integration of NEE over a given period *t* yields the Net Ecosystem Productivity (NEP):

$$NEP = -\int_{t_0}^{t_0+t} NEE\,dt \qquad (\textit{Equation 7.2)}$$

that is by definition positive when the ecosystem sequesters atmospheric carbon.

The gross primary productivity (GPP), that quantifies the amount of carbon assimilated by photosynthesis, can be derived as:

$$GPP = -\int_{t_0}^{t_0+t} (NEE - R_l - R_r - R_h)dt \qquad (Equation\ 7.3)$$

The computation of eq. 7.3 requires the knowledge of the ecosystem respiration (R_{eco}) given by the sum of the terms R_l, R_r and R_h. Neglecting the difference between day-time and night-time ecosystem respiration, R_{eco} is retrieved by a temperature response function of night-time NEE, that in absence of the photosynthetic process, equals the efflux of CO_2 to the atmosphere.

7.2 Monitoring periods at the sites of Hakasia and Tuva and objectives.

The eddy covariance technique was applied to monitor the net carbon exchange at three sites of Hakasia (Hak2, Hak3, Hak1) that represent respectively the early (5 years), intermediate (10 years) and final (climax) stage of an old field ecological succession.

Measurements at Hak1 started in July 2002 and lasted until December 2004 with some breaks during cold months (Jan-Apr 03, Nov-Apr 04) when the vegetative activity was absent. At the other sites the eddy covariance systems were running in parallel with Hak1 although for limited periods (Hak2, Jul 02-Jun 03; Hak3, May 04-Dec 04) that were nevertheless long enough to characterize the CO_2 exchange during the whole vegetative season and some winter months, allowing to assess the carbon balance on a 12 months basis.

The issues addressed by the study were:

(i) the assessment of the carbon budget

(ii) the partitioning of the net CO_2 flux (NEE) into the components of assimilation (GPP) and ecosystem respiration (R_{eco}), and the characterization of their seasonal and interannual variability.

(iii) the analysis of the response of GPP and R_{eco} to the main environmental drivers (temperature, soil moisture, solar radiation, vapour pressure deficit).

These issues were analyzed under the perspective of the carbon cycling dynamics over the temporal stages of the old field succession. Moreover, the attention was focused on the impact that a fire, burst in March 2004 at Hak1, had on the carbon balance of the same year and on the ecosystem functionality in respect with of CO_2 exchanges with the atmosphere. Results are illustrated in §7.4.

A short term record of eddy covariance measurements was additionally collected in July 2003 over a dry true steppe of Tuva. Results, presented in §7.5, are discussed addressing in particular the observed daily trends of NEE and their transitory perturbation as effect of rain events.

7.3 Materials and methods

7.3.1 Theoretical background

The atmosphere contains turbulent motions of upward and down ward moving air that transport trace gases such as CO_2. The eddy covariance samples these motions to determine the net difference of material moving across the canopy-atmosphere interface. In practice this task is accomplished by statistical analysis of the instantaneous vertical mass flux density, using Reynolds rules of averaging (Reynolds, 1985). The product of this operation is a relationship that expresses the mean flux density of CO_2 expressed over some time span (commonly between 30 and 60 minutes) as the covariance between fluctuations in vertical velocity (w) and the CO_2 mixing ratio ($c = \rho_c / \rho_a$, where ρ_a is air density and ρ_c is CO_2 density):

$$F = \overline{\rho_a} \cdot \overline{w'c'} \qquad \textit{(Equation 7.4)}$$

The overbars in the formula above denote time averaging and the primes represent fluctuations from the mean. As a convention, a positively signed covariance represents net CO_2 transfer into the atmosphere and a negative value denotes an uptake of CO_2 from the atmosphere by the underlying canopy. The same formula would apply to calculate the flux density of any other trace gas taking into account the covariance of the fluctuations in vertical velocity and the mixing ratio of the chemical species. The equation defining the conservation of mass provides theoretical guidance for implementing the eddy covariance technique.

The conservation of a general scalar is:

$$\frac{\delta \rho_s}{\delta t} + u\frac{\delta \rho_s}{\delta x} + v\frac{\delta \rho_s}{\delta y} + w\frac{\delta \rho_s}{\delta z} = S + D \qquad \textit{(Equation 7.5)}$$

Where ρ_s is the scalar density, u,v, and w are the wind velocity components, respectively in the direction of the mean wind (x), the lateral wind (y) and normal to the surface (z). S is the source/sink term and D is molecular diffusion. After application of the Reynolds decomposition where: $u = \bar{u} + u', v = \bar{v} + v', w = \bar{w} + w', \rho_s = \overline{\rho_s} + \rho_s'$, with the overbars characterizing time averages and the primes indicating fluctuations around the average, and after integration along z and assumption of no horizontal flux divergence, we obtain:

$$\int_0^{h_m} S dz = \overline{w'\rho_s'} + \int_0^{h_m} \frac{\delta \overline{\rho_s}}{\delta t} dz + \int_0^{h_m} \bar{u}\frac{\delta \overline{\rho_s}}{\delta x} dz + \int_0^{h_m} \bar{w}\frac{\delta \overline{\rho_s}}{\delta z} dz \qquad \textit{(Equation 7.6)}$$

I II III IV V

In equation 7.6 the term I represents the scalar source/sink which corresponds to the net ecosystem exchange (NEE) when the scalar is CO_2; term II represents the eddy flux at the height h_m (the height at which instruments are installed) and is noted as F_c for CO_2. Under conditions of atmospheric stationarity and horizontal homogeneity, all other terms on the right-hand side of equation 7.6 decay and the measurement by eddy covariance is equivalent to the source/sink term. However these conditions are not always met and also the other terms have to be taken into account. Term III represents the storage of the scalar below the measurement height. Storage term is positive when CO_2 produced by respiratory effluxes accumulates in the ecosystem, particularly under the canopy of dense vegetation: this phenomenon may be observed during night-time hours with calm winds and poor turbulent mixing conditions. Although the average of the storage term is zero over a daily cycle, making this term not affecting long term summations of NEE, in the short term it may be an important part of the CO_2 exchanged by the ecosystem and it should be taken into account.

Term IV represents the flux by horizontal advection and is significant when horizontal gradient of the scalar exists, as in the case of non homogeneous terrain or at night over sloping terrain, when the CO_2 produced by respiration is removed by drainage. Term V represents the flux by vertical advection: vertical velocity (w) and consequently vertical advection term were found typically to be zero over low crops (Aubinet et al., 2000), while above tall vegetation such as forest canopies this mechanism is not negligible.

Few experiments aimed at quantifying advective transport of CO_2 in forest ecosystems were conducted in recent years (Aubinet et al., 2003; Marcolla et al., 2005; Feigenwinter, 2004), and indicate that advection fluxes were usually significant during calm nights. However, in most cases, the measurement uncertainty was too large to allow their precise estimation, suggesting that advection measurement systems should be improved in order to enable such estimates to be made. In this sense, particular attention should be paid to the estimation of the vertical velocity above the canopy and to the vertical profiles of the horizontal velocity and horizontal CO_2 gradient below the canopy. On the other hand, direct measurements of advective fluxes require a very complicated set up to allow at today routine measurements at each site.

7.3.2 Implementation of eddy covariance flux measurements.

Continuous measurements of wind speed along three orthogonal components (u,v,w), sonic temperature (T_s), CO_2 (ρ_c) and water vapour (ρ_v) molar densities were carried out with an array of instruments including a 3D sonic anemometer (1012R3, Gill Instruments, UK) and a fast response open path infra-red gas analyzer (LI7500, LiCor Inc., USA) mounted on the top of a 4.5 m tower. The raw data from each 30 min. period were recorded at a rate of 20 Hz and stored into separate files on a laptop computer. Calibration of the IRGA was done at regular intervals of 1 month for CO_2 using a gas mixture referenced to NOAA/CMDL standard. Zeroes for both CO_2 and water

vapour channels were calibrated with pure N_2 gas. The eddy flux system used approximately 4 A at 12 V and was powered by six 12V -190 Ah batteries which were charged daily for 2 hours by a generator placed 50 m E from the tower, downstream of dominant winds. In case exhaust gases were blown towards the tower, data collected during the operation of recharge were rejected.

	Hakasia			Tuva
Site / Variable	Hak1	Hak2	Hak3	Yamaligh
PPFD	●	●	●	
Diffuse PPFD	●			
Rg		●	●	●
Rn	●	●	●	●
T air (2.5m)	●	●	●	●
RH (2.5m)	●	●	●	●
Precipitation	●			
Atm. Pressure	●			●
T soil (-0.05, -0.1 m)	●	●	●	●
SM (0-0.3m)	●	●	●	●
G (-0.05m)	●	●	●	●

Table 7.1. Atmospheric and soil physical variables measured (●) at the micromteorological stations in Hakasia and Tuva.

Standard meteorological and soil parameters were measured continuously: photosynthetic photon flux density (PPFD), diffuse PPFD, global radiation (Rg) and net radiation (Rn) were measured at the height of 3 m by quantum sensors (SKP215, SKP1110, Skye, UK) and a net radiometer (Q7, REBS, USA), respectively. Air temperature (Tair) and relative humidity (RH) were measured at the height of 2.5 m with a shielded sensor (HP102, TecnoEl, Italy). Precipitation was measured with a tipping bucket rain gauge (ARG100, TecnoEl, Italy), atmospheric pressure was measured by a barometer (TP800, TecnoEl, Italy). Soil temperature (Tsoil) was measured at the depths of 0.05 and 0.1 m by thermistors (107, Campbell Scientific, UK) and soil moisture (SM) was measured with a time-domain reflectometer (CS615, Campbell Scientific, UK) as an averaged value up to the depth of 0.3 m. Soil heat flux (G) was measured by a heat flux plate (HFT1, Rebs, USA) buried at the

depth of 0.05m. All channels from sensors were scanned every 30 seconds and data were stored as 30 minute averages by a data-logger (CR10X, Campbell Scientific, UK).

The physical parameters measured at each station are listed in table 7.1. The equipment used in the campaigns included two sets of instruments of the same type and model. One set was reserved for the site of Hak1 and the second set was moved around different locations according to the scientific plan. Some instruments were not included in both sets: precipitation data for the sites of Hakasia refer to the Hak 1 site, where the only rain gauge was installed; atmospheric pressure was measured at Hak1 only, justified by the small differences in elevation among sites in Hakasia. Global radiation and PPFD, needed in the data processing, when not both available, were mutually retrieved by the relation Rg [Wm^{-2}]=0.52 PPFD [$\mu mol\ m^{-2}\ s^{-1}$].

7.3.3 Data processing.

Raw data were elaborated online by the software MASE (Manca, 2003), that performs statistical calculations on the high frequency (20Hz) raw data. First and second order statistical moments of the components wind speed vector and of the measured scalars were computed for 30 minutes time intervals after transformation of the instantaneous values by a linear detrending algorithm. A 3D coordinate rotation was applied to the raw means and second moments of wind speed in order to align *u* parallel to mean wind speed to nullify *v* and *w* (first and second rotations) and to nullify the lateral momentum flux density ($\overline{w'v'}$) (third rotation). The third rotation was applied for angles up to 10°, otherwise omitted.

7.3.3.1 Computation of fluxes.

7.3.3.1.1 Sensible heat flux

The flux of sensible heat is defined as:

$$H = \rho_m C_p \cdot \overline{w'T'} \qquad \textbf{(}\textit{Equation 7.7)}$$

Where ρ_m is the density of moist air [kg m^{-3}], C_p is the specific heat of moist air (1110 J $K^{-1}kg^{-1}$), and $\overline{w'T'}$ is the covariance between fluctuations of the vertical wind speed and the air temperature. The air temperature (T) is deduced from sonic temperature (T_s) using:

$$T_s = T\ (1 + 0.51 \cdot q) \qquad (\textit{Equation 7.8}\textbf{)}$$

where q is the specific humidity given by the ratio of the weight of water vapour [g H_2O] and the weight of air [g air].

The covariance of vertical wind speed and air temperature ($\overline{w'T'}$) can be calculated according to Liu et al. (2001), on the basis of $\overline{w'T_s'}$, using the following:

$$\overline{w'T'} = \overline{w'T_s'} - 0.51 \cdot \overline{w'q'} \cdot \overline{T} + \frac{2 \cdot \overline{T}}{\overline{c^2}} \cdot (\overline{u'v'} \cdot \overline{u} \cdot A + \overline{v'w'} \cdot \overline{v} \cdot B) \qquad \textit{(Equation 7.9)}$$

where c is the speed of sound , A and B are factors depending on the geometry of the anemometer used.

The application of equations 7.8 and 7.9 to derive T and $\overline{w'T'}$ requires the knowledge of q that can be calculated only knowing the mixing ratio of water vapour (v), not measured by an open path IRGA. For this reason the sonic temperature (T_s) was used as an approximation of the air temperature (T) in all the algorithms used for flux calculation. As a consequence the covariance $\overline{w'Ts'}$ is systematically higher than the covariance $\overline{w'T'}$ calculated as in eq.7.8 and the magnitude of the bias is related to the magnitude of the water vapour flux. Manca (2003) reports an average overestimation of 10% analyzing data collected over a temperate forest.

7.3.3.1.2 Carbon dioxide and latent heat fluxes

The use of an open path gas analyzer to measure CO_2/H_2O has an impact on the computation of the flux covariance. This sensor does not measure the mixing ratio (c,v) but the molar density (ρ_c, ρ_v) expressed in [moles m^{-3}] which in principle may vary by adding molecules to or removing them from a controlled volume or by changing the size of the controlled volume. The last is done when pressure, temperature and humidity change in the atmosphere. When measuring the eddy flux covariance in terms of molar density, then the flux density of CO_2 (F_c) and H_2O (F_w) across the atmosphere-ecosystem interface is expressed as:

$$F_c = \overline{w\rho_c} = \overline{w'\rho_c'} + \overline{w}\,\overline{\rho_c} \qquad \textit{(Equation 7.10)}$$

$$F_w = \overline{w\rho_v} = \overline{w'\rho_v'} + \overline{w}\,\overline{\rho_v} \qquad \textit{(Equation 7.11)}$$

where the second term on the right hand side of the equations 7.10 and 7.11 is the product of the mean vertical velocity and CO_2/H_2O densities. The mean vertical velocity is non zero and arises from air density fluctuations. In practice the magnitude of $\overline{w}$ is too small to be detected by the sonic anemometer, so it is computed on the basis of temperature (T) and humidity density (ρ_v) fluctuations. Accordingly CO_2 flux (F_c) and water vapour flux (F_w) were calculated as the product of the mean covariance of vertical wind speed fluctuations (w') and the CO_2/H_2O density

fluctuations (ρ'_c, ρ'_v) added by terms to account for air density fluctuations over mean vertical velocity according to the equation (Webb, Pearman, Leuning, 1980):

$$F_c = \overline{w'\rho'_c} + \frac{m_a}{m_v}\frac{\overline{\rho_c}}{\overline{\rho_a}}\overline{w'\rho'_v} + \left(1 + \frac{\overline{\rho_v} m_a}{\overline{\rho_a} m_v}\right)\frac{\overline{\rho_c}}{\overline{T}}\overline{w'T'} \qquad \textit{(Equation 7.12)}$$

$$F_w = \left(1 + \frac{\overline{\rho_v} m_a}{\overline{\rho_a} m_v}\right) + \left(\overline{w'\rho'_v} + \frac{\overline{\rho_v}}{\overline{T}}\overline{w'T'}\right) \qquad \textit{(Equation 7.13)}$$

where ρ_a is dry air density, m_a and m_v are molecular weight of air and water vapour respectively.

The latent heat flux (LE) is defined as:

$$LE = \frac{\lambda M_w F_w}{1000} \qquad \textit{(Equation 7.14)}$$

Where M_w is the molar mass of water (0.018015 kg mol^{-1}) and λ (J kg^{-1}) is the latent heat of vaporization of water, which is a function of air temperature:

$$\lambda = (3147.5 - 2.37 \cdot T\ )10^3 \qquad \textit{(Equation 7.15)}$$

7.3.3.2 Spectral corrections

Remembering that the turbulent flow in the boundary layer of the atmosphere is produced by the superimposition of eddies of different size that, if measured at one point generate fluctuations of the measured variables (wind, scalar concentrations) of different frequency, it is common to express the turbulent vertical flux of a scalar (T_s, ρ_c, ρ_v) as the integration between 0 and ∞ of the co-spectral density of the vertical wind and a generic scalar (Kaimal and Finnigan, 1994):

$$\overline{w's'} = \int_0^\infty C_{ws}(f)df \qquad \textit{(Equation 7.16)}$$

where f is the frequency and $C_{ws}(f)$ is the co-spectral density at the frequency f.

In reality the measured turbulent flux $\overline{w's'_{meas}}$, underestimates the whole turbulent flux because the integral range is limited in the low frequency by the observation duration (30min) and by high

pass filtering of original data (linear detrending), and in the high frequency by the response of instruments.

The measured turbulent flux may be thus expressed by the integration over frequencies of the co-spectral density multiplied by a transfer function (TF) characterizing the process:

$$\overline{w's'_{meas}} = \int_0^\infty TF(f)C_{ws}(f)df \qquad \textit{(Equation 7.17)}$$

In order to correct fluxes for spectral losses a correction factor (CF) based on the ratio of the turbulent flux free from high and low pass filtering and the measured turbulent flux is applied:

$$CF = \frac{\int_0^\infty C_{ws}(f)df}{\int_0^\infty TF(f)C_{ws}(f)df} = \frac{\int_0^\infty C_{ws}(f)df}{\int_0^\infty TF_{HF}(f)TF_{LF}(f)C_{ws}(f)df} \qquad \textit{(Equation 7.18)}$$

where the general transfer function is separated into two functions accounting respectively for low (TF_{LF}) and high (TF_{HF}) frequencies. The transfer function characterizing high frequency losses (TF_{HF}) of an eddy covariance system was described by Moncrieff (1997) as the product of individual transfer functions each accounting for a particular instrumental effect.

The software MASE (Manca, 2003) calculates spectral corrections factors to quantify the loss of low and high frequency components of CO_2 and energy fluxes using a combination of a theoretical (Moncrieff, 1997) and experimental methods (Aubinet, 2000) based on the following steps:

1. Calculation of an experimental transfer function for high frequency losses by comparing normalized co-spectra of vertical wind velocity and sonic temperature (which represent the entire turbulent sensible heat flux density without losses) to co-spectra of vertical wind velocity and measured concentrations of CO_2/H_2O.
2. Calculation of transfer functions for high frequency losses due to limited instrumental sampling frequency (T_d) and path averaging (T_w) and combination with the experimental transfer function to obtain a single transfer function for the high frequency losses (TF_{HF}).
3. Calculation of a transfer function (TF_{LF}) for low frequency losses induced by the high-pass filtering effect of the linear detrending.

4. Combination of the retrieved TF_{LF} an TF_{HF} in to the equation 7.18 to calculate the correction factors for the covariances of the vertical wind and the sonic temperature ($\overline{w'Ts'}$), the CO_2 concentration ($\overline{w'\rho_c'}$) and the water vapour concentration ($\overline{w'\rho_v'}$).

The correction factors must be applied to all the covariance terms that appear in the equations (7.7, 7.12, 7.13) to account for spectral losses in H, LE, F_c.

7.3.3.3 Net Ecosystem Exchange

NEE was computed correcting *Fc* for the CO_2 storage term F_{st} (μmol CO_2 $m^{-2}s^{-1}$), based on the one point CO_2 concentration measured by the open-path IRGA.

$$NEE = F_c + F_{st} \qquad \textit{(Equation 7.19)}$$

$$F_{st} = \frac{h\Delta\rho_c}{\Delta t} \qquad \textit{(Equation 7.20)}$$

where $\Delta\rho_c$ is the difference in CO_2 molar density (μmol m^{-3}) between two consecutive records, h is the height of the column of air up to the level of the IRGA (m), Δt is the time interval between two consecutive records (s).

7.3.3.4 Despiking

Flux series were screened for the detection of anomalous values arising from sensors malfunctioning caused in particular by interference of water condensation, rain drops, snow or insects with the optical path of the IRGA. Fluxes associated to CO_2 concentrations out of the typical range of values for the site or to variance of the 30 min signal of CO_2 over an empirical threshold of the 97.5 percentile, were rejected.

Spikes remained in the half hourly were detected by using an algorithm according to Papale et al. (2006).

The algorithm is based on the position of each half hourly value with respect to the values just before and after and it is applied to blocks of 13 days and separately for daytime and night-time data. These night-time and daytime periods have been extended adding one value form the other period at the borders, needed to calculate *di*; night-time data were selected according to a global radiation (*Rg*) threshold of $20Wm^{-2}$, cross-checked against sunrise and sunset data derived from the local time and standard sun geometrical routines. The outlier detection was based on the double-differenced time series, using the median of absolute deviation about the median (MAD).

For each NEEi half hourly data the d value is calculated as:

$$d_i = (NEE_i - NEE_{i-1}) - (NEE_{i+1} - NEE_i) \qquad \textit{(Equation 7.21)}$$

and the value is flagged as spike when:

$$d_i < Md - z \cdot MAD \cdot 0.6745$$

$$d_i > Md - z \cdot MAD \cdot 0.6745$$

where *Md* is the median of the differences, MAD is defined as MAD = median (|di −Md|)
and z is a threshold value.
The z value was set to 5.5, an intermediate threshold, that is more conservative than 4, conventionally used, but less than 7.

7.3.3.5 The underestimation of night-time fluxes and the u_* correction

It was shown by several authors (Aubinet et al., 2000; Gu et al., 2005), that eddy flux measurements can underestimate the net ecosystem exchange during periods with low turbulence and thus limited air mixing.
This underestimation acts as a selective systematic error: it only occurs during the night when there is a net emission of CO_2 by the ecosystem leading to an underestimation of the ecosystem respiration and to biased (overestimated) carbon sequestration.
The most probable cause of error is the presence of small scale movements associated with drainage flows or land breezes that take place in low turbulence conditions and create a decoupling between the soil surface and the canopy top (Massman and Lee, 2002). In these conditions, advection becomes an important term in the flux balance and cannot be neglected.
To overcome the night flux problem the data corresponding to low turbulence periods, individuated as those below a certain threshold of friction velocity (u_*), are rejected and replaced (gapfilled) by a modelled flux based on turbulent conditions. The friction velocity (Stull, 1988) is defined as:

$$u_* = \left[\overline{u'w'}^2 + \overline{v'w'}^2\right]^{\frac{1}{4}} \qquad \textit{(Equation 7.22)}$$

The u_* correction should be applied after adding to Fc the flux storage term (F_{st}) in order to avoid a double count of the CO_2 stored in the canopy air that would be removed by the turbulence as soon as it restarts in the early morning. An accurate assessment of the storage term would imply the monitoring of a CO_2 concentration vertical profile in the canopy. Nevertheless this estimation is often based solely on the CO_2 concentration at the tower top which, in forest ecosystems, is known to yield an insufficient quantification of the CO_2 stored in the canopy air since it does not take into account the large concentration increase in the lower air layers.

7.3.3.6 The u_* threshold selection and uncertainty

The u_*-threshold was specifically derived for each site using a 99% threshold criterion on night-time data as described by (Reichstein et al., 2005). For the determination of the u_*- threshold, the data set is split into six temperature classes of equal sample size (according to quantiles) and for each temperature class, the set is split into 20 equally sized u_*- classes. The threshold is defined as the u_*-class where the average night-time flux reaches more than 99% of the average flux at the higher u_*-classes. The threshold is only accepted if for the temperature class, temperature and u_* are not or only weakly correlated ($|r|<0.4$) The final threshold is defined as the median of the thresholds of the (up to) six temperature classes. This procedure is applied to the subsets of four 3-month periods (January–March, April–June, July–September and October–December) to account for seasonal variation of vegetation structure. The u_*-threshold is reported for each period, but the whole data set is filtered according to the highest threshold found (conservative approach). To be more conservative, in addition to the data acquired when u_* was below the threshold, the first half hour measured with good turbulence conditions after a period with low turbulence is also removed. This procedure is repeated 100 times within a bootstrapping technique to asses the uncertainty of the u_* threshold. The u* thresholds found for the sites of Hakasia are reported in table 7.2.

Site	Hak1 (2002)	Hak1 (2003)	Hak1 (2004)	Hak2	Hak3
u* [ms^{-1}]	0.039	0.042	0.057	0.042	0.033

Table 7.2. Values of u_* threshold for the rejection of night-time CO_2 flux data calculated according to Reichstein et al. (2005)

7.3.3.7 Gapfilling

The gap-filling of the eddy covariance data was performed through methods that are similar to the Look Up Table (LUT) and Mean Diurnal Variation (MDV) methods described in Falge et al. (2001), but that consider both the covariation of fluxes with meteorological variables and the temporal auto-correlation of the fluxes.

In the algorithm used (Reichstein et al, 2005), three different conditions are identified:

1. Only the data of direct interest are missing, but all meteorological data are available

2. Also air temperature or VPD is missing, but radiation is available

3. Also radiation data is missing.

In case (I), the missing value is replaced by the average value under similar meteorological conditions within a time-window of ±7 days. Similar meteorological conditions are present when Rg, Tair and VPD do not deviate by more than 50 Wm^{-2}, 2.5 °C, and 5.0 hPa, respectively. If no similar meteorological conditions are present within the time window, the averaging window is

increased to ±14 days. In case (II) the same approach is taken, but similar meteorological conditions can only be defined via Rg deviation less than 50Wm^{-2} and the window size is first not further increased. In case (III) the missing value is replaced by the average value at the same time of the day (±1 h), i.e. by the mean diurnal course. In this case, the window size starts with ±0.5 days, i.e. similar to a linear interpolation from available data at adjacent hours. If after these steps the values could not be filled, the procedure is repeated with increased window sizes until the value can be filled.

7.3.3.7.1 Gapfilling of winter time NEE

Large gaps in data during winter months, when the eddy covariance stations were not operative, were filled assuming NEE=R_{eco} and modeling the soil temperature response of R_{eco} by the non-linear regression method (Falge et al., 2001). The parameterization of an exponential function (equation 7.23) was based on the 30 min. NEE data collected during the months of November and December although for periods of different duration depending on the site and on the year of measurement.

$$NEE_{winter} = R_{eco} = a \cdot e^{bT_{soil}} \qquad \textit{(Equation 7.23)}$$

where NEE_{winter} is the net ecosystem exchange when vegetation is not active (November-April), a and b are fitted parametes and T_{soil} is the soil temperature measured at the depth of 5cm.

Site		Coefficient	Std. Error	t	P
Hak1	a	0.182	0.006	26.385	<0.0001
	b	0.208	0.012	16.686	<0.0001
	R^2	0.045			
Hak2	a	0.122	0.013	9.100	<0.0001
	b	0.255	0.013	20.008	<0.0001
	R^2	0.249			
Hak3	a	0.151	0.019	7.962	<0.0001
	b	0.269	0.033	8.160	<0.0001
	R^2	0.0867			

Table 7.3. Parameters and R^2 of the exponential function used for winter time NEE at sites of Hakasia (NEE=R_{eco}=ae^bT_{soil}).

Since temperature record was available for the site of Hak1 only, winter soil temperature at the other sites was derived from a linear relation with T_{soil} measured at Hak1: ($T_{soil\text{-}Hak3}$=1.097($T_{soil\text{-}Hak1}$)-0.6282, R^2=0.962; $T_{soil\text{-}Hak2}$=0.7683 ($T_{soil\text{-}Hak1}$)-0.5667, R^2=0.962). Gaps in winter soil temperature, as occurred after the fire event of 4 March 04 at Hak1 that caused the destruction of the temperature sensor, were filled by linear interpolation.

7.3.3.8 Flux partitioning

The partitioning of NEE into the component of GPP was obtained as:

$$GPP = R_{eco} - NEE \qquad \textit{(Equation 7.24)}$$

where the ecosystem respiration, R_{eco}, was retrieved applying the algorithm by Reichstein et al. (2005), that derives a short-term temperature sensitivity of R_{eco} from eddy covariance data based on the exponential regression model (Lloyd & Taylor, 1994):

$$R_{eco} = R_{ref} e^{E_0 (1/(T_{ref} - T_0) - 1/(T - T_0))} \qquad \textit{(Equation 7.25)}$$

Regressions were performed for subperiods of 15 days, with consecutive time windows overlapping 10 days, in order to estimate the temperature sensitivity parameter E_0, setting the reference temperature to 10°C and keeping constant the parameter T_0 at -46.02°C as in Lloyd and Taylor (1994). After an E_0 parameter representative for the whole monitoring period was estimated, the temperature independent level of respiration (R_{ref}) was estimated for consecutive 4 days periods by nonlinear regression using the Lloyd & Taylor model, fixing all parameters except R_{ref}.. R_{ref} parameters estimated were assigned to the "centre of gravity" of the data of each period and were then linearly interpolated between the estimates producing a continuous time series.

7.3.4 Quality control

7.3.4.1 Energy balance closure

To assess the accuracy of eddy covariance measurements, the sum of turbulent heat fluxes is compared with the available energy, that is the net radiative flux minus storage flux densities in the air, the soil and the biomass. The slope of the linear regression expressing the relation between the sum of sensible heat (H) and latent heat (LE), including storage terms, versus the difference of net radiation (Rn) and soil heat flux (G) indicates the energy balance closure.

$$H + LE + st. = a_0 + a_1(R_n - G) \qquad \textit{(Equation 7.26)}$$

Where a_1 is the slope of the linear fit and a_0 is the intercept on the y axis.

In order to test the energy balance closure, it is necessary to compute the heat storage (*st.*) within the canopy. In the case of this study, since the temperature of biomass was not monitored, the storage term included only the heat storage in the air (sensible S_a, and latent S_w, heat), and in the soil (S_g), computed as:

$$S_a = \int_0^{hm} \rho_a C_p \frac{dT}{dt} dz \qquad \textit{(Equation 7.27)}$$

$$S_w = \int_0^{hm} \lambda M_w \frac{d\rho_v}{dt} dz \qquad \textit{(Equation 7.28)}$$

$$S_g = \int_0^{z_r} \rho_s c_s \frac{dT_s}{dt} dz \qquad \textit{(Equation 7. 29)}$$

where $\rho_{a(s)}$, are the air and soil density (kg m^{-3}), C_p is the air specific heat (J K^{-1} kg^{-1}), and $T_{a(s)}$ are the air and soil temperature (K), λ the latent heat of vaporisation of water (J kg^{-1}), ρ_v is the molar density of water vapour (mol m^{-3}), M_w is the molar weight of H_2O and z_r the depth of soil heat flux plates (0.05m).

As for the CO_2 storage, the derivatives were approximated by finite differences between two successive measurements while the integrals are approximated by weighted sums of the measured variables at different heights The dry soil specific heat was taken as 850 J kg^{-1} K^{-1} (Campbell, 1985) and the dry soil density was measured by sampling at each site.

The energy balance closure at sites in Hakasia, obtained taking into consideration 30 min. data, (fig 7.1, 7.2, 7.3) was between 78% and 90%, a result in agreement with the mean imbalance in the order of 20% found for the sites of the FLUXNET network (Wilson et al., 2002).

7.3.4.2 Stationarity Test and Integral Turbulence Test

Additionally, the stationarity test and the integral turbulence characteristics tests (Foken and Wichura, 1996) were applied in combination with the flagging scheme of Mauder and Foken (2004) to assess the data quality.

In the stationarity test, 30 minute mean covariances between the vertical velocity component and a measured scalar (CO_2, H_2O, Ts), are compared with the 6 covariance values averaged over 5 minute periods (part of the same 30 minute period).

In the integral turbulence characteristics test, the comparison is between semi-empirical (function of atmospheric stability) and measured values of the quotient between standard deviation of vertical velocity, horizontal velocity and/or temperature and u*, depending on the flux in case (vertical velocity is applied to all fluxes).

For both tests if the difference (in the case of stationarity test the largest difference of the 6 sub-sets) is lower than 30%, the correspondent calculated flux is flagged 0 in the test, if it is between 30% and 100% is flagged 1 and if the difference is higher than 100% is flagged 2.

Results of the tests are combined to produce a single flag value in such in a way that if both test result in flag 0, then the final flag is 0; if at least one result in flag 1, then the final flag is 1; finally, if at least one is flagged 2, then the final flag is 2.

The flag 0 represents data of highest quality, capable of use in fundamental research; flag 1 is for data for use in long term observation programs; and flag 2 is for bad quality data.

7.3.4.3 Footprint analysis

The extent to which an upwind source located at a certain distance from the measurement point contributes to the observed flux is termed flux footprint. The footprint analysis is used to estimate the fraction of the flux contributed by the sources within an homogeneous fetch, assuming uniform surface sources.

Inversely it is possible to calculate the upwind distance for a given percentage of cumulated footprint when the adequacy of a fetch in certain wind direction has to be evaluated. Varying footprints can be a source of errors and uncertainties that can affect the data quality, particularly if the ecosystem is inhomogeneous and patchy (Göckede et al., 2006).

A footprint analysis was performed for the sites of Hakasia (Hak1, Hak2, Hak3), considering the fetch at 70% of the cumulated footprint calculated by the software MASE applying the model of Schuepp et al. (1990). The result displayed in fig 7.4, 7.5, 7.6, evidences that the fetch is approximately enclosed in a radius of 500 m, confirming the adequacy of the selected spots for the establishment of the flux towers which were situated at bigger distances from the bordering fields with different vegetation cover.

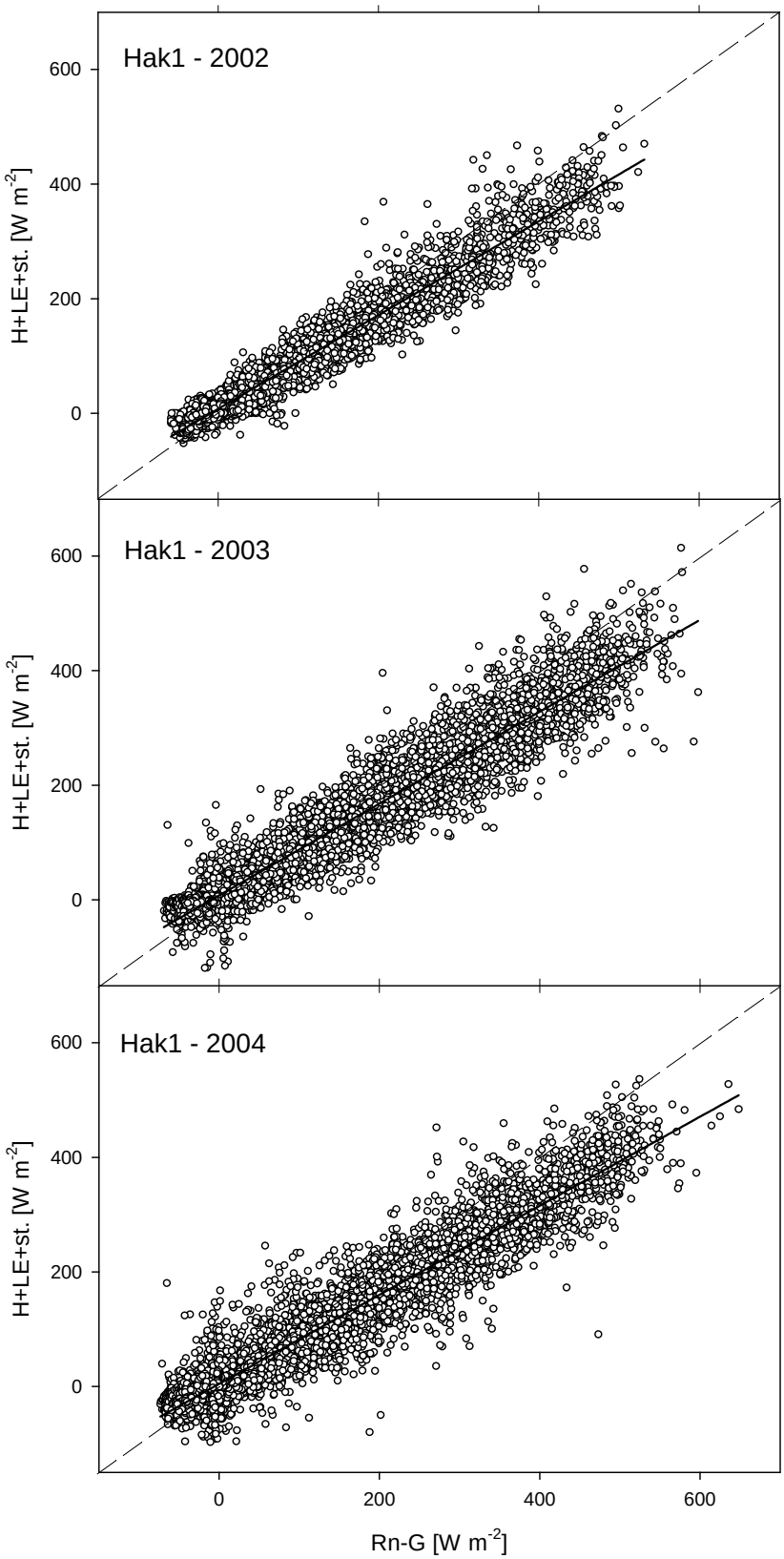

Figure 7.1. Energy balance closure at Hak1 site for the year 2002 (top), 2003 (middle) and 2004 (bottom). The dashed line is the 1:1 slope of the panel, the solid line is the linear regression of the plot.

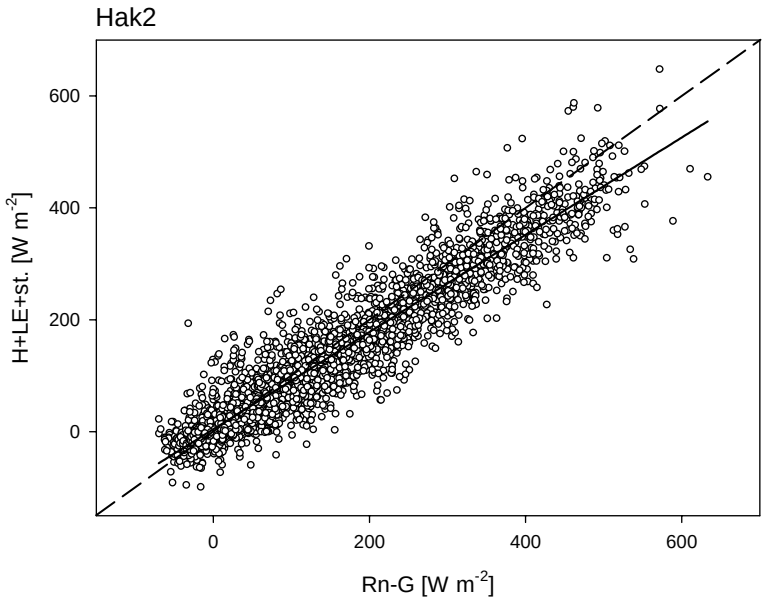

Figure 7.2. Energy balance closure at Hak2 site. The dashed line is the 1:1 slope of the panel, the solid line is the linear regression of the plot.

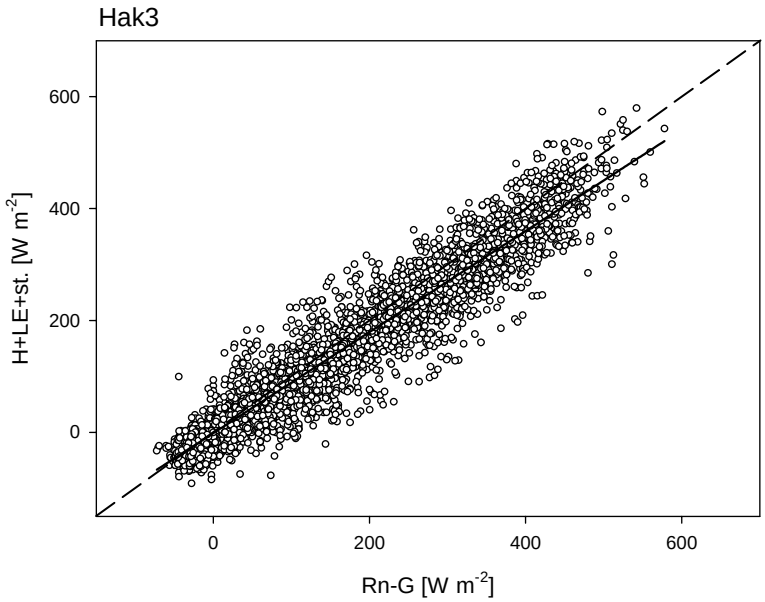

Figure 7.3. Energy balance closure at Hak3 site. The dashed line is the 1:1 slope of the panel, the solid line is the linear regression of the plot.

	a_0	a_1	R^2	n
Hak 1 (2002)	7.605	0.818	0.963	4372
Hak1 (2003)	7.639	0.801	0.954	8307
Hak1 (2004)	4.564	0.777	0.940	10712
Hak 2	4.397	0.868	0.948	5483
Hak3	-1.301	0.902	0.953	8207

Table 7.4. Parameters of the relation $H+LE+st.=a_o+a_1(Rn-G)$ retrieved by linear regression from the plots in fig. 7.1-7.3. The parameter a_1 (slope of the regression line) indicates the degree of closure of the energy balance.

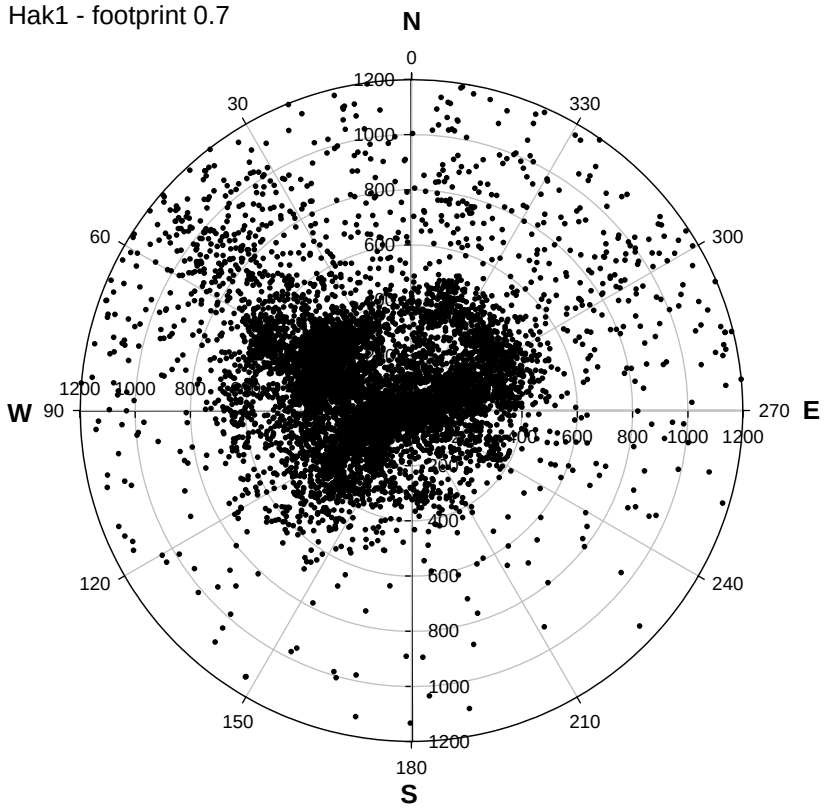

Figure 7.4. Upwind distance (fetch) [m] of measured fluxes at the site of Hak1 for 70% of the cumulated footprint.

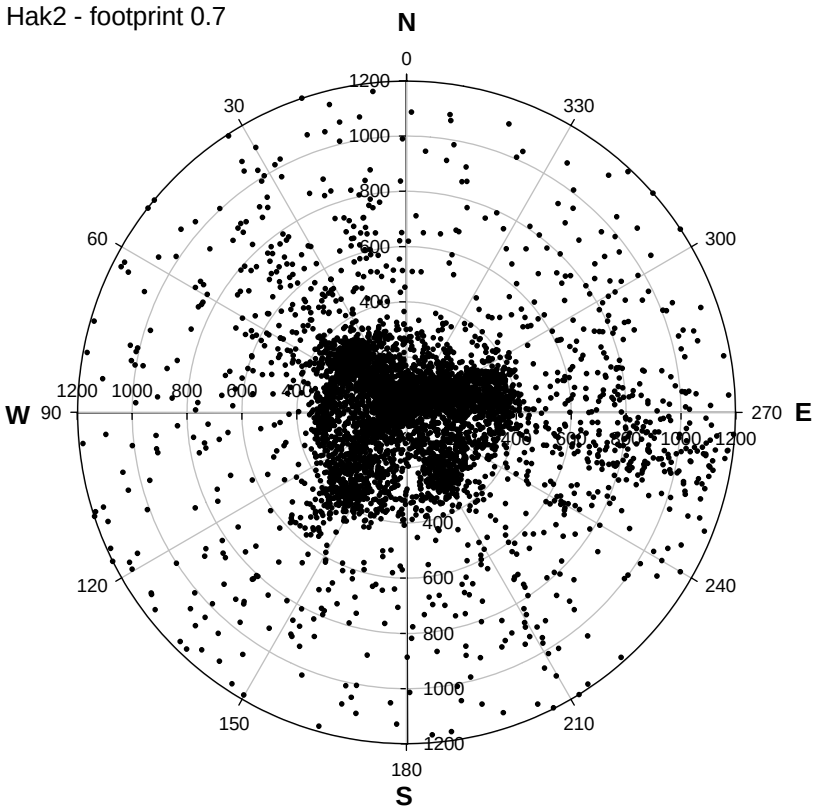

Figure 7.4. Upwind distance (fetch) [m] of measured fluxes at the site of Hak2 for 70% of the cumulated footprint

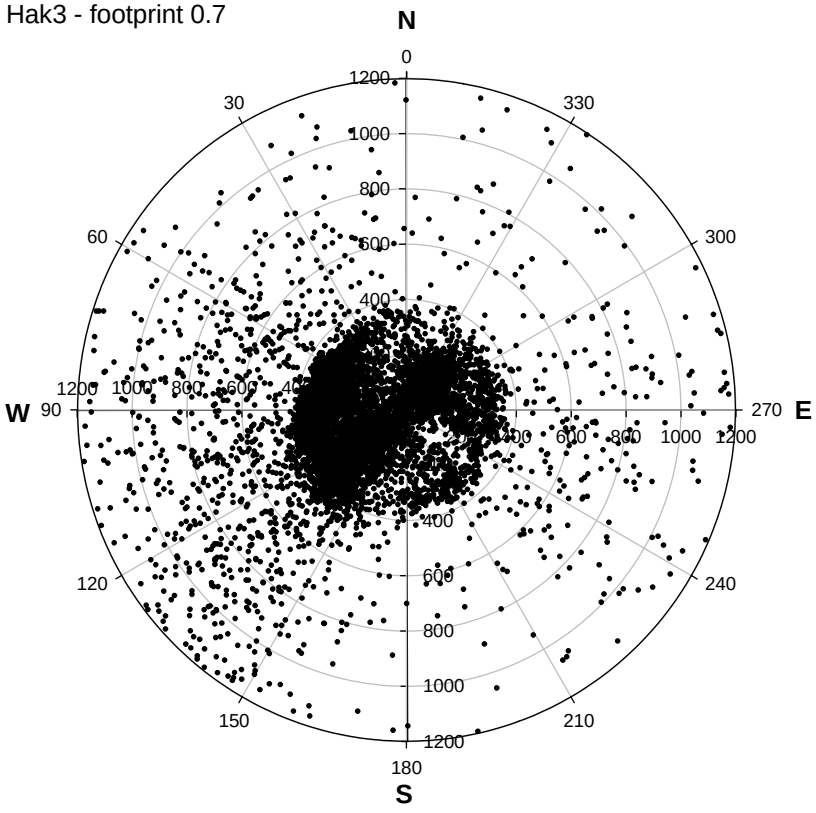

Figure 7.6. Upwind distance (fetch) [m] of measured fluxes at the site of Hak3 for 70% of the cumulated footprint.

7.4 Carbon dioxide fluxes over a true bunchgrass steppe and old field ecosystems of Hakasia.

7.4.1 Daily course of NEE

The monthly average diurnal cycles of NEE is presented in fig. 7.7. The trends reported are limited to the periods when eddy covariance measurements were performed and hence exclude the cold months when NEE was modeled (Jan-Apr 2002, Nov-Apr 2003). Values of NEE are typically positive during night hours due to the CO_2 efflux to the atmosphere due to ecosystem respiration and negative during daytime when assimilation is greater than respiration and the system uptakes carbon, except in winter months when CO_2 is constantly released to the atmosphere although at a very low rate. The integration of average NEE over the daily cycle yields a carbon uptake from May to September. In October CO_2 effluxes prevail on the poor carbon assimilation, determining a net source of CO_2 that becomes smaller in following months when respiratory activity lowers along with temperature.

In 2002 the strongest sink was recorded in August at the site of Hak1 (steppe) when the average diurnal course of NEE reached -4.26 $\mu molCO_2m^{-2}s^{-1}$, while at the site of Hak2 (old field – 5yr) it was observed earlier, in July, and of a greater magnitude (average minimum NEE: -6.05 $\mu molCO_2m^{-2}s^{-1}$). At both sites maximum respiration was observed in July when the average of nocturnal NEE was 2.57 $\mu molCO_2m^{-2}s^{-1}$ and 3.32 $\mu molCO_2m^{-2}s^{-1}$ at Hak1 and Hak2 respectively. The daily cycle of NEE showed a clear daytime uptake until October with a minimum of -0.77 $\mu molCO2m^{-2}s^{-1}$ at Hak1 and a more pronounced uptake of -1.15 $\mu molCO_2m^{-2}s^{-1}$ at Hak2. Since November average respiration ranged between 0.12 and 0.20 $\mu molCO_2m^{-2}s^{-1}$ at both sites. It should be noted that the trend of daily NEE of winter months shows a flexion in the central hours of the day, switching to negative values. In November the mean of minimum NEE was -0.19 $\mu molCO_2m^{-2}s^{-1}$at Hak1 and -0.41 $\mu molCO_2m^{-2}s^{-1}$ at Hak2. Such trend can be explained by the photosynthetic activity of the residual live biomass, at least in the month of November, when temperature during daytime is above the minimum for the process. However it should be also considered that recently, it was suggested that heat dissipation from open path gas analyzers may cause apparent off-season uptake rates (Burba et al., 2006). Since the proposed flux correction assumes a near-vertical exposure of the sensor, whereas in practice the sensor is tilted, and because the method is still being developed, we did not apply any specific correction. Anyway, given the extremely low reduction of NEE and its limited occurrence over the day, this bias has a definitely negligible effect on the carbon balance.

The absolute maximum and minimum NEE recorded in 2002 were -8.43 $\mu molCO_2m^{-2}s^{-1}$ and 4.37 $\mu molCO_2m^{-2}s^{-1}$ at Hak1, while -11.02 $\mu molCO_2m^{-2}s^{-1}$ and 6.95 $\mu molCO_2m^{-2}s^{-1}$ at Hak2.

In 2003 the maximum carbon uptake at Hak 1 was observed in June at Hak1 with an average minimum NEE of -5.71 $\mu molCO_2m^{-2}s^{-1}$ while respiration was highest on average in July (2.65 $\mu molCO_2m^{-2}s^{-1}$). At Hak2 measurements lasted until the first beginning of July: results, in this case not valid for the whole season, show monthly averaged minimum and maximum NEE in June (-10.1 $\mu molCO_2m^{-2}s^{-1}$and 3.19 $\mu molCO_2m^{-2}s^{-1}$ respectively). In comparison, the average respiration at Hak1 in June was 2.40 $\mu molCO_2m^{-2}s^{-1}$.

Absolute maximum and minimum NEE recorded in 2003 were -10.59 $\mu molCO_2m^{-2}s^{-1}$ and 5.70 $\mu molCO_2m^{-2}s^{-1}$ at Hak1 while -15.45 $\mu molCO_2m^{-2}s^{-1}$ and 10.76 $\mu molCO_2m^{-2}s^{-1}$ at Hak2.

In 2004 the month of most intense carbon uptake was June for both sites of Hak1 and Hak3. Minimum NEE was on average -7.98 $\mu molCO_2m^{-2}s^{-1}$ and -7.97 $\mu molCO_2m^{-2}s^{-1}$ for Hak1 and Hak3 respectively. Respiration was on average higher in July at Hak1 (3.82 $\mu molCO_2m^{-2}s^{-1}$) while at Hak3 it was observed in June (3.14 $\mu molCO_2m^{-2}s^{-1}$). The dryness of the month of July caused the peak of carbon uptake to lower on average to -5.31$\mu molCO_2m^{-2}s^{-1}$ when at Hak1 it was maintained at levels close to June (-7.25 $\mu molCO_2m^{-2}s^{-1}$). The month of October 2004 was warmer than in previous monitored years (Δ= +4.28°C than in 2002 and +1.64°C than in 2003) and the observed monthly averaged course of NEE resulted shifted towards an increased source. Absolute maximum and minimum NEE recorded in 2004 were -13.82 $\mu molCO_2m^{-2}s^{-1}$ and 8.71 $\mu molCO_2m^{-2}s^{-1}$ at Hak1 while -14.58 $\mu molCO_2m^{-2}s^{-1}$ and 10.84 $\mu molCO_2m^{-2}s^{-1}$ at Hak3.

7.4.2 Trend of daily integrated NEE

The seasonal pattern of daily integrated NEE (fig. 7.8-7.11) displays an evident carbon uptake starting within the first half of May up to the end of September, except on cloudy days when the systems turn into carbon sources. Some days of net carbon uptake are also possible in October, while isolated winter days with slightly negative NEE (>=-0.5 gC $m^{-2}d^{-1}$) are due to the inability of the despiking procedure to eliminate negative signed spikes in the NEE series beyond the sensitivity of the method.

In the monitored months of 2002 the peak of carbon uptake at Hak1 was -2.81 gC $m^{-2}d^{-1}$ on the 2 nd August. After that the sink strength declined until the CO_2 exchange set to an average winter efflux of 0.15 gC $m^{-2}d^{-1}$. Shortly before the onset of the growing season of 2003 an increase of the source was observed up to its maximum on 27th April (0.48 gC $m^{-2}d^{-1}$). The first day resulted in a net carbon uptake was the 2 nd May (-0.23 gC $m^{-2}d^{-1}$). In the second half of May the sink magnitude rapidly increased up to a maximum of -2.38 gC $m^{-2}d^{-1}$ recorded on 26 th June. The sink activity was sustained until mid August when it was still -2.10 gC $m^{-2}d^{-1}$ on 10 August and declined afterwards as the senescence phase of vegetation progressed. In 2004 a similar seasonal pattern was observed but the maximum uptake was enhanced to -3.64 gC $m^{-2}d^{-1}$ on 9 th June and it was followed by a more rapid decline of the carbon uptake capacity than in 2003.

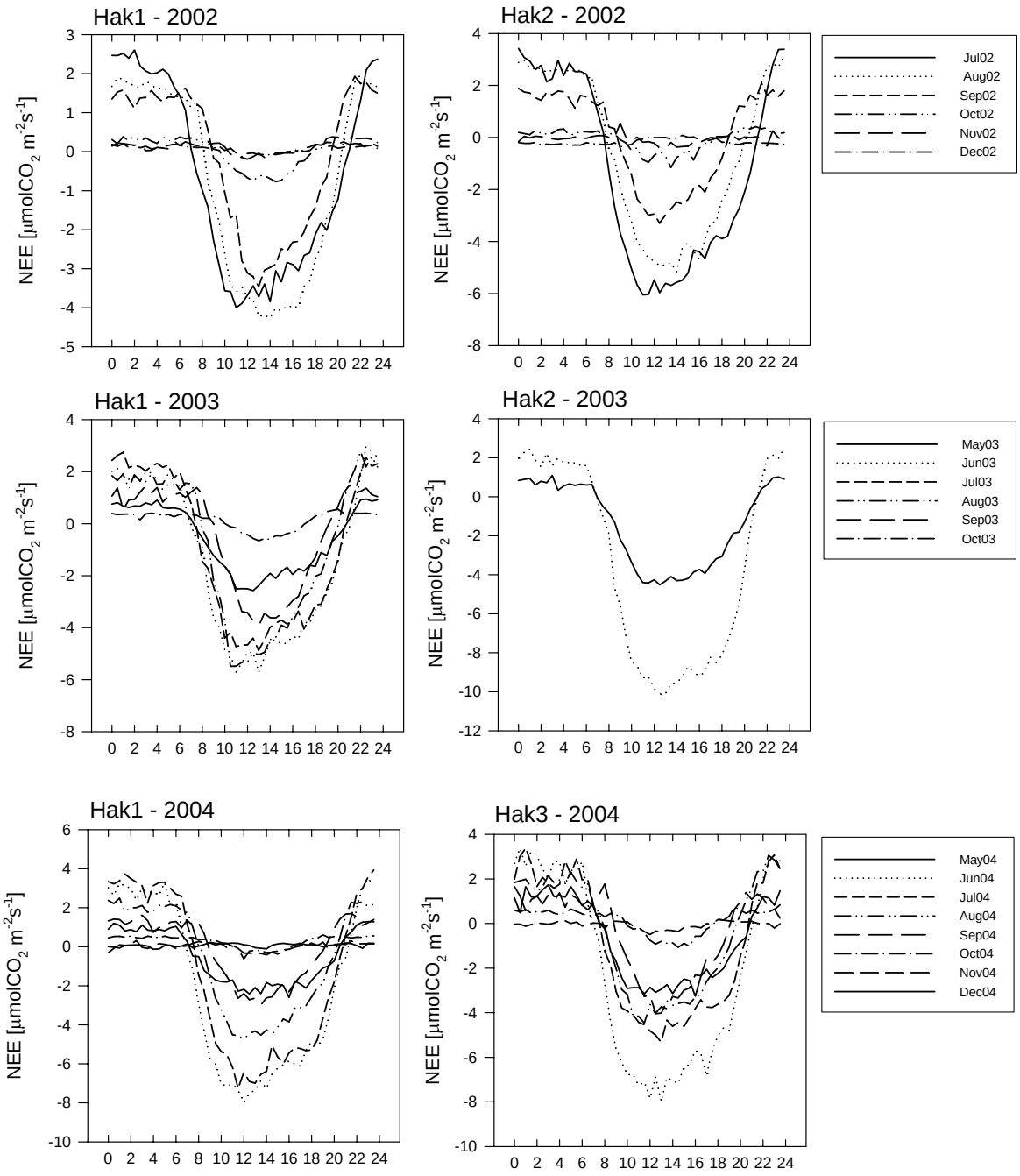

Figure 7.7. Monthly averaged diurnal cycles of net ecosystem CO_2 exchange (NEE) over the natural steppe (Hak1; left column) and the old agricultural field sites (Hak2, Hak3; right column) for the years 2002, 2003 and 2004.

The seasonal pattern of daily integrated NEE of Hak2 was similar to what observed for Hak1 in 2002 although it was characterized by a wider fluctuations. The peak of daily integrated NEE at Hak2 was -2.59 gC $m^{-2}d^{-1}$ in 2002 (4th August), whereas in 2003 the sink was noticeably enhanced reaching -5.39 gC $m^{-2}d^{-1}$ on 7 June.

The trends of daily integrated NEE of Hak3 and Hak1 were almost overlapped until June. The peak of carbon uptake at Hak3 coincided with that of Hak1 in time and magnitude (-3.65 gC $m^{-2}d^{-1}$ on 9

June). However at this site a sensible reduction in carbon uptake is observed in July when the ecosystem acts even as a source (maximum daily NEE: 1.22 gC $m^{-2}d^{-1}$ on 25th July) due to drought.

7.4.3 Partitioning into R_{eco} and GPP

Day to day variability in daily integrated GPP was tightly modulated by daily PPFD and the intensity of daily assimilation was correlated to the amount of live biomass (proxy for leaf area). Nevertheless it should be noted the existence of a lag since the maximum daily GPP always preceded the peak of live biomass and took place during the phase of stem elongation. In 2002 maximum daily GPP at Hak1 was 5.46 gC $m^{-2}d^{-1}$ on 1st August, while at Hak2 it was 6.32 gC $m^{-2}d^{-1}$ on 27th July. In 2003 daily GPP peaked at 5.30 gC $m^{-2}d^{-1}$ at Hak1 on 21st June and at 9.29 gC $m^{-2}d^{-1}$ at Hak2 on 11th June. In 2004 it was 7.30 gC $m^{-2}d^{-1}$ on 27th June at Hak1 and 7.37 gC $m^{-2}d^{-1}$ on 19th June at Hak2. During periods with particular dry environmental conditions given by concurrent high air temperature and vapour pressure deficit, a reduction in daily integrated GPP was observed. This situation can be observed in the GPP trend of Hak1 in the first half of July 2003 and 2004 and even more clearly in that of Hak3 during the first three weeks of July 2004.

Daily integrated R_{eco} was correlated with T_{soil}, and maximum values of daily integrated R_{eco} are reached in July when on average soil temperature is highest. In 2002 maximum daily R_{eco} was 4.18 gC $m^{-2}d^{-1}$ at Hak1 on 21st July and 4.24 gC $m^{-2}d^{-1}$ at Hak2 on 28th July; in 2003 it was 4.07 gC $m^{-2}d^{-1}$ at Hak1 on 23rd July and 6.50 gC $m^{-2}d^{-1}$ at Hak2 on 5th July; in 2004 it was 5.33 gC $m^{-2}d^{-1}$ at Hak1 on 17th July and 4.34 gC $m^{-2}d^{-1}$ at Hak3 on 24th July.
Daily R_{eco} showed also to be linearly dependent on daily GPP. The site specific relations linking daily GPP to daily R_{eco} are the following:

Hak1: $R_{eco}=0.645*GPP+0.172$, $R^2=0.903$, $n=920$
Hak2: $R_{eco}=0.538*GPP+0.226$, $R^2=0.832$, $n=365$
Hak3: $R_{eco}=0.604*GPP+0.160$, $R^2=0.854$, $n=366$

This provides an explanation for the decrease of R_{eco} during drier periods, remarkably at Hak3 in July 2004, when the reduced GPP exerts a stronger control than temperature on the response of ecosystem respiration.

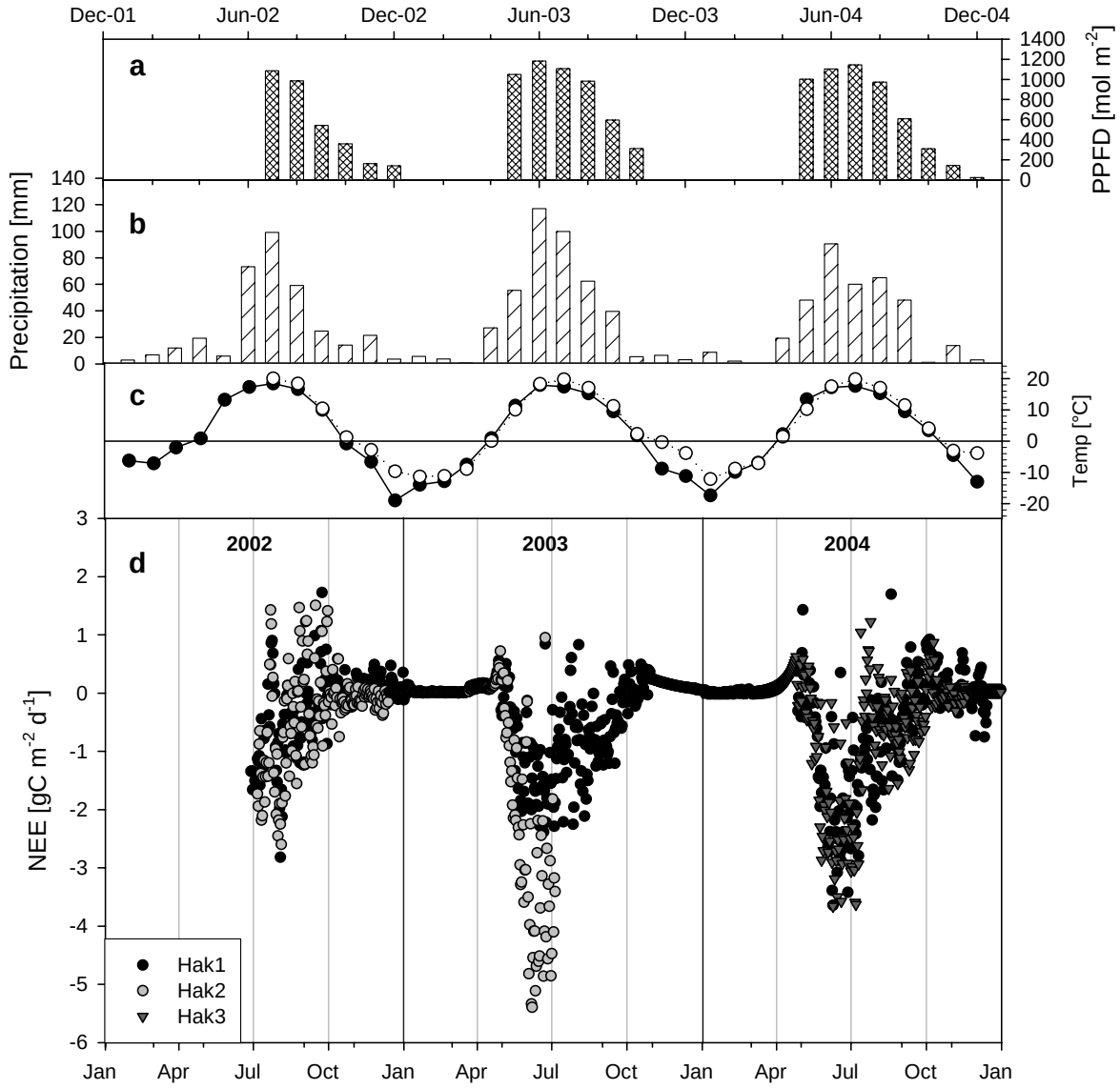

Figure 7.8. A: monthly cumulated photosynthetic photon flux density (PPFD). B: monthly precipitation (data from Hak1 station integrated with data from Shira meteo station for missing months). C: average monthly air temperature and soil temperature (depth:0.1m) measured at Hak1 (solid and open circles respectively); daily net ecosystem exchange (NEE) for the sites Hak1, Hak2 and Hak3.

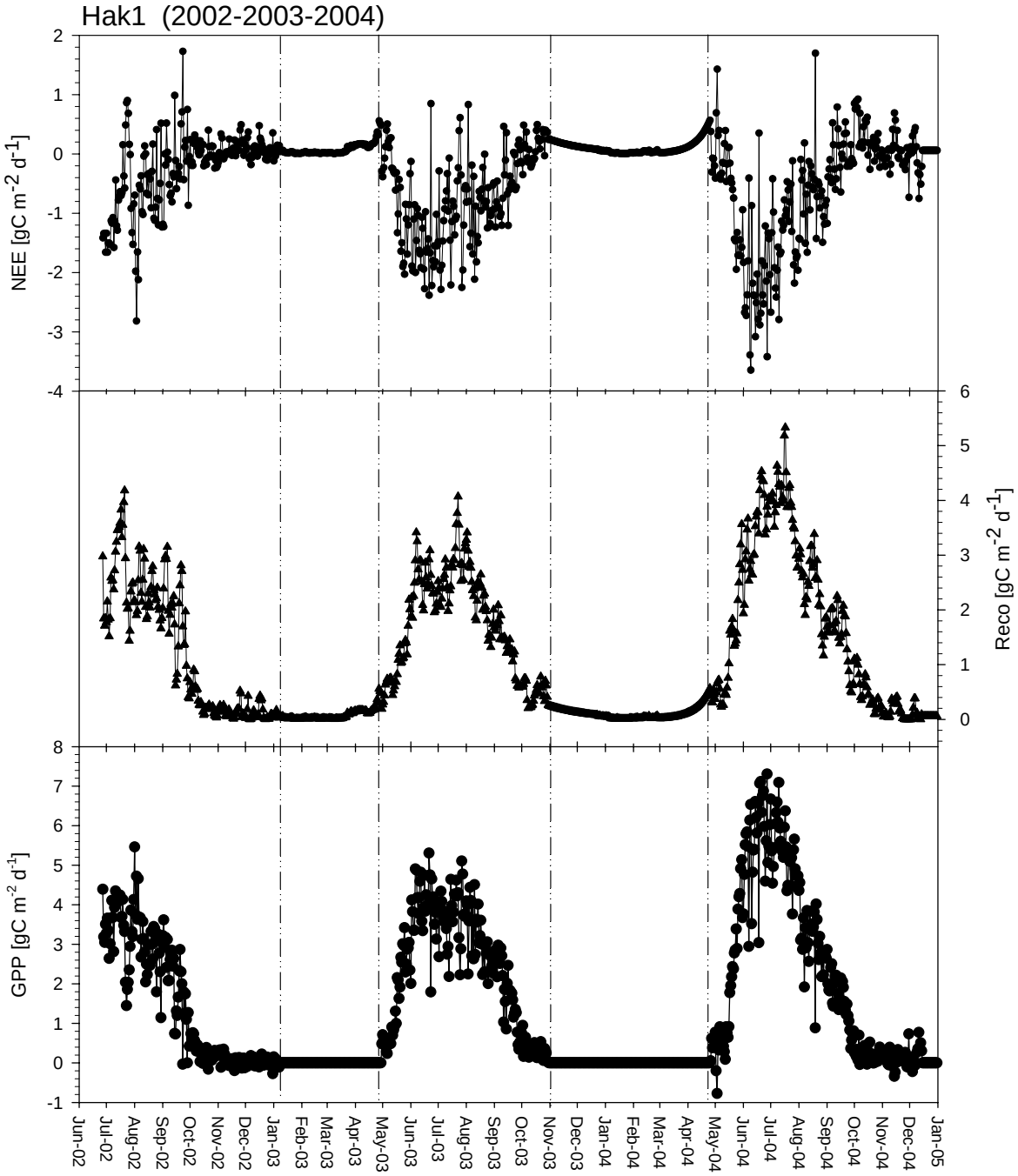

Figure 7.9. Daily integrated net ecosystem exchange (NEE) above the natural steppe site (Hak1) partitioned into ecosystem respiration (R_{eco}, middle panel) and gross primary productivity (GPP, bottom panel). Dashed vertical lines delimitate modelled fluxes during dormant season.

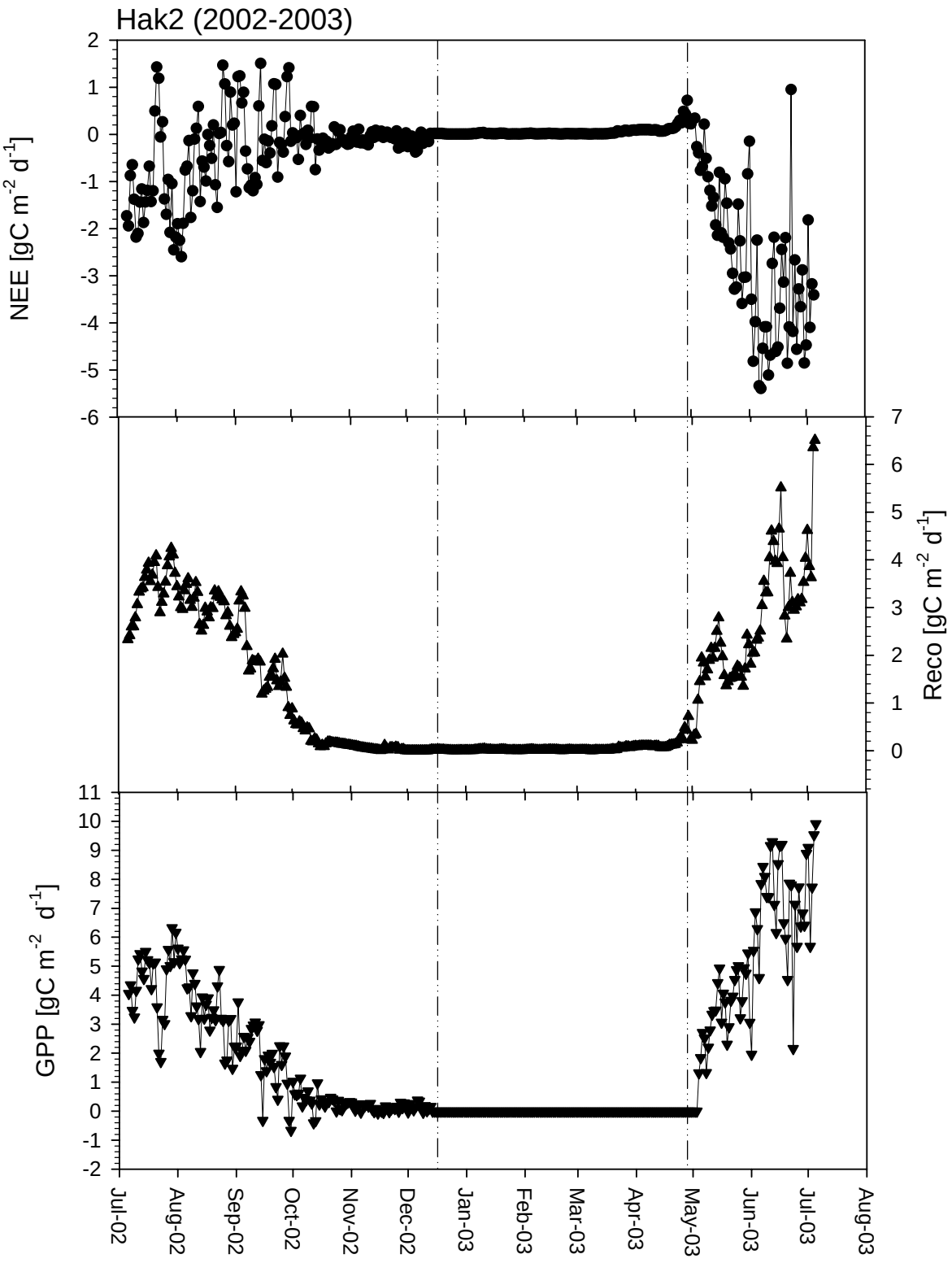

Figure 7.10. Daily integrated net ecosystem exchange (NEE) over the old field site of Hak2 partitioned into ecosystem respiration (R_{eco}, middle panel) and gross primary productivity (GPP, bottom panel). Dashed vertical lines delimitate modelled fluxes during dormant season.

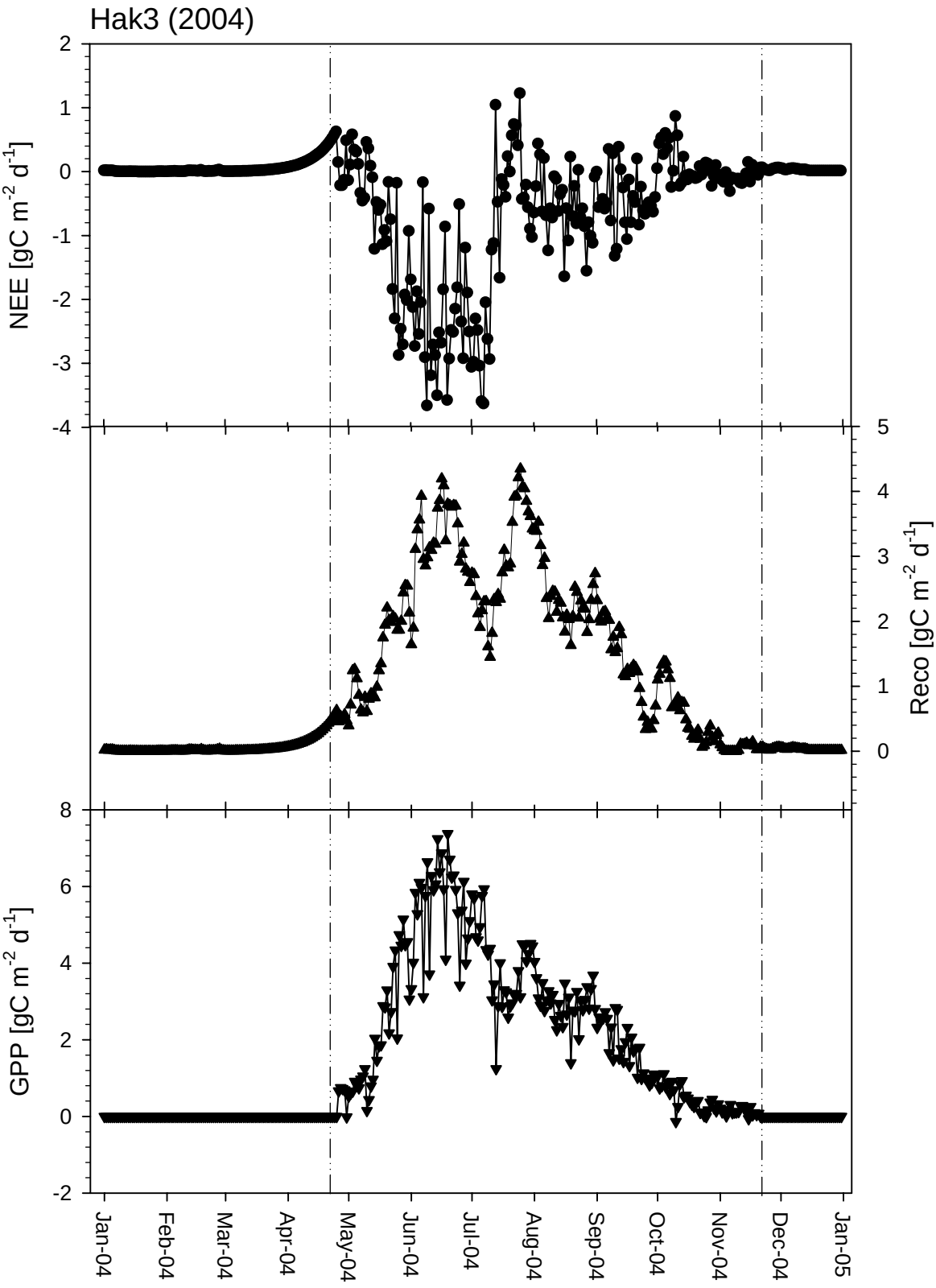

Figure 7.11. Daily integrated net ecosystem exchange (NEE) over the old field site of Hak3 partitioned into ecosystem respiration (Reco, middle panel) and gross primary productivity (GPP, bottom panel). Dashed vertical lines delimitate modelled fluxes during dormant season

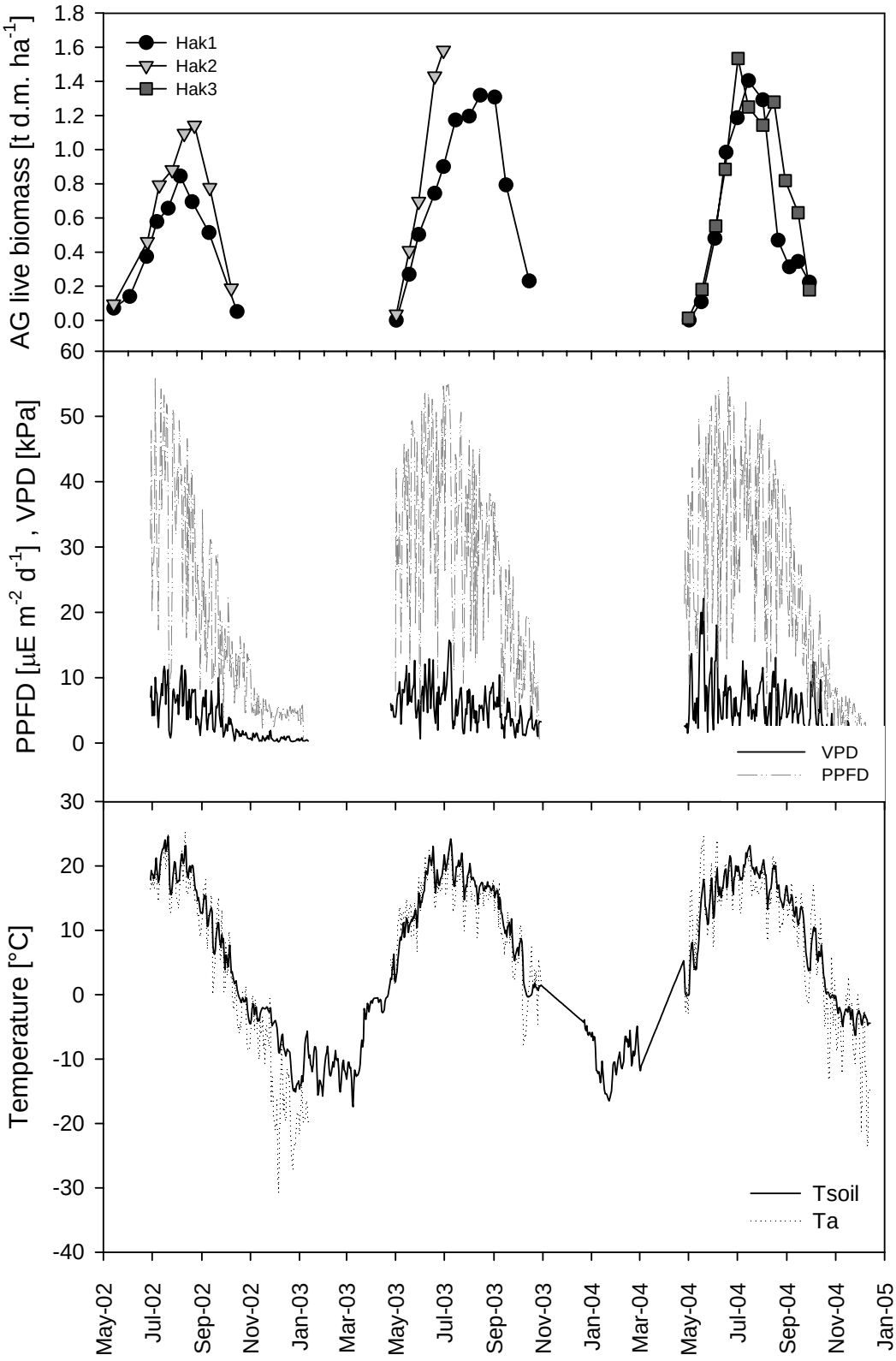

Figure. 7.12. Top panel: trend of aboveground live biomass for the sites of Hak1, Hak2, Hak3. Middle panel: trend of daily integrated PPFD and VPD. Bottom panel: trend of air temperature and soil temperature (depth: 0.1m). Meteorological variables measured at Hak1 site.

7.4.4 Carbon balance

After the integration of NEP over 12 month periods, all sites were found to be sinks for atmospheric carbon. The annual carbon balance of the steppe ecosystem (Hak1) varied from a minimum carbon sequestration of 98.9 $gCm^{-2}yr^{-1}$ to a maximum of 130.4 $gCm^{-2}yr^{-1}$ depending on the year. The lowest refers to the period from July 2002 to June 2003 and it is affected by the low uptake of the summer months of 2002; in 2003 the carbon budget was 114.4 $gCm^{-2}yr^{-1}$ while the higher carbon uptake observed in the growing season following the fire event, caused the ecosystem to be a net sink of 130.4 $gCm^{-2}yr^{-1}$ in the year 2004.

The old agricultural field ecosystems were characterized by a stronger capacity of carbon sequestration than the steppe ecosystem (table 7.5). The magnitude of the sink decreases over time from the early successional stage towards the mature stage represented by steppe vegetation. At Hak2 the NEP cumulated over the period from July 2002 to July 2003 was 216.2 $gCm^{-2}yr^{-1}$ (Δ=+117.3 $gCm^{-2}yr^{-1}$ in respect with NEP of Hak1); at Hak3 in 2004 it was 143.3 $gCm^{-2}yr^{-1}$ (Δ=+12.9 $gCm^{-2}yr^{-1}$ compared to Hak1), although in this last case, it should be taken into account that the small difference between the two sites is mostly due to the enhanced sink of Hak1 in that particular year.

The relation that best describes the NEP of the old field succession stages across time is a negative exponential function tending asymptotically to the NEP of the steppe (fig. 7.13). The NEP attributed to the steppe stage is an average value of 114.5 $gCm^{-2}yr^{-1}$ that, following a prudent approach, is supposed to be reached after 100 years after land use change. However the magnitude NEP declines rather sharply in the first years of the succession development and reaches values typical for steppe already after 20-25 years. The trend cannot be characterized for the period from the abandonment of croplands and subsequent start of the succession up to the age of 5 years. A relevant influence in this time window must be played by vegetation encroachment dynamics in a way that, assuming a condition of the agricultural lands near to the equilibrium in respect with the carbon cycle (Larionova, 2003), the sink strength of abandoned fields increases after land use change proportionally to the cover of early successional species. The encroachment process depends mostly on the seed bank and on the size of the fields and is responsible for determining the time of the succession when the peak of carbon sequestration is reached.

The higher carbon sequestration capacity of recovering grassland ecosystems lies primarily behind a larger amount of synthesized organic carbon by photosynthesis (table 7.5, fig.7.14-7.16). The highest GPP observed was 647.8 $gCm^{-2}yr^{-1}$ at Hak2 relative to the period July 2002 – June 2003, when at Hak1 it was 439.7 $gCm^{-2}yr^{-1}$ (Δ=+208.1 $gCm^{-2}yr^{-1}$). At Hak 3 it was 526.3 $gCm^{-2}yr^{-1}$ in 2004 that was larger than the average GPP observed at Hak1 during the whole monitoring period (478.3 $gCm^{-2}yr^{-1}$) by +48 $gCm^{-2}yr^{-1}$, but lower than that of 2004 (551 $gCm^{-2}yr^{-1}$). In this particular year ecosystem though respiration at Hak1 was also enhanced in respect with previous years and higher than at Hak3. Apart from this case, ecosystem respiration (TER or R_{eco}) was in general higher over recovering grasslands than over the steppe ecosystem. Similarly to GPP, ecosystem

respiration was highest in the early successional stage (Hak2: 431.6 $gCm^{-2}yr^{-1}$) and decreased over time (Hak3: 377.2 $gCm^{-2}yr^{-1}$; average Hak1: 349.2 $gCm^{-2}yr^{-1}$)

	Jul 02-Jun 03		2003	2004	
	Hak1	Hak2	Hak1	Hak1	Hak3
GPP [gC m^{-2} yr^{-1}]	439.7	647.8	444.2	551.0	526.3
TER [gC m^{-2} yr^{-1}]	340.6	431.6	329.9	420.6	377.2
NEP [gC m^{-2} yr^{-1}]	**98.9**	**216.2**	**114.4**	**130.4**	**143.3**
TER/GPP	0.77	0.67	0.74	0.76	0.72
GPP (May-Oct) [gC m^{-2}]	436.2	642.4	443.8	542.1	514.1
TER (May-Oct) [gC m^{-2}]	322.4	423.2	312.4	401.5	364.6
NEP (May-Oct) [gC m^{-2}]	113.4	219.2	131.3	140.6	149.6

Table 7.5. NEP, TER and GPP cumulated over 12 months or over the growing season only (May-Oct) of the steppe ecosystem (Hak1) compared with the former agricultural fields (Hak2, Hak3). In bold characters the figures of annual carbon balance.

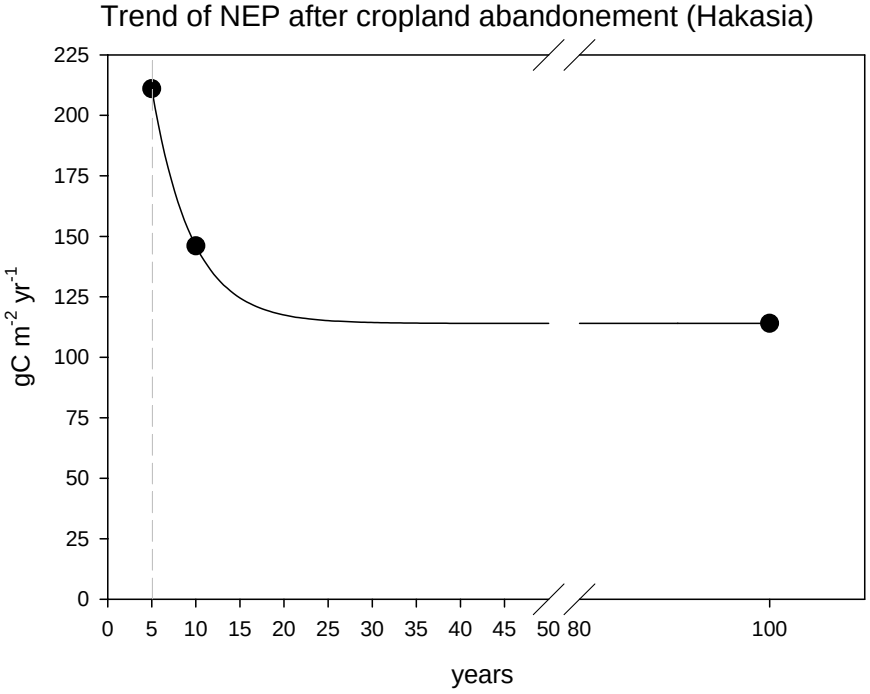

Figure 7.13. Trend of the carbon budget in relation to the age of the stages of succession after agricultural abandonment (Hak2: 5 years; Hak3: 10 years). The negative exponential trend tends asymptotically to the carbon balance of the climax stage, represented by steppe. The area of the panel within the y axis and the grey dashed line is initial phase of succession that cannot be reconstructed.

The quantity of carbon respired back to the atmosphere constituted a fraction of the assimilated carbon that varied in a limited range (0.67-0.77) for all the examined ecosystems . In particular it

was lowest for the early successional stage and highest for the steppe stage. A general relation, for all sites and years, between TER and GPP is expressed by the relation *TER= 0.5 GPP+118.35* (R^2=0.88, n=5), underlying the high degree of correlation of the two components of the carbon balance on annual basis.

The cumulated NEP over the period from May to October can be generally used for a very good approximation of the yearly carbon budget. Ecosystem respiration during the remaining months (November-April) was indeed estimated to account for not more than (2%-5.5%) of the annual value. The assimilation activity is restricted to the months from May to October and the GPP cumulated over this period is basically equal to the annual value.

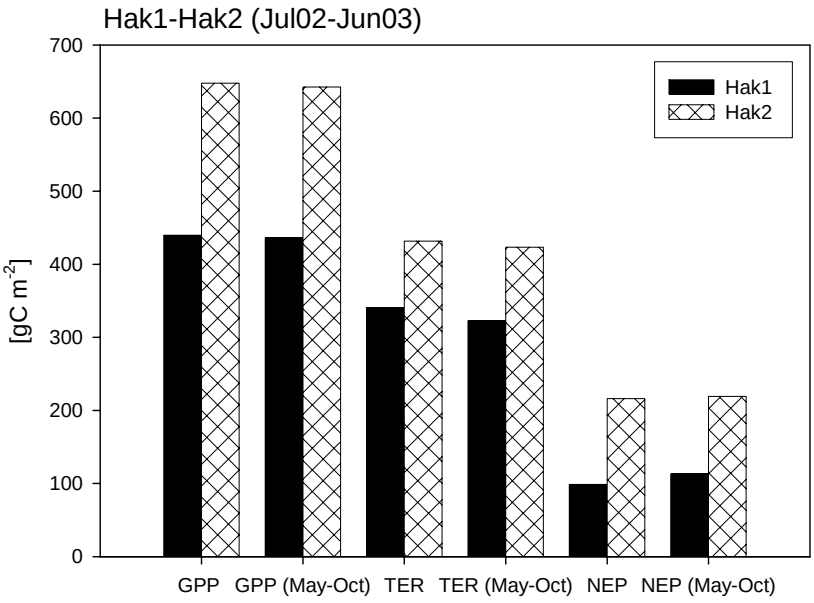

Figure 7.14.Comparison of the sites Hak1 and Hak2 in respect with GPP, TER and NEP on 12 month basis and restricted to the months of the growing season (May-Oct) resulted from the CO_2 flux monitoring from July 2002 to June 2003.

On 4 March 2004 the steppe at the Hak1 site was run by a fire. The event was recorded at 3:30 a.m. The soil, given the season of the year, was frozen and soil temperature at the depth of 5 cm was -11.8°C. After a field survey in April it was noted that only the grass biomass was burnt while no evidence of underground burning was found.

In order to include the loss of carbon caused by the fire in the carbon balance of Hak1, the amount of carbon in the burnt biomass was assessed from the aboveground biomass stock of 15 October 2003, being the last record available. The conversion factor from biomass to carbon was set to 0.45 (IPCC, 2003). Decomposition process during winter time is typically slowed down because of extremely low air temperatures, so the stock of aboveground biomass is likely to have decreased

little from mid October to March when daily mean temperature was -11.9°C with fluctuations between -29.7°C and +4.5°C.

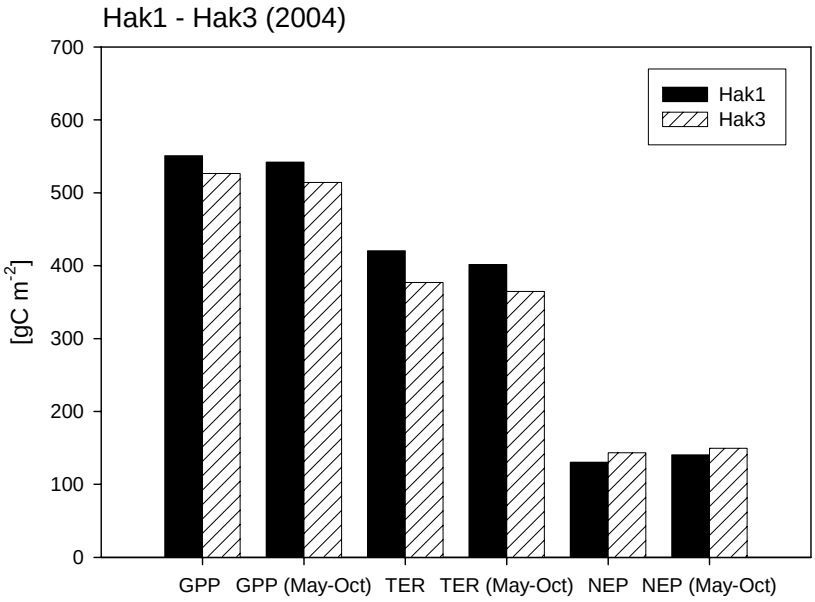

Figure 7.15. Comparison of the sites Hak1 and Hak3 in respect with GPP, TER and NEP on annual basis and restricted to the months of the growing season (May-Oct) resulted from the CO_2 flux monitoring in the year 2004.

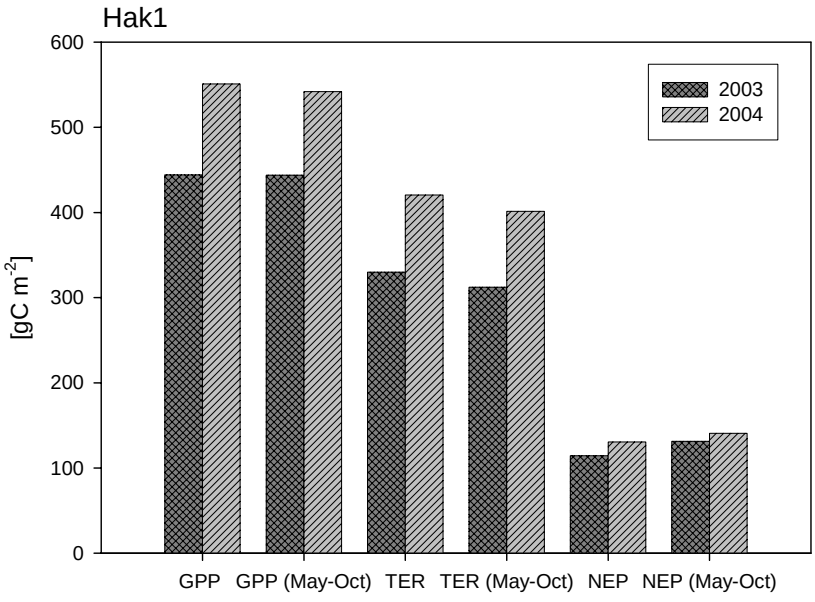

Figure 7.16. Comparison of GPP, TER and NEP on annual basis and restricted to the months of the growing season (May-Oct) of the steppe ecosystem (Hak1)in the year 2003 and 2004.

The carbon released during fire, calculated as above, was 119.0 gCm^{-2}. Subtracting this term to the NEP of Hak1 in 2004, we obtain a carbon balance of +11 $gCm^{-2}yr^{-1}$ (fig.7.17). This result clearly indicates that the steppe ecosystem is able to recover the amount of carbon lost as a consequence of fire within a single growing season thanks to an enhanced carbon sequestration capacity. The fire exerts its effect in almost nullifying the carbon sequestration of the steppe ecosystem in the year of occurrence, but substantially does not intact the stored carbon that was sequestered in previous years. Information on the frequency of fire events would be needed to assess the Net Biome Productivity (NBP) that considers the carbon sequestration capacity in the long term including the carbon losses due to fire and the fate of exported biomass (in case of grazing management).

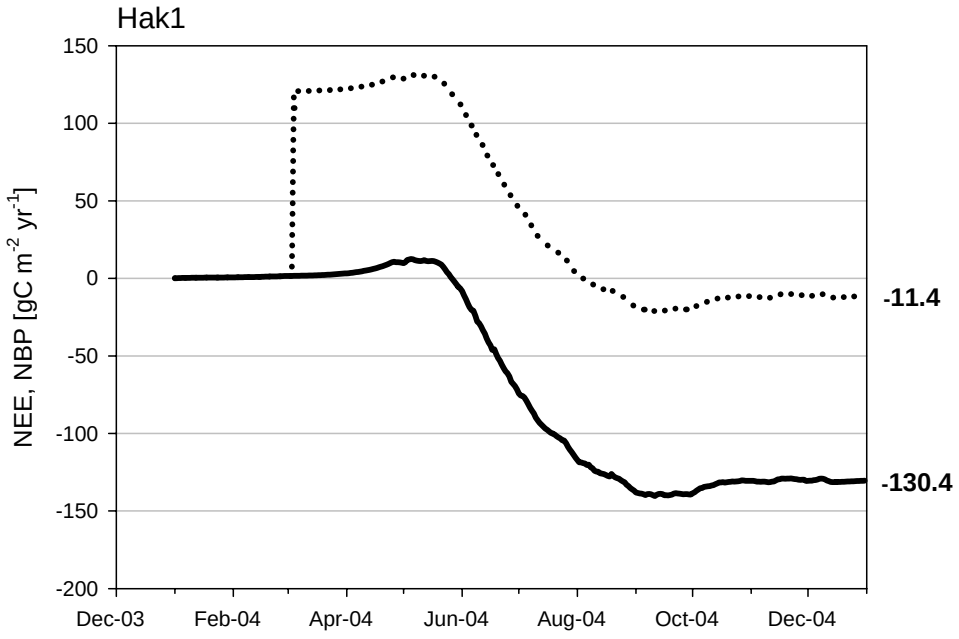

Figure 7.17. Cumulated NEP of Hak1 over the year 2004 (solid line) and after accounting for the estimated loss of carbon due to a fire on 4 March 2004 (dotted line).

7.4.5 Response of ecosystem respiration to soil temperature and soil moisture

The response of ecosystem respiration to soil temperature (measured at the depth of 0.1 m) was derived from a regressive analysis using a set of exponential equations and refining the analysis with other type of equations (sigmoid) when the exponential type did not provide the best fit. Regressions were performed on nighttime CO_2 fluxes binned by 10 consecutive records, filtered for the appropriate u_* threshold. The exponential equations used included a Q10 type (eq 7.30) and the Lloyd and Taylor (1994) function (eq. 7.31):

$$R_{eco} = R_{ref} \cdot Q_{10}^{\left(\frac{T_{soil}-10}{10}\right)} \qquad \textit{(Equation 7. 30)}$$

$$R_{eco} = R_{ref} \cdot e^{308.56 \cdot \left[\left(\frac{1}{56.02}\right) - \left(\frac{1}{T_{soil}+46.02}\right)\right]} \qquad \textit{(Equation 7. 31)}$$

where the parameter R_{ref} is the soil repiration at 10°C, Q_{10} is the factor of increase of soil respiration for a positive change in soil temperature of 10°C ($Q_{10}=R_{eco\ (Tsoil+10)}/R_{eco(Tsoil)}$). The Loyd and Taylor function assumes a variable Q10 value. The sigmoid function used (Schlentner and Van Cleve, 1985) has the following general equation:

$$R_{eco} = a + \frac{1}{b + c^{\left(\frac{10-T_{soil}}{10}\right)}} \qquad \textit{(Equation 7. 32)}$$

Where a, b and c are fitted parameters.

In a further step the analysis of the environmental control of soil respiration was extended focusing on the soil moisture factor. The residuals of the function that best explained the R_{eco} vs T_{soil} relation were plotted against the corresponding soil moisture (SM) values, furthermore a bivariate gaussian function was used to analyze the response of ecosystem respiration to both soil temperature and soil moisture.

$$R_{eco} = a \cdot e^{\left[-0.5 \cdot \left(\frac{SM-SM_0}{b}\right)^2 + \left(\frac{T_{soil}-T_{soil0}}{c}\right)^2\right]} \qquad \textit{(Equation 7. 33)}$$

where SM_0, T_{soil0}, a, b and c are fitted parameters.

Ecosystem respiration at Hak1 showed Q_{10} values of 2.48 and 2.54 in 2002 and 2003 respectively while a remarkably enhanced value of 3.35 in 2004 (table 7.6, fig 7.18, 7.19). The two exponential functions used in the regressive analysis performed quite similarly although the best fit was obtained by fitting a Lloyd and Taylor function in the case of the 2002 and 2003 data set, while for the dataset of 2004 the best relation was yielded by Q_{10} function.

The Q_{10} retrieved by the temperature response of R_{eco} at Hak2 was 2.51, close to that of Hak1 in the same period of measurements although respiration rates where higher than at Hak1 as witnessed by the higher R_{ref} values.

Hak3 displayed the lowest Q_{10} (2.12), that was due to the depression of respiration rates at high soil temperature combined with low soil moisture. In this case the fit was improved using a sigmoid function.

Soil moisture varies in respect with soil temperature following approximately a bell shaped trend. It is lowest in cold months, maximum between 5°C to 15°C and tends to decrease for T_{soil}>15°C during periods far from rain events. Soil water content was on average higher at the steppe site

Hak1 rather than in the old agricultural field sites Hak2 and Hak3. The distribution of the residuals of the soil temperature response function (Lloyd and Taylor type) of Hak1 across soil moisture does not evidence any significant trend. However the model tends to underestimate respiration rates when soil moisture falls in an interval of 30% and soil temperature is between 10°C and 20°C. In 2004 the interval of soil moisture where the model tended to an underestimation of R_{eco} was shifted to 35%-40%. The adoption of a bivariate model to describe R_{eco} as function of soil temperature and moisture yields better determination indexes and clearly highlights the role of soil moisture in modulating the CO_2 effluxes (table 7.7, fig.7.20, 7.21). Given the same soil temperature, R_{eco} increases for growing soil moisture levels up to about 0.3 m^3m^{-3} after which reaches a plateau or slightly decreases, possibly due to the effect of water saturation in soil pores. In 2004, the ecosystem respiration at Hak1 did not level even at the highest values of soil moisture. Since in that year these conditions occurred in mid June during the phase of most intense growth of vegetation, it is likely that large availability of water in the soil boosted the assimilation activity of vegetation and consequently root respiration rates.

Both the sites of Hak2 and Hak3 exhibited a negative significant decrease in ecosystem respiration at lower soil water content conditions that could not be explained by the temperature response function (Lloyd and Taylor type). Analyzing the behaviour of R_{eco} against both soil temperature and water content, we observe patterns similar to those of Hak1, with maximum respiration rates for SWC around 30%. However, while at Hak3 R_{eco} tends to a slight decrease for soil water content levels above 30%, at Hak2 the SWC range is limited in the upper end to this threshold and the resulting pattern of R_{eco} is always positively correlated to soil moisture.

Site/year	Function type	R^2	Parameters	value	Std. Error	t	P
Hak1-2002	Q10	0.801	R_{ref}	1.0841	0.0534	20.3006	<0.0001
			Q_{10}	2.4870	0.1350	18.4242	<0.0001
	Lloyd &Taylor	0.840	R_{ref}	1.1868	0.0384	30.8971	<0.0001
Hak1-2003	Q10	0.683	R_{ref}	0.9500	0.0595	15.9654	<0.0001
			Q_{10}	2.5414	0.2065	12.3066	<0.0001
	Lloyd &Taylor	0.689	R_{ref}	1.0052	0.0302	33.3158	<0.0001
Hak1-2004	Q10	0.838	R_{ref}	1.0186	0.0524	19.4394	<0.0001
			Q_{10}	3.3599	0.2137	15.7240	<0.0001
	Lloyd &Taylor	0.816	R_{ref}	1.2972	0.0333	38.9767	<0.0001
Hak3	Q10	0.596	R_{ref}	1.1303	0.0748	15.1161	<0.0001
			Q_{10}	2.1266	0.1536	13.8482	<0.0001
	Lloyd &Taylor	0.624	R_{ref}	1.0773	0.0378	28.4976	<0.0001
	Sigmoid	0.654	a	0.2713	0.0764	3.5492	0.0005
			b	0.4298	0.0395	10.8714	<0.0001
			c	37.7314	24.8972	1.5155	0.1318
Hak2	Q10	0.676	R_{ref}	1.1997	0.1013	11.8442	<0.0001
			Q_{10}	2.5121	0.2568	9.7835	<0.0001
	Loyd &Taylor	0.701	R_{ref}	1.2810	0.0555	23.0905	<0.0001

Table 7.6. Type, determination index and parameters of the non-linear functions used to describe the response of ecosystem respiration to soil temperature.

Site/year	Equation type	R^2	Parameters	value	Std. Error	T	P
Hak1-2002	Gaussian	0.889	SM_0	0.280	0.006	43.524	<0.0001
			T_{soil0}	22.537	1.336	16.860	<0.0001
			a	3.411	0.240	14.166	<0.0001
			b	0.087	0.011	7.794	<0.0001
			c	9.594	0.780	12.289	<0.0001
Hak1-2003	Gaussian	0.696	SM_0	0.311	0.044	7.059	<0.0001
			T_{soil0}	32.432	11.852	2.736	0.0073
			a	3.560	1.933	1.841	0.0685
			b	0.174	0.123	1.414	0.1604
			c	13.886	4.532	3.064	0.0028
Hak1-2004	Gaussian	0.868	SM_0	0.549	0.241	2.271	0.0244
			T_{soil0}	56.386	31.794	1.773	0.0780
			a	28.978	47.294	0.612	0.5409
			b	0.241	0.151	1.593	0.1131
			c	18.987	7.402	2.565	0.0112
Hak3	Gaussian	0.710	SM_0	0.307	0.012	24.882	<0.0001
			T_{soil0}	32.219	9.672	3.331	0.0011
			a	4.550	1.917	2.373	0.0189
			b	0.106	0.015	6.823	<0.0001
			c	13.963	3.915	3.565	0.0005
Hak2	Gaussian	0.768	SM_0	0.872	3.474	0.251	0.8024
			T_{soil0}	37.120	16.708	2.221	0.0289
			a	43.675	401.517	0.108	0.9136
			b	0.335	0.916	0.365	0.7155
			c	14.488	5.261	2.753	0.0072

Table 7.7. Multiple determination index and parameters of gaussian functions retrieved by regressive analysis of ecosystem respiration versus soil temperature and soil moisture.

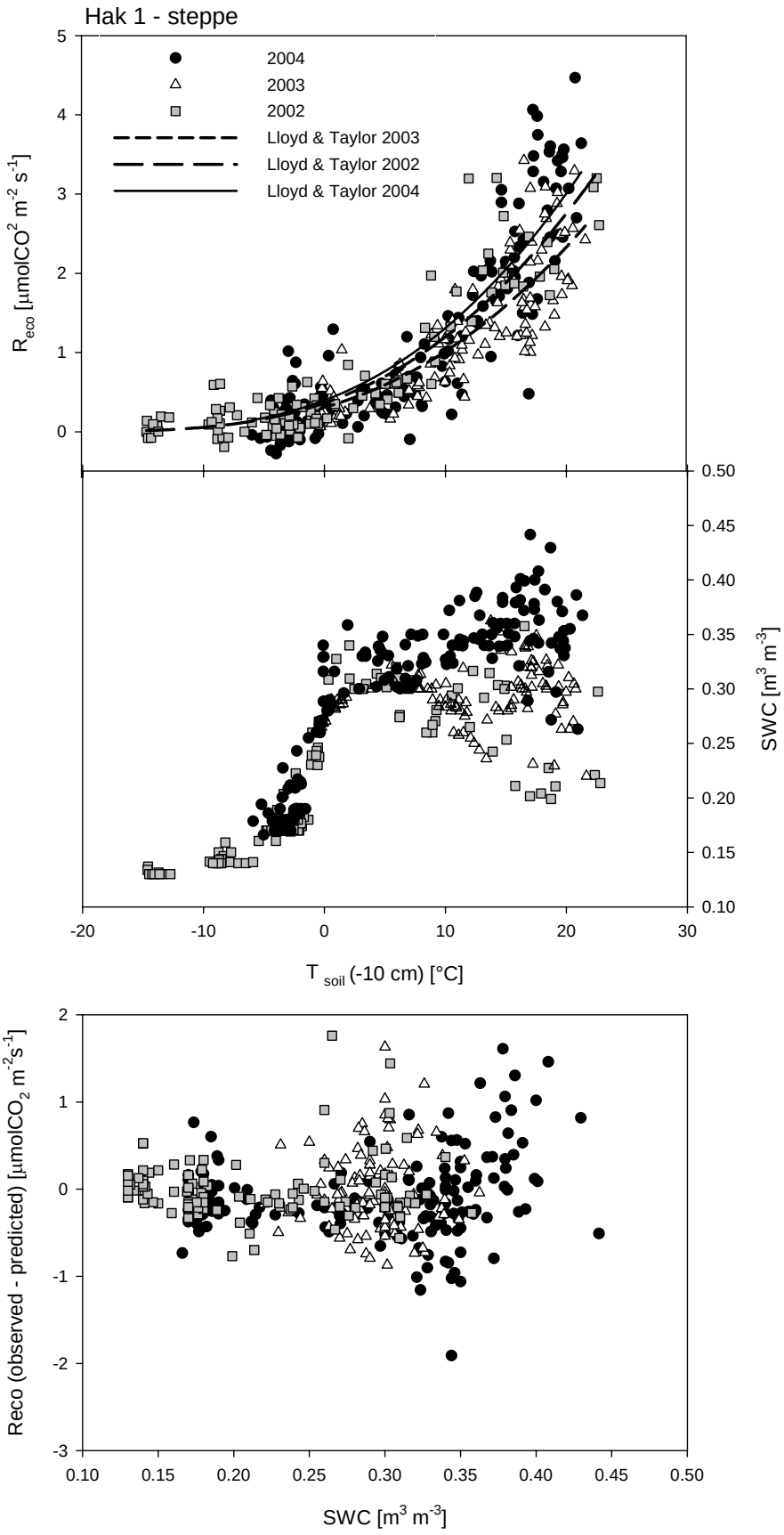

Figure 7.18. Top panel: response of R_{eco} against soil temperature (at the depth 0.01m) for the Hak1 site in the years 2002, 2003, 2004. R_{eco} values were binned by 10 consecutive records. The three

plots were fitted by Lloyd and Taylor function. Middle panel: soil water content(depth: 0-30 cm) plotted against soil temperature. Bottom panel: residuals of the Lloyd and Taylor function plotted against soil water content.

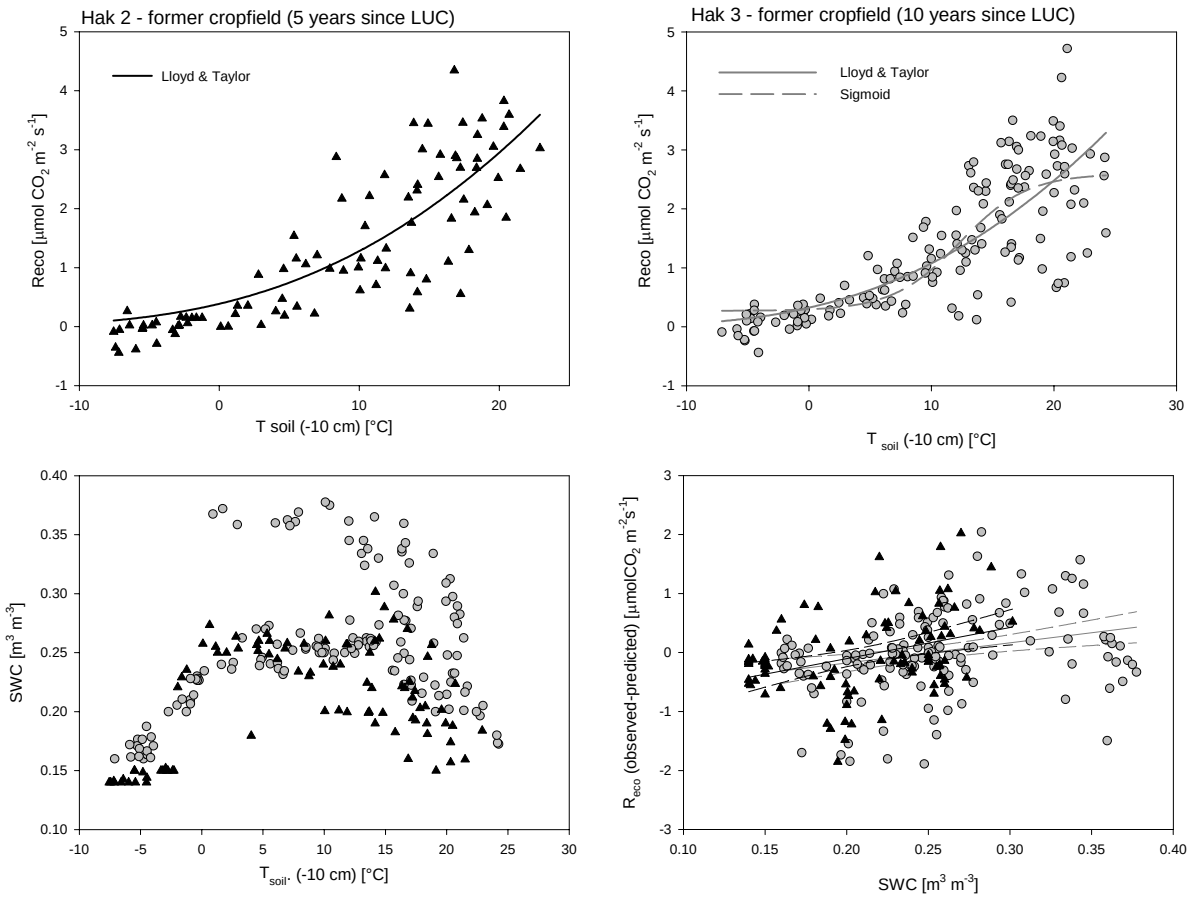

Figure 7.19. Top left panel: response of R_{eco} (values binned by 10 temporally consecutive records) against soil temperature (at the depth 0.01m) for the Hak2 site fitted by Lloyd and Taylor function. Top right panel: response of Reco against soil temperature (at the depth 0.01m) for the Hak3 site fitted by Lloyd and Taylor and sigmoid type functions. Bottom left panel: soil water content (depth: 0-30 cm) plotted against soil temperature for Hak2 (black triangles) and Hak3 (grey circles) sites. Bottom panel: residuals of the Lloyd and Taylor function plotted against soil water content for Hak2 (black triangles) and Hak3 (grey circles) sites; linear regression (solid line) and 95% confidence limit (dashed lines) for both series.

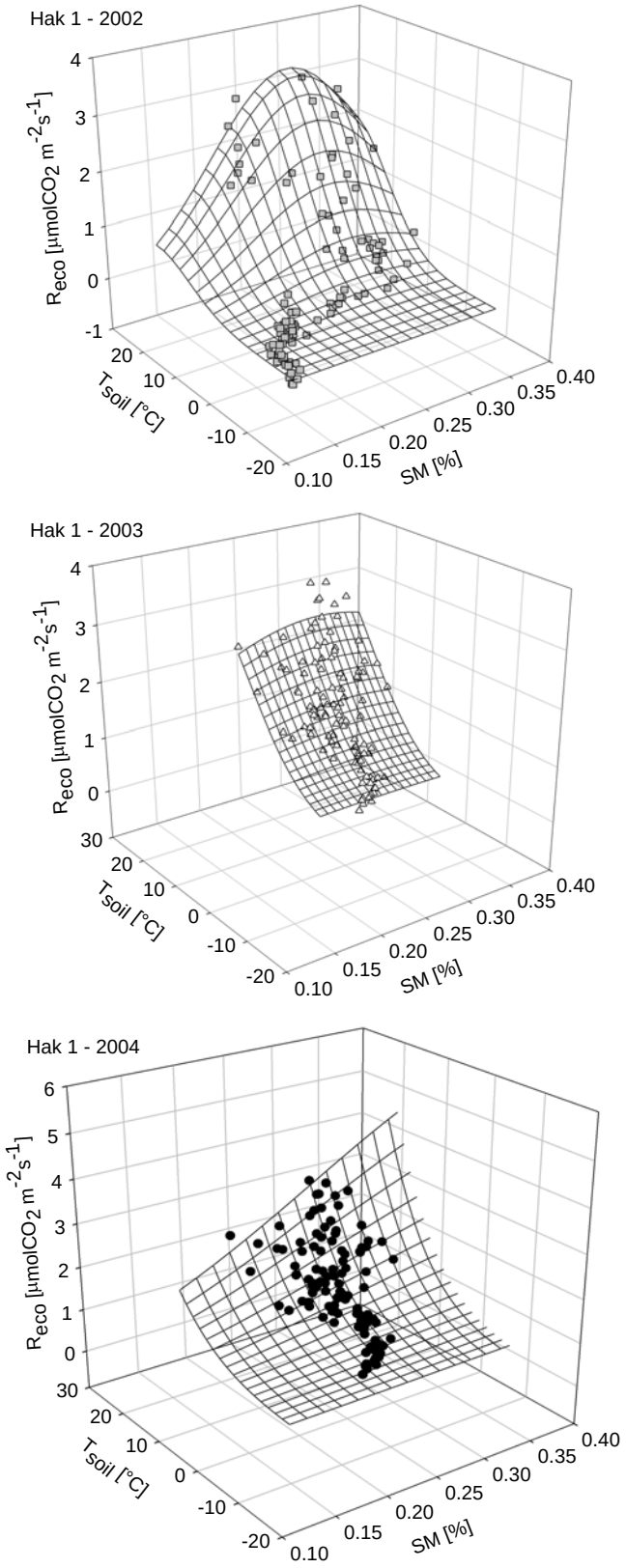

Figure 7.20. Plots of ecosystem respiration (R_{eco}) against soil temperature measured at the depth of 0.1m and soil moisture averaged over a depth of 30 cm at the site of Hak1 in the year 2002(top graph), 2003 (middle), and 2004 (bottom).

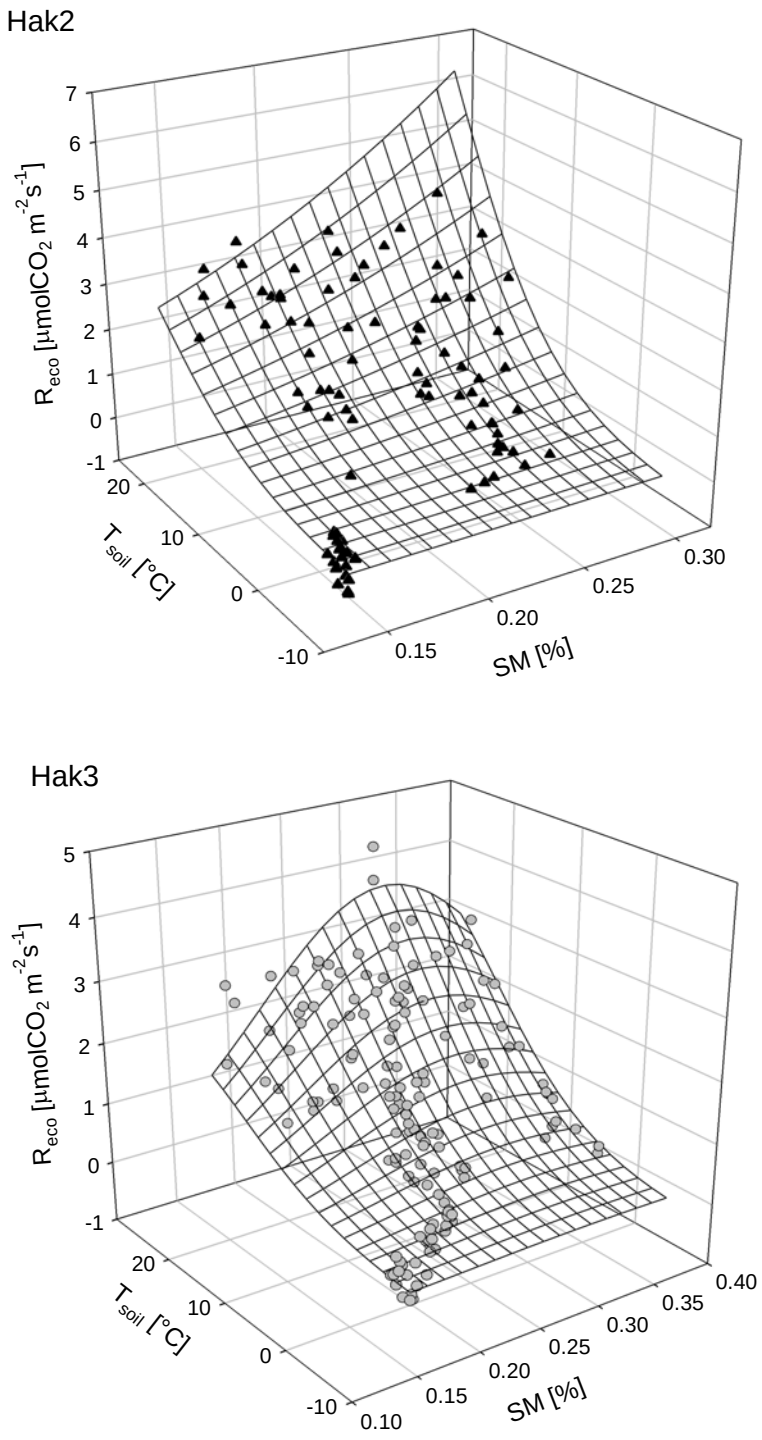

Figure 7.21. Plots of ecosystem respiration (R_{eco}) against soil temperature measured at the depth of 0.1m and soil moisture averaged over a depth of 30 cm at the site of Hak2 (above), and Hak3 (below).

7.4.6 Response of GPP to photosynthetically active radiation, air temperature and vapour pressure deficit.

The response of gross photosynthesis to radiation was analyzed by plotting the 30 minutes averaged GPP against incident PPFD and fitting the plot by a rectangular hyperbolic function as in Flanagan (2002):

$$GPP = \frac{\alpha \cdot PPFD \cdot A_{\max}}{\alpha \cdot PPFD + A_{\max}} \qquad \textit{(Equation 7. 34)}$$

Where α [mol CO_2 mol^{-1} photons] is the initial slope of the light response curve, that is the apparent quantum yield, and A_{max} [μmolCO_2 $m^{-2}s^{-1}$] is the photosynthetic rate at saturating PPFD. The light curve was fitted on monthly sets of data from March to October. The month of May was split into two fortnights (1-15, 16-31 May) in order to separate the low fluxes observed at the onset of the vegetative season from the higher rates typical of the second half of the month reducing the overall scatter of the plot.

Both apparent quantum yield and the maximum GPP increase from early May (fig. 7.22), reach the peak in June or July depending on the year, and following the senescence of vegetation decrease until returning to the original levels in October. At the steppe site of Hak1, the parameter α ranged from 0.002÷0.003 mol CO_2 mol^{-1} photons up to 0.028÷0.032 mol CO_2 mol^{-1} in the seasons 2002 and 2003. In 2004 the apparent quantum yield from the second half of May to July was always above 0.035 and reached 0.04 mol CO_2 mol^{-1} in June. The maximum GPP was 2.2÷4.7 μmolCO_2 $m^{-2}s^{-1}$ at the beginning and end of the growing season; the highest A_{max} in the seasons 2002 and 2003 is observed in September, however this result should be related to the inappropriateness of the hyperbolic function when the response of GPP to PPFD tends to be linear as in this specific case. The highest values of A_{max} during the seasons 2002 and 2003, disregarding the above mentioned case, was reached in the period between June and August 8.9÷10.6 μmolCO_2 $m^{-2}s^{-1}$. In the same time window of 2004 A_{max} was higher compared to the previous seasons, reaching a maximum of 15.5 μmolCO_2 $m^{-2}s^{-1}$ in June, but declining sharply in August (10.1 μmolCO_2 $m^{-2}s^{-1}$), after a particularly dry (-40% of precipitation in respect with 2002 and 2003) month of July.

The apparent quantum yield of recovering grassland ecosystems was generally slightly higher than that of steppe. In the case of the early successional stage (Hak2) it reached a maximum 0.35 mol CO_2 mol^{-1} photons in June 2003, while for the intermediate stage (Hak3) it reached 0.46 mol CO_2 mol^{-1} photons in June 2004. The grassland at Hak2 was characterized by a much higher A_{max} than Hak1 especially in the season 2003 when it reached 22.0 μmolCO_2 $m^{-2}s^{-1}$ in the month of June, with a difference of a factor 2 in respect with photosynthetic rates observed at Hak1. The intermediate successional stage displayed a similar A_{max} compared to the steppe ecosystem

although it was subject to a substantial reduction in July 2004 and to a lesser extent also in August. Anyway, if to compare the parameters retrieved for Hak3 with those of Hak1 in the previous seasons, excluding thus the post fire enhancement of GPP in 2004, both A_{max} and α result higher.

The parameter α resulted positively correlated to the average aboveground live biomass and air temperature of the examined periods at all sites (fig. 7.24-7.26). The parameter A_{max} on the contrary was mainly driven by the amount of live biomass. This paradigm represents a key to the interpretation of the different response of GPP to sun radiation among sites, to its variability from year to year and within the same growing season.

Differences in air temperature provide an explanation for different apparent quantum yields observed at the in the early and late growing season given similar amounts of green biomass. Recovering grasslands, characterized by higher live biomass stocks than the steppe ecosystem, display higher photosynthetic rates at saturating light. Also the general improvement in the carbon assimilation capacity of the season 2004 in respect with that of 2003 can be related to a higher aboveground biomass. An exception is represented by the noticeable enhancement of the light response parameters of the steppe ecosystem after the fire event in spring 2004 that is not justified by changes either in green biomass or in temperature in that particular year. This finding underlines the effect of fire as a fertilizing agent, likely due to the larger availability of mineral nutrients for plants, especially nitrogen, contained in the ashes of the burnt biomass, that leads to an improved carbon assimilation capacity of the steppe ecosystem.

A paired analysis of the change in half-hourly GPP of steppe and old field ecosystems against air temperature and vapour pressure deficit (VPD) in the months of July and August (Hak1 vs Hak2 in 2002; Hak1 vs Hak3 in 2004) revealed that the steppe ecosystem was more steady in respect with the environmental control on the photosynthetic process than recovering grasslands (fig. 7.27, 7.28). In each examined month and for both sites compared, the VPD increased linearly with air temperature, while GPP decreased starting from air temperature values of about 26°C up to minimum values for air temperatures of about 30°C or more (maximum T was 36°C recorded at Hak2 in August 2002). The reduction in GPP is was definitely pronounced for recovering grasslands in both July and August (Hak2: ≈-30% ; Hak3: ≈-45%) while the steppe ecosystem maintained GPP at levels of 80-90% in respect with the temperature optimum for the process.

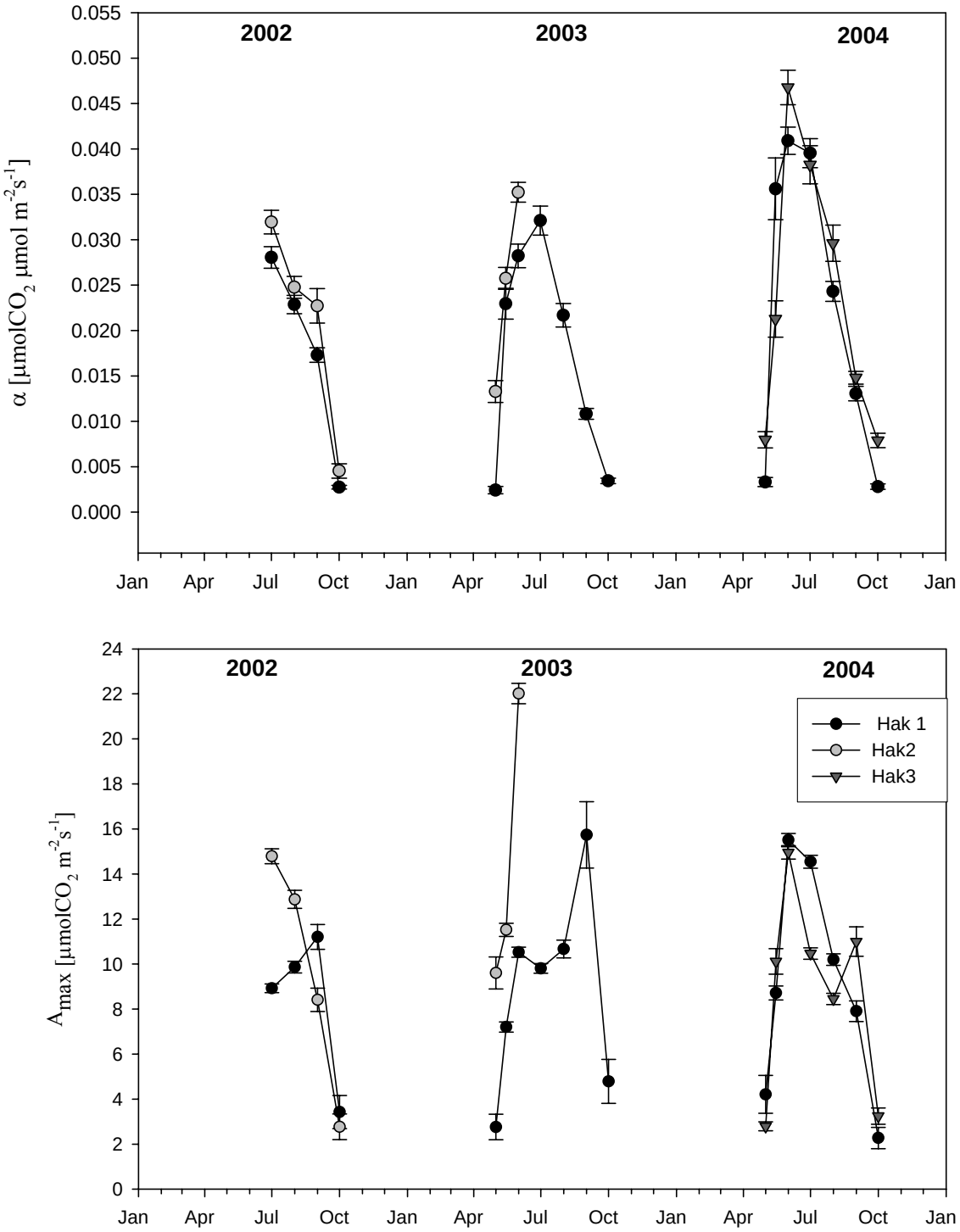

Figure 7.22. Parameters of the light curves (mean ± std.error) retrieved from regressive analysis of half hourly GPP against incident PPFD for the sites of Hak1, Hak2, Hak3. Trend of apparent quantum yield (α)(above) and maximum GPP at saturating irradiance (A_{max})(below) across the growing season (May-October). The plots have a monthly time step. In 2002 plots start since July; the month of May was divided into two fortnights to focus in more detail on the onset of photosynthetic activity.

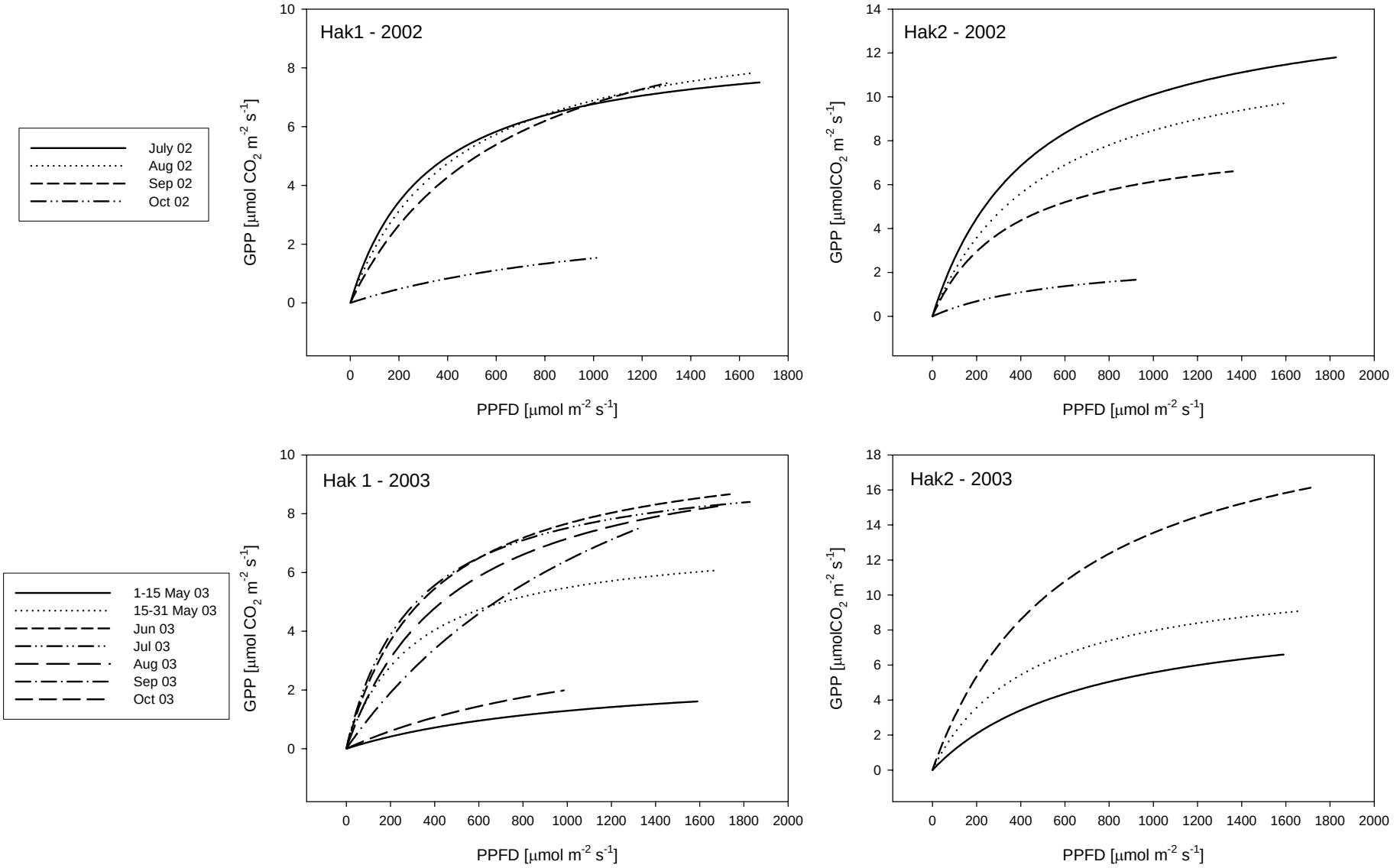
July 02
Aug 02
Sep 02
Oct 02
Hak1 - 2002
Hak2 - 2002
Hak 1 - 2003
Hak2 - 2003
1-15 May 03
15-31 May 03
Jun 03
Jul 03
Aug 03
Sep 03
Oct 03
GPP [µmol CO2 m-2 s-1]
GPP [µmolCO2 m-2 s-1]
PPFD [µmol m-2 s-1]

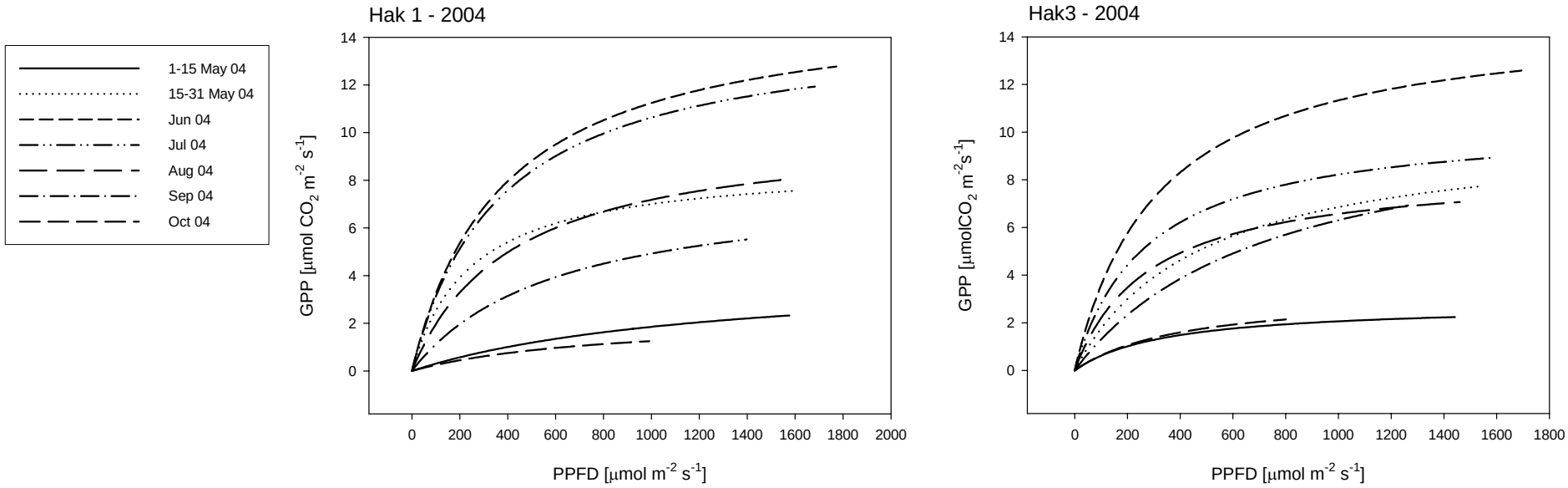

Figure 7.23. Light curves for the months from May to October of 2002, 2003 and 2004 for all the sites (continues from previous page). Curves are rectangular hyperbola with general equation ($GPP=\alpha*PPFD*A_{max}/(\alpha*PPFD+A_{max})$) retrieved from the regression of half hourly GPP against incident PPFD. The month of May was split into two fortnights to focus more accurately on the onset of photosynthetic activity at the beginning of the season.

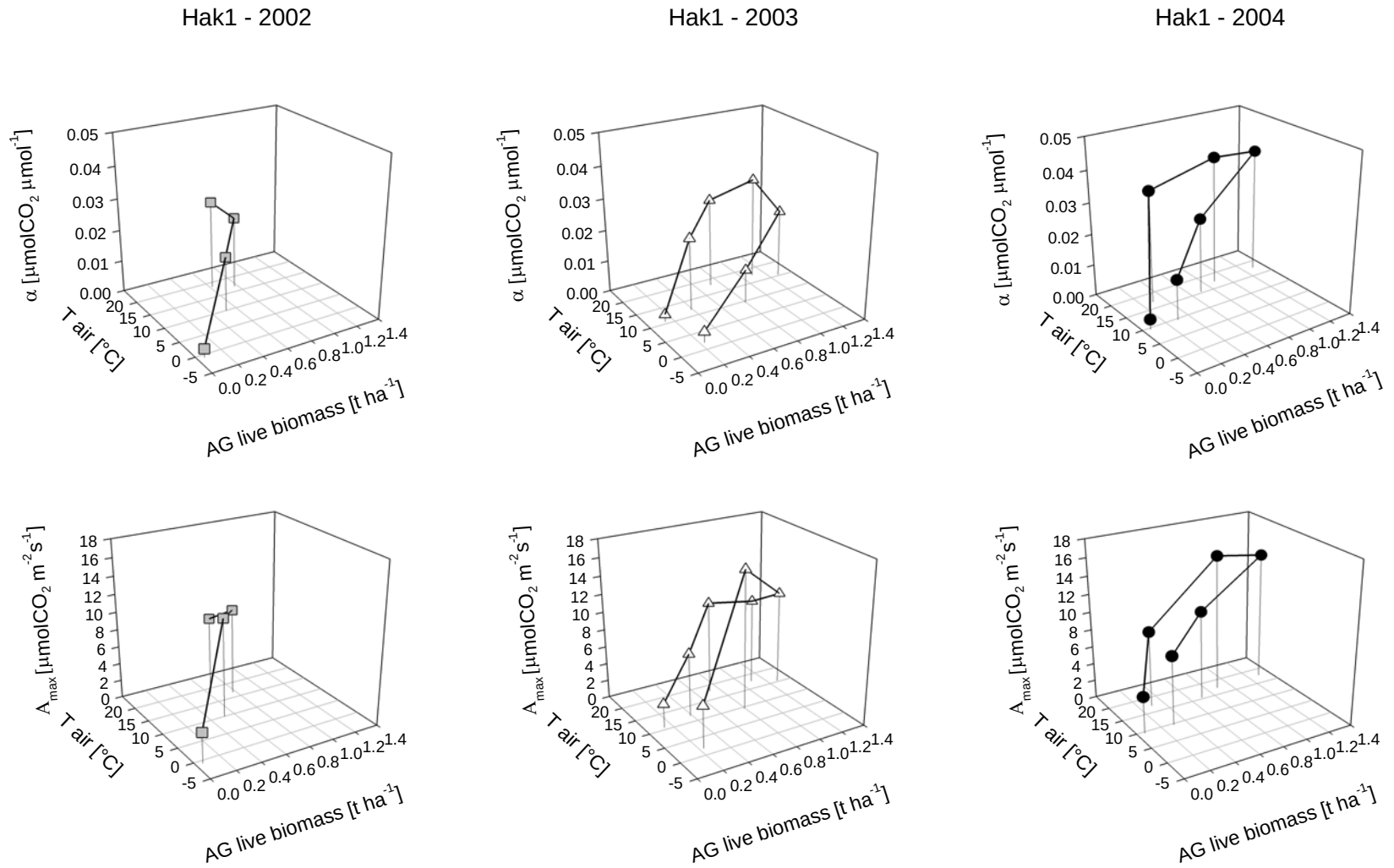

Figure 7.24. Parameters of the light curves of the site Hak1 plotted against the average amount of aboveground live biomass and air temperature. Above: apparent quantum yield (α). Below: maximum GPP at saturating PPFD (A_{max}).

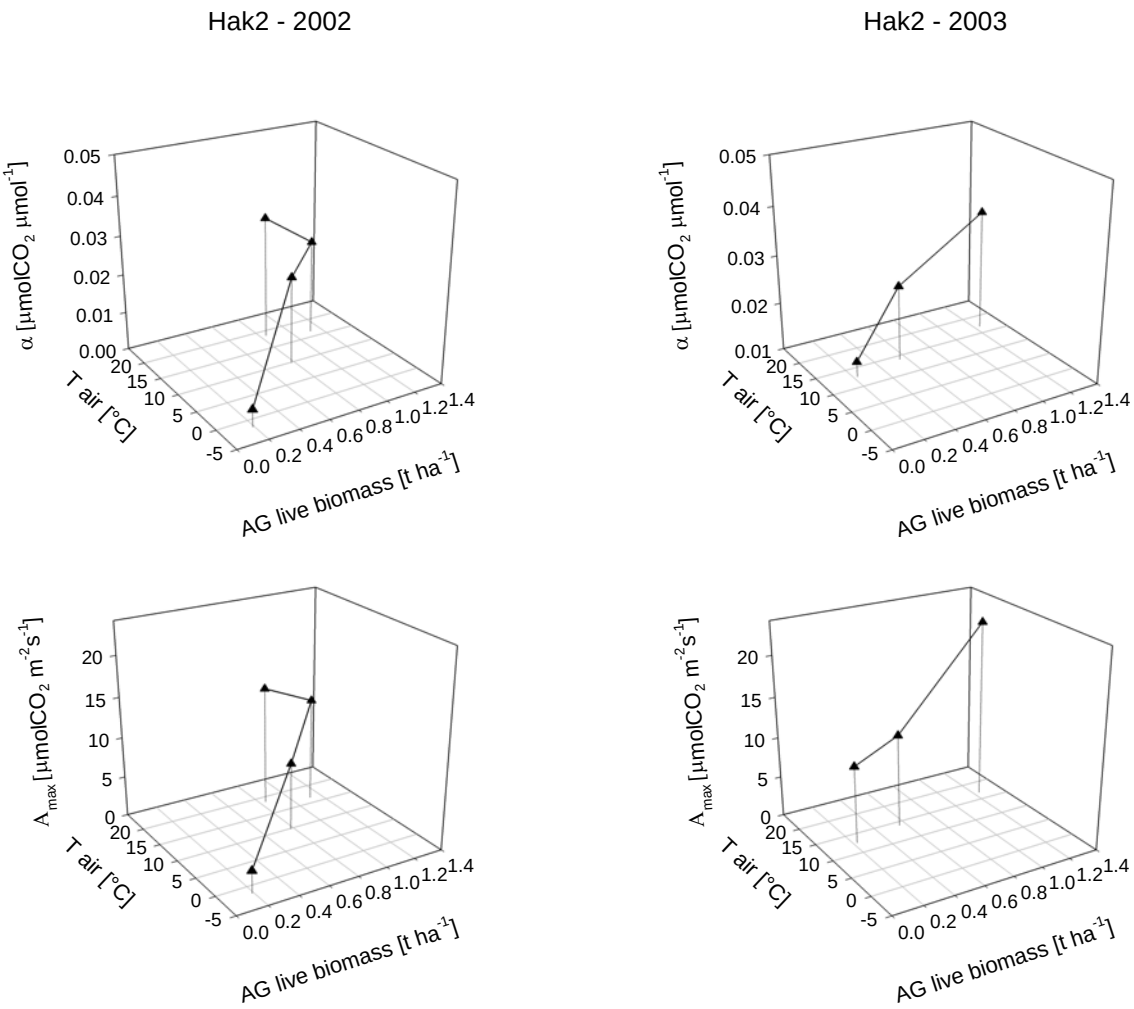

Figure 7.25. Parameters of the light curves of the site Hak2 plotted against the average amount of aboveground live biomass and air temperature. Above: apparent quantum yield (α). Below: maximum GPP at saturating PPFD (A_{max}).

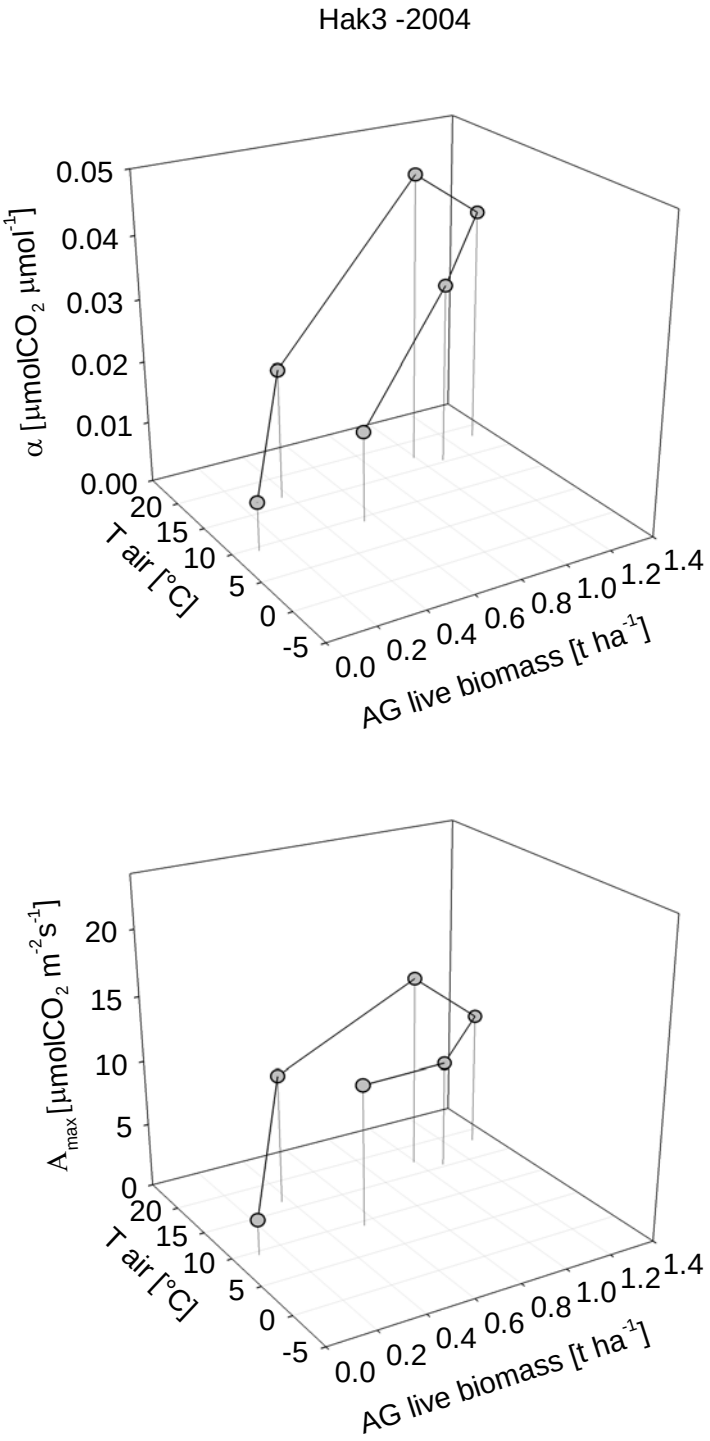

Figure 7.26. Parameters of the light curves of the site Hak3 plotted against the average amount of aboveground live biomass and air temperature. Above: apparent quantum yield (α). Below: maximum GPP at saturating PPFD (A_{max}).

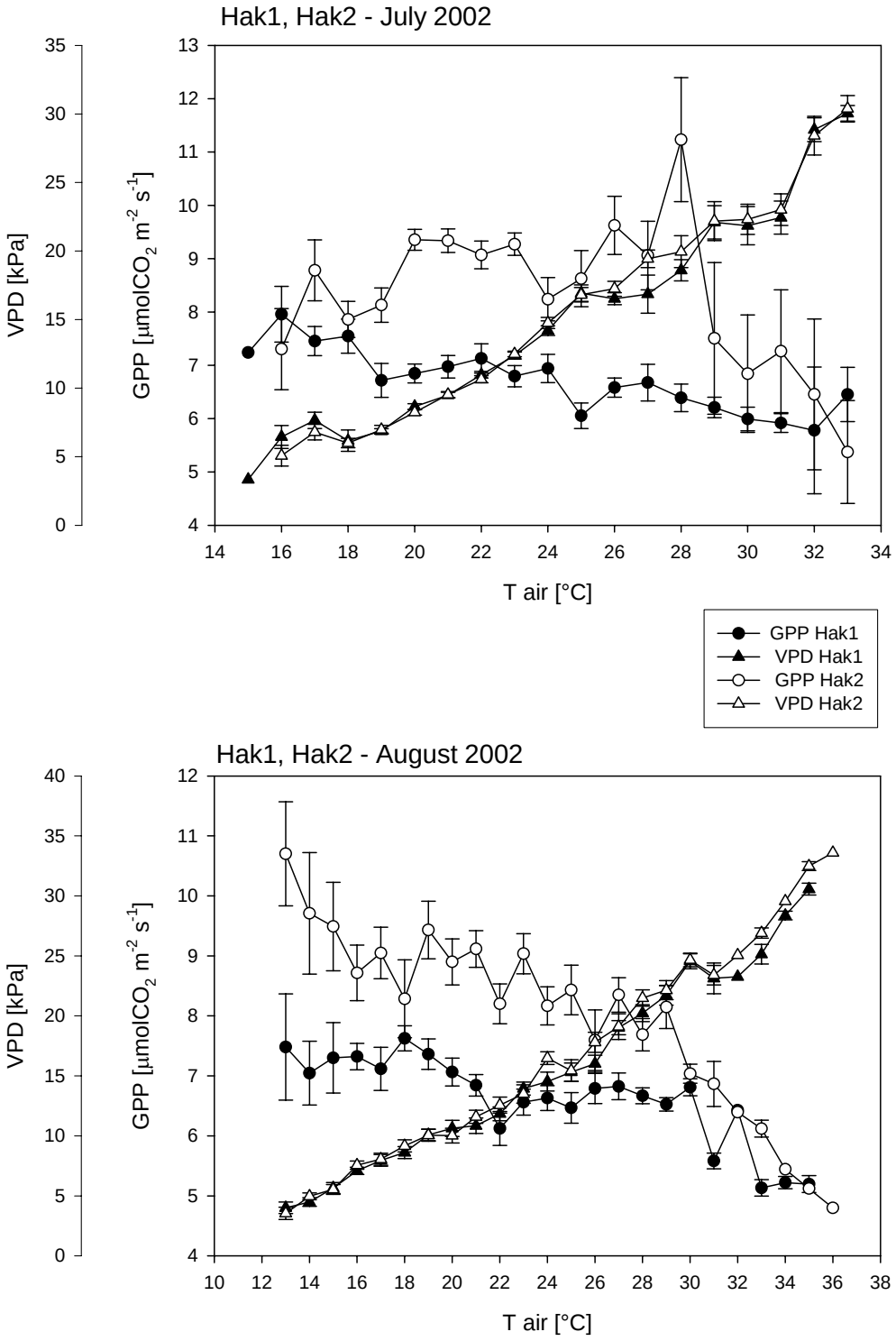

Figure 7.27. Comparison of reduction in GPP at increasing air temperature and vapour pressure deficit between the natural steppe (Hak1) and the early stage of succession (Hak2) in the months of July (above) and August (below) 2002.

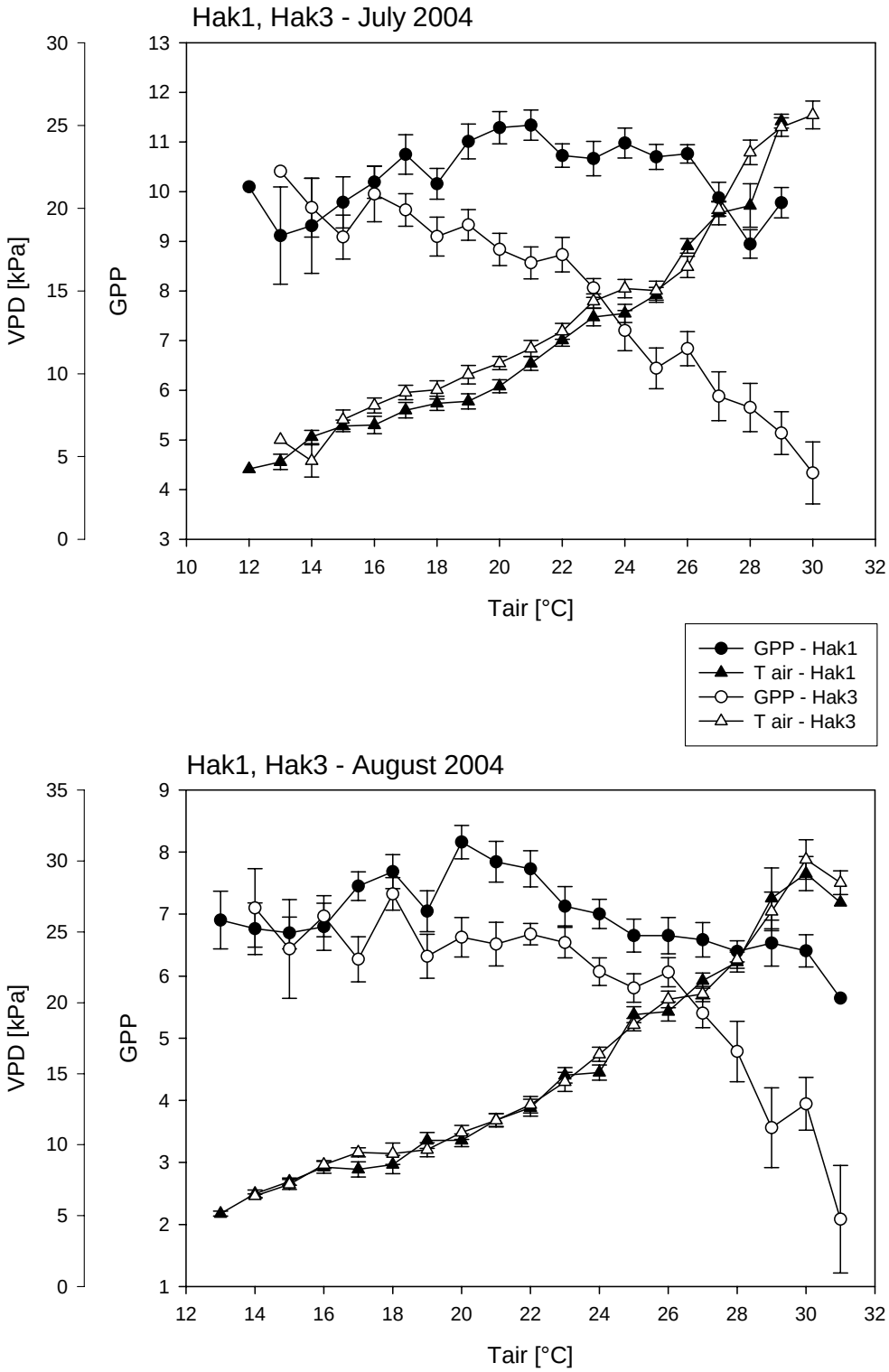

Figure 7.28. Comparison of reduction in GPP at increasing air temperature and vapour pressure deficit between the steppe (Hak1) and the intermidiate stage of succession (Hak3) in the months of July (above) and August (below) 2004.

7.4.7 Water Use Efficiency.

The evapotranspiration over the steppe ecosystem cumulated from May to October (July to October in 2002) was found to balance approximately the amount of precipitation fallen during the same period, whereas it was found systematically lower over the old fields (tab 7.8). The maximum divergence in evapotranspiration was observed in the month of July (-26% at Hak2 in 2002 and -17% at Hak3 in 2004) and over the whole span of the growing season the difference was -15% at Hak2 (Jul-Oct 02) and -11% at Hak3 (May-Oct 04).
It is thus evident that the higher carbon sequestration of old field ecosystems compared to the steppe ecosystem, do not occur at the expenses of larger water losses.
The water use efficiency of photosynthesis (WUE_{Ph}) is defined as the ratio between the carbon assimilated and the water lost by transpiration (Tr) (Larcher, 2003)

$$WUE_{Ph} = \frac{A}{Tr} \qquad [\mu mol\ CO_2/mmol\ H_2O] \qquad \textit{(Equation 7. 35)}$$

The water vapour flux measured at ecosystem scale is the result of both evaporation and transpiration. Since the two components of are not discernible, it is not possible to compute precisely the water use efficiency using eq.7.35., that is then approximated as the ratio of micromoles of carbon fixed through photosynthesis (GPP) per mole of water evaporated from the land surface (transpiration + soil evaporation) (E).
We calculated the average GPP/E ratio for 10 days time windows on the basis of daily cumulated GPP and E. The operation was performed for the months from May to October (in 2002 from July) for all sites.

The ratio GPP/E varied according to a similar pattern for all sites (fig. 7.29). It was lowest in the beginning of May at the onset of the growing season and rapidly increased until, already in the last ten days of the month, reached levels that were maintained, with some fluctuations, across the rest of the season as long as the end of September. In October water use efficiency declined sharply. Excluding the two fringe months of the growing season, the steppe ecosystem displayed an average WUE of 2.3 μmol CO_2/mmolH_2O both in 2002 and in 2003 while in summer 2004 it was 2.6 μmol CO_2/mmolH_2O. Old field ecosystems displayed on average better WUE than the steppe ecosystem, being 3.1 μmol CO_2/mmolH_2O for the early stage of succession (Hak2) in 2002 and 2.7 μmol CO_2/mmolH_2O for the intermediate stage (Hak3).

Year	Month	Rain (mm)	ETP Hak1 (mm)	ETP Hak2 (mm)	ETP Hak3 (mm)
2002	Jul	99.12	78.47	62.17	
	Aug	59	57.99	54.90	
	Sep	24.75	37.17	31.07	
	Oct	14.19	15.59	14.39	
	Σ	**197.06**	**189.23**	**162.53**	
2003	May	55.41	46.23		
	Jun	117.17	87.45		
	Jul	99.89	80.41		
	Aug	62.38	64.60		
	Sep	39.53	37.41		
	Oct	5.4	15.14		
	Σ	**379.78**	**331.23**		
2004	May	48.08	56.45		48.75
	Jun	90.5	92.14		78.20
	Jul	60	80.48		68.23
	Aug	65	60.90		59.66
	Sep	48.02	32.25		35.87
	Oct	1.2	14.07		10.90
	Σ	**312.8**	**336.28**		**301.61**

Table 7.8. Monthly cumulated precipitation and evapotranspiration at the sites of Hak1, Hak2, Hak3. Precipitation was measured at the site of Hak1 only.

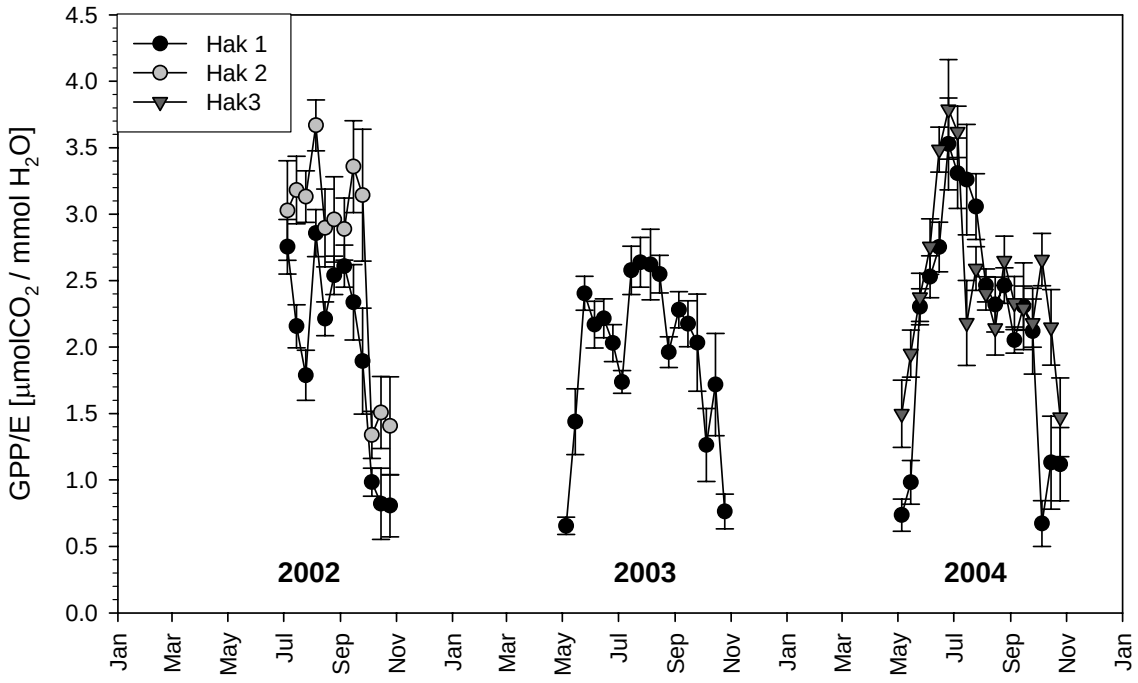

Figure 7.29. Average (± std. error) ratio of GPP/E for 10 day periods during the vegetative season (May- Oct).

7.4.8 Discussion

The carbon balance of the investigated sites was within the ranges for temperate grasslands reported in literature confirming that these ecosystems predominantly act as a sink for atmospheric CO_2. The carbon sequestration of the true steppe ecosystem (range: 98.9-130.4 $gCm^{-2}yr^{-1}$) was similar to that of lowlands and low to medium mountain grasslands of various management in Europe (Lelystad-The Netherlands: 143.5 $gCm^{-2}yr^{-1}$; Monte Bondone-Italy: 160.4 $gCm^{-2}yr^{-1}$; Neustift-Austria: 81.3 $gCm^{-2}yr^{-1}$; Grillenburg-Germany: 146.2 $gCm^{-2}yr^{-1}$; Hegihatsal-Hungary: 54.3 $gCm^{-2}yr^{-1}$) which all have a shorter growing season compared to more productive grasslands over the continent (Gilmanov et al., 2007). However for these European sites the NEP is given by larger GPP (1083-1600 $gCm^{-2}yr^{-1}$) and R_{eco} (940-1545 $gCm^{-2}yr^{-1}$) components, at least by a factor three compared to the studied steppe ecosystem.

The NEP found for the steppe of Hakasia was also in agreement with the carbon balance estimates of North American grassland ecosystems (§2.2, table2.1.) although some of these, composed predominantly by C_4 plants, show larger carbon sequestration ,up to 274 $gCm^{-2}yr^{-1}$ (Sukyer et al, 2003), while the net ecosystem productivity of (unmanaged or extensively managed) C_3 grasslands ranges from a condition of equilibrium (Sukyer & Verma, 2001) up to a sink of 133 $gCm^{-2}yr^{-1}$ (Valentini et al., 1995) depending also on the inter-annual variability of precipitation that favors carbon uptake.

The magnitude of assimilation and respiration rates in the case of C_3 grasslands, with a minimum NEE between -8 to -14 $\mu molCO_2m^{-2}\text{-}s^{-1}$ and a maximum NEE in the range of 3.5 and 7 $\mu molCO_2m^{-2}\text{-}s^{-1}$ (Flanagan et al., 2002; Frank & Dugas, 2001, Valentini et al., 1995).was comparable to the steppe site of Hakasia.

Narrowing the analysis to steppe ecosystems only, the site of Hakasia was found more efficient in carbon sequestration than a steppe ecosystem of Mongolia (41 $gCm^{-2}yr^{-1}$) (Li et al., 2005) and within the envelope of NEP assessment for an Hungarian steppe (*pustza*) ecosystem varying between 54 and 234 $gCm^{-2}yr^{-1}$ (Barcza et al., 2003; Gilmanov et al., 2007).

Results of carbon accumulation rates of old agricultural fields of Hakasia (Hak2: 216 $gCm^{-2}yr^{-1}$; Hak3: 130 $gCm^{-2}yr^{-1}$) converge with estimates of soil carbon stock changes in abandoned fields for a variety of soil types in Russia (§3.3, table 3.3) (range 43-161 $gCm^{-2}yr^{-1}$). Taking into account that those estimates do not refer not to the annual increment but the mean carbon build up over a minimum period of 14 years and a maximum of 47 years and considering that chernozem soils are recognized as the most productive among steppes soils, the estimated carbon sink of the 5 years old field (Hak2) could easily be consistent with the mentioned estimates.

The seasonality of net ecosystem exchange observed at the sites of Hakasia was typical for northern temperate grassland ecosystems (Falge et al., 2002) displaying the highest GPP/R_{eco} ratio in the first third of the growing season after 30-45 days since the onset of plants activity and uptaking CO_2 with a decreasing intensity until the whole vegetation enters in winter dormancy. On the annual time scale the amount of carbon respired by ecosystems equals a lower fraction of gross

primary productivity (range 0.67-0.77) than found for European grasslands with similar carbon sequestration capacity to the sites of Hakasia (range 0.86-0.96), yet close to the ratio reported by Law et al.(2002) for north American temperate continental grasslands (0.74). A feature of steppe and recovering grassland sites of Hakasia is the particularly small CO_2 source during winter months due to extremely cold temperature (<=5.5% of the total CO_2 emitted), which allows the ecosystems to minimize the loss of carbon uptaken during the growing season. In a review on respiration of Russian soils Kudeyarov & Kurganova report that the contribution of the cold period (from November to April) to the annual CO_2 emissions in different types of ecosystems in the southern part of Moscow region varied from 21 to 26%. However in dependence of particularly cold winters, the contribution of in the same period decreased to 11-15%. Accordingly, in tundra region, the soil CO_2 efflux during cold months is estimated to be less than 10%. Because of the climatic pattern of Hakasia region, with poor precipitation between November and April (archive mean 45 mm), and strong winds, the snow cover does not generally exceed 10 cm and the soil is exposed to intense freezing. Thus the process of soil respiration results limited and soil CO_2 fluxes in the cold period range between 0.036 and 0.77 $gCO_2m^{-2}d^{-1}$ with a mean soil temperatures at 5cm from the surface of -6.1°C, that drops to local minima between -15 and -17°C.

These results are in agreement with studies in arctic tundra ecosystems. For example, Fedorov-Davydov and Gilichinsky (1993) found that winter respiratory losses for a *Vaccinium-Cetraria* community in Russia ranged from 0.0 to 0.81 g CO_2 m^{-2} d^{-1} during October (−1.4 °C) to February (−20.3 °C), resulting in an estimated total respiratory loss of 75 g CO_2 m^{-2} for the seven-month winter period (in Hakasia winter respiration ranged 33 to 77 g CO_2 m^{-2} from November to April).. Zimov et al. (1993) reported an average winter respiratory loss (December–February) of 0.55 g CO2 m^{-2} d^{-1} for arctic tundra soils in northeastern Russia. Oechel et al. (1997) found that average respiratory loss in moist tussock tundra in Alaska (October–late May) was 1.1 g CO_2 m^{-2} d^{-1}. Respiratory losses were 0.25 g CO_2 m^{-2} d^{-1} for the late fall/early winter period at an automorphic arctic tundra site near Kolyma in northeast Siberia with mean air temperatures of −19.3 °C.

Low winter temperatures can thus be reckoned as a factor at the basis of the carbon sequestration capacity of continental temperate grasslands that would be threatened by a future scenario of climate warming because of the reduced length of the frost period and increased temperature with a consequent enhanced winter soil respiration.

The trend of NEP over time of the old field succession observed for sites of Hakasia matches the classical conception of bioenergetics of ecosystem development described by Odum (1969), although with some difference. According to that model in the early stage of ecological succession the gross photosynthesis exceeds the rate of ecosystem respiration while as succession occurs the GPP/R_{eco} ratio tends to 1. Odum uses indeed the GPP/R_{eco} ratio to indicate the state of maturity of a succession. However, the steppe site, that represents the final stage of the old field succession, is characterized by a ratio >1. It is to arguable that steppe ecosystems are constantly in succession

because of disturbances such as fire or grazing at different levels of intensity. The accumulation of carbon takes place thanks to the high belowground productivity that represents a route for inputs of organic matter, part of which remains sequestered in soil, forming the organic carbon rich chernozem soils (Bazilievich et al., 1988; Afanasyeva, 1966). The formation of such kind of soil under steppe vegetation suggests that these kind of ecosystems can continue to uptake atmospheric carbon for long times without reaching an equilibrium. Other factors that could play a role in explaining the sink capacity of the steppe ecosystem are the effect of CO_2 fertilization and nitrogen depositions; for instance Ciais et al. (2005) suggest that CO_2 fertilization may account for 50% of increased NPP in Siberia, much more than in Europe and the Amazon.

7.4.9 Conclusions

The net ecosystem productivity (NEP) of different temporal stages of the old field succession denoted a net gain of atmospheric carbon (sink). The magnitude of carbon sequestration was highest (2.1 tC $ha^{-1}yr^{-1}$) in the earlier stage (5 years since land use change) and decreased across the time of succession up to 1.1 tC ha^{-1} yr^{-1} for the climax stage represented by a typical steppe cenosis. Such pattern of the carbon balance was yielded from the decrease of gross primary productivity (GPP) after the earlier stage, whereas ecosystem respiration was found to be linearly correlated to carbon assimilation.

The carbon sequestered during the vegetative season from May to October is substantially a fair approximation of the yearly NEP since ecosystem respiration during the rest of the year (November-April) leads to modest losses of carbon, being not larger than 5.5% of annual CO_2 effluxes.

The processes of photosynthesis and respiration of the old field ecosystems, although characterized by higher rates of CO_2 exchange compared to the steppe ecosystem, were found more prone to limitation under more hot and dry environmental conditions of summer months. The resulting effect was a temporary reduction in the carbon sequestration capacity, which in the case of the steppe ecosystem was less pronounced.

After a fire event the steppe ecosystem reacted enhancing its carbon sequestration capacity and offset the carbon loss from the burnt biomass within a single growing season (NBP: 0.11 tC ha^{-1} yr^{-1}). On a eco-physiological basis the increase in the sink strength was determined by an enhancement of apparent quantum efficiency and maximum photosynthetic capacity per unit of green biomass.

7.5 Carbon dioxide fluxes over a dry bunchgrass steppe in the Ubs-Nur hollow (Tuva).

A campaign aimed at monitoring CO_2 fluxes over a typical dry true steppes in the Republic of Tuva, was carried out in July 2003 at the site of Yamaligh, within a cluster of the Ubs Nuur Hollow Reserve. The area of a dry true bunchgrass steppe selected for the monitoring of CO_2 exchanges had an homogeneous vegetation cover of about 50%, stretching around over flat terrain for several kilometres except towards the north, where a rocky outcrop bordered the plain at not less than 1500 m from the micrometeorological station.

Observations lasted 10 days, from 12th to 21th July, and were preceded by a very dry period which characterized the beginning of the summer and delayed the on set of the growing season. As a consequence grass was still little developed when measurements were about to start, while after some rain events occurred since 13th July and continued at intervals during the following days, a vigorous development of vegetation was observed. In such period after the stem elongation some species reached the flowering phase.

It is thus reasonable to state that monitoring of CO_2 fluxes took place during a period of intense gaseous exchange between plants and the atmosphere, which likely represented the peak of carbon assimilation during the season.

Total above ground biomass, sampled on 22nd July over 10 square plots with the size of 0.5m^2, was 1.64±0.63 t d.m.ha^{-1} (mean±s.d.), of which 1.16±0.57 t d.m.ha^{-1} was represented by dead biomass, including dead stems from the previous season and litter, while live biomass accounted for 0.48 ± 0.38 t ha^{-1}. The amount of aboveground biomass, being less by about 30% than that in 2004, witnesses the particular conditions of low productivity of the year.

7.5.1 Carbon dioxide flux measurements

Activities included eddy covariance measurements of CO_2 and were carried with the same instrumental set up and according to the data processing protocol described in § 7.2, except for differences in data elaboration concerning the despiking and gapfilling techniques used, described hereafter.

Gaps in data series, produced after the removal of spikes mostly caused by the interference of rain drops during and after rain events with the optical path of the gas analyzer (simply based on visual screening of outliers), were filled through non linear regressions (Falge et al., 2001) linking CO_2 fluxes with environmental drivers. In particular day time gaps (PPFD>0) were filled with modelled NEE as function of photosynthetic photon flux density (PPFD) using a rectangular hyperbolic function, and night time gaps (PPFD=0) by a bivariate gaussian model of NEE_{nigth} as function of

soil temperature (ST) and soil water content (SWC). The equations applied for daytime and night-time gapfilling respectively are the following:

$$NEE = R_{eco} - \frac{\alpha \cdot PPFD \cdot A_{\max}}{\alpha \cdot PPFD + A_{\max}} \qquad \textit{(Equation 7.36)}$$

(when PPFD>0)

$$NEE_{night} = \mathrm{Re}co = a \cdot \exp(-0.5 \cdot (((SWC - SWC_0)/b)^2 + ((ST - ST_0/c)^2))$$

(Equation 7.37)

(when PPFD=0)

where R_{eco}, α, A_{max}, a,b,c,SWC_0, ST_0 are parameters of the equations.

The aim of gapfilling the data in this specific case is to integrate NEE fluxes at daily scale and examine the day to day variation in the carbon exchange with the atmosphere. Since the monitoring period is short, the cumulated carbon budget is not of particular interest, although even few days of measurements in a key moment of the season can provide useful information on the magnitude of carbon fluxes of this steppe ecosystem and on the control exerted by environmental factors.

Additional measurements of soil CO_2 effluxes were carried out by a closed dynamic system for soil respiration measurements (LiCor 6400-09, LiCor Inc., Nebraska, USA) over 10 plots spaced out by 30 m and distributed around the tower along the N-S and W-E directions. Plots were equipped with PVC collars to avoid disturbance of superficial soil layers given by the insertion of the chamber.

7.5.2 Results and discussion

The sum of sensible and latent heat fluxes, added with terms accounting for the storage of energy in the compartments of air and soil (Aubinet, 2003), reached 80% of the measured incoming energy in the system (*Rn-G = 0.80 (H+LE)+2.78* ; r^2=0.94) (fig.7.30).

Half-hourly minimum NEE over the monitoring period was -3.66 $\mu molCO_2\ m^{-2}s^{-1}$ and maximum night-time NEE, correspondent to R_{eco}, was 3.82 $\mu molCO_2\ m^{-2}s^{-1}$. The pattern of CO_2 fluxes trend (fig. 7.31) was evidently driven by two contrasting environmental conditions: a phase characterized by low water availability following poor summer precipitation, broken by several rain events spaced by days of sunny weather. Since the station was not equipped with a rain gauge, the amount of precipitation fallen in the monitoring period can be approximated to 32 mm, as recorded at the nearest meteorological station in the village of Erzin. Soil moisture at the site was particularly low, ranging from a minimum of 0.073 $m^3\ m^{-3}$ at daytime to a maximum of 0.083 $m^3\ m^{-3}$ at night the first of day of measurements and incrementing gradually in the following days after rain water inputs till reaching a minimum and maximum of the daily fluctuation of 0.096 and 0.083 $m^3\ m^{-3}$ respectively. Only on the last day after about 24 hours of rain, the soil water content reached 0.127

m^3 m^{-3}. On the first morning of measurements (13th July-doy 194), when the first modest rain events took place alternated to hours of clear sky, maximum carbon uptake was -1.74 μmolCO_2 $m^{-2}s^{-1}$. On 14th July (14 July -doy 195) the minimum NEE (-3.66 μmolCO_2 $m^{-2}s^{-1}$) was observed.

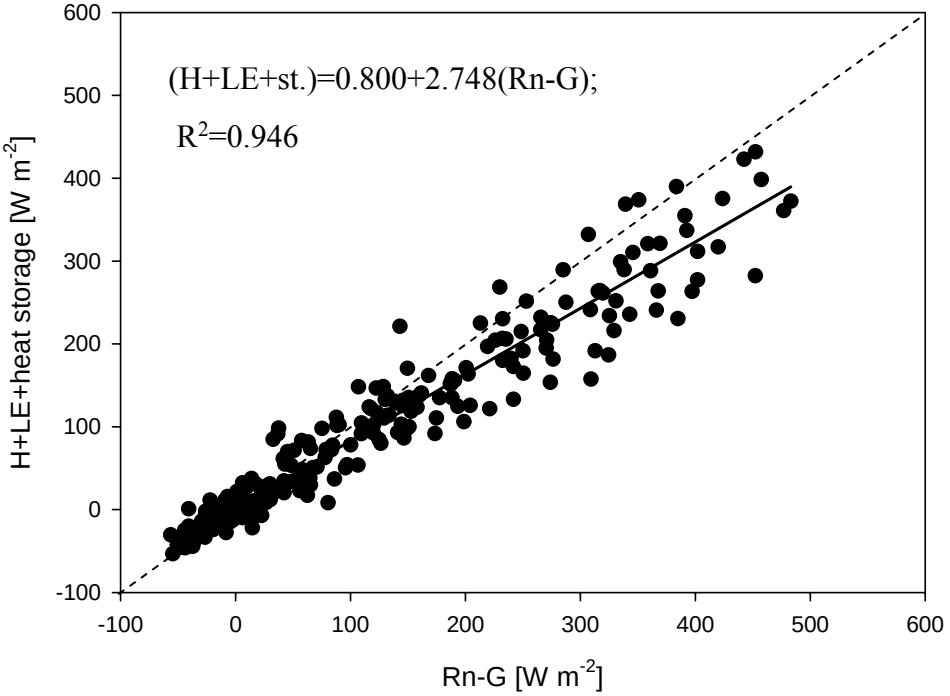

Figure. 7.30. Energy balance closure at the Yamaligh site. The heat storage term accounts for heat storage in the soil layer between 0 and 5 cm depth and the sensible and latent heat in the column of air below the height of the sonic anemometer (5m).

In these two days, the ecosystem was a net sink of atmospheric CO_2 (maximum daily NEP: -0.29 $gCm^{-2}d^{-1}$); afterwards it turned into a carbon source because of increased respiration rates (fig. 7.32). In the night of doy 195 the maximum Reco was 2.69 μmolCO_2 $m^{-2}s^{-1}$, already doubled compared to previous days. More abundant rain fell in the night of doy 196 and during the whole following day (16th July-doy 197) the effluxes from ecosystem respiration were greater than carbon assimilation by photosynthesis, determining a net loss of 1.28 $gCm^{-2}d^{-1}$, despite the cloudless sky conditions. The increase in CO_2 effluxes following the rain was consistent with independent measurements of soil respiration taken by soil chamber. Soil respiration around midday of doy 197 was 2.74 μmolCO_2 $m^{-2}s^{-1}$; this rate is greater by a factor 2.5 than that measured in the preceding and following days. The observed respiration pulses after the rain events are a known phenomenon (Xu and Baldocchi, 2004), and are especially notable during the dry season as a consequence of quickly stimulated microbial activity.

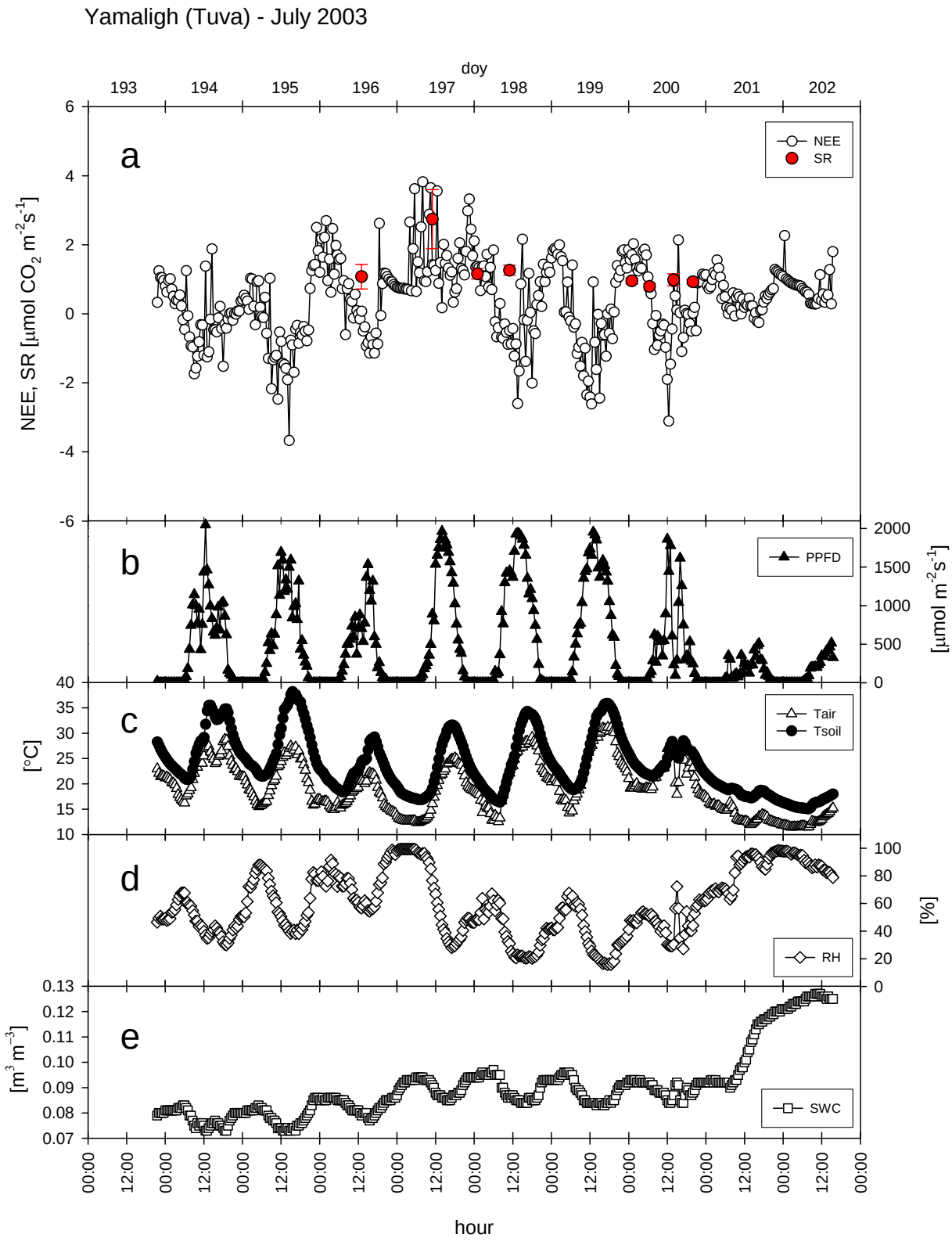

Figure 7.31. Trends, along the monitoring period of :a) net ecosystem exchange (NEE) and single chamber based measurements of soil respiration (SR) (mean±s.d.); b) photosynthetic photon flux density (PPFD); c) air temperature and soil temperature (at-5 cm); d) relative air humidity e) soil water content averaged over 0-30 cm of depth. Each point in the graph refers to 30 min. averages.

In the following two days (17-18 July), both with almost clear sky during the whole span of the day, daily NEP ranged between 0.05 and 0.28 gC $m^{-2}d^{-1}$, denoting the role of the steppe as a weak source of carbon to the atmosphere despite the assimilative activity of the vegetation.

Li et al. (2005) monitoring carbon fluxes by eddy covariance technique in a grazed steppe of central Mongolia in the same year, report minimal NEE and maximum R_{eco} of -3.6 and 1.2 $\mu molCO_2\ m^{-2}s^{-1}$ respectively, both observed in the month of July. The magnitude of CO_2 fluxes measured in the steppe of Tuva is almost enclosed in this range although on average higher R_{eco} was observed. Enhanced ecosystem respiration following rain pulses was detected also in the steppe site of Mongolia, whereas this was associated to an increase of NEE in the first weeks of the growing season and was even larger during the rain period itself. However during the increasing period of green leaf area index rain pulses usually caused a decrease in NEE, because of the larger stimulation on photosynthesis than on respiration. Interestingly Li et al. (2005) also found that from late July to early August the ecosystem switched from a carbon sink to a carbon source because of water stress.

Analyzing the response of NEE to photosynthetic active irradiance in the time window between doy 176 and 210, Li et al. (2005) retrieved an apparent quantum yield (α) of 0.0075±0.0010 (mean± std. error) and a A_{max} of 4.66±0.23 $\mu molCO_2 m^{-2}s^{-1}$. The same analysis for the steppe of Yamaligh in the period between doy 194 and 201 yielded a lower α (0.0028±0.0007) but a similar A_{max} (4.2593±1.0940) (fig.7.33).

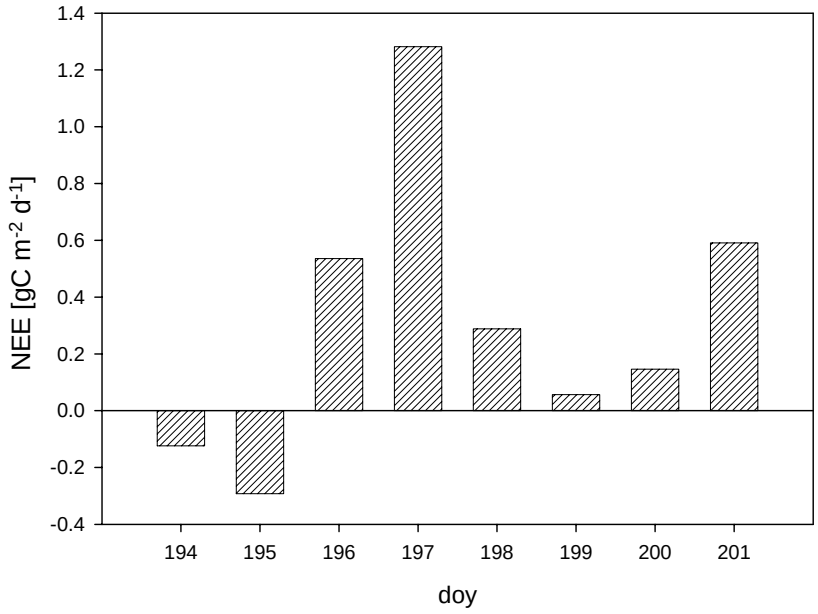

Figure 7.32. Daily net ecosystem exchange (NEE) from the julian doy 194 to 201 (13-20 July). Positive values denote a source of CO_2 to the atmosphere.

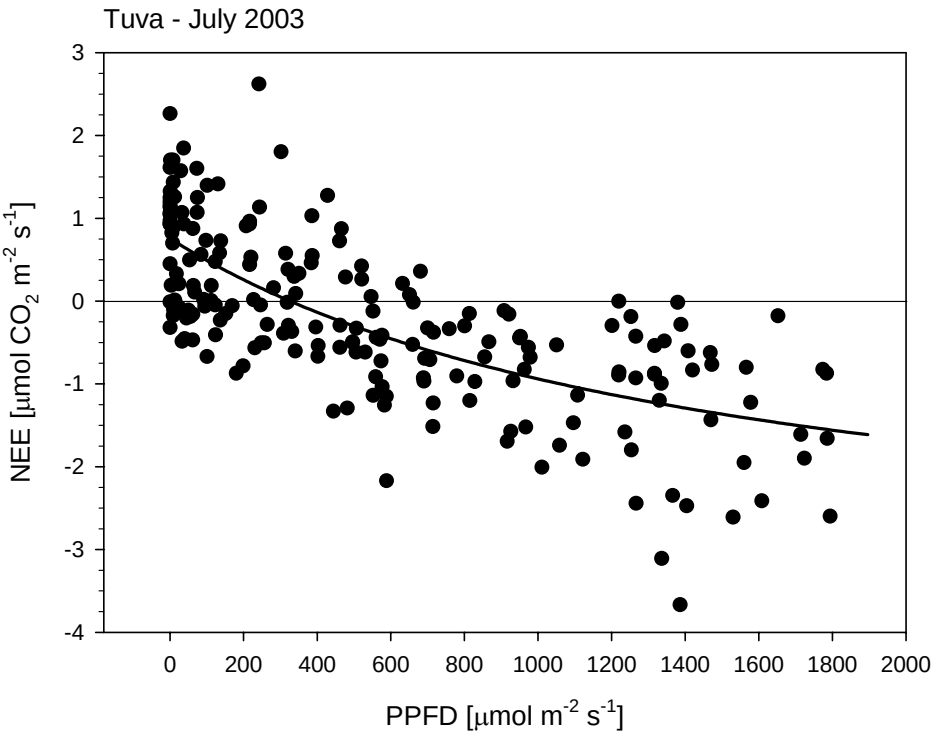

Fig 7.33. Response of net ecosystem exchange (NEE) to photosynthetic active irradiance (PPFD) based on the whole set of data collected in the time window between doy 193 and 202 (12-21 July) A regressive analysis on the basis of a rectancular hyperbolic function was performed. General equation, parameters retrieved, and statistical results as follows:

$NEE= R_{eco}-(\alpha*A_{max}*PPFD)/(\alpha*PPFD+A_{max})$

R= 0.71758409; Rsqr = 0.51492692; Adj Rsqr = 0.51002720
Standard Error of Estimate= 0.7232

	Coefficient	*Std. Error*	*t*	*P*
α	*0.0028*	*0.0007*	*3.9972*	*<0.0001*
A_{max}	*4.2593*	*1.0940*	*3.8932*	*0.0001*
R_{eco}	*0.7555*	*0.1061*	*7.1213*	*<0.0001*

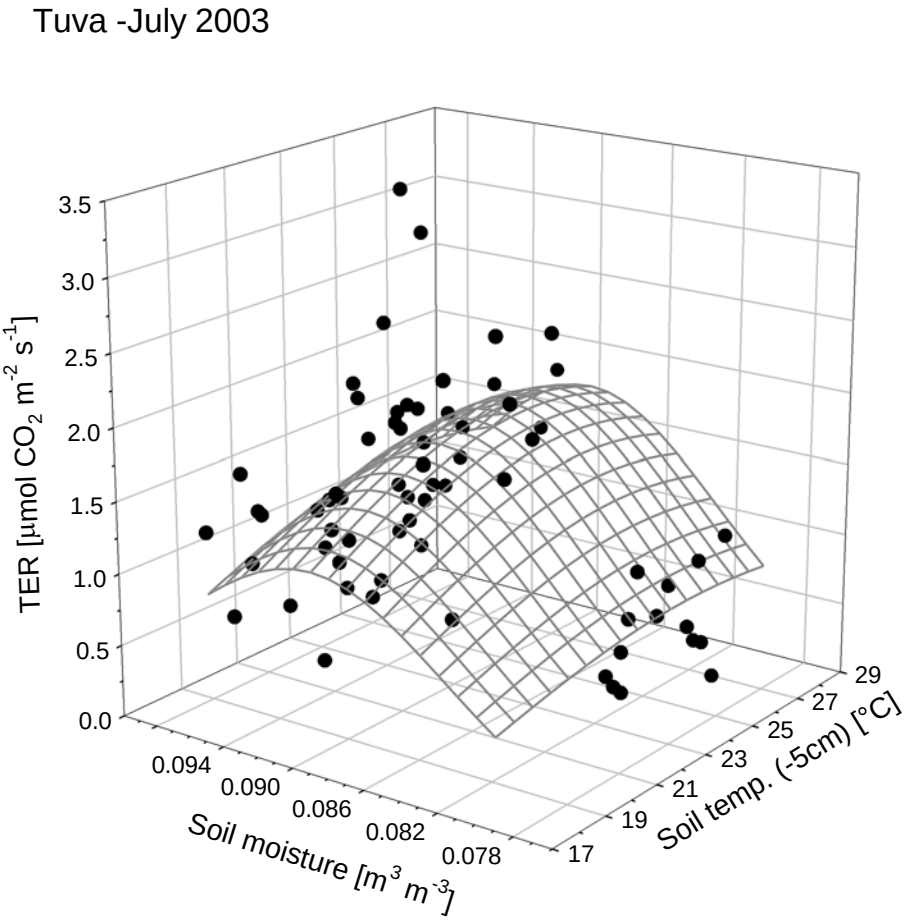

Fig 7.34. Bivariate model of the response of total ecosystem respiration (TER) to soil temperature measured at 5 cm depth and soil moisture (averaged over a 0-30cm profile). General equation, parameters and statistical results of the regression are shown below.

$NEE_{night} = R_{eco} = a*exp(-0.5*(((SWC-SWC_0)/b)^2 + ((St-ST_0)/c)^2))$

R= 0.54052915; Rsqr = 0.29217177; Adj Rsqr = 0.24650543
Standard Error of Estimate = 0.5858

	Coefficient	***Std. Error***	***t***	***P***
SWC_0	*0.0901*	*0.0011*	*81.6726*	*<0.0001*
ST_0	*25.2957*	*3.2266*	*7.8397*	*<0.0001*
a	*1.8364*	*0.1894*	*9.6959*	*<0.0001*
b	*0.0074*	*0.0014*	*5.1897*	*<0.0001*
c	*8.7385*	*5.0668*	*1.7247*	*0.0896*

7.5.3 Conclusions

The dry true steppe of Yamaligh responded dynamically to rain events with respiratory pulses which exceeded the assimilative capacity at a stage of the season when maximum growth rates of vegetation are generally observed. The positive daily NEE observed after rain events, denoting an overall loss of CO_2 to the atmosphere, may be up to 5 times larger in magnitude than the sequestration of atmospheric CO_2 (negative daily NEE) that characterizes the ecosystem in periods far from precipitations.

The short time window of investigation, together with the anomalous poor precipitation at the site in the period of early summer, are two factors that prevent the collected data set in Tuva from being generally representative for typical summer CO_2 fluxes of this kind of ecosystem. Nevertheless it was possible to find similarities in the functionality, between the steppe of Yamaligh and a short-grass steppe ecosystem of Mongolia in respect with the CO_2 exchanges with the atmosphere.

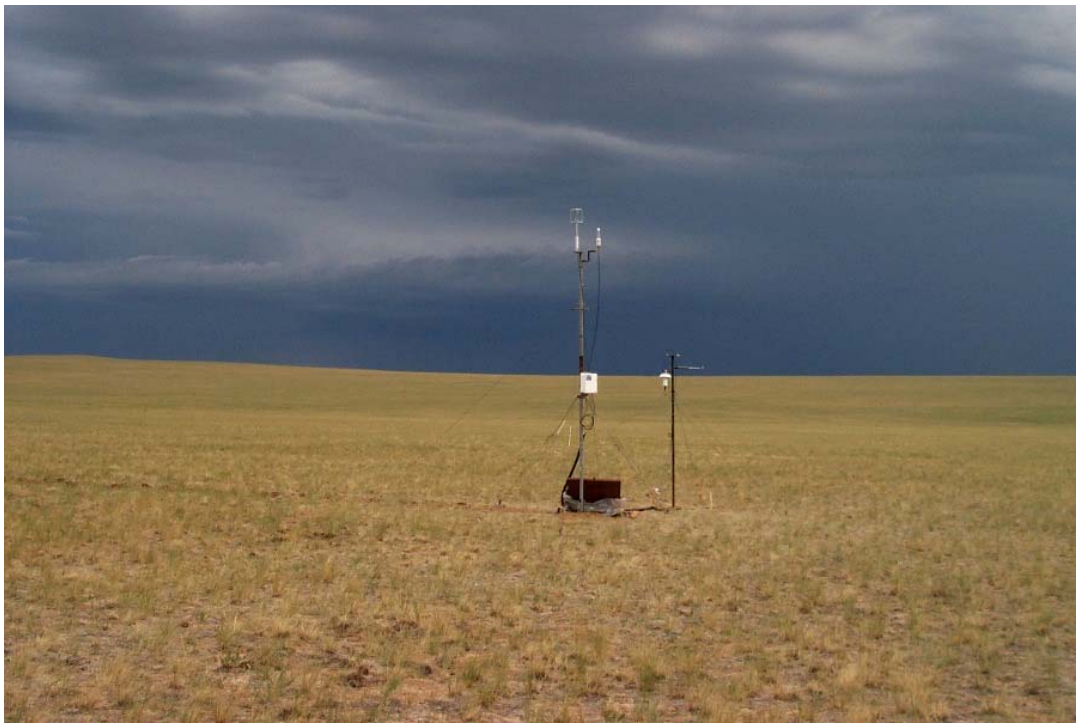

Eddy covariance station at the site of Yamaligh (Republic of Tuva) – July 2003

Winter landscape of the former agricultural land of the Solionozonoe collective farm (Republic of Hakasia) – January 2003

Plants of Atermisia spp., predominant in the early stages of the old field succession, confer the typical glaucous colour to the canopy layer – July 2002

Eddy covariance station at site of Hak1(Republic of Hakasia) – July 2003

8 Chamber based measurements of CO_2 effluxes: partitioning of root-derived soil CO_2 effluxes and control of photosynthesis over soil respiration

8.1 Soil respiration: underlying processes

After photosynthesis, CO_2 flux from soil remains the second largest carbon flux in most ecosystems, and can account for 60–90% of total ecosystem respiration (Goulden et al., 1996; Longdoz et al., 2000).

The three carbon pools that can be recognized as sources of CO_2 efflux from soil include (1) the soil organic matter (SOM), (2) above and below ground dead plant residues, and (3) organic substances released by living roots such as exudates, secretions, and sloughed-off root cells. The last group is frequently described as rhizodeposits (reviewed by Nguyen, 2003). Despite large differences in chemical composition, turnover times in the soil, and contribution to the total CO_2 efflux, these three pools have no sharp boundaries. There are many dead plant residues in the soil that are partly humified, thus part of SOM, and there are many rhizodeposits that originated from dead roots or root parts (root turnover).

There are two main groups of organisms: heterotrophic and autotrophic organisms. The most important heterotrophs in the soil can be subdivided into two broad groups: (1) soil microorganisms (bacteria, fungi, actinomycetes and protozoans) and (2) soil macrofauna (macroscopic invertebrates and small mammals). The contribution of soil macrofauna to total CO_2 efflux from soils is usually only a few percent (Ke et al., 2005). Most CO_2 evolved by heterotrophic soil organisms is respired by microorganisms such as bacteria, non-mycorrhizal and mycorrhizal fungi, and actinomycetes. This component of soil CO_2 flux is referred to as 'microbial respiration'. Although the direct contribution of soil macrofauna is small, they can greatly increase microbial respiration not only by fragmentation and comminution of plant residues (Couteaux et al., 1991; Bonkowski et al., 2000), but also by predation of some groups of microorganisms (Griffiths, 1994; reviewed by Bonkowski, 2004). This intensifies their turnover rate and results in increasing CO_2 efflux from the soil (Mikola and Setala, 1998; Wardle et al., 1998; Lavelle and Gilot, 1994). Plants are the most important autotrophs contributing to CO_2 efflux from soil by root respiration.

Within the broad groupings described above, Kuzyakov (2006) suggests that the following five sources are the main contributors to total soil CO_2 efflux:

(1) microbial decomposition of SOM in root free soil without undecomposed plant remains, frequently referred to as 'basal respiration'.

(2) microbial decomposition of SOM in root affected or plant residue affected soil (defined 'rhizosphere priming effect' or 'priming effect', respectively).

(3) microbial decomposition of dead plant remains.

(4) microbial decomposition of rhizodeposits from living roots, frequently referred to as 'rhizomicrobial respiration'.

(5) root respiration.

It is important to note that pedogenic or anthropogenic acidification of soils containing $CaCO_3$ can also contribute to the CO_2 efflux. However, on the subannual, annual and decadal time scales, which are usually used in the soil CO_2 flux measurements, its contribution is marginal. The $CaCO_3$-derived CO_2 usually accounts for not more than 3–4 gC m^{-2} y^{-1}.

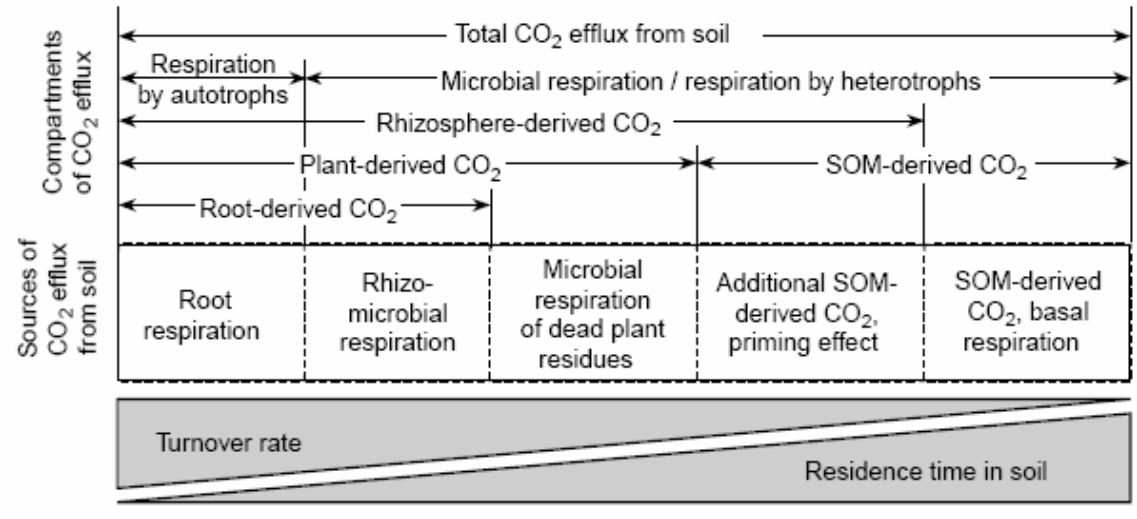

Figure 8.1.Sources of biogenic CO_2 effluxes from soil, ordered according to turnover rates and mean residence time of C in soil. (after Kuzyakov, 2006)

Rates of soil respiration are largely dependent upon soil temperature and moisture conditions (Singh & Gupta, 1977; Schlentner & Van Cleve, 1985). Seasonal changes in soil microclimate play an important role in defining seasonal differences in soil CO_2 emissions within sites, and climatic differences generate different soil respiration rates among distant sites (Raich & Potter, 1995). Other soil factors potentially influencing rates of soil respiration *in situ* include the availability of carbon substrates for microorganisms (Seto & Yanagiya, 1983), plant root densities and activities (Ben-Asher et al., 1994), soil organism population levels (Singh & Shukla, 1977), soil physical and chemical properties (Moore & Knowles, 1989).

Among these factors temperature has been the abiotic factor most associated with soil CO_2 flux in reviews of global patterns of soil CO_2 flux (Lloyd and Taylor, 1994; Raich and Potter, 1995), but heating of the soil is primarily caused by solar radiation and consequently, soil temperature and light availability to canopies are correlated at diurnal and annual time scales.

Recent studies have indeed highlighted the tight correlation between gross primary productivity (GPP) or canopy photosynthesis and soil respiration (Craine et al., 1999; Kuzyakov and Cheng, 2001; Janssens et al., 2001; Tang et al., 2005).

Monitoring of soil respiration in a natural steppe of Hakasia (Hak1) over selected days of the growing season also evidenced the correlation of soil respiration to photosynthetic active radiation over the course of a day, whereas soil temperature was a weaker driver (fig. 8.2-8.5).

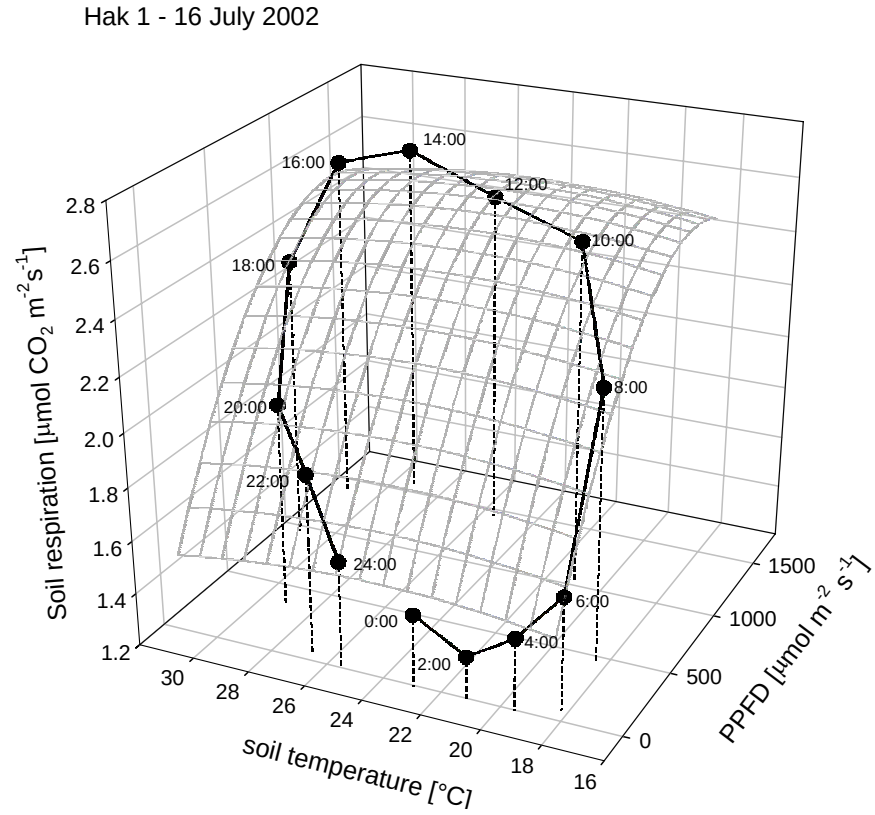

Figure 8.2.Daily dynamic of soil respiration (SR) measured at 2h time intervals over a steppe of Hakasia (Hak 1) on 16 July 2002 by a portable soil respiration chamber (LI 6400, LiCor, USA) plotted against photosynthetic active radiation flux (PPFD) and soil temperature (ST) measured at 0.1 m depth. The general equation and parameters of the regressive model used to fit the data (grey surface) are the following:

*SR=y0+a*PPFD+b*ST+c*PPFD^2+d*ST^2; R = 0.968; Rsqr = 0.937; Adj Rsqr = 0.906*

Standard Error of Estimate = 0.1389

	Coefficient	*Std. Error*	*t*	*P*
y0	*0.7487*	*1.5894*	*0.4710*	*0.6502*
a	*0.0015*	*0.0003*	*4.9981*	*0.0011*
b	*0.0662*	*0.1314*	*0.5038*	*0.6280*
c	*-0.0000*	*0.0000*	*-2.8671*	*0.0209*
d	*-0.0014*	*0.0027*	*0.5083*	*0.6250*

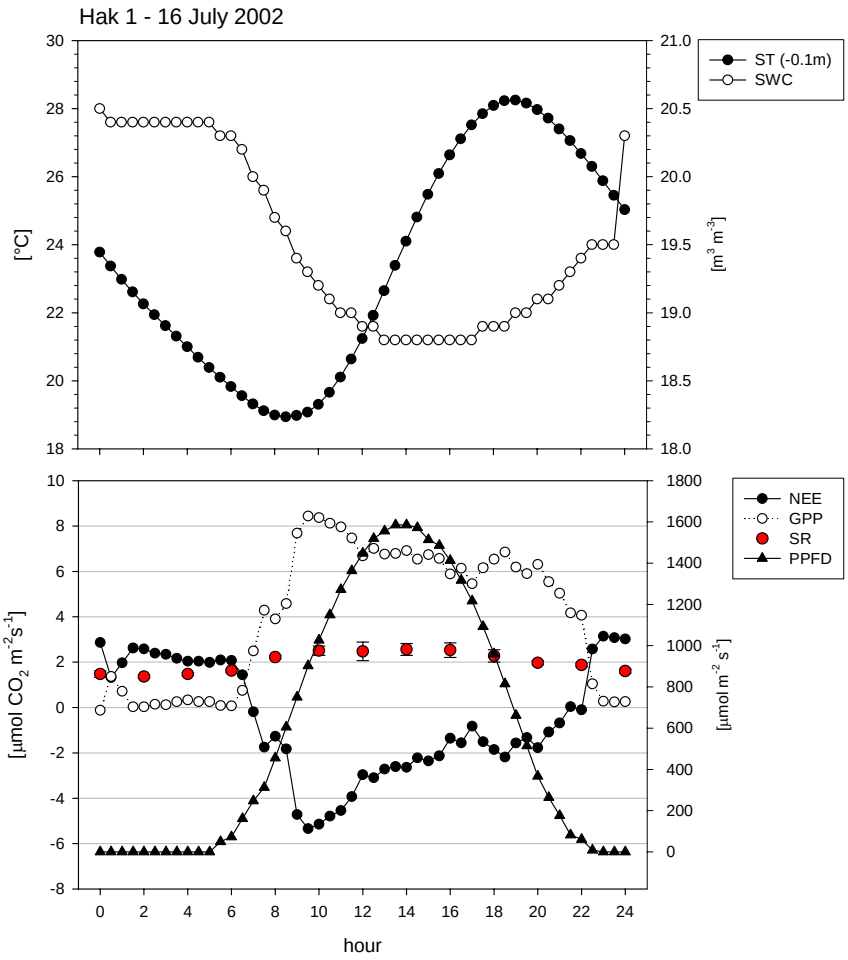

Figure 8.3. Above: trend of 30 min average of soil temperature (ST) and soil water content (SWC) on 16th July 2002 at Hak1. Below: trend of 30 min mean net ecosystem exchange (NEE), gross primary productivity (GPP) , photosynthetic photon flux density (PPFD). Trend of soil respiration (SR) measured by soil flux chamber (6400-09, LiCor, USA).

Ecophysiological studies consistently demonstrate tight linkage between photosynthesis and carbohydrate supply to roots as and between carbohydrate supply and root respiration (Amthor, 1994; Lambers et al., 1996; Szaniawski and Kielkiewicz, 1982). Therefore, studies of factors affecting root carbohydrate status, such as light or defoliation, often find that factors influencing carbohydrate supply explain patterns of root respiration better than does temperature (Bassirirad et al., 1993; Fukuoka et al., 1996; Percival et al., 1996). It is reasonable to predict that controls over plant carbon gain and allocation could provide key links between light availability, its interception and soil CO_2 flux. This ecophysiological perspective has generally not been applied to ecosystem studies of soil CO_2 flux, yet it is important, for example, in analyses of climate warming, which would entail an increase in temperature without a change in light supply. In such a scenario, the pre-warming relationship between temperature and soil CO_2 flux may not apply.

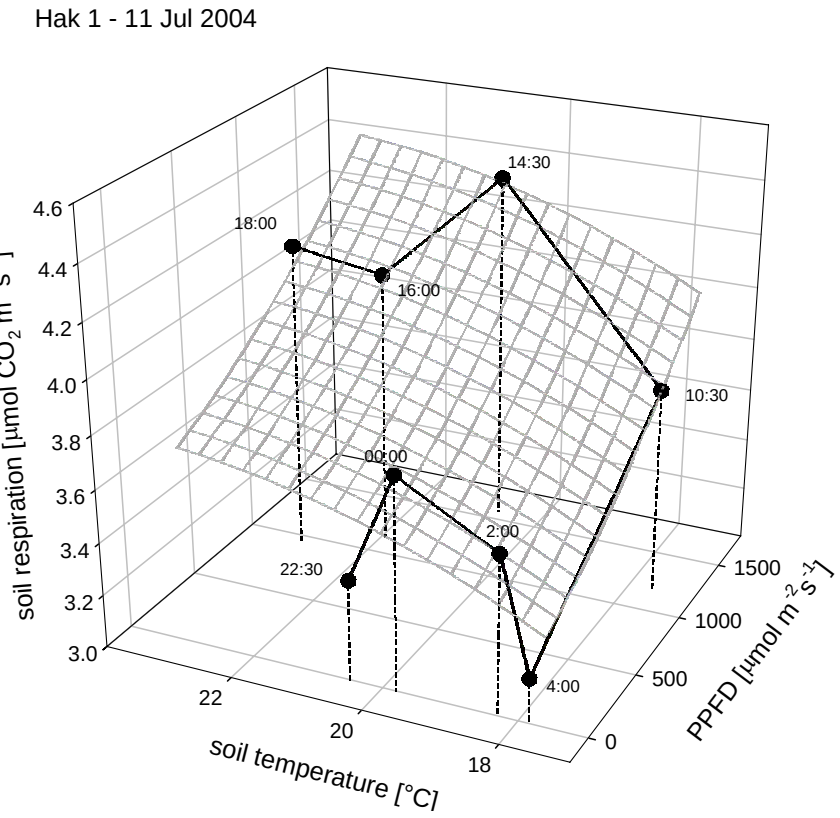

Figure 8.4 Daily dynamic of soil respiration (SR) measured at 2h time intervals over a steppe of Hakasia (Hak 1) on 11 July 2004 by a portable soil respiration chamber (SRC1, fitted to an EGM2,PP Systems, UK) plotted versus photosynthetic active radiation flux (PPFD) and soil temperature (ST) measured at 0.1 m depth. The general equation and parameters of the regressive model used to fit the data (grey surface) are the following:

*SR=y0+a*PPFD+b*ST+c*PPFD^2+d*ST^2; R = 0.905; Rsqr = 0.819; Adj Rsqr = 0.579. Standard Error of Estimate = 0.2576*

	Coefficient	*Std. Error*	*t*	*P*
y0	*-1.8443*	*21.0197*	*-0.0877*	*0.9356*
a	*0.0003*	*0.0011*	*0.2384*	*0.8269*
b	*0.4617*	*2.1214*	*0.2176*	*0.8417*
c	*0.0000*	*0.0000*	*0.1389*	*0.8983*
d	*-0.0095*	*0.0533*	*-0.1787*	*0.8696*

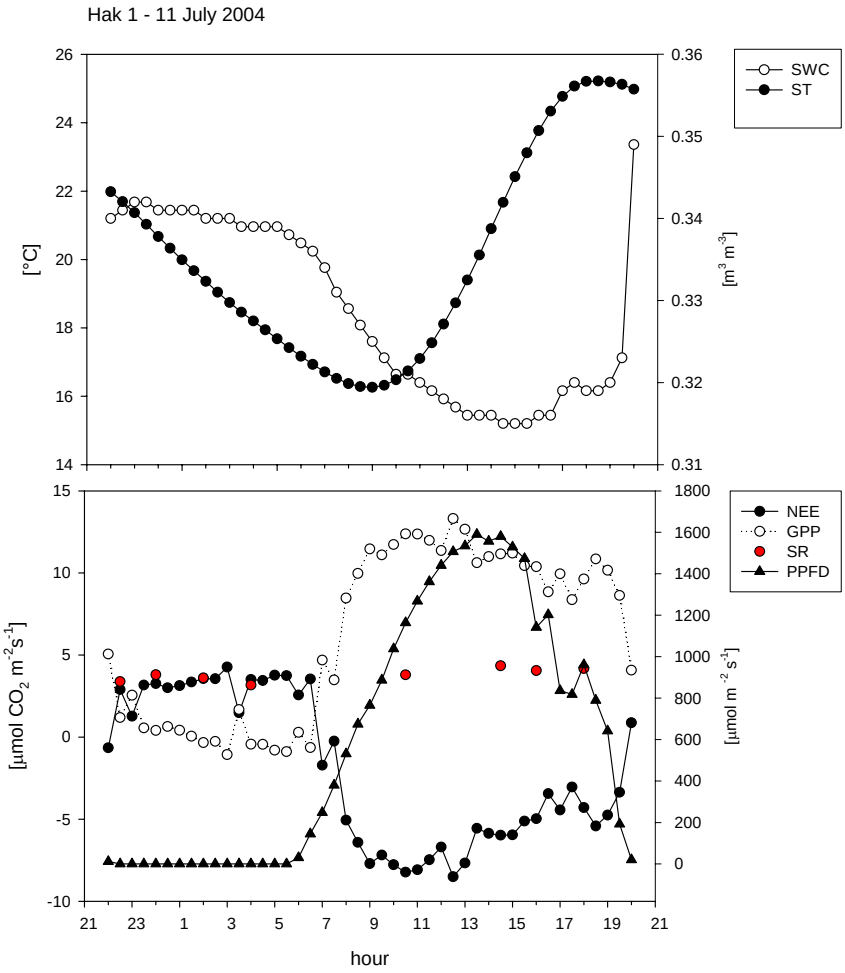

Figure 8.5 Above: trend of 30 min average of soil temperature (ST) and soil water content (SWC) across 10th and 11th July 2004 at Hak1. Below: trend of 30 min mean of net ecosystem exchange (NEE), gross primary productivity (GPP) , photosynthetic photon flux density (PPFD). Trend of soil respiration (SR) measured by soil flux chamber (SRC1 fitted to EGM2, PP Systems, UK).

8.2 Field experiments

Two manipulative experiments were conducted in a steppe of Hakasia with the following objectives:

1. To quantify the contribution of autothrophic and heterothrophic respiration to total soil CO_2 efflux (study case 1)
2. To address the influence of factors that affect carbohydrate source on soil CO_2 flux, by testing the effect of reduced light intensity and removal of aboveground biomass on soil respiration. (study case 2)

8.2.1 Applied methods for soil CO_2 flux measurement partitioning

The methods applied in the experiments (root removal, trenching, clipping and shading) are part of a group of non-isotopic techniques, used for the partitioning of autotrophic and heterotrophic respiration (Hanson, 2000; Kuzyakov, 2006) and are illustrated below.

In all methods applied the estimate of root contribution (RC) to total soil respiration flux (SR) is retrieved indirectly by difference between the control and the manipulated plots.

$$RC = SRc - SRm \qquad \textit{(Equation 8.1)}$$

where *SRc* is the soil respiration flux from not manipulated (control) plots and *SRm* is the soil respiration flux from treated plots.

8.2.1.1 Root exclusion

The root exclusion method is any procedure that indirectly estimates the root contribution by measuring soil respiration with and without the presence of roots (i.e., no direct measurements of bare root tissue are made).

Existing root exclusion techniques may be categorized into three broadly defined areas:

(1) root removal – roots are removed, soil is placed back in reverse order of removal, and further root growth is prevented by barriers (alternatively, roots may be removed after a series of soil respiration measurements)

(2) trenching – existing roots are severed by trenching at a plot boundary but not removed, and a barrier is installed to inhibit future root growth.

(3) gap analysis – aboveground vegetation is removed from relatively large areas (e.g., clearcutting in forests) and soil respiration measurements in the gap are compared to soil respiration data for a forested area.

Root exclusion studies are most useful if the measurements extend through a complete annual cycle, but over such a long period there is the possibility of reinvasion of roots into previously root free zones. For this reason, root exclusion approaches based on trenching or gaps would be improved if periodic or post- experiment sampling for residual root density was conducted. Such sampling would ensure that gaps or barriers provide complete exclusion of root regrowth during experiments.

Root exclusion approaches share the problem that root severance and/or removal results in increased soil moisture, which can affect decomposition and respiration rates. In some systems (i.e., very dry or very wet sites) and at certain times of the year, differences in moisture between root exclusion zones and intact zones must be taken into account.

One of the biggest concerns with the trenching approach is the influence of residual decomposing roots left in the trenched plots and their contribution to total soil respiration. Ewel et al. (1987) addressed this problem by allowing several months to pass after trenching before collecting CO_2 efflux data and by periodically sampling fine root biomass in the trenched plots.

Kzyakov (2006) points out as one of the main shortcomings of the root removal techniques that the decomposition of SOM and other plant residues is dependent, not only on the physical effects (water regime and temperature balance) of vegetation on soil, but also on direct biological effects due to the presence of living roots (Kuzyakov, 2002a,b; Paterson, 2003). For instance, the CO_2 evolved as a consequence of the rhizosphere priming effect may be 2–3 times larger than that of basal respiration (Cheng et al., 2003).

8.2.1.2 Shading and clipping.

Shading or clipping of aboveground plant parts in grasslands (Craine et al., 1999) or clear felling in forests have been used as less-invasive alternatives to root exclusion, which avoid any influence of root-removal on soil conditions by partitioning of SOM-derived and root-derived CO_2. These methods are based on stopping leaf photosynthesis and thus excluding new assimilate transport to the roots. The advantage of these approaches is that shortly after the treatment (days), the water content and the nutrient turnover in the shaded or clipped treatment are nearly the same as in the untreated control. However, the disadvantage of these methods is that, although the flow of recent assimilate is interrupted, previously-fixed carbon in plant organic compounds can be used for root respiration and rhizodeposition. Thus, the contribution of root-derived CO_2 to the total soil CO_2 flux is not completely removed. The application of these techniques to many plants requires caution as plant carbon allocation is affected in two ways. Defoliation of grasses increases the sink strength for leaf growth and reduces below-ground carbon allocation (Detling et al., 1979; Holland and Detling, 1990). In addition, many plants store some of the carbon assimilated prior to defoliation in their roots, and utilize these carbon reserves for regrowth following cutting (Johansson, 1993). Increases in exudation and root and rhizosphere respiration after clipping have been reported (Paterson et al., 2003; Fu and Cheng, 2004). These effects, especially changes of carbon allocation patterns, have a significant effect on microbial community structure, and lead to differences in, but not elimination of root derived CO_2 fluxes in clipped and un-clipped treatments.

8.3 Case study 1- Partitioning of soil respiration of heterotrophic and autotrophic origin in a natural steppe of Hakasia

8.3.1 Soil CO_2 fluxes: partitioning

The objective of this study was to partition the heterotrophic component of soil respiration in a natural steppe of Hakasia (Hak1) over the growing season of 2004 from May to September. The interest behind this manipulative experiment was on the one hand to disclose the seasonal dynamics of heterothrophic respiration and derive the authothrophic component by difference with total soil respiration; on the other hand to quantify the term of cumulated soil respiration of heterothrophic origin, setting the base for the assessment of the carbon budget with the ecological inventory approach, described in chapter 9.

Soil respiration was measured weekly using a closed dynamic system (SRC1 chamber connected to EGM2, PP Systems,UK) over 10 plots selected within the footprint area of the eddy covariance station along N-S and W-E directions and spaced out of 30 m, where PVC collars (diameter 10 cm; height 6 cm) were inserted approximately 3 cm deep in the ground. Collars were located in the space between graminoids tussocks and the possible live stems within the surface inscribed by the collar were clipped to avoid measuring CO_2 fluxes originated else than from the soil.

Heterotrophic component of soil respiration flux was measured at weekly frequency applying two variants of the root exclusion method (root removal and trenching) over 6 additional plots having a surface of (40x40) cm^2 by 30 cm of depth, adjacent to the plots located along the W-E direction. In three of these plots the extracted soil was cleaned from roots and was placed back into each pit and further root growth was prevented by barriers placed on the lateral faces; while in the remaining three plots, roots were severed by trenching but not removed, and barriers were installed to inhibit future root growth. Regrowth of grass from germination in the plots was inhibited by frequent checks of the experimental area and removal of seedlings found. To address the problem of enhanced soil CO_2 efflux rates due to residual decomposing roots left in the trenched plots, we allowed 12 months to pass after trenching before collecting soil CO_2 efflux data. No significant difference was observed (α=0.05) in soil CO_2 effluxes (two-tailed T-test: P T<t 0.17) nor soil temperature (two-tailed T-test: P T<t 0.79) between plots with the result being independent of the technique applied.

8.3.2 Results and discussion

Soil respiration fluxes measured by chambers responded to soil temperature according to a linear relation (*SR=0.22(Tsoil)-0.42*; R^2=0.88; n=23). Values ranged from a minimum of 0.64 and 0.24 $\mu molCO_2\ m^{-2}\ s^{-1}$ in the beginning of May and in the end of September respectively, to a maximum of 4.3 $\mu molCO_2\ m^{-2}\ s^{-1}$ in middle July (fig.8.6). Heterotrophic fraction of soil respiration represented almost the whole soil CO_2 efflux in early May before the onset of vegetation and was

also linearly correlated to the soil temperature (*Rh=0.17(Tsoil)-0.18*;R^2=0.72; n=23). R_h values reached maximum values in the time window between end of June and beginning of August (2.79 – 3.71 μmolCO_2 m^{-2} s^{-1}) when R_h represented on average about 68% of soil respiration. The autotrophic component of soil CO_2 effluxes, retrieved as the difference between measurements of soil respiration and its heterotrophic fraction, was greater during periods of biomass growth, (from 1.34 to 1.75 μmolCO_2 m^{-2} s^{-1} in late July). In general, the magnitude of root respiration, cumulated for each time interval between measurements, was proportional to the photosynthetic activity, albeit with considerable scatter (*Ra=0.16*GPP-0.15*; R^2=0.56; n=20); however it is possible to reduce substantially the scatter of this relation by analyzing the response to gross primary productivity only for the periods from May to July (R^2=0.75) (fig.8.7), as during the remaining part of the season the values of root respiration associated to lower levels of photosynthesis suggest that the support for root respiration was provided mostly at the expenses of the plants reservoirs of carbon, possibly from the translocation of carbon from the aboveground to the belowground biomass. It also cannot be excluded that inside the manipulated plots the absence of roots formed in the current season, that undergo decomposition at the end of the summer, result in a lower CO_2 efflux from heterotrophic origin, leading to an overestimation of the autotrophic component. Nevertheless this explanation unlikely applies to the month of July, when, according to sequential biomass samplings, it was registered a consistent increment in roots biomass.

Using a linear interpolation of soil fluxes between measurements dates, the cumulated value of soil respiration for the whole monitoring period, was 417.2 gCm^{-2} partitioned into 332.7 gCm^{-2} (79%) from heterotrophic respiration and 84.5 gCm^{-2} (21%) from autotrophic origin (fig.8.6). From the modelled ecosystem respiration based on eddy covariance measurements, it is possible to quantify the CO_2 effluxes within the time window of this study (May-September) as representative for 92% of the correspondent yearly total. We thus conclude that the result of the partitioning of soil respiration found can be fairly extended to annual scale too.

Published results of field based data sets on soil respiration partitioning from non forest ecosystems (Hanson, 2000) show that the percentage of root contribution is spread throughout the entire range with an overall average of 36%, although time steps of the estimates vary from daily, to monthly and annual. Taking in consideration the experiments conducted on grasslands ecosystems at yearly time step, Kucera and Kirkham (1971) found a root contribution of 40% in a tall grass prairie.

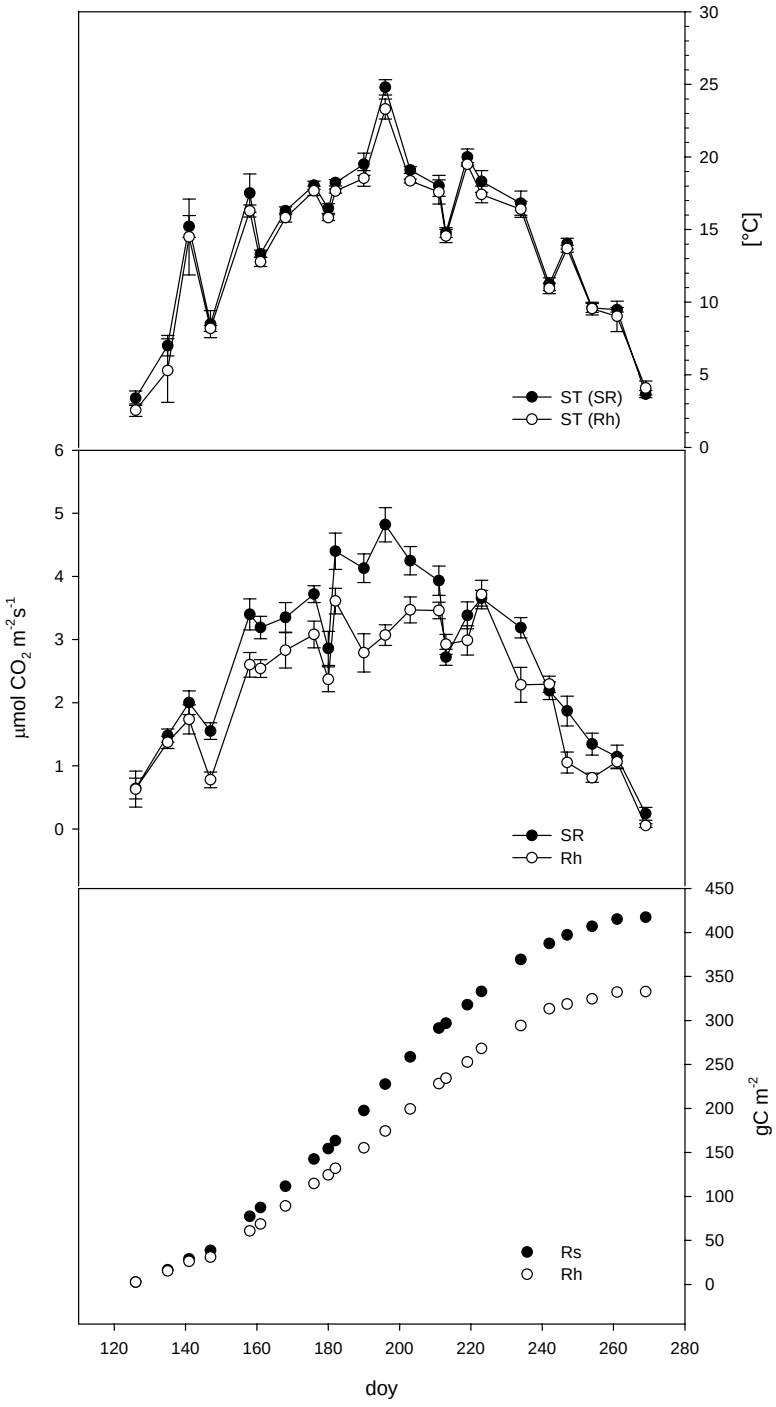

Figure 8.6.Above: trend of soil temperature (-10 cm) (mean ± standard deviation.) measured in plots for total soil respiration measurements (black dots) and plots for heterothrophic respiration measurements (white dots). Middle: trend of soil respiration (black dots) and heterotrophic component of soil respiration (open dots) measured by chamber technique (error bars: ± standard error). Below: trend of cumulated soil respiration (Rs) (black dots) and heterotrophic respiration (Rh) (white dots).

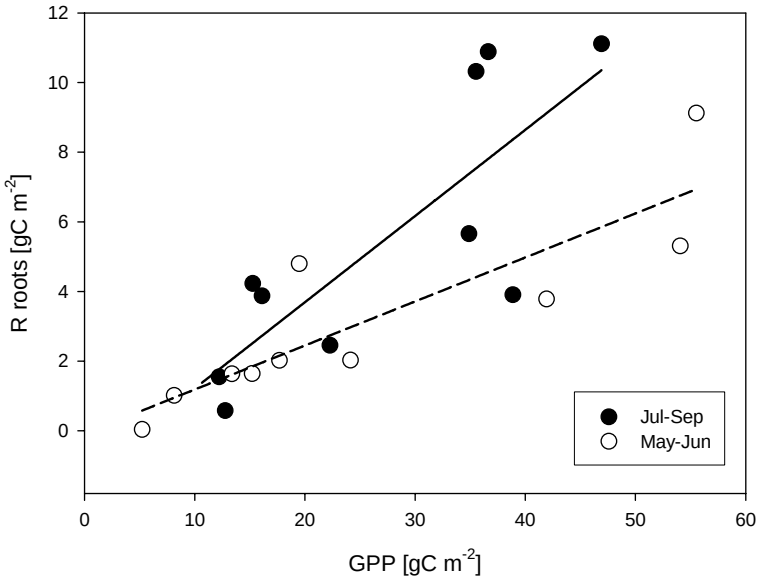

Figure 8.7. Relation between root respiration (R roots) and gross primary productivity (GPP) cumulated over the periods between measurements assuming linear variation of root respiration within each period. The linear regression for the early summer (white dots, dashed line) gives a slope of 0.12 ($P<0.01$, $r^2=0.75$) while for the late summer (black dots, solid line) the ratio of R roots/GPP is 0.24 ($P>0.01$, $r^2=0.64$)

8.4 Case study 2- Photosynthesis control on soil respiration in a natural steppe of Hakasia.

8.4.1 Materials and methods

The study was performed in late July 2004 over a natural graminoid small-tussock steppe in Hakasia (Hak1). Plots were located within the footprint of the tower in a rectangular area containing a total of 30 plots distributed in 6x5 rows; the area of each plot was 0.25 m^2 (50x50 cm) and rows were separated by buffer stripes of 1 m width. Plots were randomly assigned to be clipped, shaded or left as control so that 10 plots per each thesis were individuated (fig.8.8). Plastic (PVC) collars (d=11cm; h=6 cm) were inserted approximately 3 cm into the ground in the middle of each plot, 2 days before the beginning of the measurements. Soil CO_2 flux measurements were performed using a closed dynamic soil respiration system (EGM2, PP-Systems) fitted with a soil respiration chamber (SRC1, PP Systems, UK) and started before the treatment was applied in order to verify the homogeneity of the groups of plots assigned to different thesis in respect with the soil CO_2 fluxes. Soil temperature at 5 cm depth was also measured for each plot by a probe connected to soil chamber system. These first sets of measurements were performed on 20th and on 24th July; after that standing aboveground biomass was clipped, leaving the litter in place, in the plots

selected for the suppression of photosynthetic activity, while a polyethylene net covering the canopies and the sides of the plots facing E,S,W directions was used to shadow the plots where light intensity had to be reduced. A PAR radiometer (SKP215, Skye) was installed under the cover of the net in order to quantify the reduction of incoming radiation in the shadowed plots by comparison with the total incoming PAR radiation measured at the tower site; two thermistors (CS107, Campbell Scientific) to monitor soil temperature were inserted at 5 cm depth in a clipped and in a shadowed plot respectively and all data were stored as 30 min. averages by a data logger (CR10, Campbell Scientific). Soil CO_2 flux measurements were taken again from 26th July and were carried on daily for five days in the hours between 10 and 11:30 a.m. In such time-window of the day indeed soil temperatures showed the least divergence between treatments (fig.8.9) and photosynthetic activity of plants was already on set by several hours though not limited by water vapour deficit.

Data were analyzed testing differences in soil CO_2 flux rates and soil temperature among treatments using one-way ANOVA (Prism4, GraphPad Software Inc.); in case of significative differences in variances, Tukey's post hoc test was furtherly performed to detect which treatment differed significantly.

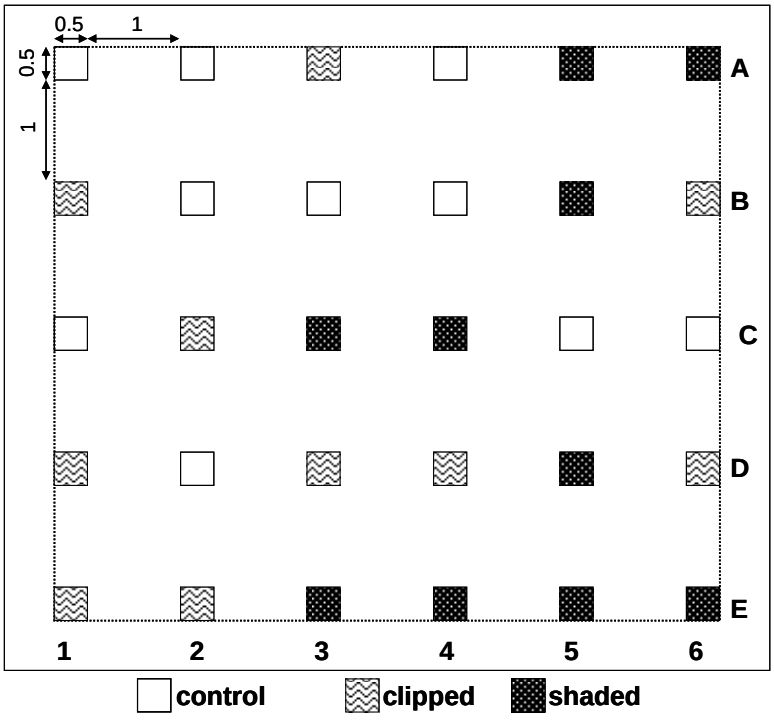

Figure 8.8. Scheme of the experimental design: a number of 30 plots (0.5x0.5m^2) were randomly assigned to control, shaded and clipped treatments.

8.4.2 Results and discussion

Analyzing data by one way ANOVA, no significative difference neither in soil CO_2 efflux nor in soil temperature was observed ($P>0.05$) between the three groups of plots designated for the treatments before any manipulation was performed.

After the beginning of the experiment the reduction in PAR flux over the shaded plots for the whole period of measurements was 76.5% with the peak of PPFD reaching 326.4±89.9 μmol $m^{-2}s^{-1}$ against full incoming PAR radiation of 1325.9±349.9 μmol $m^{-2}s^{-1}$ (fig 8.9).

Soil respiration rates in both clipped and shaded treatments were smaller than in control plots: these differences were highly significant ($p<0.001$) either performing ANOVA for the whole set of measurements grouped by treatment than analyzing separately only the results of the last day of measurements when the reduction of soil respiration rates was 75% and 79.5% for the shaded and the clipped plots respectively (Tab.8.1).

It was not observed any significant difference in soil temperature between control and clipped plots during measurements ($P<0.0001$), while soil temperature in shaded plots differed on average by -0.9 °C ($P<0.001$) compared to control plots. However the reduced soil respiration in the shaded plots by a mean of -28.5% does not seem to be justified by the effect of the slightly lower soil temperature as evidenced comparing treatments on the basis of functional response of soil respiration to temperature (fig.8.11). The regressive analysis of soil CO_2 effluxes against soil temperature using a simple exponential function confirms indeed a depression of soil respiration, in both clipped and shaded treatments keeping soil temperature constant.

The ratio between soil CO_2 flux in clipped plots and in control plots was negatively correlated with time since clipping (Spearman r=-0.96), while the ratio between soil CO_2 flux in shaded plots and in control plots did not decline progressively with time (fig.8.10) but resulted positively correlated to the amount of PAR radiation of the day before the date of measurements. (Spearman r=0.84).

Soil respiration in clipped plots was higher than in shaded plots: if on one side the absence of carbohydrates supply from photosynthetic activity would lead to expect an opposite result, on the other hand the effects of increased labile organic matter to the microbial food chain coming from roots death after clipping and the higher root respiration stimulated by the restoration of aboveground sprouts can provide an explanation. Craine (1999) found similarly a lower reduction of soil respiration in clipped plots (-19%) than in shaded plots (-40%) after two days since the application of treatment in a temperate grassland.

Although we did not measure root respiration in the shade experiment, the results are consistent with Fukuoka et al. (1996), where shaded cabbage seedlings had lower results of root respiration than unshaded seedlings. This would imply that in our shading experiment, the decreases in soil CO_2 flux in shaded plots partly were due to decreases in root respiration.

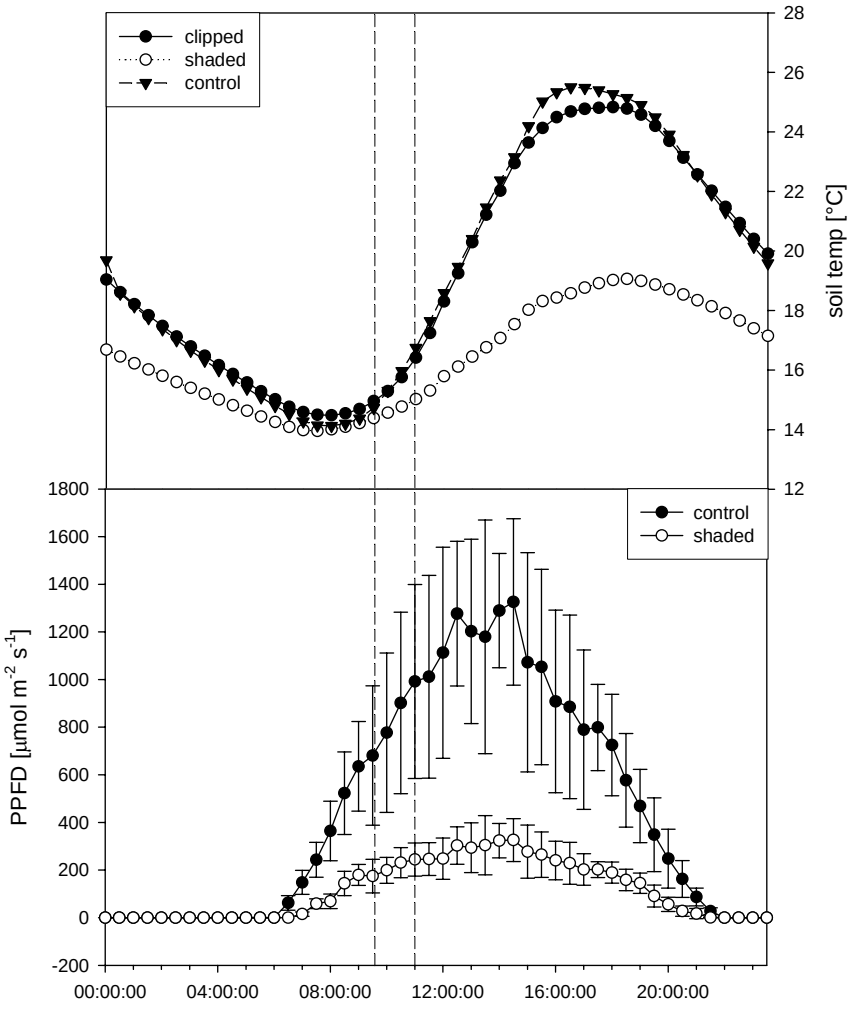

Figure 8.9. Above: average daily trend of soil temperature measured at a depth of 5 cm by thermistors under a clipped and a shaded plot; control refers to soil temperature measured in an undisturbed area in the proximity of eddy covariance station. Below: average daily trend of PPFD measured above the canopies at the eddy covariance station (control) and under the shading net (shaded) during the dates of measurements (24^{th}-30^{th} July). Vertical bars indicate standard deviation. The dashed vertical lines delimitate the time window when soil CO_2 flux was measured.

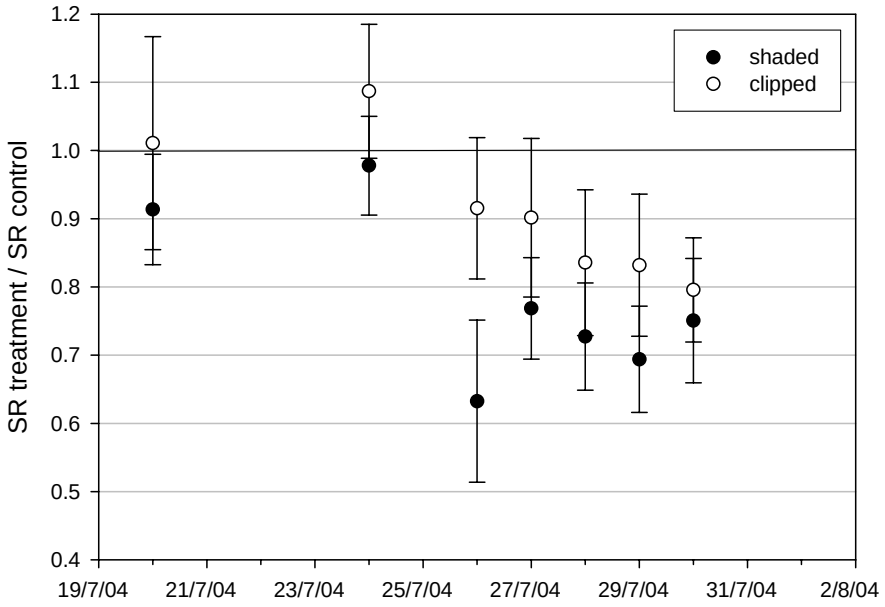

Figure 8.10 Trend of soil CO_2 fluxes in shaded and clipped plots normalized by soil CO_2 fluxes in control plots before and after the treatment (mean±s.d).

		Group of plots			
	parameter	**control**	**clipped**	**shaded**	**ANOVA**
Before treatment	Soil CO_2 flux [$\mu molCO_2\ m^{-2}s^{-1}$]	4.04±0.13	3.87±0.26	4.23±0.11	n.s.
	% respect to control		104.8	94.5	
	Soil temperature [°C]	18.61±0.20	18.64±0.18	18.49±0.17	n.s.
After treatment (entire set)	Soil CO_2 flux [$\mu molCO_2\ m^{-2}s^{-1}$]	$3.27±0.09^a$	$2.82±0.09^b$	$2.33±0.05^c$	P<0.0001
	% respect to control		85.6	71.4	
	Soil temperature [°C]	$16.61±0.13^a$	$16.79±0.16^a$	$15.63±0.08^b$	P<0.0001
After treatment (last day)	Soil CO_2 flux [$\mu molCO^2\ m^{-2}s^{-1}$]	$2.92±0.09^a$	$2.43±0.13^b$	$2.03±0.07^c$	P<0.001
	% respect to control		79.6	75.0	
	Soil temperature [°C]	$15.74±0.21^a$	$15.69±0.19^a$	$15.13±0.07^b$	P<0.05

Table 8.1. Average soil CO_2 flux and soil temperature for each treatment during distinct phases of the experiment (mean ± s.e) and results of ANOVA. Superscript letters denote significant differences (P<0.05) between treatments after performance of Tukey's post hoc test.

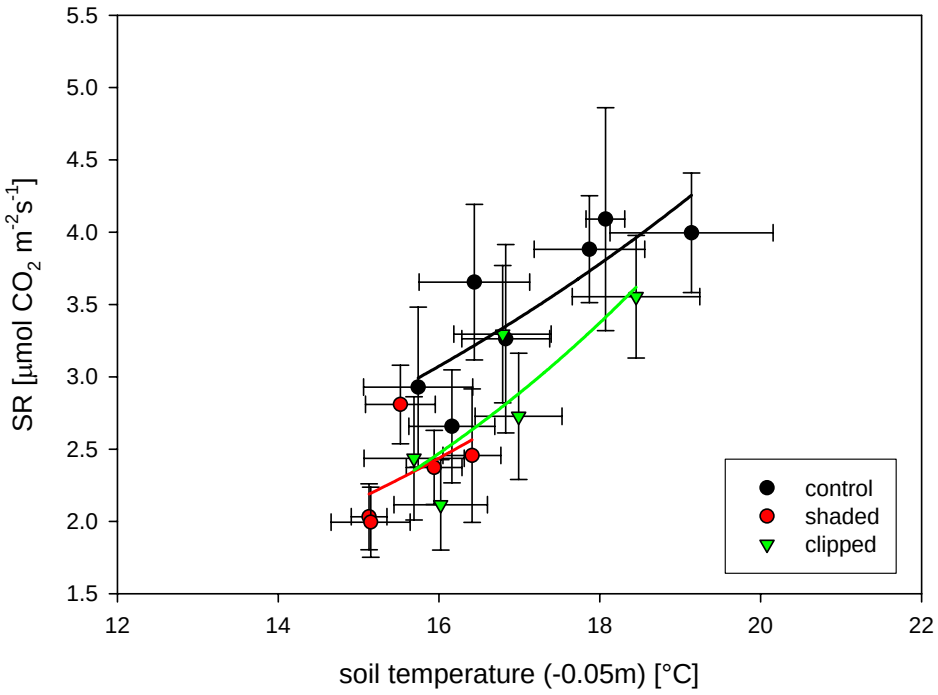

*Figure 8.11. Response of soil CO_2 flux to soil temperature measured at the depth of 0.05m of control plots and treated (shaded, clipped) plots. Error bars represent standard deviation Data were fitted with an exponential functions having general equation: SR=a*exp(b*Tsoil).*
(control: a=0.58±0.32, b=0.10±0.03, R^2=0.68),
(shaded: a=0.33±0.67, b=0.12±0.12, R^2=0.24),
(clipped: a=0.20±0.19, b=0.15±0.05, R^2=0.70).

8.5 Conclusions

The soil CO_2 effluxes of authothrophic origin represented a variable fraction of total soil respiration along the growing season in a natural steppe ecosystem, ranging between 18% and 50% (average 25%) during the periods of most intense plants growth, from mid May to the end of July. Over the whole growing season (May-September) heterothrophic respiration accounted for 21% of total soil respiration, a result that can be considered valid also at annual scale given the very low soil respiration activity in the remaining months of the year.

Factors affecting plant canopy carbon status and carbohydrate supply to roots had large effects on soil respiration in this grassland ecosystem, independent of the physical environment (temperature). Ecophysiological studies consistently show that factors affecting photosynthesis and whole plant carbon gain strongly influence carbon allocation belowground and root respiration at the daily time scale. The reduction of soil CO_2 efflux in clipped and shaded plots in respect with control, 6 days after the treatment, was 20.4% and 25% respectively This study clearly links whole plant carbon gain and soil CO_2 flux, which has been historically modelled ignoring factors that are associated with carbohydrate sources to roots. Such effort towards an improvement of modelling CO_2 effluxes

to the atmosphere could be relevant in a future climate scenario of temperate regions where together with increased temperature also cloudiness will be enhanced because of higher evapotranspiration.

9 Multiple constrained estimate of NEP by eddy covariance and ecological inventory approach.

The use of micrometeorological methods, such as the eddy covariance (E.C.) technique has the advantage of providing Net Ecosystem Production (NEP) at ecosystem scale, including also the role of soil net uptake or release. However E.C., when applied over complex landscapes must include measurements of atmospheric storage, flux divergence and advection in the experimental set up (Baldocchi, 2003): these requirements are often too demanding for long term measurements and usually not implemented. For these reasons is very critical to provide additional cross checks and verification between EC method and inventory type assessment. In this respect there are few studies which directly address a comparison of NEP derived by inventories of carbon pool changes and measured by eddy covariance.

Few studies show that EC measurements are converging with independent values produced by measuring changes in biomass and soil carbon (Curtis et al., 2002;Valentini et al., 2003), however validation of results of carbon budget retrieved by E.C. against measurements of changes of ecosystem carbon stocks is often problematic because the increments of biomass in root systems may be difficult to determine and the changes in soil carbon content may require long-term observations to be detected with statistical significance (Smith, 2004; Conen 2003).

Steppe ecosystems represent a case in which the assessment of carbon balance may be performed with relative simplicity through a multiple constraint approach cross-validating the eddy covariance measurements with independent NEP. Indeed, the structure of the vegetation of these ecosystems offer the possibility of collecting increments of the root system through periodic biomass measurements and to measure soil respiration excluding the contribution of root respiration in a less complicated way than for forest ecosystems. In addition conditions for negligible advective transport and homogeneous flux source areas (footprints) are more frequently met in this type of ecosystems, making steppes an ideal test-case for cross verification of eddy covariance and inventory techniques for annual carbon balance determination.

We analyzed the carbon balance of a true steppe ecosystem of Hakasia during the period 26th April-30th September 2004. During this campaign we monitored continuously CO_2 fluxes at ecosystem scale using the eddy covariance method and carried on samplings of phytomass fortnightly, in order to assess net primary productivity, and weekly measurements of soil respiration trying to partition the CO_2 effluxes into autotrophic and heterotrophic components by an experiment of root exclusion.

Hence, our main objective was to assess the NEP as the difference between NPP and heterotrophic respiration to provide an independent constraint on meteorologically based estimates of the same variable. Importantly we quantify uncertainties in both approaches by (i) analyzing results of NPP assessments retrieved by different methodologies, (ii) by comparing night time chamber based efflux measurements with ecosystem respiration retrieved by E.C. technique and further assessments of error sources in the eddy fluxes.

9.1 Materials and methods

9.1.1 Net primary productivity

In this study we assessed net primary productivity using three methods:

1)

$$NPP(AG,BG) = \Sigma(\Delta((AG,BG)bmass + (AG,BG)Totdead)) =$$
$$= \Sigma(\Delta(AGTotmat + BGTotmat)); \Delta > 0$$

Singh et al (1975) *(Equation 9.1)*

2)

$$NPP(AG,BG) = \Sigma(\Delta(AG,BG)bmass + \Delta(AG,BG)Totdead + (r_{(ag,bg)} \cdot (AG,BG)Totdead))$$
$$= \Sigma(\Delta AGTotmat + \Delta BGTotmat + (r_{(ag,bg)} \cdot (AG,BG)Totdead))$$

Long et al (1989); after Weigert & Evans (1964). *(Equation 9.2)*

3)

$$NPP(AG) = \Sigma(\Delta((AG)bmass + (AG)Totdead)); \Delta > 0$$
$$NPP(BG) = \Delta BGTotmat(ingrowth\_cores)$$

(Equation 9.3)

where *AGbmass*= aboveground live matter; *AGTotdead*= aboveground total dead matter; *BGbmass*= belowground live biomass; *BGTotdead*= belowground total dead matter; *AGr*=aboveground relative rate of decomposition; *BGr*= belowground relative rate of decomposition; *AGTotmat*= aboveground total matter; *BGTotmat*= belowground total matter; *BGTotmat(ingrowth_cores)*= belowground total matter in in growth cores.

The selection of the methods was done in order to cover a wide range of estimates, knowing the typical tendency of each method to yield systematically higher or lower results for NPP than the ensemble average.

All methods were already introduced in §6.2, where their conditions for applicability, merits and flaws are discussed. In particular, method 3 is a combination of distinct approaches for the separate estimation of aboveground and belowground net primary productivity: it indeed assesses aboveground NPP as in method (1), while belowground NPP is given by root biomass increments

measured by the method of ingrowth cores (Jordan and Escalente, 1980; Persson, 1983; Cuevas and Medina, 1988; Neill, 1992; Fisk et al., 1998; Johnson and Matchett, 2001). In method 2, decomposition of dead matter was modelled as a function of time on the base of a negative exponential equation parametrized on results of decomposition experiments after Titlianova (1977) (refer to § 6.2.2 for detailed explanation).

9.1.2 Eddy covariance measurements

CO_2 flux monitoring was performed in accordance with the eddy covariance technique, with an array of instruments including a 3D sonic anemometer (1012R3, Gill Instruments, UK) and a fast response open path infra-red gas analyzer (LI7500, LiCor Inc., USA) mounted on the top of a 4.5 m tower. The instrumental set up was completed by sensors for the monitoring of atmospheric forcings in the atmospheric surface layer and parameters of the soil. Details of the instrumental set up, modality and frequency of calibration of the IRGA, and procedure of flux calculation were the same as all the eddy covariance systems operated in our research activities and were already described in §7.3.2 and §7.3.3.

Data gaps included also rejected NEE values associated to low turbulence conditions (low u_*) which accounted for 15.1% of data. The u_* threshold was defined according with Reichstein et al., 2005 and Papale et al., 2006 using a bootstrapping technique (100 samplings). The selected threshold value is the median of the 100 thresholds found and in this case is 0.06 m s-1. It is possible also to define an uncertainty or variability of the u_* threshold looking to the distribution of the 100 u_* values obtained with the bootstrapping; in this application we assessed the annual NEE also filtering the data using 5^{th} and 95^{th} percentile values of u_* threshold estimate (0.04 and 0.085 m s^{-1} respectively).

Gaps totalized 30.1% of data series, 1.4% being due to IRGA maintenance and calibration, power outages and blockage of the system and the remaining 28.7% to removal of spikes, bad quality data and fluxes associated to low turbulence conditions.

To assess the accuracy of eddy covariance measurements, we analyzed the linear regression between the sum of sensible heat (H) and latent heat (LE) versus the difference of net radiation (Rn) and soil heat flux (G):

$$H + LE = a_0 + a_1(R_n - G) \qquad \textit{(Equation 9.4)}$$

obtaining a closure of the energy balance of 0.78 (a), an intercept of 7.9 (a_0) with R^2=0.91.

Before data gapfilling, NEE was computed correcting Fc for the CO_2 storage term (*Fst*, μmol CO_2 $m^{-2}s^{-1}$), based on the one point CO_2 concentration from the open-path IRGA of the eddy covariance system, as in (Flanagan, 2002):

$$F_{st} = \frac{h\Delta\rho_c}{\Delta t} \qquad \textit{(Equation 9.5)}$$

where $\Delta\rho_c$ is the difference in CO_2 molar density (μmol m^{-3}) between two consecutive records, h is the height of the column of air up to the level of the IRGA (m), Δt is the time interval between two consecutive records (s).

In absence of a CO_2 profile system, this approach might be acceptable because storage term sums tend to zero on daily (-3.8 10^{-3} gC d^{-1}) and seasonal time scale (Baldocchi, 2003; Anthoni et al., 1999), not influencing the estimates of NEP. However, it is still possible that the storage term might not account for all the CO_2 released affecting 30 min NEE, because of spatial heterogeneity of storage in the control volume below the measurement height (Finnigan et al., 2003), or because under stable conditions respired CO_2 might accumulate in micro-topographic troughs (Xu and Baldocchi, 2004).

9.1.2.1 Gapfilling

The gapfilling procedure was performed applying separately three techniques, for the purpose of comparing their effect on the result of the carbon balance: (1) nonlinear regressions (Falge, 2001), (2) Marginal Distribution Sampling (MDS) method (Reichstein et al. 2005) and artificial neural networks (ANN) (Papale and Valentini, 2003)

9.1.2.1.1 Non linear regressions.

Missing data at daytime (PPFD>0) were filled by using rectangular hyperbolic light response functions (Falge et. al., 2001) fitted to NEE for 15 days time windows:

$$NEE = \frac{F_{\max}\alpha Q_p}{\alpha Q_p + F_{\max}} + R_{eco} \qquad \textit{(Equation 9.6)}$$

where Q_p is the incident photosynthetically active radiation (μmol m^{-2} s^{-1}), F_{max} (μmol m^{-2} s^{-1}) is the maximum CO_2 flux at infinite light, α the apparent quantum yield and R_{eco} the ecosystem respiration.

Night time gaps according to the nonlinear regression method were filled by using exponential relationships, retrieved for 1 month time windows, between night-time NEE sorted by periods of high turbulence (u_*>=0.06 m s^{-1}) and soil temperature (T_{soil}) measured at 10 cm depth:

$$NEE_{night} = R_{eco} = a\exp^{bTsoil} \qquad \textit{(Equation 9.7)}$$

where a and b are empirical coefficients.

9.1.2.1.2 Marginal Distribution Sampling

In the application of MDS method, given the fact that meteorological data were available without gaps, missing values of NEE were replaced by average values under similar meteorological conditions within a time window of ±7 days. Similar meteorological conditions are present when global radiation (R_g), air temperature (T_{air}) and vapour pressure deficit (VPD) do not deviate by more than 50 Wm^{-2}, 2.5 °C and 5.0 hPa respectively. If no similar conditions were present within the time window the averaging window was increased and similar conditions were defined only based on Rg or simply the measurement time

9.1.2.1.3 Artificial Neural Networks

The feed-forward backpropagation artificial neural networks (ANNs) are non-linear data based models able to reproduce continuous non-linear functions. The relations between input and output variables are found using training algorithms and a dataset of real observations (Papale and Valentini, 2003). After the training phase the ANN can be applied to other cases starting only from the input values, showing a good generalization capacity.

For this application the ANN have been trained using as input meteorological data (air temperature, photosynthetic photon flux density, air humidity) and the [sin] and [cos] operators of the julian day for the seasonal pace, while the output was the eddy covariance NEE measurements. The examples selected for the ANN training were only the half hourly data collected at Hak 1 site in 2004 under good conditions (after spike removing and u_* filtering) and where all the input variables were available. The trained ANN have been then applied to the half hours where the input were available but the output missing.

9.1.2.2 Flux partitioning

The partitioning of NEE into the component of GPP was then obtained as:

$$GPP = R_{eco} - NEE \qquad \textit{(Equation 9.8)}$$

where the ecosystem respiration, R_{eco}, was retrieved using the two following approaches:

1) Extrapolating daytime ecosystem respiration from temperature response functions used for gapfilling of night-time NEE according to the non linear regression method.

2) Applying the algorithm by Reichstein et al. (2005), that derives a short-term temperature sensitivity of R_{eco} from eddy covariance data based on the exponential regression model (Lloyd & Taylor, 1994):

$$R_{eco} = R_{ref} e^{E_0 (1/(T_{ref} - T_0) - 1/(T - T_0))}$$ *(Equation 9.9)*

Regressions were performed for subperiods of 15 days, with consecutive time windows overlapping 10 days, in order to estimate the temperature sensitivity parameter E_0, setting the reference temperature to 10 °C and keeping constant the parameter T_0 at -46.02 °C as in Lloyd and Taylor (1994). After an E_0 parameter representative for the whole monitoring period was estimated, the temperature independent level of respiration (R_{ref}) was estimated for consecutive 4 days periods by nonlinear regression using the Lloyd & Taylor model, fixing all parameters except $R_{ref.}$ Rref parameters estimated were assigned to the "centre of gravity" of the data of each period and were then linearly interpolated between the estimates producing a continuous time series.

9.1.3 Soil CO_2 fluxes

Soil respiration was measured weekly using a closed dynamic system (EGM2, PP Systems,UK) over 10 plots selected within the footprint area along N-S and W-E directions and spaced out of 30m, where PVC collars (diameter 10 cm; height 6 cm) were inserted approximately 3 cm deep in the ground. Collars were located in the space within plants tussocks and the possible live stems within the surface inscribed by the collar were clipped to avoid measuring CO_2 fluxes originated else than from the soil.

Heterotrophic component of soil respiration flux was measured at weekly frequency applying two variants of the root exclusion method (root removal and trenching) over 6 additional plots whose dimensions were (40x40) cm^2 of surface by 30 cm of depth, adjacent to the plots located along the W-E direction.(§8.3)

Further measurements of CO_2 effluxes, aimed at monitoring night time ecosystem respiration by an alternative method to eddy covariance, were performed using a cylindrical cuvette with diameter of 150 mm and height of 140 mm (CPY-2, PP Systems, UK) connected to the EGM2, designed to allow for closed system measurement of CO_2 fluxes in low plant canopies and soil. Measurements were taken over eight plots located close to the PVC collars aligned along the W-E direction, inserting the cuvette in the soil by the sharpened metal rim at its base and enclosing the canopies within the cuvette's volume.

9.1.4 Uncertainty analysis in inventory and eddy covariance based estimates of NEP

The uncertainties of biometric and of soil CO_2 fluxes measurements associated only to sampling errors, not accounting for systematic errors arising for instance from instruments readings, were calculated as 95% confidence interval around the mean value of each set of measurements; the uncertainty of NPP assessment and of the cumulated value of heterotrophic respiration were

computed applying the following rules for combining uncertainties by addition (1) and multiplication (2) (IPCC,GPG 2000):

(1) $$U_{total} = \frac{\sqrt{(U_1 x_1)^2 + (U_2 x_2)^2 + ... + (U_n x_n)^2}}{x_1 + x_2 + ... + x_n}$$ *(Equation 9.10)*

(2) $$U_{total} = \sqrt{U_1^2 + U_2^2 + ... + U_n^2}$$ *(Equation 9.11)*

where: U_{total} is the percentage uncertainty in the sum of the quantities (half the 95% confidence interval divided by the total (i.e. mean) and expressed as a percentage); x_i and U_i are the uncertain quantities and the percentage uncertainties associated with them, respectively.

Estimates of uncertainty in eddy covariance CO_2 fluxes, arising from the accumulation of either random instrument errors and systematic errors of various kinds, were addressed following Ehman et al. (2002). Considering the random variability of hourly eddy covariance fluxes as 30%, chosen as a conservative threshold (Hollinger & Richardson, 2005; Moncrieff at al., 1996), and that the daily NEE values derive from the sums of hourly CO_2 fluxes measurements, we calculated the random error in the mean flux for one mean daily cycle as in Goulden et al. (1996):

$$Er = pr\sqrt{\frac{\sum_{i=1}^{N}(Fi)^2}{N}}$$ *(Equation 9.12)*

where *pr* is the random error (%) applied to each half-hour data, N is the number of flux measurements in one day (48), and *Fi* is the ith flux measurement of the daily cycle.

The combined effect of random errors over NEE estimate decays with the square root of the number of summands, such that $Er(Nd) = Er/\sqrt{Nd}$ where *Nd* is the number of days. Being the magnitude and sign of systematic errors unknown and given the systematic error on one mean diurnal cycle as the sum of the individual systematic errors

$$Es = ps\sum_{i=1}^{N} Fi$$ *(Equation 9.13)*

where *ps* is the systematic error (%).

We only allowed 50% of the standard random cancellation of half hourly errors on daily totals of NEE and no cancellation in the accumulation of daily totals on long term NEP. The assessment of uncertainties of NEP for the whole period was completed with the quantification of errors deriving

from the gapfilling procedure and with the analysis of sensitivity of the cumulated NEP versus the u_*. The first was accounted for as the deviation of results yielded by the application of the different gapfilling techniques; while the latter was analyzed selecting an interval between the 5th and 95th percentile values of u_* threshold estimate (0.04 and 0.85 m s^{-1} respectively). The restriction of such analysis to a particular range of u_* is justified by the intention of evaluating the uncertainty of the NEP assessment related to the selection of a determined u_* threshold within a valid range, and excludes therefore lower u_* values for which the overestimation of the NEP would be obvious (Barford et al., 2001).

9.2 Results

9.2.1 Biomass dynamics and assessment of NPP

At the date of the first biomass sampling (1 May), the growing season had still not begun, as evidenced by the absence of live aboveground biomass (fig.9.1). The dead aboveground biomass was 0.39 t ha^{-1}, a value by far lower than the typical amount of dry grass in spring recorded during previous campaigns at the same site, because the steppe was run by a fire in March 2004, which nevertheless burnt the grass stems and affected moderately the amount of litter in the area. The peak of aboveground live biomass was reached in the middle of July with 1.40 t d.m. ha^{-1} that corresponded also to the peak of total aboveground biomass (2.09 t d.m. ha^{-1}); after this stage the quantity of aboveground biomass remained substantially steady as the decrease of living biomass since the second half of August, associated to the beginning of the senescence phase, was compensated by the increase in dead biomass. In September however there was a new sprout of grass which is visible in the sustained level of live AG biomass after its previous rapid decline. The comparative analysis of the trend of live and dead aboveground biomass from May to July reveals their synchronous increase, which apart from being the evidence of mortality induced by intra and inter-specific competition is also determined by the overlapped development phases of different kind of grass cenosis along the growing season.

The amount of belowground biomass ranged between 88%-95% of total biomass along the monitoring period (Fig.9.1) and it was characterised by the same growth pattern of AG biomass

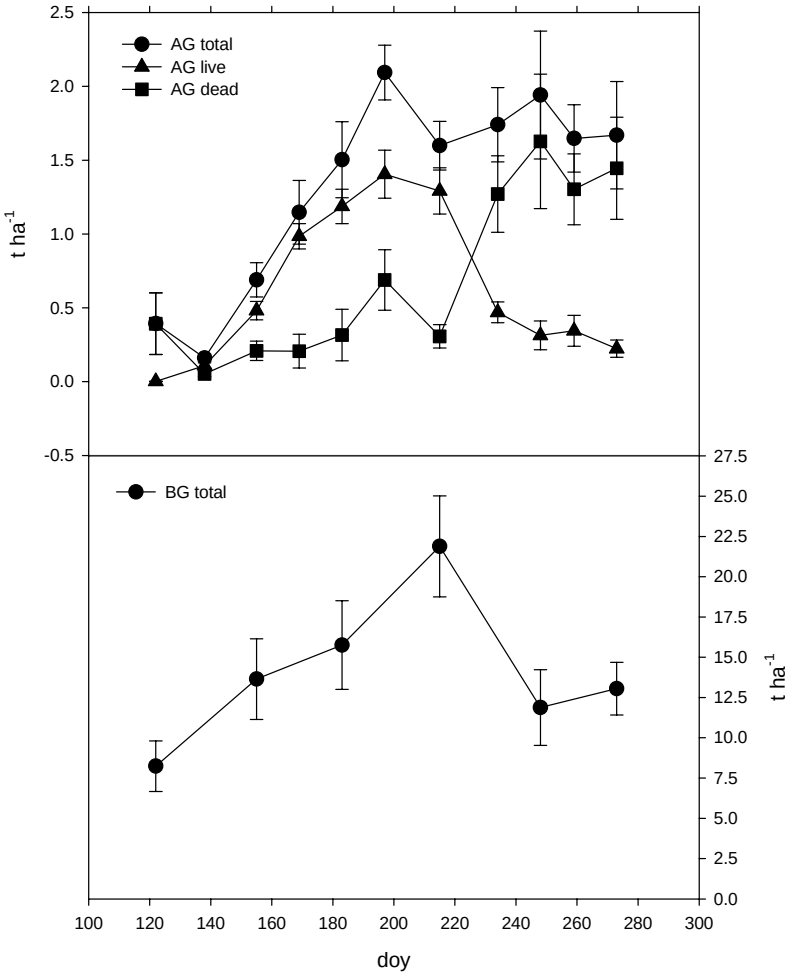

Figure 9.1. (above) Trend of aboveground biomass sorted into live and dead; (below) trend of belowground biomass including live and dead biomass. Error bars indicate the 95% confidence interval.

from May to August, reaching its peak on the sampling of 1 August (doy 214) (21.8 t d.m ha^{-1}). During August the amount of roots biomass decreased significantly as an evidence of the intense decomposition activity, while in September a new increment attributable to a late seasonal sprout of root productivity before winter senescence was recorded. It seems reasonable to doubt that the fire occurred during winter burnt part of the belowground biomass because the difference in the quantity of roots, collected in the root ingrowth cores at the end of the previous growing season (15 October 2004) and at the beginning of May 2004 respectively, likely depended on the sole process of decomposition (≈-40%).

The assessment of NPP for the whole period of observations (May-September) varied sensibly depending on the method used (fig.9.2, 9.3): method 1 (sum of positive increments of AG,BG biomass) led to 7.70±3.15 tC ha^{-1} (95% confidence limit); method 2 (sum of changes in AG,BG biomass with adjustment for decomposition) led to 3.87±1.03 tC ha^{-1} while according to method 3

(sum of positive increments in AG biomass; BG NPP determined by roots growth within ingrowth cores) the NPP was 2.89±0.77 tC ha^{-1}. The averaged assessment of NPP was therefore 4.82±1.65 tC ha^{-1}. The proportion of NPP allocated belowground was 87%, 84% and 71% according to methods 1, 2 and 3 respectively (fig.9.3).

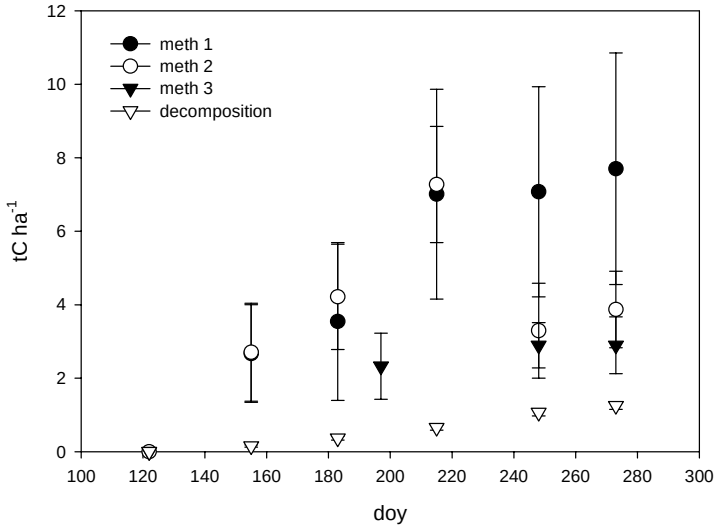

Figure 9.2. NPP assessed by three methods (black dots: sum of positive changes in biomass; white dots: sum of changes in biomass with adjustment for decomposition; black triangles: sum of positive changes in AG biomass and BGNPP assessed by ingrowth cores) along the biomass sampling dates of the growing season. Amount of dead biomass decomposed (white triangles). Error bars indicate the 95% confidence interval of the estimate based exclusively on the propagation of sampling errors.

Methods 1 and 2 differ only by the term of decomposition until the total biomass reaches the maximum, after that the assessment of NPP provided by method 2 drops because the decline in belowground biomass in August is not traded off by the estimation of the amount of decomposed biomass in that period. The divergence in the results of the two methods is thus likely due to the underestimation of the carbon lost in the process of decomposition which is most intense during summer months because of favourable conditions such as high temperatures and precipitation. Total modelled decomposition is equal indeed to 1.25±0.1 tC ha^{-1} for the period from May to September, which corresponds only to 16% and 31% of NPP estimated with method 1 and 2 respectively. Although the extrapolation of the estimate of amount of decomposed matter for a whole year would lead to a substantially sensible result (since the model is parameterized on the base of annual rates of biomass decomposition of central Asian steppes), decomposition rates can be significantly different over limited time windows leading to underestimate (during summer) NPP when applying method 2.

On the other hand method 1 tends to overestimate systematically the real NPP (Scurlock et al., 2002) because it incorporates in the sum only terms associated to a positive change in biomass, although they can be related to the effect of sampling error and not to a real increase in primary productivity. Contrary to the methods 1 and 2, method 3 does not keep track of the increment in biomass in September leading to the lowest estimate of NPP with the the lowest root-shoot ratio. The possibility of simultaneous growth and decomposition of root biomass within the ingrowth cores, as it likely happened at the end of the summer, is the main flaw of this method and leads to an underestimation of the belowground primary productivity. In spite of this, method 3 is the only one that allows to limit the magnitude of the uncertainty of NPP assessment by measuring directly the increments in biomass and not to deduce them by differences in biomass stocks.

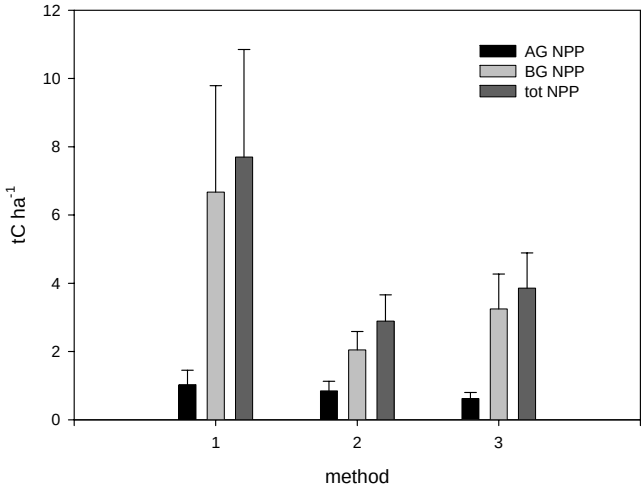

Figure 9.3. Above ground (AG), Belowground (BG) and total NPP assessed according to methods applied.

9.2.2 Soil CO_2 fluxes

The report of results of measurements of total soil respiration and its component of heterothrophic origin, across the season, as well as an analysis of the main ecological drivers regulating the process, was provided in § 8.3. Using a linear interpolation of soil fluxes between measurements dates, the cumulated value of soil respiration for the whole monitoring period, was 417.2 gCm^{-2} partitioned into 332.7 gCm^{-2} (79%) from heterotrophic respiration and 84.5 gCm^{-2} (21%) from autotrophic origin (fig.9.4).

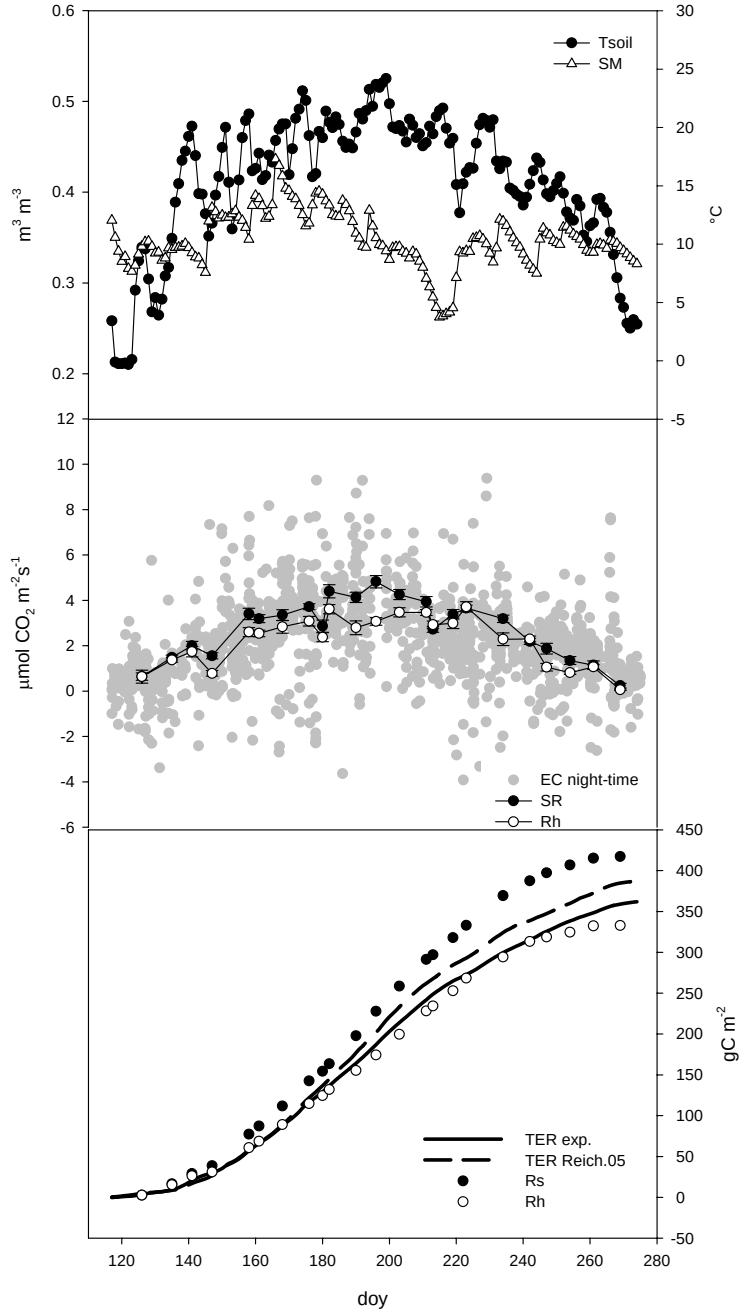

Figure 9.4. Above: trend of daily average of soil temperature (-5cm) (black dots) and soil moisture (white triangles). Middle: trend of soil respiration (black dots) and heterotrophic component of soil respiration (open dots) measured by chamber technique (error bars: ±standard error), total ecosystem respiration by eddy covariance (grey dots) measured during night-time; Below: trend of cumulated ecosystem respiration modelled with exponential model (lower solid line), with Reichstein 2005 model (upper dashed line); cumulated soil respiration (Rs) (black dots) and heterotrophic respiration (Rh) (white dots).

9.2.3 Comparison between eddy covariance system and chamber based measurements of total ecosystem respiration

Ecosystem respiration measured by chamber CPY2 was up to six fold greater than the correspondent measured values by eddy covariance when friction velocity was below the threshold of 0.06 m s^{-1}, confirming the failure of the E.C. system in measuring the whole magnitude of night time fluxes in conditions of low atmospheric turbulence (fig.9.5). Nevertheless, sorting the chamber measurements taken when u_* was greater than 0.06 ms^{-1}, the comparison between the two techniques evidences a fairly good match of ecosystem respiration values with chamber based fluxes being on average still higher than eddy covariance measurements ($R_{eco}(CPY2)=1.15*R_{eco}(EC)-0.07$; R^2=0.83; n=7): differences in fluxes did not overcome 1.21 μmolCO_2 m^{-2} s^{-1} and were limited in the range -2%÷+36% in respect with the eddy covariance measurements.

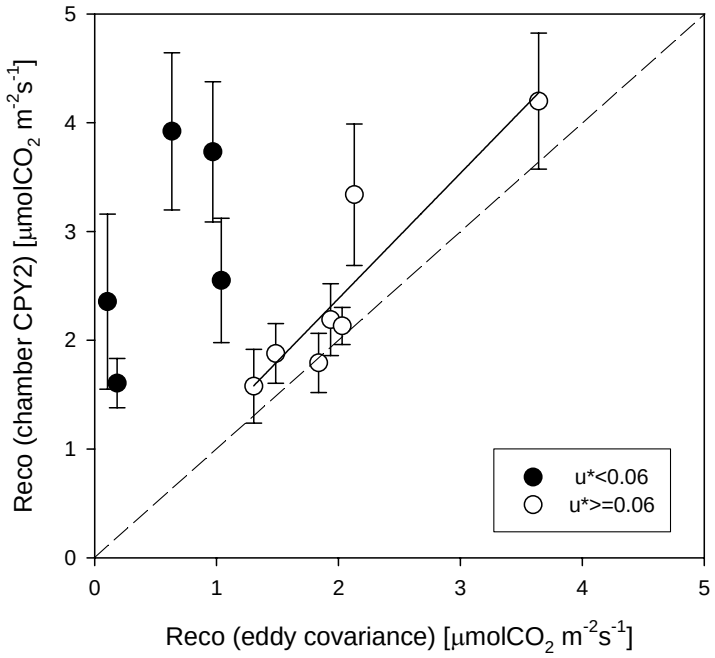

Figure 9.5. Comparison of eddy covariance and chamber based measurements of ecosystem respiration for conditions of friction velocity above 0.06 ms^{-1} (white dots) and below 0.06 m s^{-1} (black dots) . Error bars stand for standard error of chamber CO_2 flux measurements.

9.2.4 Eddy covariance measurements

During the first two weeks of May the ecosystem was a small source of carbon with mean daily NEP values of about 0.08 gC $m^{-2}d^{-1}$: in this period daily NEP ranged widely between -0.41 and 1.42 gC $m^{-2}d^{-1}$ and it was modulated by pronounced fluctuations in air temperature controlling respiratory activity while the vegetative season was on setting (Fig.9.6). After 15th May (doy 136), carbon assimilation increased due to the start of the growing season induced an uptake of CO_2

which rapidly reached its maximum (-3.59 gC $m^{-2}d^{-1}$ the 9th of June- doy 161) and kept sustained with a daily average of -2.15 gC $m^{-2}d^{-1}$ throughout the month of June. From July the daily NEP values started declining yet denoting a sink activity throughout the month August, with GPP slightly higher than TER, with a resulting daily average NEP of -1.41 and -0.63 gC $m^{-2}d^{-1}$ in the months of July and August, respectively. The magnitude of both respiratory and photosynthetic CO_2 fluxes reduced further in September, when average daily NEP was -0.05 gCd^{-1} and until, in the last week of September both GPP and TER dropped to ±0.8 gC $m^{-2}d^{-1}$ leading to a net flux close to zero.

The cumulated NEP over the period 26th April – 30th September was 150.5, 149.8 and 154.7 gC m^{-2} according to the methods of gapfilling of non linear regression, MDS and ANN (average of NEP assessments: 151.7 gC m^{-2}). (fig.9.7). The application of different methods for the gapfilling provided a deviation in results of 4.9 gCm^{-2} representing 0.3% of average cumulated NEP.

NEP estimate showed an average increase of 6.7 gC m^{-2} when u_* threshold was set to 0.04, which was more pronounced when gapfilling with non linear regression method (7.2 gC m^{-2}) and less applying the ANN method (6.3 gC m^{-2}), while at the upper limit (u_*=0.085 ms^{-1}) NEP decreased on average by -6.6 gC m^{-2} (Fig.9.8). The weight of uncertainty over NEP estimate dependent on the u_* threshold selection can thus be approximated as ±4.4%.

The overall assessment of the uncertainty of the carbon budget retrieved by eddy covariance measurements was ±31.6 gCm^{-2}, that corresponds to 20% of the cumulated flux. The cumulated value of TER over the monitoring period, based on simple exponential relations between night-time respiration and soil temperature, was 361.9 gCm^{-2} while adopting the model of Reichstein (2005) it was 387.7 gCm^{-2} (average 374.8 gCm^{-2}). The divergence of 25.8 gCm^{-2} between the two estimates of TER does not arise from systematic higher outputs by the model of Reichstein et al (2005), while results of both models are respectively either higher and lower along the season without highlighting any particular systematic difference. The cumulated GPP over the same period was 512.5, 537.5 and 542.4 gCm^{-2} (average 530.8 gCm^{-2}) obtained by difference of NEP gapfilled by non linear regression and TER modelled with simple exponential model, and by difference of NEP gapfilled with MDS, ANN methods and TER resulted from Reichstein et al. (2005) model . Cumulated total ecosystem respiration assessed by E.C technique (taking into account chamber based measurements) consisted of about 89% heterotrophic soil CO_2 effluxes, but it resulted lower than total soil respiration by about 11%, although by definition it should be higher. Two factors should be taken anyway considered when comparing results of CO_2 effluxes retrieved by distinct techniques: primarily that the uncertainty of cumulated total soil respiration (about 30%) overcomes the difference between TER and SR; moreover that chamber based measurements of soil CO_2 effluxes were performed during daytime hours, when CO_2 flux rates are typically higher compared to nighttime rates.

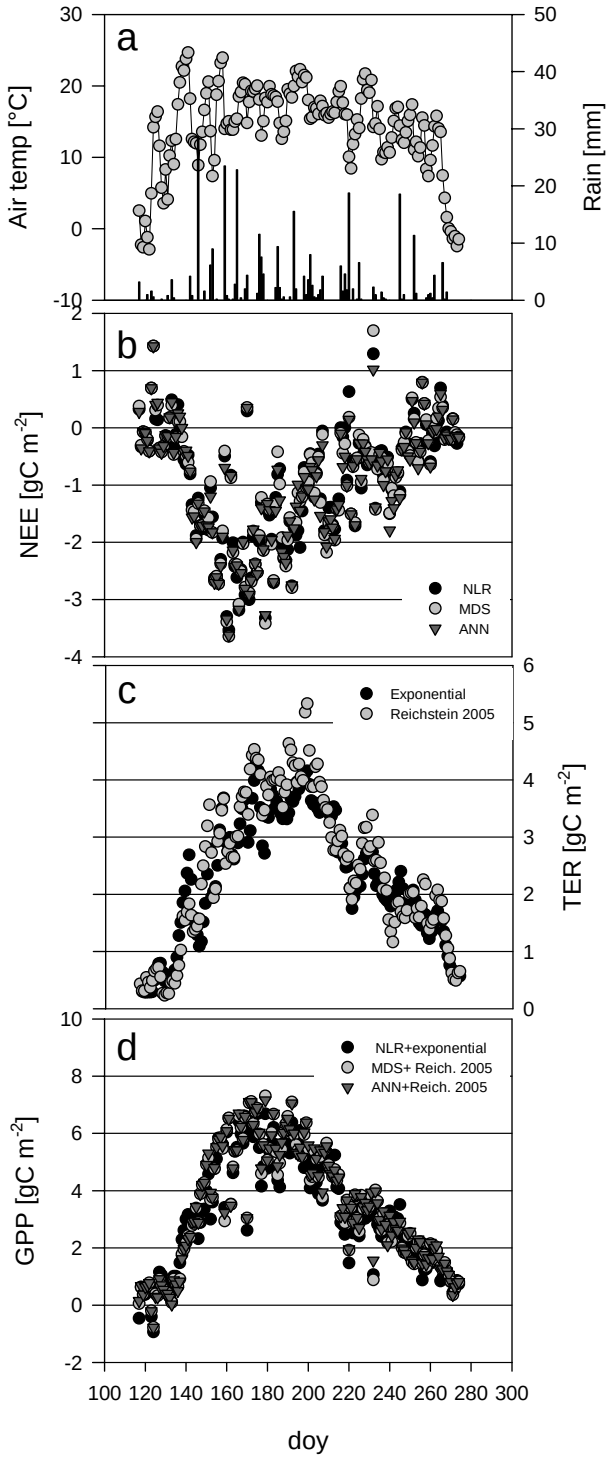

Figure 9.6. (a): trend of daily average air temperature (white dots) and precipitation (black bars).(b): trend of daily NEE gapfilled with NLR, MDS and ANN methods. (c) trend of daily TER modelled with simple exponential relations and Reichstein 2005 algorithm. (d) daily GPP obtained as difference between: 1. NEE gapfilled with non linear regression method and TER modelled with simple exponential relations; 2.NEE gapfilled with MDS method and TER modelled according to Reichstein 2005; 3. NEE gapfilled with ANN method and TER modelled as in Reichstein 2005.

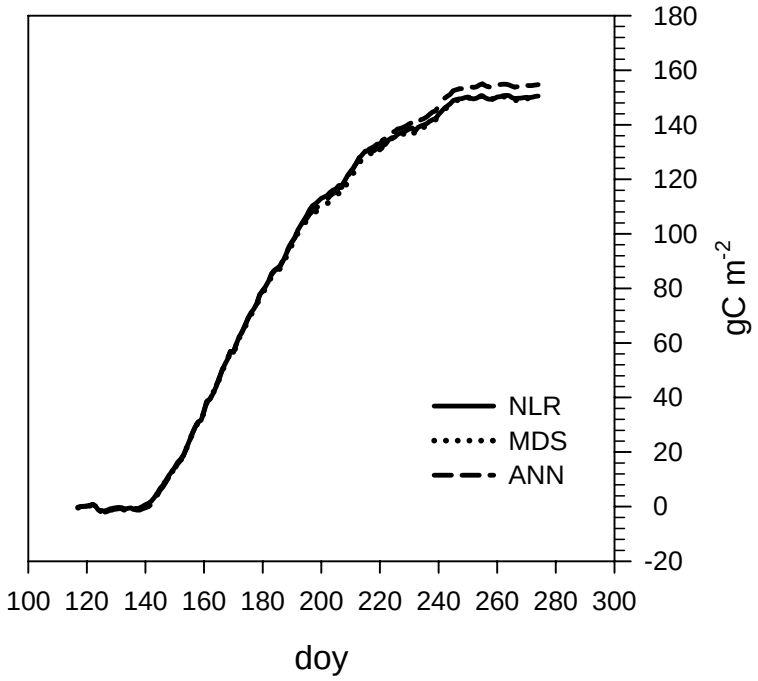

Figure 9.7. Cumulated NEP with gaps filled by non linear regressions method (solid line), MDS (dotted line), ANN (dashed line).

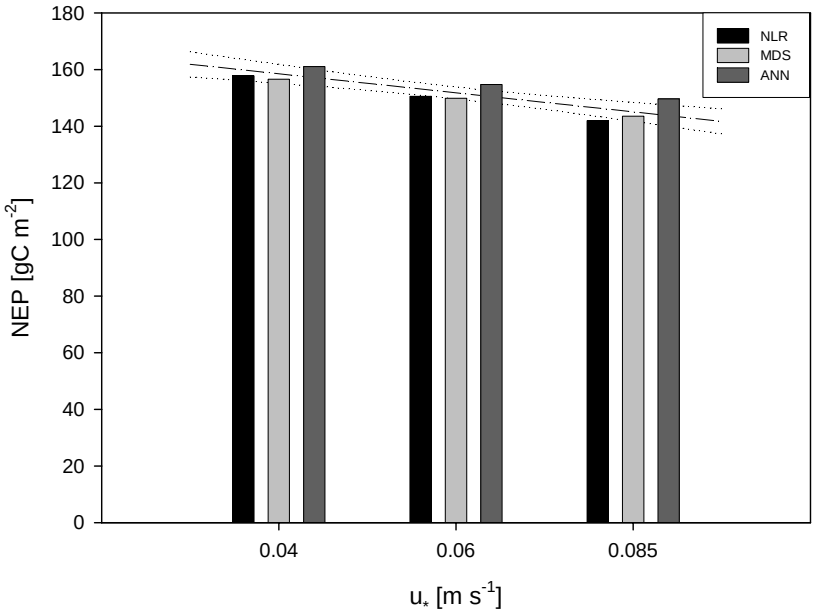

Figure 9.8 Analysis of sensitivity of NEP, obtained with different gapfilling methods (NLR, MDS, ANN) versus the value of u_* selected as threshold for rejection of night-time eddy covariance fluxes within a range of 0.04 and 0.085 ms^{-1} corresponding to the 5th and 95th percentile of the results from the iterative procedure for u_* threshold determination.

9.2.5 Comparison of carbon budget by ecological inventory and eddy covariance.

The net ecosystem production assessed by the method of ecological inventory was 150.1±196 gC where the uncertainty refers to the confidence interval at 95% (table 9.1). This estimate was smaller than the NEP retrieved by the E.C technique by 1.6 gC (-1.0%). The discrepancy of NEP assessment through the application of the two methods can be defined as negligible if compared with the results of the most favourable of similar works (Barford et al., 2001; Curtis et al., 2002; Ehman et al., 2002) which report differences between E.C and inventory based estimates of the carbon budget up to 30%. Despite of this substantial agreement of results, the inventory based assessment suffers from a large uncertainty, more than 1.3 times the NEP, which makes not possible to clearly individuate the role of the steppe ecosystem as a carbon sink or source using this approach.

	assessment [gC m^{-2}]	uncertainty ±	remark
1. NPP	482.8	165.5	(0.95 confidence interval)
2. Rh (heterotrophic respiration)	332.7	105.2	(0.95 confidence interval)
3. NEP (ecological inventory)	150.1	196.1	(0.95 confidence interval)
4. NEP (eddy covariance)	151.7	31.6	
Δ (4-3)	1.6		(1.0% of NEP)

Table 9.1. Comparison of assessment of NEP by ecological inventory and eddy covariance approaches

9.3 Discussion

The remarkable difference in the results of NPP assessment depending on the methods applied has already been highlighted by a review on the subject (Scurlock, 2002) and this case study further confirms such findings (minimum 6.42 t d.m.ha^{-1}; maximum 15.75 t d.m.ha^{-1}). However, the results obtained by various methods, with the exception of method 3 that is lower , fall within the range of NPP typical reported for natural steppes of temperate northern China and Central Asia (7.3-22.0) t

d.m. ha^{-1} (Ni, 2004; Scurlock 2002). Since NPP assessment method being characterized by biases whose magnitude and often sign are not known we envisage the necessity of following multiple methods, chosen according to the criterion of accounting for both trends of above and belowground biomass dynamics when data are available, and of providing an averaged estimate of NPP and the deviation among produced results. The shares of uncertainties in the assessments of belowground and aboveground NPP were 39.2% and 35.2% respectively however the belowground compartment, representing the largest fraction of biomass, is the source of an uncertainty in NPP more than 5 times larger than the aboveground one. In this study the average sampling error over all the sampling dates, with a number of 20 units per each sampling, was 19% for aboveground and 18% for belowground biomass, at a level of significance of 95%. We estimate the number of sampling units needed to lower the error to 10% as 54 for aboveground biomass and 58 for belowground: such number of samples would determine an uncertainty of 26% in belowground NPP and 22% in aboveground NPP.

The site, characterized by almost flat terrain (slope 2% along N-S direction) and by homogeneous vegetation cover far beyond the area of the footprint which during night-time and in conditions of developed turbulence (u_*>0.1 ms^{-1}) extended on average to 725 m upwind from the sensors according to the model of Schuepp et al., 1990, offers in principle the requirements for the application of the eddy covariance technique without complications arising from the necessity of accounting for advective and flux divergence terms in order to produce defensible estimates of CO_2 fluxes, as in the case of complex terrain sites (Baldocchi, 2003; Aubinet et al., 2003). Comparing the relative frequency of wind versus wind directions during night-time for conditions of low and high turbulence (u_*<0.06; u_*>0.06) we did not detect any difference evidencing the presence of katabatic winds that could drain CO_2 along the gentle slope during stable atmospheric conditions. Moreover the frequency of winds blowing along the slope of the terrain is only related to very few events (<2% of total distribution) and therefore the potential overall contribution of katabatic flows to the total flux is likely negligible. The analysis of night-time fluxes evidenced the underestimation of ecosystem respiration by eddy covariance during period with low turbulence: in case of u_*<0.06 we observed a correlation of u_* with the CO_2 fluxes. This result is confirmed also by independent chamber based measurements of ecosystem respiration being larger than eddy covariance based measurements when u_* was under the selected threshold. This bias, widely observed in eddy covariance studies (Black et al., 1996; Goulden et al., 1996; Grace et al., 1996; Moncrieff et al., 1996; Mahli et al., 1998; Aubinet et al., 2000; Baldocchi et al., 2000) is corrected by replacing the underestimated effluxes in low wind conditions with fluxes modelled on the base of unbiased measurements taken over a certain threshold of friction velocity and represents reasonably a crucial issue for addressing an accurate assessment of the carbon budget. In this study we found that the variability of the NEP assessment arising from the selection of a determined u_*

threshold contributed to about 40% of the total uncertainty in the result and was of the same magnitude of the uncertainty originated from the selection of different gapfilling techniques.

9.4 Conclusions

Both eddy covariance and ecological inventory methodologies face significant difficulties, resulting in potential systematic biases of unknown magnitude or sign that are currently the subject of significant efforts in the ecological and the micrometeorological communities. This study is not intended to be an absolute validation of one methodology against the other and in the accurate evaluation of the uncertainties of each approach, but it tries to focus on the merits and flaws of each method providing a comparison of results of net ecosystem productivity for a specific environment, steppe plains, where it is possible to minimize the sources of errors for both methodological approaches. Our conclusions are the following:

1. The carbon balance of the monitored natural steppe showed, according to micrometeorological measurements, an uptake of carbon of 151.7 ±31.6 gCm^{-2}, cumulated during the growing season from May to September. This result was in agreement with an independent estimate through ecological inventory which yielded a sink of 150.1 gC (Δ=1.6 gCm^{-2}) although this method was characterized by a large uncertainty (±130%) considering the 95% confidence interval of the estimate.
2. Eddy covariance measurements underestimated night-time CO_2 effluxes when friction velocity was below 0.06 ms^{-1} as evidenced also by the comparison with independent chamber based measurements of ecosystem respiration. To account for this bias measured fluxes under $u_* < 0.06$ were rejected and replaced with modelled NEE: the sensitivity of the resulting NEP to the selection of the u_* threshold, chosen within the 5th and 95th percentile of its estimate (0.04-0.085 ms^{-1}), was quantified in ±4.4%.
3. In a site whose conditions are considered suitable to perform unbiased eddy covariance flux measurements due to the missed capture of advective flux components, the multiple constrained assessment of NEP showed a fair match between the results of the techniques used.
4. Belowground processes in steppe ecosystems account for a pre-eminent part of the carbon exchange: in particular efforts to better quantify the dynamics of root biomass (growth and turnover) have to be undertaken in order to reduce the uncertainties in the assessment of NPP. This assessment should be preferably based on the application of multiple methods, each one characterized by its own pros and cons.

10 Synthesis of the main findings and outlook on the role of steppe zone of Russian Federation in the global carbon cycle.

This thesis presents an analysis of the carbon cycle of steppe ecosystems and recovering steppes after agricultural use located in the steppe zone of Central Asia. It provides a quantitative characterization of the carbon pools, of the patterns of carbon allocation within the systems, of the CO_2 exchanges between the biosphere and the atmosphere, as well as of the response of CO_2 fluxes to environmental drivers. The research areas, located in the Republic of Hakasia and in the Republic of Tuva (Russian Federation), included true bunchgrass steppes and neighbouring old agricultural fields hosting different temporal stages of recovering grassland.

Finding 1:The former agricultural use of steppe lands caused a considerable loss of soil organic carbon.

Large areas of the territory of Eurasia occupied by steppes have been historically converted to agricultural use. In both the studied areas a large fraction of steppes were converted into crop fields during the 50's, while since the early 90's the process of abandonment of cultivated land started. Within about 40 years, cultivations caused a loss of organic carbon, as resulted from the systematically lower carbon stocks found in fields of Hakasia and Tuva, compared to steppes. The difference in carbon stocks was not less than (46-52%) and affected both the soil organic carbon pool, 80-92% of the lost carbon , and the belowground biomass pool for the remaining part.

Finding 2: Steppes store a higher fraction of biomass in the belowground pool compared to old field ecosystems; the latter ones are characterized by a higher aboveground net primary productivity.

The biomass carbon stock of steppes of Hakasia and Tuva was found to be stored mainly in the belowground pool, with a proportion ranging 88-94%, thanks to the highly developed root system of perennial species. In old fields, belowground biomass was still predominant but the share of biomass found in the aboveground pool, from 12 up to 42%, was larger than in steppes.

The assessment of net primary productivity at sites of Hakasia, evidenced that the organicated carbon is allocated primarily to the root system, with a fraction varying between 70% and 90% for both steppe and old field ecosystems.

Aboveground net primary productivity was found systematically higher in old fields than in steppes, while it was not possible to establish a clear ranking of belowground net primary productivity because of the uncertainty in its assessment.

Finding 3: Old fields recover actively the carbon lost during previous agricultural use, hence acting as a sink for atmospheric carbon. The magnitude of the sink declines over time, but the sink capacity is maintained also once the mature stage of steppe vegetation is reached.

CO_2 exchanges between ecosystems and the atmosphere where monitored by micrometeorological (eddy covariance) technique over three stages of an old field succession in Hakasia, represented by an early stage (5 years since land use change), an intermediate stage (10 years) and a mature stage (steppe).

Yearly CO_2 exchange estimates showed that all the examined ecosystems were carbon sinks, with a strenght declining from the early stage (2.1 tC ha^{-1}) to the the steppe ecosystem (1.1 tC ha^{-1}). Also the amounts of carbon assimilated by photosynthesis (GPP) and released to the atmosphere through ecosystem respiration (R_{eco}) decreased over the stages of the succession, yielding the observed trend in the NEP.

The carbon budget of the true steppe, estimated additionally using the ecological inventory methodology, agreed with the result obtained with the micrometeorological technique.

Finding 4: The functionality of steppes is characterized by a higher stability compared to earlier stages of succession.

Monitoring CO_2 exchanges over the old field succession in Hakasia revealed that, even if characterized by lower carbon assimilation than old field ecosystems, the steppe ecosystem displayed a less pronounced reduction of the photosynthetic process in response to extreme high air temperature and air dryness conditions, maintaining its efficiency.

Moreover, it was observed that a spring fire burst over the steppe ecosystem was followed by an enhanced carbon sequestration that could completely offset the amount of carbon lost from the burnt biomass. The storage of the greatest fraction of biomass belowground in steppe ecosystems minimizes the volatilization of carbon of aboveground biomass during fires and facilitates the prompt recover of the grass cover.

10.1 Role of steppe zone of the Russian Federation in the global carbon cycle

The finding that the carbon cycle of steppe ecosystems, as well as the one of old fields located in the steppe region, is not in equilibrium with the atmosphere and results in a net uptake of carbon, might imply a significant contribution of the Eurasian steppe biome, given its vast area, to explain part of the carbon sink attributed to the lands of the temperate and boreal zones of the northern hemisphere.

The ultimate scope of this study was not an upscale of the results obtained at ecosystem level to a broader spatial level, such as the whole steppe biome. However, in generalizing the results obtained for Hakasia, some considerations should be made. Steppe ecosystems of Eurasia are indeed widely differentiated and distributed according to ecological/climatic patterns: true steppes in semi arid climate represent only one typology of steppe vegetation. Less productive steppes of arid lands and desert steppes found in hyperarid climates reasonably would be less efficient in carbon sequestration than true steppes. The same concept holds for the carbon balance of old fields, since the abandonment of agriculture took place preferentially in the least productive southern croplands of the former Soviet Union, especially in Kazakhstan.

An assessment of the potential for carbon sequestration limited to the territory of Russian Federation would be, for the reasons mentioned above, more appropriate since the steppe zone of this country hosts more mesic steppes, like true and meadow steppes, to which results found in this study can be likely extended.

The Russian Federation covers $17.1 \cdot 10^6$ km^2. An analysis of the land cover distribution in the Russian Federation derived from various global data sets (IGBP, USGS, GE, BATS) displays a fraction of grassland and agricultural lands of 15.7% (Van der Molen et al., in prep.), while according to the FAOSTAT (2007) database, agricultural lands cover 13% of the territory and are composed by 5.2% of permanent pastures and by 7.5% of arable land and permanent crops (tab. 10.1). The estimate of the reduction in arable land and permanent crops in the Russian Federation that followed the collapse of the Soviet system, is 9.3 10^6 ha between 1992 and 2003; part of these old fields ($3.9 \cdot 10^6$ ha) moved into the pasture land use category (tab. 10.2). The areas with steppe cover falls into the category grasslands and pastures, subtracted of the included area of abandoned fields.

Assuming that no further abandonment of agricultural land took place after 2003 and considering that the recovering grasslands developed over abandoned fields have at present an average age of 10 years, we can attribute to these areas the NEP of the intermediate (10 yr) stage of the old field succession of Hakasia. On the other side, we can attribute to the category (grasslands + pastures) the NEP of the mature (steppe) stage. The result is an assessed sink of 0.17 Pg C yr^{-1} over the steppe zone of the Russian Federation (tab 10.3), generated in greatest part from steppes (93%) and with a not negligible contribution of old field ecosystems (7%).

Land use/land cover of Russian Federation			
	Area [10^6 km^2]	Area [%]	source
Grassland + agricultural land	2.68	15.7	(IGBP, USGS, GE, BATS)
Agricultural land (A+B)	2.16	12.6	FAOSTAT
Arable land and permanent crops (A)	*1.24*	7.5	
Pastures (B)	*0.92*	5.1	

Table 10.1 Area and fraction of the territory of Russian Federation under grassland and agricultural land use.

Changes in land use of agricultural lands of Russian Federation (1992-2003) - FAOSTAT			
Category	Area [10^6 km^2]		Δ [10^6 km^2]
	(1992)	(2003)	
Agricultural land (A+B)	2.21	2.16	-0.05
Arable land and permanent crops (A)	*1.33*	*1.24*	-0.09
Pastures (B)	*0.88*	*0.92*	+0.04

Table 10.2. Areas under different use in agricultural lands of Russian Federation in 1992 and 2003 and changes (Δ) occurred.

Carbon sequestration potential in the steppe zone of Russian Federation				
Land use		Area [10^6 ha]	NEP [tC ha^{-1}yr^{-1}]	C sink [10^6 tC yr^{-1}]
Non agricultural land	Grassland	52.0	1.14	59.3
Agricultural land	Pastures	88.0	1.14	100.3
	Old fields	9.3	1.30	12.1
				171.7

Table 10.3. Assessment of the carbon sequestration potential (C sink) of steppes and old fields of Russian Federation. Steppes fall under both the categories grassland and pastures. Net ecosystem productivity attributed to different categories refer to results of CO_2 flux monitoring in a true steppe and an old field at 10 years after abandonment in Hakasia.

The result obtained is undoubtedly a coarse assessment, that could be improved only if more information on the carbon balance of these ecosystems for a wider spectrum of climatic, edaphic, and management (grazing pressure) conditions was available. However it highlights the importance of the steppe zone as a potential hot spot in the global carbon cycle.

10.2 Conclusive remarks

.

The Eurasian steppe biome very likely functions as a sink for atmospheric carbon exerting a not negligible role in the global carbon balance.

Former agricultural fields in the steppe zone of Eurasia, being characterized by a higher carbon sequestration capacity than steppe ecosystems, also contribute actively to this sink.

The spatialization of the carbon balance observed at sites in the steppe region of the Republic of Hakasia, to assess the magnitude of the sink of steppes and old fields ecosystems in the Russian Federation, suggests a carbon sequestration of 0.17 PgC yr^{-1}.

Further research should improve the understanding of the carbon balance of Eurasian steppe and old agricultural field ecosystems addressing:

(i) its interannual and spatial variability, determined by differences in climatic, edaphic, and management conditions.

(ii) the dynamics of carbon sequestration capacity of the old field succession, focusing in particular on the earliest stage after land use change and on the duration of the enhanced carbon sequestration over the late stages compared to steppes.

(iii) a more accurate determination of belowground carbon cycle processes, that hold the key for the capacity of carbon sequestration of these ecosystems.

Bibliography

Introduction

Bousquet P., Ciais Ph., Peylin P., Ramonet M. and Monfray P. (1999). Inverse modeling of annual atmospheric CO_2 sources and sinks. 1. Methods and control inversion. J. Geophys. Res., 104 (D21), 26161-26178.

Dixon R. K., Brown S., Houghton R. A., Solomon A. M., Trexler M. C., Wisniewski J. (1994). Carbon pools and flux of global forest ecosystems. Science, 263, 185-190.

Gurney K., Law R. M., Denning A. S., Rayner P.J., Baker D., Bousquet Ph., Bruhwilerk L., Y., Chen H., Ciais Ph., Fan S., Fung I.Y., Gloor M., Heimann M., Higuchi K., John J., Maki T., Maksyutov S., Masarie K., Peylin Ph., Prather M.l, Pak C.B., Randerson J., Sarmiento J., Taguchi S., Takahashi T. and Yuen C.W. (2002). Towards robust regional estimates of CO_2 sources and sinks using atmospheric transport models. Nature, 415, 626–630.

Houghton, R.A. (2003) Revised estimates of the annual net flux of carbon to the atmosphere from changes in land use and land management. Tellus, 55B, 378-390.

IPCC (2007) Climate Change 2007: The Physical Science Basis – Summary for Policymakers. Contribution of Working Group I to the Fourth Assessment Report of the Intergovernmental Panel on Climate Change approved at the 10th Session of Working Group I of the IPCC, Paris, February 2007.

Keeling C.D., Piper S.C. and Heimann M. (1989). A three dimensional model of atmospheric CO_2 transport based on observed winds: 4. Mean annual gradients and interannual variations. In: D.H. Peterson (Editor), Aspects of Climate Variability in the Pacific and the Western Americas. Geophysical Monograph. American Geophysical Union, Washington D.C., pp. 305-363.

Kolchugina T. P. and Vinson T. P. (1993). Carbon sources and sinks in the former Soviet Union. Global Biogeochemical Cycles, 7, 291-304.

Li S.G., Asanuma J., Eugster W., Totani A., Liu J.J., Urano T., Oikawa T., Davaa G., Oyunbaatar D. and Sugita M. (2005). Net ecosystem carbon dioxide exchange over grazed steppe in central Mongolia. Global Change Biology, 11, 1941-1955.

Liski J., Korotkov A.V., Prins C.F.L., Karjalainen T., Victor and D. G. Kauppi P.E. (2003). Increased Carbon Sink In Temperate And Boreal Forests. Climatic Change, 61, 89–99.

Millennium Ecosystem Assessment, (2005). Ecosystems and Human Well-being: Synthesis. Island Press, Washington, DC. A.,

Nilsson S., Shvidenko A., Stolbovoi V., Gluck M., Jonas M. and Obersteiner M. (2000). Full carbon account for Russia. Interim Report IR-00-021. International Institute for Applied Systems Analysis, Laxenburg, Austria.

Prentice I.C., Farquhar G.D., Fasham M.J.R., Goulden M.L., Heimann M., Jaramillo V.J., Khehgi S., Le Quéré C., Scholes R.J. and Wallace D.W.R. (2001). The carbon cycle, and atmospheric carbon dioxide. In: Climate Change 2001: The scientific basis. Contribution of working group I to the third assessment report of the intergovernmental panel on climate change. Houghton J.T., Ding Y., Griggs D.J., Noguer M., Van der Linden P.J., Dai X., Maskell K. and C.A. Johnson (Eds.) pp. 183-237, Cambridge University Press, Cambridge, United Kingdom and New York, NY, USA.

Rödenbeck C., Houweling S., Gloor M. and Heimann M. (2003). CO_2 flux history 1982-2001 inferred from atmospheric data using a global inversion of atmospheric transport. Atmos. Chem. Phys. 3, 1919-1964.

Shvidenko A. and Nilsson S. (2003). A synthesis of the impact of Russian forests on the global carbon budget for 1961–1998. Tellus B, 55, 391–415.

Tans et al. (1990) Observational constraints on the atmospheric CO_2 budget. Science 247, 1431-1438.

Chapter 1

Alekhno A.N., Busko E.G., Voronov A.G. (1995). Structure and dynamica of vegetation cover. In: The Uvsu-Nuur experiment. Part 1. Intellekt Press, Moscow. P.59-159.

Gorshkova A.A. (1990). Features of productivity formation of of steppe communities in central Tuva. In: Information problems of research of the biosphere. The Uvs-Nuur hollow is a natural model of the biosphere. Pushino. P. 184- 200.

Isachenko A.G. and Shalapnikov A.A. (1989). Landscapes. Mysl Press. Moscow. 503 p.

Kamenetskaya I.V. (1949). The influence of meteorological conditions on seed reproduction in plants of Streletskaya steppe. Byull. Mosk. Ova. Ispyt. Prir, 54(4): 83-89. (in Russian)

Kuminova, A. V., Zvereva, G.A., Lamanova, T.G. (1976). Steppes. In: Vegetation cover of Khakasia. NAUKA Press, Novosibirsk. 95-152 p.

Kuminova A.V. (1982). Vegetation cover of the Ulug-Khem region of the Tuvan ASSR. NAUKA Press, Novosibirsk. 5-28 p.

Lavrenko A.M. and Karamysheva Z.V. (1993). Steppes of former Soviet Union and Mongolia. In: Ecosystems of the World. Natural Grasslands. Northern Hemisphere and Resumè. Coupland, R, (editor), Elsevier, Amsterdam, 3-59.

Lavrenko E.M. (1956). Steppes and agricultural lands replacing steppes. In: Vegetation cover of the USSR: Explanations for Geobotanical map of the USSR. V. 2. Academy of Sciences Press, Moscow-Leningrad. p.595-730.

Lavrenko E.M., Karamysheva Z.V., Nikulina R.I. (1991). Steppes of Asia. NAUKA Press, Leningrad, 146 p.

Lavrenko E.M., Volkova E.A., Karamysheva Z.V. (1988). Botanical-geographical and cartographical research in Mongolian People's Republic. In: Natural conditions, vegetation cover and animals of Mongolia. Pushino, p. 137-159.

Lavrenko A.M. (1970). Division of the Black Sea- Kazakhstan subregion of the Eurasian steppe region. Bot. Zh., 55: 609-625. (in Russian)

Lavrenko A.M. (1970). Division of the Central Asian subregion of the Eurasian steppe region. Bot. Zh., 55: 1734-1741. (in Russian)

Shalyt M.S. (1950). The underground parts of some meadow, steppe and desert plants and phytocenosis, 1. Tr. Bot. Inst.Akad. Nauk USSR, Ser.3, Gobot., 6: 205-442. (in Russian)

Shalyt M.S. (1952). The underground parts of some meadow, steppe and desert plants and phytocenosis, 2. Tr. Bot. Inst.Akad. Nauk USSR, Ser.3, Gobot., 8: 71-139. (in Russian)

Volkova V.G., Kochurov B.I., Khakimzyanova F.I. (1979). The contemporary status of steppes in the Minusinsk hollow. NAUKA Press, Novosibirsk. 90 p.

Yershova E.A. (1982). On the characteristics of steppe vegetation of the West Tuva mountains. In: vegetation communities of Tuva. NAUKA Press, Novosibirsk. P. 109-121.

Chapter 2

Ajwa H.A, Rice .C.W., Sotomayor D. (1998). Carbon and nitrogen mineralization in tallgrass prairie and agricultural TO soil profiles. Soil Science Society of America Journal 62: 942–951.

Barnwel T.O, Jackson R.B., Elliott E.T., Burke I.C., Paustian K., Paul E.A., Donigan A.S., Patwardhan A.S., Rowell A., Weinrich K. (1992). An approach to assessment of management impacts on agricultural soil carbon. Water, Air and Soil Pollution 64: 423–435.

Bol R., Amelung W., Friedrich C. (2004). Role of aggregate surfaces and core fraction in the sequestration of carbon from dung in a temperate grassland soil. European Journal Soil Science 55: 71–77.

Boone R.D. (1994). Light-fraction soil organic matter: origin and contribution to net nitrogen mineralization. Soil Biology and Biochemistry 26, 1459-1468.

Bremer E., Janzen H.H., Johnston A.M. (1994). Sensitivity of total, light fraction and mineralizable organic matter on management practices in a Lethbridge soil. Canadian Journal of Soil Science 74, 131-138.

Bruce J.P., Frome M., Haites E., Janzen H., Lal R., Paustian K. (1999). Carbon sequestration in soils. Journal of Soil and Water Conservation 54: 382–389.

Cambardella C.A., Elliot E.T. (1992). Particulate soil organic-matter changes across a grassland cultivation sequence. Soil Science Society of America Journal 56, 777-783.

Cambardella C.A., Elliot E.T. (1993). Carbon and nitrogen distribution in aggregates from cultivated and native grassland soils. Soil Science Society of America Journal 57, 1071-1076.

Cao M.K., Woodward F.I. (1998). Net primary and ecosystem production and carbon stocks of terrestrial ecosystems and their responses to climate change. Global Change Biology 4: 185–198.

Christensen B.T. (1996). Matching measurable soil organic matter fractions with conceptual pools in simulation models of carbon turnover: Revision of model structure. In: Evaluation of Soil Organic Matter Models (eds Powlson DS, Smith P, Smith JU), NATO ASI Series 1, Vol. 38. Springer-Verlag, Berlin.

Christensen B.T.. (1996). Carbon in primary and secondary organomineral complexes. In: Stewart BA, ed. Structure and organic matter storage in agricultural soils. Boca Raton, FL, USA: CRC Press, 97–165.

Conant R.T., Paustian K., Elliott E.T. (2001). Grassland management and conversion into grassland: effects on soil carbon. Ecological Applications 11: 343–355.

Coupland R.T. (1979). The nature of grassland. In: Coupland RT, ed. Grassland ecosystems of the world. Cambridge, UK: Cambridge University Press, 23–31.

Darrah P.R. (1996). Rhizodeposition under ambient and elevated CO_2 levels. Plant and Soil 187: 265–275.

Dugas W.A., Heuer M.L., Mayeux H.S. (1999). Carbon dioxide fluxes over bermudagrass, native prairie, and sorghum. Agricultural and Forest Meteorology, 93, 121–139.

Emmerich W.E., (2004). Carbon dioxide fluxes in a semiarid environment with high carbonate soils Agricultural and Forest Meteorology 122 (1–2), 127–128.

Eswaran H., Vandenberg E., Reich P. (1993). Organic carbon in soils of the world. Soil Science Society of America Journal 57: 192–194.

Fitter A.H., Self G.K., Brown T.K., Bogie D.S., Graves J.D., Benham D., Ineson P. (1999). Root production and turnover in an upland grassland subjected to artificial soil warming respond to radiation flux and nutrients, not temperature. Oecologia 120: 575–581.

Flanagan L.B., Wever L.A., Carlson P.J. (2002). Seasonal and interannual variation in carbon dioxide exchange and carbon balance in a northern temperate grassland. Global Change Biology 8, 599–615.

Frank A.B., Dugas W.A. (2001). Carbon dioxide fluxes over a northern, semiarid, mixed-grass prairie. Agricultural and Forest Meteorology, 108, 317–326.

Giardina C.P., Ryan M.G. (2000). Evidence that decomposition rates of organic carbon in mineral soil do not vary with temperature. Nature 404: 858–861.

Gifford R.M., Roderick M.L. (2003). Soil carbon stocks and bulk density: spatial or cumulative mass coordinates as a basis of expression? Global Change Biology 9: 1507–1514.

Gordon W.S., Jackson R.B. (2000). Nutrient concentrations in fine roots. Ecology 81: 275–280.

Hungate B.A., Holland E.A., Jackson R.B., Chapin F.S., Mooney H.A., Field C.B. (1997). The fate of carbon in grasslands under carbon dioxide enrichment. Nature 388: 576–579.

IPCC (2001). Climate change 2001: the scientific basis. contribution of working group 1 to the third assessment report of the intergovernmental panel on climate change. Houghton J.T., Ding Y., Griggs D.J., Noguer M., van der Linden P.J., Dai X., Maskell K., Johnson C.A., eds. Cambridge, UK, Cambridge University Press.

Jenkinson D.S. (1990). The turnover of organic carbon and nitrogen in soil. Philosophical Transactions of the Royal Society of London Series B – Biological Sciences 329: 361–368.

Jobbágy E.G., Jackson R.B. (2000). The vertical distribution of soil organic carbon and its relation to climate and vegetation. Ecological Applications 10: 423–436.

Joffre R., Ågren G.I. (2001). From plant to soil: litter production and decomposition. In: Mooney HA, ed. Terrestrial global productivity. San Diego, CA, USA: Academic Press, 83–99.

Jones M.B., Donnelly A. (2004). Carbon sequestration in temperate grassland ecosystems and the influence of management, climate and elevated CO_2.New Phytologist 164:423-439.

Kalbitz K., Solinger S., Park J.H., Michalzik B., Matzner E. (2000). Controls on the dynamics of dissolved organic matter in soils: a review. Soil Science 165: 277–304.

Kirschbaum M.U.F. (2000). Forest growth and species distribution in a changing climate. Tree Physiology 20: 309–322.

Kyzyakov Y., Domanski G. (2000). Carbon input by plants into the soil. Review. Journal of Plant Nutrition and Soil Science, 163, 421-431.

Lal R., Henderlong P., Flowers M. (1998). Forages and row cropping effects on soil organic carbon and nitrogen contents. In: Stewart BA, ed. Management of carbon sequestration in soil. Boca Raton, FL, USA: CRC Press, 365–379.

LeCain D.R., Morgan J.A., Schuman G.E., Reeder J.D., Hart R.H. (2002). Carbon exchange and species composition of grazed pastures and exclosures in the shortgrass steppe of Colorado. Agriculture Ecosystems and Environment 93: 421–435.

Li S.G., Asanuma J., Eugster W., Totani A., Liu J.J., Urano T., Oikawa T., Davaa G., Oyunbaatar D. and Sugita M. (2005). Net ecosystem carbon dioxide exchange over grazed steppe in central Mongolia. Global Change Biology 11, 1941-1955.

Loiseau P., Soussana J.F. (1999). Elevated CO_2, temperature increase and N supply effects on the accumulation of below-ground carbon in a temperate grassland ecosystem. Plant and Soil 212: 123–134.

Meyers, T. P. (2001). A comparison of summertime water and CO_2 fluxes over rangeland for well-watered and drought conditions. Agric. For. Meteor., 106, 205–214.

Miller R.W., Donahue R.L. (1990). Soils: an Introduction to Soils and Plant Growth, 6th edn. Prentice Hall Inc, New Jersey, USA.

Nosberger J., Blum H., Fuhrer J. (2000). Crop ecosystem responses to climatic change: productive grasslands. In: Hodges HF, ed. Climate change and global crop productivity. Wallingford, UK: CAB International, 271–291.

Novick K.A., Stoy P.C., Katul G.G., Ellsworth D.S., Siqueira M.B.S., Juang J., Oren R. (2004). Carbon dioxide and water vapor exchange in a warm temperate grassland. Oecologia 138, 259–274.

Ojima D.S., Parton W.J., Schimel D.S., Scurlock J.M.O., Kittel T.G.F. (1993). Modeling the effects of climatic and CO_2 changes on grassland storage of soil-C. Water Air and Soil Pollution 70: 643–657.

Parton W.J., Scurlock J.M.O., Ojima D.S., Schimel D.S., Hall D.O. (1995). Impact of climate change on grassland production and soil carbon worldwide. Global Change Biology 1: 13–22.

Post W.M., Kwon K.C. (2000). Soil carbon sequestration and land-use change: processes and potential. Global Change Biology 6: 317–327.

Reeder J.D., Schuman G.E. (2002). Influence of livestock grazing on C sequestration in semi-arid mixed-grass and short-grass rangelands. Environmental Pollution 116: 457–463.

Schlesinger W.H. (1977). Soil respiration and changes in soil carbon stocks. In: Mackenzie FT, ed. Biotic feedbacks in the global climatic system. Will the warming feed the warming? Oxford, UK: Oxford University Press.

Schuman G.E., Janzen H.H., Herrick J.E. (2002). Soil carbon dynamics and potential carbon sequestration by rangelands. Environmental Pollution 116: 391–396.

Schuman G.E., Reeder J.D., Manley J.T., Hart R.H., Manley W.A. (1999). Impact of grazing management on the carbon and nitrogen balance of a mixed grass rangeland. Ecological Applications 9: 65–71.

Skjemstad J.O., LeFeuvre R.P., Prebble R.E. (1990). Turnover of soil organic matter under pasture as determined by ^{13}C natural abundance. Australian Journal of Soil Research 28, 267-276.

Soussana J.F., Pilegaard K., Ambus P., Berbigier P., Ceschia E., Clifton-Brown J., Czobel Sz., de Groot T., Horva´t L., Hensen A., Jones M., Kasper G., Martin C., Milford C., Nagy Z., Neftel A., Raschi A., Rees R.M., Skiba U., Stefani, P., Saletes S., Sutton M.A., Weidinger T. (2004). Annual greenhouse gas balance of European grasslands. First results from the GreenGrass project. In: Weiske, A. (Ed.), Leipzig. Greenhouse Gas Emissions from Agriculture—Mitigation Options and Strategies. Conference Proceeding, pp. 25– 30.

Spycher G., Sollins P., Rose S. (1983). Carbon and nitrogen in the light fraction of a forest soil: Verticle distribution and seasonal patterns. Soil Science 135, 79-87.

Suyker A.E., Verma S.B., Burba G.G. (2003). Interannual variability in net CO_2 exchange of a native tallgrass prairie. Global Change Biology, 9, 255–265.

Suyker, A. E., and Verma S.B. (2001). Year-round observations of the net ecosystem exchange of carbon dioxide in a native tall grass prairie. Global Change Biol., 3, 279–290.

Thornley J.H.M., Cannell M.G.R. (1997). Temperate grassland responses to climate change: an analysis using the Hurley pasture model. Annals of Botany 80: 205–221.

Trumbore S. (2000). Age of soil organic matter and soil respiration: radiocarbon constraints on belowground C dynamics. Ecological Applications 10: 399–411.

Valentini R., Gamon J.A., Field C.B. (1995). Ecosystem gas exchange in a California grassland: seasonal patterns and implications for scaling. Ecology 76, 1940– 1952.

Whitehead D.C. (1995). Grassland nitrogen 4–5. Wallingford, UK: CAB International.

Zan C.S., Fyles J.W., Girouard P., Samson R.A. (2001). Carbon sequestration in perennial bioenergy, annual corn and uncultivated systems in southern Quebec. Agriculture Ecosystems and Environment 86: 135–144.

Chapter 3

Bolin B., Sukumar, R. (2000). Global perspective. In: Land Use, Land Use Change and Forestry, pp.23-51, Cambridge University Press, Cambridge, UK.

Boone R.D. (1994) Light fraction soil organic matter: origin and contribution to net nitrogen mineralization. Soil Biology and Biogeochemistry, 26, 1459-1468.

Bremer E., JanzenH.H., Johnston A.M. (1994) Sensitivity of total, light fraction and mineralizable organic matter on management practices in a Leithbridge soil. Canadian Journal of Science 74, 131-138.

Cambardella C.A., Elliot E.T. (1992). Particulate soil organic matter changes across a grassland cultivation sequence. Soil Science Society of America Journal 56, 777-783.

Cambardella C.A., Elliot E.T. (1993). Carbon and nitrogen distribution in aggregates from cultivated and native grassland soils. Soil Science Society of America Journal 57, 1071-1076.

Cerri C.C., Volkoff B., Andreaux F., Leopoldo P.R. (1991). Nature and behaviour of organic matter in soils under natural forest and after deforestation, burning and cultivation, near Manaus. Forest Ecology and Management, 38, 247-257.

Chen S. (1996). Inner Asian grassland degradation and plant transformation, in Culture and Environment in Inner Asia, The pastoral economy and the environment, Durham: Duke University Press, 1: 111-123.

Christensen B.T (1992). Physical fractionation of soil and organic matter in primary particle size and density separates. Advances in Soil Science 20, 1-90.

Christensen B.T. (1996). Matching measurable soil organic matter fractions with conceptual pools in simulation models of carbon turnover: Revision of model structure. In: Evaluation of Soil Organic Matter Models (eds Powlson D.S., Smith P., Smith J.U.), NATO ASI Series 1, Vol. 38. Springer-Verlag, Berlin.

Chuluun T., Ojima D. (2002). Land use change and carbon Cycle in arid and semi-arid lands of East and Central Asia. Sicence in China (Series C) vol. 45, 48:54.

Chuluun, T., Ojima, D. (1999). Climate and grazing sensitivity of the Mongolian rangeland ecosystem, in Proceedings of the VI International Rangeland Congress on "People and Rangelands: Building the Future", Townsville, Queensland, Australia, 2: 877-878.

Conant R.T., Paustian K., Elliot E.T. (2001). Grassland management and conversion into grassland : effects on soil carbon. Ecological Applications, 11, 343-355.

Dobrovolsky G. V. and Urusevskaya I. S. (1984). *Soil geography*. MGU, Moscow, 415 pp. (in Russian).

Ellis J., Lee R..Y. (1999). Collapse of the Kazakhstan livestock sector: Catastrophic convergence of ecological degradation, economic transition and climate change, Report on "Impacts of privatization on livestock and rangeland management in semiarid Central Asia", London: Overseas Development Institute.

Enkhee J. (2000). The Mongolian tradition of legal culture and the grassland management in Inner Mongolia today, in Proceedings of the International Symposium on "Nomads and Use of Pastures Today", 194-199.

Fearnside P.M., Barbosa R.I. (1996). Soil carbon changes from conversion of forest to pasture in Brazilian Amazonia. Forest Ecology and Management, 108, 147-166.

Graetz, D., (1994). Changes in Land Use and Land Cover, A Global Perspective, eds. Meyer, W., Turner II, B., Cambridge: Cambridge University Press, 287-328.

Grubler A. (1994). Human driving force: technology, in Change in Land Use and Land Cover, A Global Perspective (eds. Meyer, W., Turner II, B.), Cambridge: Cambridge University Press, 287-328.

Guo L.B., Gifford R.M. (2002). Soil carbon stocks and land use change: a meta analysis. Global Change Biology 8, 345-360.

Houghton R.A. (2003). Revised estimates of the annual net flux of carbon to the atmosphere from changes in land use and land management 1850–2000. Tellus 55B, 378-390

Houghton R.A., Hackler J.L. (2001). Carbon flux to the atmosphere from Land Use Changes: 1850 to 1990. ORNL/CDIAC-131, NDP-050/R1 (http://cdiac.esd.ornl.gov/ndps/ndp050.html).

Humprey C., Sneath D. (1999). The End of Nomadism? Society, State and the Environment in Inner Asia, Durham: Duke University Press.

IPCC. (2000). Summary for policy makers: Land Use, Land Use Change and Forestry. A special report for the Intergoernamental Panel on Climate Change, Geneva, Switzerland.

Jenkinson D.S. (1990). The turnover of organic carbon and nitrogen in soil. Philosophical Transactions of the Royal Society of London B 329, 361-368.

Kerven C., Lunch C. (1999). The future of pastoralism in Central Asia, Proceedings of the 6th International Rangleland Congress on "People and Rangelands: Building the Future", 2: 1042-1048.

Kharin N., Tateishi R., Harahsheh H. (1999). Degradation of the drylands of Asia, Centre for Environmental Remote Sensing (CEReS), Chiba University.

Kharin N.G. (1996). Strategy to combat desertification in Central Asia, Desertification Control Bulletin, 29: 29-34.

Kharin N. G., Kalenov G. S., Kiril'tseva A. A. (1993). Explanatory note to the map of human-induced land degradation in the Aral Sea Basin: scale 1:250000, Ashkhabad: Desert Research Institute.

Kyzyakov Y., Domanski G. (2000). Carbon input by plants into the soil. Review. Journal of Plant Nutrition and Soil Science, 163, 421-431.

Larionova A.A., Rozanova L.N., Yevdokimov A.M., Yermolayev A.M., Kurganova I.N. and Blagodatsky S.A. (2003). Land use change and management effect on carbon sequestration in soils of Russia's Taiga zone. Tellus 55B, 331-337.

Mahli Y., Baldocchi D.D., Jarvis P.G. (1999). The carbon balance of tropical, temperate and boreal forests. Plant, Cell and Environment, 22, 715-740.

Miller .R.W., Donahue R.L. (1990). Soils: an Introduction to Soils and Plant Growth, 6th edn. Prentice Hall Inc, New Jersey, USA.

Nilsson S., Shvidenko A., Stolbovoi V., Gluck M., Jonas M. and Obersteiner M. (2000). In: *Full carbon account for Russia. Interim Report IR-00-021*, International Institute for Applied Systems Analysis, Laxenburg, Austria, 180 pp.

Oades J.M. (1993). The role of biology in the formation, stabilization and degradation of soil structure. Geoderma 56, 377-400.

Orenchi S. (2000). Study on the issue of the stock system of grassland: extracts of the theory, in Proceedings of the International Symposium on "Nomads and Use of Pastures Today", 223-229.

Pankova E. I. and Novikova A. F. (2000). Soil degradation processes on agricultural lands of Russia. *Eurasian Soil Sci.* 33, 319–330.

Parton W.J, Stewart J.W.B., Cole C.V. (1988). Dynamics of C, N, P and S in grassland soils: a model. Biogeochemistry 5, 109-131.

Post W.M., Kwon K.C. (2000). Soil carbon sequestration and land use change: process and potential. Global Change Biology, 6, 317-327.

Qu G., Li J. (1994). Population and environment in China, Boulder: Lynne Rienner Publishers.

Reardon-Anderson J. (1996). Land use and society in Machuria and Inner Mongolia during the Qing Dynasty, Environmental History, 503-530.

Skjemstad J.O., LeFeuvre R.P., Prebble R.E. (1990). Turnover of soil organic matter under pasture as determined by ^{13}C natural abundance. Australian Journal of Soil Research 28, 267-276.

Sparling G.P., Shepherd T.G., Kettles H.A. (1992). Changes in soil organic C, microbial C and aggregate stability under continuous maize and cereal cropping, and after restoration to pasture in soils from the Manawatu region, New Zealand. Soil Tillage Research, 24, 225-241.

Spycher G., Sollins P., Rose S. (1983). Carbon and nitrogen in the light fraction of a forest soil: Vertical distribution and seasonal patterns. Soil Science 135, 79-87.

Tserendash, S.(2000). Pasture resource: utilization and management in Mongolia. Proceedings of the International Symposium on "Nomads and use of pastures today", 141-143.

Chapter 4

Cherepnin L.M. (1953). Flora and vegetation of the south of the Krasnoyarsk territory. PhD. Krasnoyarsk. 30 p.

Conen F., Mikhail V.Y., Sambuu A.D. (2003). Potential for detecting changes in soil organic carbon concentrations resulting from climate change. Global Change Biology 9, 1515-1520.

Folland C.K., Karl T.R. (2001). Observed climate variability and change. In: Climate Change (2001): The Scientific Basis (eds Houghton J.T., Ding Y., Griggs D.J., Noguer M., van der Linden P.J., Dai X., Maskell K., Johnson C.A.), pp. 99–181. Cambridge University Press, Cambridge.

IPCC (2001). Climate Change 2001: The Scientific Basis. Contribution of Working Group I to the Third Assessment Report of the Intergovernmental Panel on Climate Change [Houghton J.T., Ding Y., Griggs D.J.,. Noguer M., van der Linden P.J., Dai X.,. Maskell K, and Johnson C.A. (eds.)]. Cambridge University Press, Cambridge, United Kingdom and New York, NY, USA, 881 pp.

Parton W.J., Ojima D.S., Schimel D.S. (1994). Environmental change in grasslands: assessment using models. Climatic Change, 28, 111–141.

Parton W.J., Scurlock J.M.O., SCOPEGRAM Group Members *et al*. (1995). Impact of climate change on grassland production and soil carbon worldwide. Global Change Biology, 1, 13–22.

Stolboboi V.(2000). Soils of Russia: Correlated with the Revised Legend of the FAO Soil Map of the World and World Reference Base for Soil Resources. Research Report, RR-00-13. IIASA, Laxenburg, Austria, 112 pp.

Thornthwaite C.W. (1933). The Climates of the Earth. Geographical Review, Vol. 23, No. 3, pp. 433-440.

Chapter 5

Conen F., Yakutin M.V., Sambuu A.D. (2003). Potential for detecting changes in soil organic carbon concentrations resulting from climate change. Global Change Biology 9, 1515-1520.

Dymyna G.D.(1982). Productivity of steppe communities of Central Tuva // Steppe vegetation of Siberia and some features of its ecology. - Novosibirsk: Nauka. Sib. Branch, P.86-94. (in Russian)

Eber W. (1991). Morphology in modern ecological studies. In: Esser, G., Overdieck, D. (eds.) Modern ecology: basic and applied aspects, Elsevier, Amsterdam, pp.3-20.

Gorshkova A.A. (1990). Features of productivity formation in steppe communities of Central Tuva // Informational problems of biosphera studying. Ubsu Nur hollow-natural model of the biosphera. – Pushino, P.184-200. (in russian)

Guo L.B., and Gifford R.M. (2002). Soil carbon stocks and land use change: a meta analysis. Global Change Biology 8, 345-360.

Knops J.M.H., and Tilman D. (2000). Dynamics of soil nitrogen and carbon accumulation for 61 years after agricultural abandonment. Ecology, 81, 88-98.

Kurbatskaia S.S. (1996). Dynamics of ecosystems of steppes and semideserts in Ubsu-Nur hollow // Global monitoring and UbsuNur hollow. – M.: Intellect, P. 15-18. (in Russian)

Kyrgys Ch.S. (1997). Productivity of dry steppe used as a winter pasture // Stable development of small nationalities of Central Asia and steppe ecosystems. – Kyzyl, Slovo, P. 80-83. (in Russian)

Larcher W. (2003). Carbon utilization and dry matter production. In: Physiological plant ecology: ecophysiology and stress physiology of functional groups, Springer-Verlag, pp.139-162.

Matson P.A., Parton W.J., Power W.J., Swift, M.J. (1997). Agricultural intensification and ecosystem properties. Science 277, 504-508.

Mironicheva-Tokareva N.P. (1998). Dynamics of vegetation during an overgrowing of dumps (On the example of KATEK). - Novosibirsk: Nauka. Sib. Branch,172 p. (in Russian)

Post W.M., and Kwon K.C. (2000). Soil carbon sequestration and land-use change : processes and potential. Global Change Biology 6, 317-328.

Sale P.J.M. (1974). Productivity of vegetable crops in a region of high solar input. Carbon balance of potato crops. Aust J Plant Physiol 1, 283-296.

Schulze E.D., Beck E., Müller-Hohenstein K.(2005). Plant Ecology, Springer Verlag, Heidelberg, Pp. 648-661.

Shmidt M.W.I., Skjemstadt J.O., Gehrt E., Kögel-Knaber I., (1999). Charred organic carbon in German chernozemic soils. Eur J Soil Sci 50, 351-365.

Titlianova et al. (2003). Productivity of steppes. In : Gadghiev I.M., Korolyuk A.Yu., Tytlianova A.A. et al., Steppes of Central Asia. Khmelev, V.A. editor, Novosibirsk, SB RAS, Pp. 95-112 (in Russian).

Titlyanova A.A., Kosyh N.P., Mironicheva-Tokareva N.P. (1996). Belowground parts of plants in grassland ecosystems. - Novosibirsk: Nauka. Sib. Branch, 128 p. (in Russian)

Torn M., Lapenis A.G., Timofeev A., Fischer M.L., Babikov B.V. and Harden J.W. (2002). Organic carbon and carbon isotopes in modern and 100-year-old-soil archives of the Russian steppes. Global Change Biology 8, 941-953.

Volkova V.G., Kochurov B.I., Hakimzyanova F.I. (1979). Up-to-date conditions of the steppes of Minusinskaya hollow. – Novosibirsk: Nauka. Sib. Branch, 90 p. (in Russian)

Yakutin M.V., Romanova I.P (1996). Carbon stores in belowground biomass, microbiomass and humus of dry steppes of UbsuNur hollow // Global monitoring and UbsuNur hollow. – M.: Intellect, P. 30-33.

Chapter 6

Coupland R.T. (1992). Mixed prairie. Grasslands of the world (ed. by R.T. Coupland), pp. 151–182. Cambridge University Press, Cambridge.

Cuevas E., and Medina E. (1988). Nutrient dynamics within Amazonian forests. II. Fine root growth, nutrient availability, and leaf litter decomposition, Oecologia, 76, 222–235.

Fahey. T. J., and Hughes J. W. (1994). Fine root dynamics in a northern hardwood forest ecosystem, Hubbard Brook Experimental Forest, NH. Journal of Ecology 82, 533–548.

Fisk M.C., Schmidt S. K. and Seastedt T. R. (1998). Topographic patterns of above- and belowground production and nitrogen cycling in alpine tundra, Ecology, 79, 2253–2266.

Gill R.A., Jackson R.B. (2000). Global patterns of root turnover for terrestrial ecosystems. New Phytologist 147: 13-31.

Gower S.T., Krankina O., Olson R.J., Apps M., Linder S., Wang C. (2001). Net primary production and carbon allocation patterns of boreal forest ecosystems. Ecological Applications 11: 1395-1411.

Hiu D., Jackson R.B. (2005). Geographical and interannual variability in biomass partitioning in grassland ecosystems: a synthesis of field data. New Phytologist doi:10.1111/j.1469-8137.2005.01569.x

IPCC. (2003). Good Practice Guidance for LULUCF Sector, Intergovernmental Panel on Climate Change, Cambridge University Press, Cambridge, UK.

Jackson R.B., Schenk H.J., Jobbágy E.G., Cnadell J., Colello G.D., Dickinson R.E., Field C.B., Friedlingstein P., Heimann M., Hibbard K., Kicklighter D.W., Kleidon A., Neilson R.P., Parton W.J., Sala O.E. & Sykes M.T. (2000). Belowground consequences of vegetation change and their treatment in models. Ecological Applications, 10, 470–483.

Johnson L.C., Matchett J. R. (2001). Fire and grazing regulate belowground processes in tallgrass prairie. Ecology, 12, 3377–3389.

Jordan C.F., and Escalante G. (1980). Root productivity in an Amazonian rain forest, Ecology, 6, 14–18.

Koukura Z., Mamolos A.P., Kalburtji K.L. (2003). Decomposition of dominant plant species litter in a semi arid grassland, Applied Soil Ecology, 23, 13-23.

Lauenroth W.K. (2000). Methods of estimating belowground net primary production. Methods in ecosystem ecology (ed. by O.E., Sala, R.B., Jackson, H.A. Mooney & R.W. Howarth), pp. 58–71. Springer, New York.

Lieth H. (1975). Modeling the primary productivity of the world. In: Lieth, H., Whittaker, R.H. eds. Primary productivity of the biosphere. Berlin, Germany: Springer-Verlag, 237-263.

Long S.P., Moya E.G., Imbamba S.K., Kamnalrut A., Piedade M.T.F., Scurlock J.M.O., Shen Y.K. & Hall, D.O. (1989). Primary productivity of natural grass ecosystems of the tropics: a reappraisal. Plant and Soil, 115, 155–166.

McNaughton S.J., Osterheld M., Frank D.A. & Williams K.J. (1989). Ecosystem-level patterns of primary productivity and herbivory in terrestrial habitats. Nature, 341, 142–144

Melillo J.M., McGuire A.D., Kicklighter D.W., Moore III B., Vorosmarty C.J. and Schloss A.L. (1993). Global climate change and terrestrial net primary production. Nature 363: 234–240.

Miyazaki S., Yasunari T., Miyamoto T., Kaihotsu I.,Davaa G., Oyunbataar D., Natsagdorj L., Oki T. (2004). Impact of seasonal and interannual rainfall variability on grassland vegetation in central Mongolia. Geographycal Research Abstracts, vol.6, 04567.

Milner C. & Hughes R.E. (1968). Methods for the measurement of the primary production of grassland. Blackwell Scientific, Oxford.

Neill C.(1992), Comparison of soil coring and ingrowth methods for measuring belowground production, Ecology, 73, 1918–1921.

Ni J. (2004). Estimating net primary productivity of grasslands from field biomass measurements in temperate northern China. Plant Ecology 174: 217-234.

Olson J.S. (1963). Energy storage and the balance of producers and decomposers in ecological systems, Ecology, 44, 322–331.

Paruelo J.M., Epstein H.E., Lauenroth W.K. & Burke I.C. (1997). ANPP estimates from NDVI for the Central Grassland Region of the United States. Ecology, 78, 953–958.

Persson H. (1983). The distribution and productivity of fine roots in boreal forests, Plant and Soil, 71, 87–101.

Raich J.W., Russell A.E. & Vitousek P.M. (1997). Primary productivity and ecosystem development along an elevational gradient on Mauna Loa, Hawai'i. Ecology, 78, 707–721.

Sala O.E. & Austin A.T. (2000). Methods of estimating aboveground net primary productivity. Methods in ecosystem science (ed. by Sala O.E., Jackson R.B., Mooney H.A.& Howarth R.W.), pp. 31–43. Springer, New York.

Scurlock J.M.O., Cramer W., Olson R.J Parton W.J. and .Prince S.D. (1999). Terrestrial NPP: towards a consistent data set for global model evaluation, Ecological Applications 9: 913–919.

Scurlock J.M.O., Johnson K. and Olson R.J. (2002). Estimating net primary productivity from grassland biomass dynamics measurements. Global Change Biology 8: 736–753.

Singh J.S. & Joshi M.C. (1979). Tropical grasslands: primary production. Grassland Ecosystems of the World (ed. by R.T. Coupland), pp. 197–218. Cambridge University Press, Cambridge.

Singh J.S., Joshi M.C. (1975). Review and assessment of various techniques for estimating net aerial primary production in grasslands from harvest data. Botanical review, 41, 181-232.

Titlianova A.A. (1977). Biological Cycle of carbon in grassland ecosystems, Novosibirsk, (in Russian).

Titlianova et al. (2003). Productivity of steppes. In : Gadghiev I.M., Korolyuk A.Yu., Tytlianova A.A. et al.,Steppes of Central Asia. Khmelev V.A. editor, Novosibirsk, SB RAS, Pp. 95-112 (in Russian).

Weigert R.G., Evans F.C. (1964). Primary production and the disappearance of dead vegetation on an old field in south-eastern Michigan. Ecology 45, 49-63.

Chapter 7

Afanasjeva E.A. (1966). Chernozems of the middle Russian Upland, Nauka, Novosibirsk. (in Russian)

Aubinet M., Heinisch, B.Yernaux, M. (2003) Horizontal and vertical CO2 advection in a sloping forest, Boundary Layer meteorology, vol. 108, no3, 397-417.

Aubinet, M., Grelle, A., Ibron, A., Rannik, Ü., Moncrieff, J., Foken, T., Kowalski, A.S., Martin, P.H., Berbigier, P., Bernhofer, C., Clement, R., Elbers, J., Granier, A., Grunwald, T., Morgensterm, K., Pilegaard, K., Rebmann, C. , Snijders, W., Valentini, R., Vesala, T. (2000). Estimates of the annual net carbon and water exchange of forests: the EUROFLUX methodology. Adv. Ecol. Research, 30, 113-175.

Bazilievich N.I., Shmakova E.I., Tishkov A.A. and Tran T. (1988) Herbaceous Ecosystems of the Russian Plain, Kursk Region, in: Biological Productivity of Herbaceous Ecosystems, edited by Ulyin V.B., pp. 56-66, Nauka, Novosibirsk. (in Russian)

Baldocchi D.D. (2003). Assessing the eddy covariance technique for evaluating carbon dioxide exchange rates of ecosystems: past, present and future. Global Change Biology, 9, 479-492.

Baldocchi D., Valentini R., Running S., Oechels W.and Dahlman R. (1996). Strategies for measuring and modelling carbon dioxide and water vapour fluxes over terrestrial ecosystems. Global Change Biology, 2, 159-168.

Baldocchi D.D., Hicks B.B. and Tilden P.M. (1988). Measuring biosphere-atmosphere related gases with micrometeorological methods. Ecology, 65, 1331-1340.

Barcza Z., Laszlo H., Kondo H., Saigusa N., Yamamoto S. and Bartholy J. (2003) Carbon exchange of grass in Hungary. Tellus, 55B, 187-196.

Burba, G.G., D.J. Anderson, L. Xu and D.K. McDermitt (2006). Correcting apparent off-season CO_2 uptake due to surface heating of an open path gas analyzer: progress report of an ongoing study. 27th Conference on Agricultural and forest meteorology, 24 May 2006, San Diego, CA, USA.

Ciais, P., Janssens I., Shvidenko A., Wirth C., Malhi Y., Grace J., Schulze E.-D., Heimann M., Phillips O. and Dolman A.J. (2005). The potential for rising CO_2 to account for the observed uptake of carbon by tropical, temperate and boreal fores biomes. In: Griffiths, H. and P.G. Jarvis (Eds). The carbon balance of forest biomes. Taylor and Francis, Oxon, UK, p. 109-149.

Campbell G.S. (1985). Soil Physics with Basic. Elsevier, NewYork, USA, 150 pp.

Falge E., Baldocchi D., Tenhunen J., Aubinet M., Bakwin P. Berbigier P., Bernhofer C., Burba G., Clement P., Davis K.J., Elbers J.A., Goldstein A.H., Grelle A., Granier A., Guomundsson J, Hollinger D., Kowalski A.S., Katul G., LawB.E., Malhi Y., Meyers T., Monson R.K., Munger J.W., Oechel W., Tha Paw U K., Pilegaard K. Rannik Ü., Rebmann C., Suyker A., Valentini R., Wilson K., Wofsy S.(2002). Seasonality of ecosystem respiration and gross primary production as derived from FLUXNET measurements. Agricultural and Forest Meteorology, 113, 53-74.

Feigenwinter C., Bernhofer C. and Vogt R. (2004): The influence of advection on the short term CO_2-budget in and above a forest canopy, Boundary-Layer Meteorol., 113, 201-224.

Fedorov-Davydov D.G., Gilichinsky D.A. (1993). Features of the dynamics of CO_2 evolution from frozen soils. [Osobennosti dinamiki vydeleniya CO_2 iz merzlykh pochv]. In: Zavarzin G.A.,

Kudeyarov V.N. (Eds.), Dykhanie Pochvy [Soil Respiration]. Institute Pochvovedeniya i Fotosinteza, Pushchino, pp. 76–100

Flanagan L.B., Wever L.A. and Carlson P.J. (2002). Seasonal and interannual variation in carbon dioxide exchange and carbon balance in a northern temperate grassland. Global Change Biology, 8, 559-615.

Foken Th. and Wichura B.(1996). Tools for quality assessment of surface-based flux measurements. Agricultural and Forest Meteorology, 78, 83-105.

Frank A.B. (2002). Carbon dioxide fluxes over a grazed prairie and seeded pasture in the Northern Great Plains. Environmental Pollution, 116, 397-403.

Gilmanov T.G., Sousanna J-F., and the EUROGRASSFLUX Working group (2007). Partitioning of the tower-based net CO_2 exchange in European grasslands into gross primary productivity and ecosystem respiration components using light response functions analysis. Agriculture, Ecosystems and Environment, in press.

Göckede M., Markkanen T., Hasager C.B. and Foken T. (2006). Update of a Footprint-Based Approach for the Characterisation of complex measurements sites. Boundary-Layer Meteorology, 118, 635-655.

Gu L., Falge E.M., Boden T., Baldocchi D.D., Black T.A., Saleska S.R., Suni T., Verma S.B., Vesala T., Wofsy S.C., and Xu L. (2005).Objective threshold determination for nighttime eddy flux filtering. Agric. Forest Meteorology, 128, 179-197.

Hunt J.E., Kelliher F.M., Mcseveny T.M., Ross D.J. and Whitehead D. (2004). Long-term carbon exchange in a sparse, seasonally dry tussock grassland. Global Change Biology, 10, 1785-1800.

Kaimal K.C. and Finnigan J.J. (1994). Atmospheric boundary layer flows: their structure and measurements. Oxforf University Press, Oxforf, 289 pp.

Kato T., Tang Y., Gu S., Cui X., Hirota M., Du M., Li Y., Zhao X., Oikawa T. (2004). Carbon dioxide exchange between the atmosphere and an alpine meadow ecosystem on the Qinghai - Tibetan Plateau, China. Agricultural and Forest Meteorology, 124, 121-134.

Kuderayov V.N., Kurganova I.N. (2005). Respiration of Russian soils: database analysis, long-term monitoring, and general estimates. Eurasian Soil Science vol.38, 9, 983-992.

Larionova A.A., Rozanova L.N., Yevdokimov I.V., Blagodatsky S.A. (2003). Carbon balance in arable grey forest soils. Annales UMCS, Sec.E, 58, 193-203.

Law B.E., Falge E., Gu L., Baldocchi D.D., Bakwin P., Berbigier P., Davis K., Dolman A.J., Falk M., Fuentes J.D., Goldstein A., Granier A., Grelle A., Hollinger D., Janssen I.A., Jarvis P., Jensen N.O., Katul G., Mahli Y., Matteucci G., Meyers T., MonsonR., Munger W., Oechel W., Olson R., Pilegaard K., Paw K.T., Thorgeirsson H., Valentini R. Verma S. Vesala T., Wilson K., WofsyS. (2002). Environmental controls over carbon dioxide and water vapour exchange of terrestrial vegetation. Agricultural and Forest Meteorology, 113, 97-120.

LeCain R.D., Morgan J.A., Schuman G.E., Reeder J.D., Hart R.H. (2002). Carbon exchange and species composition of grazed pastures and exclosures in the shortgrass steppe of Colorado. Agriculture, Ecosystems and Environment, 93, 421-435.

Li S.G., Asanuma J., Eugster W., Totani A., Liu J.J., Urano T., Oikawa T., Davaa G., Oyunbaatar D. and Sugita M. (2005) Net ecosystem carbon dioxide exchange over grazed steppe in central Mongolia. Global Change Biology, 11, 1941-1955.

Liu H., Peters G. and Foken T. (2001). New equations for sonic temperature varience and buoyancy heat flux with an omnidirectional sonic anemometer. Boundary-Layer Meteorology, 199: 459-468.

Lloyd J. & Taylor J.A..(1994). On the temperature dependence of soil respiration. Funct. Ecol., 8, 315-323.

Manca G. (2003). Analysis of carbon fluxes in a cronosequence of Turkey oak (Quercus Cerris L.) of Central Italy by eddy covariance technique. PhD thesis. University of Tuscia, Viterbo. 224 P. [in Italian]

Marcolla B., Cescatti A., Montagnani L., Manca G., Kerschbeumer G., Minerbi S. (2005) Importance of advection in the atmospheric CO_2 exchanges of an alpine forest. Agricultural and Forest meteorology, vol. 130, n.3-4, 193-206.

Massman W.J. and Lee X. (2002). Eddy covariance flux corrections and uncertainties in long-term studies of carbon and energy exchanges. Agric. Forest. Meteorology, 113, 121-144.

Mielnick P.C., Dugas W.A.. (2000). Soil CO_2 flux in a tallgrass prairie. Soil Biology & Biochemistry, 32, 221-228.

Moncrief J.B., Massheder J.M., de Bruin H., Elbers J., Friborg T., Heusinkveld B., Kabat P., Scott S., Soegaard H., and Verhoef A. (1997a). A system to measure surface fluxes of momentum, sensible heat, water vapour and carbon dioxide. Journal of Hydrology, 188-189, 589-611.

Odum E.P. (1969). The strategy of ecosystem development. Science, 164, 596-604.

Oechel W.C., Vourlitis G., Hastings S.J. (1997). Cold season CO2 emission from arctic soils. Global Biogeochem. Cycles 11, 163–172.

Reichstein M., Falge E., Baldocchi D., Papale D., Aubinet M., Berbigier P., Bernhofer C., Buchmann N., Gilmanov T., Granier A., Grünwald T., Havrankova K., Illvesniemi H., Janus D., Knohl A., Laurila T., Lohila A., Loustau D., Matteucci G., Meyers T., Miglietta F., Ourcival J., Pumpanen J., Rambal S., Rotemberg E., Sanz M., Vesala T., Yakir D., Valentini R.. (2005). On the separation of net ecosystem exchange into assimilation and ecosystem respiration: review and improved algorithm. Global Change Biology, 11, 1424-1439.

Reynolds O. (1895). On the dynamical theory of incompressible viscous fluids anfd the determination of criterion. Philosophical transactions of Royal Society of London, A174, 935-982.

Ruimy A., Jarvis P.G., Baldocchi D.D., Saugier B.(1995). CO2 fluxes over plant canopies and solar radiation: a review. Adv. Ecol. Res., 26, 1-68.

Schuepp P.H., Leclerc M.Y., Macpherson J.I. and Desjardins R.L. (1990). Footprint prediction of scalar fluxes from analytical solutions of the diffusion equation. Boundary-Layer Meteorology, 50: 355-373.

Stull R.B. (1988). An introduction to boundary layer meteorology. Kluweer Academic Publisher, Dordrecht, 666 pp.

Sukyer A.E., Verma S.B., Burba G.G. (2003) Interannual variability in net CO2 exchange of a native tallgrass prairie. Global Change Biology, 9, 255-265.

Suyker A.E. and Verma S.B. (2001). Year-round observation of the net exchange of carbon dioxide in a native tallgrass prairie. Global Change Biology, 7, 279-289.

Valentini R., Matteucci G., Dolman A.J., Schulze E.D., Rebman C., Moors E.J., Granier A., Gross P., Jensen N.O., Pilegaard K., Lindroth A., Grelle C, Bernhofer C., Grünwald T., Aubinet M., Ceulemans R., Kowalski A.S., Vesala T., Rannik Ü., Berbigier P., Loustau D., Mundsson J. Gu&Eth., Thorgeirsson H., Ibron A., Morgenstern K., Clement R., Moncrieff J., Montagnani L., Minerbi S., Jarvis P.G., (2000). Respiration as the main determinant of carbon balance in European forests. Nature, 404, 861-865.

Valentini R., Gamon J.A., Field C.B. (1995). Ecosystem gas exchange in a California grassland: seasonal patterns and implications for scaling. Ecology 76, 1940– 1952.

Webb E.K., Pearman G.I., and Leuning R. (1980). Correction of flux measurements for density effects due to heat and water vapour transfer. Q. J. R. Meteorol. Soc., 106, 85-100.

Wilson K.B., Goldstein A.H., Falge E. et al. (2002). Energy balance closure at FLUXNET sites. Agricultural and Forest Meteorology, 113, 223-243.

Xu L., Baldocchi D.D. (2004). Seasonal variation in carbon dioxide exchange over a Mediterranean annual grassland in California. Agricultural and Forest Meteorology, 1232, 79-96.

Chapter 8

Amthor J. S. (1994). Plant respiratory responses to the environment and their effects on the carbon balance. *In* Plant-environment interactions. Ed. R E Wilkinson. pp 50l–54. Marcel Dekker, Inc, New York.

Bassirirad H., Caldwell M.M. and Mott K.A. (1993). Effect of root cooling on photosynthesis of *Artermisia tridentata* seedlings under different light levels. Bot. Acta 106, 22–227.

Batjes N.H., (1996). Total carbon and nitrogen in the soils of the world. European Journal of Soil Science 47, 151–163.

Ben-Asher J., Cardon G.E., Peters D., Rolston D.E., Biggar J.W., Phene C.J. & Ephrath J.E. (1994). Determining root activity distribution by measuring surface carbon dioxide fluxes. Soil Sci. Soc. Am. J. 58: 926–930.

Bonkowski M., (2004). Protozoa and plant growth: the microbial loop in soil revisited. New Phytologist 162, 617–631.

Bouma T. .J, Broekihuysen A.G.M. and Veen B.W. (1996). Analysis of root respiration *Solanum tuberosum* as related to growth, ion uptake and maintenance of biomass. Plant Physiol. Biochem. 34, 795–806.

Bowden R.D., Nadelhoffer K.J., Boone R.D., Melillo J.M., Garrison J.B., (1993). Contributions of aboveground litter, belowground litter, and root respiration to total soil respiration in a temperature mixed hardwood forest. Canadian Journal of Forest Research 23, 1402–1407.

Buchmann N. (2000). Biotic and abiotic factors controlling soil respiration rates in Picea abies stands. Soil Biology & Biochemistry 32, 1625–1635.

Cheng W.X., Johnson D.W., Fu S.L. (2003). Rhizosphere effects on decomposition: controls of plant species, phenology, and fertilization. Soil Science Society of America Journal 67, 1418–1427.

Couteaux M.M., Mousseau M., Celerier M.L., Bottner P. (1991). Increased atmospheric CO_2 and litter quality: decomposition of sweet chestnut leaf litter with animal food webs of different complexities. Oikos 61, 54–64.

Craine J., Wedin D., Stuart Chapin III. (1999). Predominance of ecophysiological controls on soil CO_2 flux in a Minnesota grassland. Plant and Soil 207: 77-86.

Detling J.K., Dyer M.I., Winn D.T. (1979). Net photosynthesis, root respiration, and regrowth of *Bouteloua gracilis* following simulated grazing. Oecologia 41, 127–134.

Fisher F.M., Gosz J.R. (1986). Effects of trenching on soil processes and properties in a New Mexico mixed-conifer forest. Biology and Fertility of Soils 2, 35–42.

Fu S., Cheng W. (2004). Defoliation affects rhizosphere respiration and rhizosphere priming effect on decomposition of soil organic matter under a sunflower species: *Helianthus annuus*. Plant and Soil 263, 345–352.

Fukuoka N., Yoshioka H., Shimizu E. and Fujiwara T. (1996). Effect of shading cabbage seedlings on their physiological processes and rooting ability after transplanting to the nursery. J. Japan. Soc. Hortic. Sci 65, 545–551.

Goulden M.L., Munger J.W., Fan S.M., Daube B.C., Wofsy S.C. (1996). Exchange of carbon dioxide by a deciduous forest: response of interannual climate variability. Science 271, 1576–1578.

Griffith, B.S. (1994). Soil nutrient flow. In: Darbyshire, J.F. (Ed.), Soil Protozoa. CAB International, Wallingford, pp. 65–92.

Hanson P.J., Edwards N.T., Garten C.T. and Andrews J.A. (2000). Separating root and soil microbial contributions to soil respiration: A review of methods an observations. Biogeochemistry 48: 115-146.

Holland C.A., Detling J.K. (1990). Plant response to herbivory and belowground nitrogen cycling. Ecology 71, 1040–1049.

Janssens I.A., Lankreijer H., Matteucci G. *et al.* (2001). Productivity overshadows temperature in determining soil and ecosystem respiration across European forests. Global Change Biology 7, 269-278.

Johansson G. (1993). Carbon distribution in grass (*Festuca pratensis* L.) during regrowth after cutting: utilization of stored and newly assimilated carbon. Plant and Soil 151, 11–20.

Killham K. (1994). Soil Ecology, Cambridge University Press, Cambridge.

Ke X., Winter K., Filser J. (2005). Effects of soil mesofauna and farming management on decomposition of clover litter: a microcosm experiment. Soil Biology & Biochemistry 37, 731–738.

Keith H., Raison R.J and Jacobsen K.L. (1997). Allocation of carbon in a mature eucalypt forest and some effects of soil phosphorus availability. Plant Soil 196, 81–99.

Kucera C.L. & Kirkham D.R. (1971). Soil respiration studies in tallgrass prairie in Missouri. Ecology 52: 912-915.

Kuzyakov K. (2006).Sources of CO_2 efflux from soil and review of partitioning methods. Soil Biology & Biogeochemistry 38: 425-448.

Kuzyakov K. Cheng W. (2001). Photosynthesis controls of rhizosphere respiration and organic matter decomposition. Soil Biology & Biogeochemistry 33, 1915-1925.

Kuzyakov Y. (2002a). Review: Factors affecting rhizosphere priming effects. Journal of Plant Nutrition and Soil Science 165, 382–396.

Kuzyakov Y. (2002b). Separating microbial respiration of exudates from root respiration in non-sterile soils: A comparison of four methods. Soil Biology & Biochemistry 34, 1619–1629.

Lambers H., Scheurwater I. and Atkin O K (1996). Respiratory patterns in roots in relation to their functioning. *In* Plant roots: the hidden half Ed. Waisel Y., Eshel A. and Kafkafi U. pp 323–362. Marce Dekker, Inc., New York.

Landsberg J..J. and Waring R,H. (1997). A generalized model of forest productivity using simplified concepts of radiation-use efficiency, carbon balance and partitioning. For. Ecol. Manag. 95, 209–228.

Lavelle P., Gilot C. (1994). Priming effect of macroorganisms on microflora: a key process of soil function? In: Ritz K., Dighton J., Giller K.E. (Eds.), Beyond the Biomass: Compositional and Functional Analysis of Soil Microbial Communities. Wiley, Chichester, pp. 173–180.

Lee M.S., Nakane K., Nakatsubo T., Koizumi H. (2003). Seasonal changes in the contribution of root respiration to total soil respiration in a cool temperate deciduous forest. Plant and Soil 255, 311–318.

Lloyd J. and Taylor J.A. (1994). On the temperature dependence of soil respiration. Funct. Ecol. 8, 315–323.

Longdoz B., Yernaux M., Aubinet M. (2000). Soil CO_2 efflux measurements in a mixed forest: impact of chamber distances, spatial variability and seasonal evolution. Global Change Biology 6, 907–917.

Mikola J., Setala H. (1998). Productivity and trophic-level biomasses in a microbial-based soil food web. Oikos 82, 158–168.

Moore T.R. & Knowles R. (1989). The influence of water table levels on methane and carbon dioxide emissions from peatland soils. Can. J. Soil Sci. 69: 33–38

Nguyen C. (2003). Rhizodeposition of organic C by plants: mechanisms and controls. Agronomie 23, 375–396.

Paterson E. (2003). Importance of rhizodeposition in the coupling of plant and microbial productivity. European Journal of Soil Science 54, 741–750.

Percival D.C., Proctor J.T.A. and Tsujita M.J (1996). Whole-plant net CO_2 exchange of raspberry as influenced by air and rootzone temperature, CO_2 concentration, irradiation, and humidity. J. Am. Soc. Hortic. Sci. 121, 838–845.

Raich J.W. and Schlesinger W.H. (1992). The global carbon dioxide flux in soil respiration and its relationship to vegetation and climate. Tellus Ser. B Chem. Phys. Meteorol. 44, 81–99.

Raich J.W. and Potter C.S. (1995). Global patterns of carbon dioxide emission from soils. Global Biogeochem. Cycles 9, 23-36.

Ross D.J., Scott N.A., Tate K.R., Rodda N.J., Townsend J.A. (2001). Root effects on soil carbon and nitrogen cycling in a *Pinus radiata* D.Don plantation on a coastal sand. Australian Journal of Soil Research 39, 1027–1039.

Schlentner R.E. & Van Cleve K. (1985). Relationships between CO_2 evolution from soil, substrate temperature, and substrate moisture in four mature forest types in interior Alaska. Can. J. For. Res. 15: 97–106

Seto M. & Yanagiya K. (1983). Rate of CO_2 evolution from soil in relation to temperature and amount of dissolved organic carbon. Jap. J. Ecol. 33: 199–205

Singh U.R. & Shukla A.N. (1977). Soil respiration in relation to mesofaunal and mycofloral populations during rapid course of decomposition on the floor of a tropical dry deciduous forest. Rev. Écol. Biol. Sol 14: 363–370

Singh J.S. & Gupta S.R. (1977). Plant decomposition and soil respiration in terrestrial ecosystems. Bot. Rev. 43: 449–529

Szaniawski R.K. and Kielkiewicz M. (1982). Maintenance and growth respiration in shoots and roots of sunflower plants grown at different root temperatures. Physiol. Plant. 54, 500–504.

Tang J., Baldocchi D., Xu L. (2005). Tree photosynthesis modulates soil respiration on a diurnal time scale. Global Change Biology 11, 1298-1304.

Van Der Werf A. (1996). Growth, carbon allocation, and respiration as affected by nitrogen supply: aspects of the carbon balance. *In* Dynamics of Roots and Nitrogen in Cropping Systems of the Semi-Arid Tropics Eds. Ito O., Johnasen C., Adu-Gyamfi J.J, Katayama K., Kumar J.V.D.K. Rao, Rego T.J. pp 145–158. Japan International Research Center for Agricultural Sciences.

Wardle D.A., Verhoef H.A., Clarholm M. (1998). Trophic relationships in the soil microfood-web:Predicting the responses to a changing global environment. Soil Biota and Global Change 4, 713–727.

Zimov S.A., Zimova G.M., Davidov S.P., Davidova A.I., Voropaev Y.V., Voropaeva Z.V., Prosiannikov S.F., Prosiannikova O.V., Semiletova I.V., Semiletov I.P. (1993). Winter biotic activity and production of CO_2 in Siberian soils: a factor in the greenhouse effect. J. Geophys. Res. 98 (D3), 5017–5023.

Chapter 9

Anthoni P.M., Law B.E., Unsworth M.H. et al. (1999). Carbon and water vapour exchange of an open-canopied ponderosa pine ecosystem, Agricultural and Forest Meteorology, 95, 151-168.

Aubinet M., Heinesch B., Yernaux M. (2003). Horizontal and vertical CO_2 advection in a sloping forest, Boundary-Layer Meteorology, 108, 397-417.

Aubinet. M., Grelle A., Ibrom A. et al. (2000). Estimates of annual net carbon and water exchange of European forests: the EUROFLUX methodology, Advances in Ecological research, 30, 113-175.

Baldocchi D. (2003). Assessing the eddy covariance technique for evaluating carbon dioxide exchange rates of ecosystems: past, present and future, Global Change Biology 9, 479-492.

Baldocchi D.D., Finnigan J.J., Wilson K.W. et al. (2000). On measuring net ecosystem carbon exchange in complex terrain over tall vegetation, Boundary Layer Meteorology, 96, 257-291.

Barford C.C., Wofsy S.C., Goulden, M.L. et al. (2001). Factors controlling long and short term sequestration of atmospheric CO_2 in a mid latitude forest, Science, 294, 1688-1691.

Batjes N.H., Sombroek W.G. (1997). Possibilities for carbon sequestration in tropical and subtropical soils, Global Change Biology, 3, 161-173.

Bird M.I., Chivas A.R., Head J. (1996). A latitudinal gradient in carbon turnover times in forest soils, Nature, 381, 143-146.

Black T.A., Den Hartog G., Neumann H. et al. (1996). Annual cycles of CO_2 and water vapour fluxes and above and within a boreal aspen stand, Global Change Biology, 2, 219-230.

Ciais P., Tans P.P., Trolier M., White J.W.C.& Francey R.J. (1995). A large northern hemisphere terrestrial CO_2 sink indicated by the $^{13}C/^{12}C$ ratio of atmospheric CO_2, Science, 269, 1098-1101.

Conen F., Mikhail V.Y., Sambuu A.D. (2003). Potential for detecting changes in soil organic carbon concentrations resulting from climate change. Global Change Biology 9, 1515-1520.

Coupland R.T. (1992). Mixed Prairie. Grasslands of the World (ed Coupland R.T), Cambridge University Press, 151-182.

Cuevas E., and Medina E. (1988). Nutrient dynamics within Amazonian forests. II. Fine root growth, nutrient availability, and leaf litter decomposition, Oecologia, 76, 222–235.

Curtis P.S., Hanson P.J., Bolstad P., Barford C., Randolph J.C., Schmid H.P., Wilson K.B. (2002). Biometric and eddy covariance based estimates of annual carbon storage in five eastern North American deciduous forests, Agricultural and Forest Meteorology, 113, 3-19.

Ehman J.L., Scmid H.P., Grimmond C.S.B. et al. (2002). An initial intercomparison of micrometeorological and ecological inventory estimates of carbon exchanges in mid-latitude deciduous forest, Global Change Biology, 8, 575-589, 202.

Fahey T.J., and. Hughes J. W. (1994). Fine root dynamics in a northern hardwood forest ecosystem, Hubbard Brook Experimental Forest, NH. Journal of Ecology 82, 533–548.

Falge E., Baldocchi D.D. Olson R. et al. (2001). Gap filling strategies for defensible annual sums of net ecosystem exchange, Agricultural and Forest Meteorology , 107, 43-69.

Finnigan J., Raupach M. (2003). Transfer of materials and energy in the soil–canopy–boundary–layer system: measurements and modelling: a perspective for the next ten years of research. Rep. Ser. Aerosol Sci. 62A, 8–11.

Fisk M.C., Schmidt S. K. and Seastedt T.R. (1998). Topographic patterns of above- and belowground production and nitrogen cycling in alpine tundra, Ecology, 79, 2253–2266.

Flanagan L.B., Wever L.A., Carson P.J. (2002). Seasonal and interannual variation in carbon dioxide exchange and carbon balance in a northern temperate grassland, Global Change Biology, 8, 599-615.

Gill R.A., Kelly R.H., Parton W.J., Day K.A., Jackson R.B., Morgan J.A:, Scurlock J.M.O., Tieszen L.L., Castle J.V., Ojima D.S. and Zhang X.S. (2002). Using simple environmental variables to estimate belowground productivity in grasslands, Global Ecology & Biogeography 11, 79-86.

Gilmanov T.G., Verma S.B., Sims P.L., Meyers T.P., Bradford J.A., Burba G.G., Sukyer A.E. (2003). Gross primary production and light response parameters of four Southern Plains

ecosystems estimated using long term CO_2 flux tower measurements, Global Biogeochemical Cycles 17, 1071.

Goulden M.L., Munger J.W., Fan S.M. et al. (1996). Measurements of carbon storage by long term eddy correlation: methods and a critical assessment of accuracy, Global Change Biology, 2, 169-182.

Grace J., Malhi Y., Lloyd J. et al. (1996). The use of eddy covariance to infer the net carbon dioxide uptake of Brazilian rain forest, Global Change Biology, 2, 209-217.

Hall D.O., Ojima D.S., Parton W.J., Scurlock J.M.O. (1995). Response of temperate and tropical grasslands to CO_2 and climate change, Jounal of Biogeography, 22, 537-47.

Hall D.O., Scurlock J.M.O (1991). Climate change and productivity of natural grassland, Annals of Botany (Supplement), 67, 49-55.

Hollinger D.Y. and Richardson A.D. (2005). Uncertainty in eddy covariance measurements and its application to physiological models Tree Physiology 25, 873– 885.

IPCC (2003). Good Practice Guidance for LULUCF Sector, Intergovernmental Panel on ClimateChange, Cambridge University Press, Cambridge, UK.

IPCC (2000). Good Practice Guidance and Uncertainty Management in Greenhouse Gases Inventories, Cambridge University Press, Cambridge, UK..

Johnson L.C., Matchett, J.R. (2001). Fire and grazing regulate belowground processes in tallgrass prairie. Ecology, 12, 3377–3389.

Jordan C.F., and Escalante G. (1980). Root productivity in an Amazonian rain forest, Ecology, 6, 14–18, 1980.

Koukura Z., Mamolos A.P., Kalburtji K.L (2003). Decomposition of dominant plant species litter in a semi arid grassland, Applied Soil Ecology, 23, 13-23.

Lauenroth W.K. (2000). Methods of estimating belowground net primary production, Methods in ecosystem science (ed. By. Sala O.E., Jackson R.B., Mooney H.A. & Howarth R.W.), 58-71. Springer, New York.

Lieth, H.F.H. (ed.) (1978). Patterns of Primary Productivity in the Biosphere, Hutchinsons Ross, Stroudsberrg , PA, 342 pp.

Lloyd J., Taylor J.A. (1994). On the temperature dependence of soil respiration., Functional Ecology, 8, 315-323.

Long S.P., Garcia Moya E., Imbamba S.K. et al. (1989). Primary productivity of natural grass ecosystems of the tropics : a reappraisal, Plant and Soil, 115, 155-166.

Long S.P., Jones M.B., Roberts M.J. (eds.) (1992). Primary Productivity of Grass Ecosystems of the Tropics and Sub-Tropics, Chapman & Hall, London.

Mahli Y., Nobre A.D., Grace J., et al. (1998). Carbon dioxide transfer over a central Amazonian rain forest. Journal of Geophysical Research, 103, 31593-31612.

Meyers T. (2001). A comparison of summertime water and CO_2 fluxes over rangeland for well watered and drought conditions, Agricultural and Forest Meteorology, 106, 205-214.

Milner C., Hughes R.E. (1968). Methods for the Measurement of the Primary Production of Grassland, IBP Handbook no.6, Blackwell, Oxford.

Moncrieff. JB., Mahli Y., Leuning R. (1996). The propagation of errors in long term measurements of land atmosphere fluxes of carbon and water, Global Change Biology, 2, 231-240.

Neill C. (1992). Comparison of soil coring and ingrowth methods for measuring belowground production, Ecology, 73, 1918–1921.

Ni J. (2004). Estimating net primary productivity of grasslands form field biomass measurements in temperate northern China, Plant Ecology, 174, 217-234.

Olson J.S. (1963). Energy storage and the balance of producers and decomposers in ecological systems, Ecology, 44, 322–331.

Papale D., Reichstein M., Canfora E., Aubinet M., Bernhofer C., Longdoz B., Kutsch W., Rambal S., Valentini R., Vesala T., and Yakir D. (2006). Towards a more harmonized processing of eddy covariance CO_2 fluxes: alogorithms and uncertainty estimation, Biogeosciences, 3, 571–583.

Papale D., Valentini R. (2003). A new assessment of European forests carbon exchanges by eddy fluxes and artificial neural network spatialization, Global Change Biology, 9, 525-535.

Paruelo J.M., Epstein H.E., Lauenroth W.K. and Burke I.C. (1977). ANPP estimates from NDVI fort he central Grassland Region of the United States, Ecology, 78, 953-958.

Persson H. (1983). The distribution and productivity of fine roots in boreal forests, Plant and Soil, 71, 87–101.

Raich J.W., Russel A.E. and Vitousek P.M. (1997). Primary productivity and ecosysytem development along an elevational gradient on Mauna Loa, Hawaii, Ecology, 78, 707-721.

Reichstein M., Falge E., Baldocchi D., Papale D., Aubinet M., Berbigier P., Bernhofer C., Buchmann N., Gilmanov T.,Granier A., Grünwald T., Havránková K. Ilvesniemi, H., Janous D., Knohl A. Laurila T., Lohila A., Loustau D., Matteucci G., Meyers T. Miglietta F., Ourcival J., Pumpanen J. Rambal S. Rotenberg E. Sanz M., Tenhunen T., Seufert G., Vaccari F., Vesala T., Yakir D., and Valentini R (2005). On the separation of net ecosystem exchange into assimilation and ecosystem respiration: review and improved algorithm, Global Change Biology 11, 1424-1439.

Sala O.E. and Austin A.T. (2000). Methods for estimating aboveground net primary productivity. Methods in ecosystem science (ed. By. Sala O.E., Jackson R.B, Mooney H.A. &. Howarth R.W.), 31-43, Springer, New York.

Schulze E.D., Wirth C., Heimann M. (2000). Managing forests after Kyoto, Science, 289, 2058-2059.

Scurlock J.M.O., Johnson K. and Olson R.J. (2002).Estimating net primary productivity from grassland biomass dynamics measurements, Global Change Biology, 8, 736-753.

Sims P.L., Risser P.G. (2000). Grasslands. In: Barbour M.G., Billings W.D. (Eds.), Northern American Terrestrial Vegetation, 2nd ed. Cambridge University Press, Cambridge, 323-356.

Singh J.S., Joshi M.C. (1979). Tropical grasslands primary production. In: Grassland Ecosystems of the World (ed. Coupland R.T.) Cambridge University Press, 197-218.

Singh J.S., Joshi M.C. (1979). Review and assessment of various techniques for estimating net aerial primary production in grasslands from harvest data, Botanical review, 41, 181—232.

Schuepp P.H., Leclerc M.Y., MacPherson J I., and Desjardins R.L. (1990). Footprint predictions of scalar fluxes using analytical solutions of the diffusion equation, Boundary–Layer Meteorol., 50, 355-373.

Smith P. (2004). How long before a change in soil organic carbon can be detected?, Global Change Biology, 10, 1878-1883.

Stolbovoi V. (2000). Soils of Russia: Correlated with the Revised Legend of the FAO Soil Map of the World and World Reference Base for Soil Resources. Research Report, RR-00-13. IIASA, Laxenburg, Austria.

Suyker A.E., Verma S.B. (2001). Year round observations of the net ecosystem exchange of carbon dioxide in a native tallgrass prairie, Global Change Biology, 7, 179-189.

Titlianova A.A. (1977). Biological Cycle of carbon in grassland ecosystems, Novosibirsk (in Russian).

Titlianova et al. (2003). Productivity of steppes. In : Gadghiev I.M., Korolyuk A.Yu., Tytlianova A.A. et al.: Steppes of Central Asia, Khmelev V.A. editors, Novosibirsk, SB RAS,. 95—112. (in Russian)

Thornthwaite C.W. (1933). The Climates of the Earth, Geographical Review, Vol. 23, 3, 433-440.

Trumbore S.E., Chadwick O.A., Amundson R.(1996). Rapid exchange between soil carbon and atmospheric carbon dioxide driven by temperature change, Science, 272, 393-396.

Valentini R., Matteucci G., Dolman A.J., Schulze E.D. (2003). The role of canopy flux measurements in global C-cycle research, in: Fluxes of Carbon, Water and Energy of European Forests, Valentini R.(ed.), Springer Verlag, 255-266.

Webb E.K., Pearman G., Leuning R. (1980). Correction of flux measurements for density effects due to heat and water vapour transfer, Quarterly Journal of Royal Meteorological Society, 106, 85-100.

Weigert R.G., Evans F.C. (1964). Primary production and the disappearance of dead vegetation on an old field in south-eastern Michigan. Ecology 45, 49-63.

Wohlfahrt G., Anfang C., Bahn M., Haslwanter A., Newesely, C., Schmitt M., Drösler M., Pfadenhauer J., Cernusca A. (2005). Quantifying nighttime ecosystem respiration of a meadow using eddy covariance, chambers and modelling. Agricultural and Forest Meteorology 128, 141–162.

Xu L., Baldocchi D.D., (2004). Seasonal variation in carbon dioxide exchange over a Mediterranean annual grassland in California. Agric. For. Meteorol. 123, 79–96.

Chapter 10

FAOSTAT (2007) Food and Agricultural Organization of the United Nations, Statistics Division, http://faostat.fao.org/site/377/DesktopDefault.aspx

Van der Molen M.K.,. Dolman A.J, Belelli Marchesini L.,Ciais P., Corradi C., Heimann M., Kuwada T., Kononov A.V., Kurbatova J., Maximov T., Moors E., Nakai T., Schulze E.D., Shibistova O., Ohta T., Valentini R., Varlagin A., Viovy N., Vygodskaya N., Zimov S. The carbon balance of the Boreal Eurasia consolidated with eddy covariance observations. (submitted to GCB, February 2007)

Acknowlegements

Generally the accomplishment of a research, especially when based on field work, relies upon the contribution of several players, who, despite of their different task and degree of involvement, are fundamental ingredients for a successful result.
After the experience of three years of research at remote sites, I feel today to have a clearer idea of all the necessary amount of work that starts with the organization of an expedition and ends, as in this case, with the completion of a doctoral thesis. For this reason, I am also well aware of how my work benefited from the support of many people whom I feel deeply obliged to thank.

My doctorate supervisor, Prof. Riccardo Valentini, for having addressed my research topic and offered chances for my cultural and professional growth.
Prof. Eugene Vaganov, director of the Sukachev Forest Institute in Krasnoyarsk, for providing our team with the use of the infrastructures in Solionoziornoe, and the Institute's staff in Solionoziornoe for their kind assistance.
Dr. Nadja Tchebakova, for her precious and, in more than one occasion, extraordinary help in managing a large number of logistic issues.
Andrej Shifman, for his valuable work in the maintenance of the stations in Hakasia.
Valentina and Marina Mariassova, for their reliable help in the everyday's life in Solionoziornoe.
Dr. Tatyana Bugaenko, for the appreciated work in the botanical description of the sites and the "personal training" in the determination of steppe's species.
Dr. Elena Parfonova, Olga Gavrichkova and all the undergraduate students from Krasnoyarsk University who took part in the collection and treatment of the biomass samples.
All my work mates in the steppe: Emanuele Presutti Saba, Stefano Giorgi, Enrico Vittorini, Guerino Cefalo, Gianluca Bonavigo, Giovan Battista Zaini, Silvia Di Paolo, Daniela Silvani, Laura Saenz de Buruaga and Riccardo Ludovisi.
My lab colleagues, Dr. Dario Papale and Eleonora Canfora, for their help with the eddy covariance data gapfilling.
Prof. Hana Santruckova, for the nice collaboration in the joint field survey in summer 2004 and the results of soil analysis.
Renato Zompanti, technician of University of Tuscia and Mario Lanini, technician of CNR-IBIMET (Florence), for their work in the set up of the micrometeorological stations in Hakasia.
Dr. Galina Zrazhevskaya and Dr. Olga Shibistova, for their efforts at Kranoyarsk customs and in the burocratical aspects that the import of scientific equipment implies.
Dr. Giovanni Manca, for the efficient and careful assistance in the first steps of the eddy covariance measurements in Hakasia.
Dr. Juliya Kurbatova, Dr. Andrej Varlagin and Dr. Sergey Grigoriev, for the friendly help in Moscow.
Dr.Chaizu Kyrgys, and Andriyan Doduk, for their support in the realization of the short campaign in the Ubs-Nur Biosphere Reserve in Tuva.
I would also like to add to this list two people who, although probably not interested in carbon related issues, contributed unintentionally to the regular development of the research workplan: a lorry driver that gave an unexpected lift travelling for 380 km from Solionoziornoe to Krasnoyarsk in June 2004, and an unknown horse rider, met in the steppes of Tuva in May 2003, that pointed me the right direction when the chances to find the place I was looking for seemed already compromised. I was really grateful for that.